JHR 86: 1–17 (2021)
doi: 10.3897/jhr.86.69998
https://jhr.pensoft.net

RESEARCH ARTICLE

JOURNAL OF Hymenoptera RESEARCH
A peer-reviewed open-access journal
The International Society of Hymenopterists

Three new species and two new records of the genus *Phaenocarpa* Foerster (Hymenoptera, Braconidae, Alysiinae) from South Korea

Ju-Hyeong Sohn[1*], Cornelis van Achterberg[2*], Gyeonghyeon Lee[1], Hyojoong Kim[1]

1 *Animal Systematics Lab., Department of Biology, Kunsan National University, Gunsan, 54150, Republic of Korea* **2** *State Key Laboratory of Rice Biology and Ministry of Agriculture / Key Lab of Agricultural Entomology, Institute of Insect Science, Zhejiang University, Hangzhou, 310058, China*

Corresponding author: Hyojoong Kim (hkim@kunsan.ac.kr)

Academic editor: Jose Fernandez-Triana | Received 11 June 2021 | Accepted 3 October 2021 | Published 29 October 2021

http://zoobank.org/5E60582B-54FE-4856-8195-8BB4A3E1A264

Citation: Sohn J-H, van Achterberg C, Lee G, Kim H (2021) Three new species and two new records of the genus *Phaenocarpa* Foerster (Hymenoptera, Braconidae, Alysiinae) from South Korea. Journal of Hymenoptera Research 86: 1–17. https://doi.org/10.3897/jhr.86.69998

Abstract

The species of the genus *Phaenocarpa* Foerster, 1863 (Braconidae: Alysiinae) from South Korea are revised, and the genus is recorded for the first time from South Korea. Three species, *Phaenocarpa artotemporalis* **sp. nov.**, *P. brachyura* **sp. nov.** and *P. lobata* **sp. nov.**, are new to Science, and two species, *P. masha* Belokobylskij, 1998 and *P. fidelis* Fischer, 1970, are newly recognized in South Korea. They are described and illustrated herein with a provision of the identification key to the Korean species. In addition, the DNA barcode region of the mitochondrial cytochrome c oxidase subunit I (*COI*) has been analyzed for the six species including *P. ruficeps* for genetic comparison.

Keywords

COI barcode, cyclostome, koinobiont, natural enemy, parasitoid wasp, systematics, taxonomy

Introduction

The subfamily Alysiinae is a relatively large taxon among the family Braconidae, and is subdivided into two tribes; the tribes Alysiini with 76 genera and Dacnusini with 31

* The authors contributed equally to this paper.

Copyright *Ju-Hyeong Sohn et al.* This is an open access article distributed under the terms of the Creative Commons Attribution License (CC BY 4.0), which permits unrestricted use, distribution, and reproduction in any medium, provided the original author and source are credited.

genera (Yu et al. 2016). The two tribes are distinguished by the presence (or absence) of fore wing vein r-m as a main key character (Shaw and Huddleston 1991). Alysiinae occurs worldwide and contains over 2,440 valid species (Yu et al. 2016), of which 180 species in 21 genera are listed in the National Species List of South Korea (NIBR 2019). This group is known as koinobiont endoparasitoids of dipterous larvae, using their mandible (with three or four teeth, rarely more or less) to break open the puparium of the host. Some of them, such as *Dacnusa sibirica* in Dacnusini, are commercially utilized in biological control for *Liriomyza trifolii* (Abd-Rabou 2006).

The genus *Phaenocarpa* Foerster, 1863 is a large and worldwide distributed genus of Alysiinae, which includes 228 species with nine subgenera (Yu et al. 2016; Zhu et al. 2017). *Phaenocarpa* species are known as koinobiont endoparasitoids, mainly in larvae of Dipteran species of Anthomyiidae, Chloropidae, Clusiidae, Drosophilidae, Muscidae, Scathophagidae, Sciomyzidae, Syrphidae and Muscidae (Wharton 1984; van Achterberg 1998, 2009).

In the Korea, Papp (1968, 1994) has recorded four species thus far; *Phaenocarpa* (*Discphaenocarpa*) *angustipera* Papp, 1968, *P.* (*Phaenocarpa*) *eunice* (Haliday, 1838), *P.* (*P.*) *picinervis* (Haliday, 1838) and *P.* (*P.*) *ruficeps* (Nees, 1812). In this study, we present new morphological characters and the barcoding sequences of the *COI* region of three new species (*P. artotemporalis* sp. nov., *P. brachyura* sp. nov. and *P. lobata* sp. nov.) and two newly recorded species (*P. masha* Belokobylskij, 1998, *P. fidelis* Fischer, 1970) plus one previously recorded species, *P. ruficeps*. Descriptions, diagnoses, an identification key and photographs of the diagnostic characters are also provided.

Materials and methods

Samples used in this study were collected with Malaise traps in South Korea at the DMZ Botanical Garden, Mandae-ri, Haean-myeon, Yanggu-gun, Gangwon-do. Sorting and preparation were done at the Animal Systematics Lab. (**ASL**), Department of Biology, Kunsan National University (**KSNU**) at Gunsan. For morphological identification, Wharton et al. (1997) and Zhu et al. (2017) were used. Morphological characters were observed with a Leica M205C stereo microscope. The Taxapad database (Yu et al. 2016) was used for references. We followed the terminology of Wharton (2002) and van Achterberg (1993). The type specimens are deposited KNA (Korea National Arboretum).

A Leica DMC2900 digital camera and a Leica M205 C microscope (Leica Geosystems AG) were used for photography and several pictures being taken for each height using multi-focusing technology. LAS V4.11 (Leica Geosystems AG) and Helicon-Focus 7 (Helicon Soft) software were used for stacking work. After stacking work, illustrations were created using Adobe Photoshop CS6.

Extraction of DNA was done in ASL, KSNU. Whole genomic DNA was extracted from the specimens by using a DNeasy Blood & Tissue kit (QIAGEN Inc., Dusseldorf, Germany) following the manufacturer's protocol. In order to conserve morphologically complete voucher specimens, DNA extraction method was used slightly modified from

'non-destructive method' by Favret (2005) and 'freezing method' by Yaakop et al. (2009). In the original protocol, the sample was crushed or wounded, and then soaked with 180 µl of buffer ATL + 20 µl of proteinase, following by three hours over incubation at 55 °C. In the slightly modified DNA extraction methods, samples were soaked with 180 µl of buffer ATL + 20 µl of proteinase K without destroying the sample, followed by 10 minutes incubation at 55 °C and then kept in a freezer at -22 °C overnight. After that the general protocol was used for the remaining steps. The primer set of LCO-1490 (5'-GGTCAACAAATCATAAAGATATTGG-3') and HCO-2198 (5'-TAAACTTCAGGGTGACCAAAAAATCA-3') was used to amplify approximately 658 bp as the partial front region of the *COI*. The polymerase chain reaction (PCR) products were amplified by using AccuPowerH PCR PreMix (BIONEER, Corp., Daejeon) in 20 µl reaction mixtures containing 0.4 µM of each primer, 20 µM of the dNTPs, 20 µM of the $MgCl_2$, and 0.05 µg of the genomic DNA template. PCR amplification was performed using a GS1 thermo-cycler (Gene Technologies, Ltd., U.K) according to the following procedure: initial denaturation at 95 °C for 5 min, followed by 34 cycles at 94 °C for 35 sec; an annealing temperature of 48 °C for 25 sec; an extension at 72 °C for 45 sec, and a final extension at 72 °C for 5 min. The PCR products were visualized by electrophoresis on a 1.5% agarose gel. A single band was observed, purified using a QIAquick PCR purification kit (QIAGEN, Inc.), and then sequenced directly using an automated sequencer (ABI Prism 3730 XL DNA Analyzer) at Macrogen Inc. (Seoul, South Korea).

Sequence alignment was performed in MEGA version 7 (Kumar et al. 2016) with ClustalW tool. To estimate the pairwise genetic distances, the *P*-distance model was conducted using MEGA version 7.

Results

A total of 589 bp of the *COI* fragments were sequenced from *P. fidelis*, *P. masha*, *P. lobata* sp. nov., *P. artotemporalis* sp. nov., *P. brachyura* sp. nov., *P. ruficeps*, which were deposited in GenBank (accession numbers MZ318083–MZ318088). Pairwise distances were estimated by using the *P*-distance model with the option for pairwise deletion. As results, the morphologically very similar *P. artotemporalis* sp. nov. showed a large genetic difference by 12% either from *P. brachyura* sp. nov. or from *P. lobata* sp. nov. In addition, *P. brachyura* sp. nov. differed by 7% from *P. lobata* sp. nov.

Table 1. *COI* pairwise genetic distances between the *Phaenocarpa* species known from South Korea.

	Phaenocarpa fidelis	*Phaenocarpa masha*	*Phaenocarpa lobata*	*Phaenocarpa artotemporalis*	*Phaenocarpa brachyura*	*Phaenocarpa ruficeps*
Phaenocarpa fidelis	0.00					
Phaenocarpa masha	0.122	0.00				
Phaenocarpa lobata	0.053	0.126	0.00			
Phaenocarpa artotemporalis	0.124	0.151	0.127	0.00		
Phaenocarpa brachyura	0.071	0.136	0.071	0.122	0.00	
Phaenocarpa ruficeps	0.097	0.121	0.087	0.139	0.107	0.00

Phaenocarpa **Foerster, 1863**

Phaenocarpa Foerster, 1863: 267; Papp 1968: 570; Fischer 1970: 409; Shenefelt 1974: 1003; Wharton 1980: 96; Chen and Wu 1994: 114; Belokobylskij 1998: 233. Type species: *Alysia picinervis* Haliday, 1838.

Synonymy. *Homophyla* Foerster, 1863 (subgenus); *Mesothesis* Foerster, 1863; *Sathra* Foerster, 1863; *Idiolexis* Foerster, 1863 (subgenus); *Asynaphes* Provancher, 1886; *Kahlia* Ashmead, 1900 (subgenus); *Stiralysia* Cameron, 1910; *Rhopaloneura* Stelfox, 1941; *Discphaenocarpa* Belokobylskij, 1998 (subgenus); *Neophaenocarpa* Belokobylskij, 1998 (subgenus); *Sibphaenocarpa* Belokobylskij, 1998 (subgenus); *Uncphaenocarpa* Belokobylskij, 1998 (subgenus); *Ussurphaenocarpa* Belokobylskij, 1998 (subgenus); *Clistalysia* Zhu, van Achterberg & Chen, 2017 (subgenus).

Diagnosis. Third antennal segment shorter than fourth segment; fore wing vein 2–SR shorter than vein 3–SR, vein CU1b longer than vein 3–CU1**.**

Biology. Koinobiont endoparasitoids of larvae of Dipteran species (Wharton 1984).

Distribution. Cosmopolitan.

Identification key to the Korean *Phaenocarpa* species

1 Temples distinctly striate ventrally; mesopleuron largely coarsely sculptured; face laterally extensively and finely striate; [wing membrane distinctly infuscate] ..... ***P. angustiptera*** **Papp, 1968**

– Temples smooth ventrally; mesopleuron largely smooth, except for area of precoxal sulcus; face laterally smooth or nearly so **2**

2 Vein r-m of fore wing bordered with blackish setae, resulting in an infuscated patch..... ***P. picinervis*** **(Haliday, 1838)**

– Vein r-m of fore wing normal, not bordered with blackish setae (Fig. 6C) .. **3**

3 Mandible very slender, approx. 2.3 times longer than wide .... ***P. eunice*** **(Haliday, 1838)**

– Mandible more robust, at most 1.9 times longer than wide (Fig. 6L) **4**

4 Scutellar sulcus evenly narrowed medially, 3–5 times wider than its median length (Fig. 6F); head more or less reddish or yellowish brown (Fig. 6D)..... ..... ***P. ruficeps*** **(Nees, 1812)**

– Scutellar sulcus wide medially, 2–3 times wider than long medially (Fig. 4F); head dark brown or black (Fig. 1D) **5**

5 First tooth of mandible gradually connected to second tooth, forming a straight or arcuate connection (Fig. 4L); first metasomal tergite subparallel-sided, 1.7–2.0 times longer than its apical width (Fig. 4H); [ovipositor sheath as long as hind tibia] ..... ***P. fidelis*** **Fischer, 1970**

– First tooth of mandible separated from second tooth by incision (Fig. 1L); first tergite gradually widened posteriorly, 1.1–1.8 times longer than its apical width (Figs 1H, 2H, 3H)..... **6**

6 Eye in dorsal view 4.0–4.5 times as long as temple (Fig. 1D); propleuron reddish brown (Fig. 1F); notauli reduced posteriorly (Fig. 1G) .... ***P. artotemporalis* sp. nov.**

– Eye in dorsal view 2.0–3.0 times as long as temple (Fig. 2D); propleuron black or orange brown (Fig. 2F); notauli usually complete (up to medio-posterior depression (Fig. 2G) or nearly so **7**

7 Mandible subparallel-sided (Fig. 2L); ovipositor sheath approx. 0.7 times as long as hind tibia (Fig. 2I); first metasomal tergite slenderer, approx. 1.4 times longer than its apical width (Fig. 2H) ..... ***P. brachyura* sp. nov.**

– Mandible distinctly widened dorsally (Fig. 5L); ovipositor sheath 1.2–1.3 times as long as hind tibia (Fig. 5I); first tergite very robust, 1.1–1.2 times longer than its apical width (Fig. 5H) **8**

8 Tarsal claws slender (Fig. 5J); third and fourth antennal segments dark brown and slender (Fig. 5B); metanotum more or less tooth-shaped protruding dorsally in lateral view (Fig. 5G); pterostigma approx. 4.2 times longer than wide (Fig. 5C); middle tooth of mandible not widened dorsally (Fig. 5L) .... ***P. masha* Belokobylskij, 1998**

– Tarsal claws robust (Fig. 3J); third and fourth antennal segments yellow and robust (Fig. 3B); metanotum obtuse dorsally in lateral view (Fig. 3F); pterostigma approx. 5.5 times longer than wide (Fig. 3C); middle tooth of mandible widened dorsally (Fig. 3L) ..... ***P. lobata* sp. nov.**

***Phaenocarpa artotemporalis* Sohn & van Achterberg, sp. nov.**
http://zoobank.org/D973E619-5FB8-4956-A043-0574073C41EB
Figure 1A–L

Type material. ***Holotype***, ♀ (KNA), **South Korea**, DMZ Botanical Garden, Mandae-ri, Haean-myeon, Yanggu-gun, Gangwon-do, 38°15'09.3"N, 128°06'40.6"E, 08–21. VIII.2017, Shin, Kim. GenBank accession no. MZ318086 for the barcoding sequence of the COI region

Comparative diagnosis. Differs from other species in the group of *Phaenocarpa* species by notauli reduced posteriorly by having the eye in dorsal view 4.0–4.5 times as long as temple (2.0–3.0 times in other species). Closely related to *P. brachyura* sp. nov., for differences see key above.

Description. ***Holotype***, ♀: length of body in lateral view 2.0 mm, length of antenna 3.2 mm, and length of fore wing 2.6 mm.

Colour. Body (Fig. 1A) entirely reddish brown; antenna brown basally, medially dark brown, Mandible pale orange.

Head. Head (Fig. 1D) width 1.9 times median length in dorsal view. Antenna (Fig. 1B) 1.6 times longer than body in female, 25-segmented. Fourth segment 1.5 times longer than third segment, 1.2 times longer than fifth segment. Eye slightly oval, 1.1 times as long as wide in lateral view. Width of face (Fig. 1E) 1.6 times its

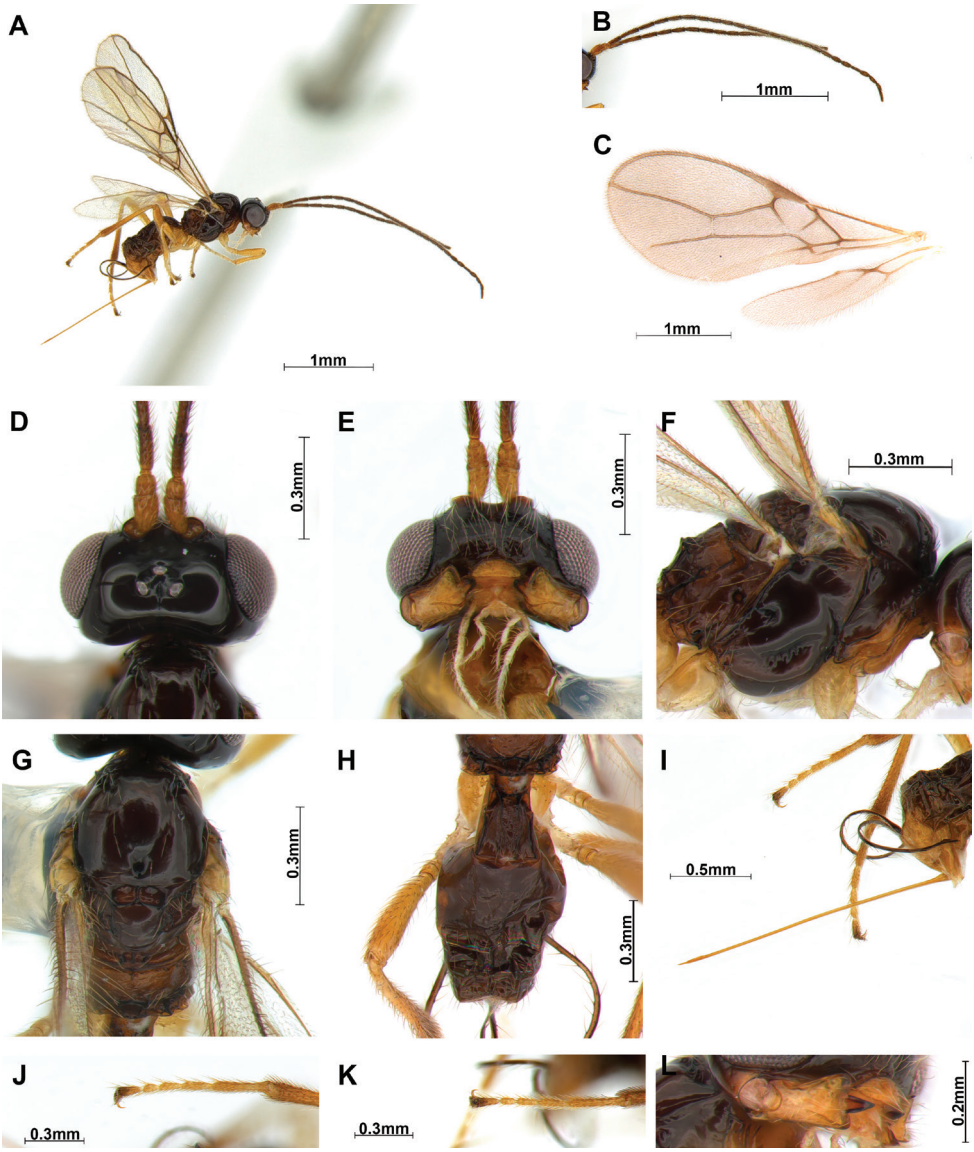

Figure 1. *Phaenocarpa artotemporalis* sp. nov., ♀ **A** body **B** antennae **C** wings **D** head, dorsal **E** head, anterior **F** mesosoma, lateral **G** mesosoma, dorsal **H** propodeum and metasoma, dorsal **I** ovipositor and its sheaths, lateral **J** tarsus, lateral **K** tarsus, dorsal **L** mandible, lateral.

height from ventral rim of antennal sockets to upper margin of clypeus; face with long setae. Eye in dorsal view 4.2 times as long as temple. Ocello-ocular line (OOL) 3.4 times longer than diameter of anterior ocellus; OOL:antero-posterior ocellar line (AOL):postero-ocellar line (POL)= 15:4:6. Stemmaticum concave. Vertex smooth and polish with fine groove. Mandible with three teeth (Fig. 1L); second tooth narrow and sharp with dark brown tip and separated from first tooth by incision. Labrum 2.5 times longer than wide. Maxillary palp 0.7 times longer than mesosoma.

Mesosoma. Mesosoma 1.9 times longer than wide in dorsal view. Mesosoma (Fig. 1G) with medio-posterior depression; notauli reduced posteriorly; scutellar sulcus with two carinae; small basal bump on hind coxa. Propodeum (Fig. 1H) entirely smooth, propodeal areola with bumpy sculpture; precoxal sulcus (Fig. 1F) distinct, with about five crenulae. Fore wing (Fig. 1C) 2.3 times as long as wide; pterostigma long and narrow, 4.4 times longer than wide; vein r of fore wing 2.0 times longer than wide; vein 1-SR+M slightly bent; 2-SR+M sclerotized; 1-SR+M:2-SR+M = 10:4; vein 2-SR:vein r:vein 3-SR = 12:3:24; first subdiscal cell of fore wing ca 0.9 times longer than wide.

Leg. Hind coxa compressed, grooved and 1.4 times longer than hind trochanter; hind femur 0.8 times longer than hind tibia; hind tibia 1.2 times longer than hind tarsus.

Metasoma. First tergite widened posteriorly, striate, and 1.8 times longer than its apical width; T1:T2 = 32:36. Setose part of ovipositor sheath (Fig. 1I) 1.4 times longer than mesosoma, 1.3 times as long as hind tibia and with long setae.

Male. Unknown.

Distribution. South Korea.

Etymology. From "artus/arctus" (Latin for narrow) and "tempus" (Latin for area behind eyes) because of the enlarged temples.

Phaenocarpa brachyura **Sohn & van Achterberg, sp. nov.**
http://zoobank.org/5E43A497-EC93-4868-AF70-09603EE830F7
Figure 2A–L

Type material. ***Holotype,*** ♀ (KNA), **South Korea,** DMZ Botanical Garden, Mandae-ri, Haean-myeon, Yanggu-gun, Gangwon-do, 38°15'09.3"N, 128°06'40.6"E, 21.VIII–05.IX.2017, Shin, Kim. GenBank accession no. MZ318087 for the barcoding sequence of the COI region

Comparative diagnosis. Runs to the East Palaearctic *P. basarukini* Belokobylskij, 1998 and to the West Palaearctic *P. curticauda* van Achterberg, 1998 because of the short ovipositor sheath (approx. 0.7 times as long as hind tibia). The new species differs from *P. basarukini* by the slightly longer ovipositor sheath (0.5–0.6 times as long as hind tibia in *P. basarukini*), first mandibular tooth distinctly lobe-shaped and middle tooth slenderer, pterostigma and hind femur wider. Differs from *P. curticauda* by the wider pterostigma, longer 1r-m of hind wing and 1-CU1 of fore wing, second tooth less widened dorsally, complete notauli, first tergite 1.4 times longer than its apical width and areola of propodeum wider.

Colour. Head black, around eye brown; antenna yellowish brown; mandible brown and apically dark brown. First tergite dark brown and mesonotum entirely black.

Head. Head (Fig. 2D) width 1.6 times median length in dorsal view. Antenna (Fig. 2B) twice as long as body, 41 segmented. Fourth segment 1.4 times longer than third segment and 1.2 times longer than fifth segment. Eye slightly oval, 1.2 times as long as wide in lateral view. Width of face (Fig. 2E) 1.6 times its height from ventral rim of antennal sockets to upper margin of clypeus; face with long setae. Eye in dorsal view 2.4 times as long as temple. Ocello-ocular line 3.0 times longer than diameter

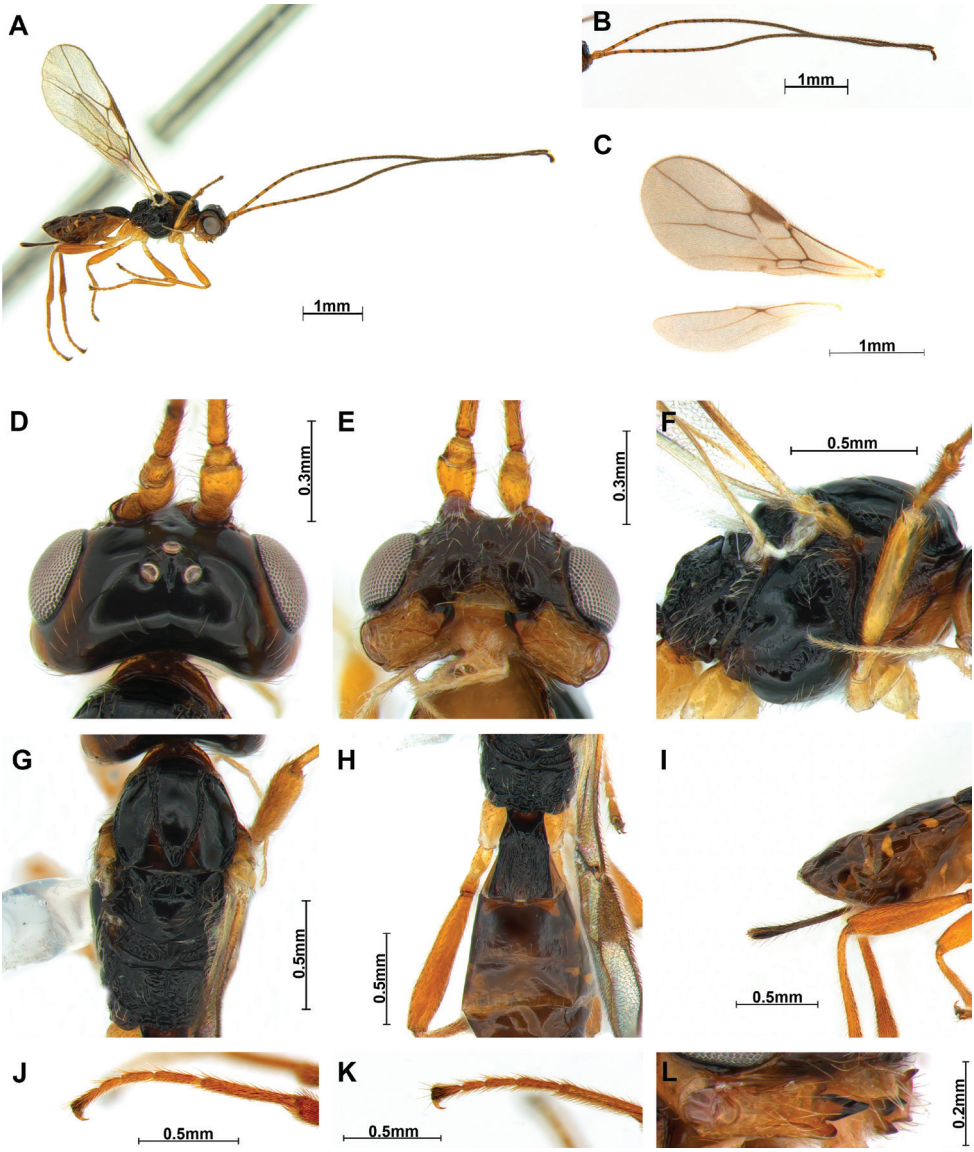

Figure 2. *Phaenocarpa brachyura* sp. nov., ♀ **A** body **B** antennae **C** wings **D** head, dorsal **E** head, anterior **F** mesosoma, lateral **G** mesosoma, dorsal **H** propodeum and T1 to T3, dorsal **I** ovipositor and its sheaths, lateral **J** tarsus, lateral **K** tarsus, dorsal **L** mandible, lateral.

of anterior ocellus; OOL:AOL:POL = 21:5:7. Stemmaticum concave. Mandible with three teeth (2L), subparallel-sided, first mandibular tooth distinctly lobe-shaped and separated from second tooth by incision. Labrum 2.9 times longer than wide. Maxillary palp 0.4 times longer than mesosoma.

Mesosoma. Mesosoma (Fig. 2G) 2.1 times longer than wide in dorsal view. Notauli crenulated, reaching medio-posterior depression; scutellar sulcus with two cari-

nae; in lateral view, mesopleuron and metapleuron with long setae. Anterior half of propodeum smooth, posterior of median carina strongly wrinkled (Fig. 2H), lateral view of propodeum not curved dorsally; precoxal sulcus (Fig. 2F) shallow and with 10 crenulae. Fore wing (Fig. 2C) 2.3 times longer than wide; pterostigma long and narrow, 2.9 times longer than wide; vein r of fore wing 1.9 times longer than wide; vein 2-SR slightly bent; vein 2-SR+M and r-m not sclerotized; vein 2-SR:vein r:vein 3-SR = 10:2:18; first subdiscal cell of fore wing ca 0.6 times longer than wide.

Leg. Hind coxa compressed, grooved and 1.3 times longer than hind trochanter; hind femur 0.7 times longer than hind tibia; hind tibia 0.8 times longer than hind tarsus.

Metasoma. First tergite widened posteriorly, striate and narrow, 1.4 times longer than its apical width; T1:T2 = 48:37. Setose part of ovipositor sheath (Fig. 2I) 0.6 times as long as mesosoma, 0.7 times as long as hind tibia and with setae.

Male. Unknown.

Distribution. South Korea.

Etymology. From "brachys" (Greek for short) and "oura" (Greek for tail) because of the comparatively short ovipositor sheath.

Phaenocarpa lobata **Sohn & van Achterberg, sp. nov.**
http://zoobank.org/39495B6E-B87D-4947-99BF-1B8C768A8320
Figure 3A–L

Type material. ***Holotype*****,** ♀ (KNA), **South Korea,** DMZ Botanical Garden, Mandae-ri, Haean-myeon, Yanggu-gun, Gangwon-do, 38°15'09.3"N, 128°06'40.6"E, 19.IX–10.X.2017, Shin, Kim. GenBank accession no. MZ318085 for the barcoding sequence of the COI region.

Comparative diagnosis. Differs from other species treated in this paper by the long pterostigma of the fore wing (approx. 5.5 times as long as wide; 2.9–4.4 times in other species). The orange antenna and the yellow and robust third and fourth antennal segments distinguish it from other *Phaenocarpa* species. Closely related to *P. masha* Belokobylskij, 1998, for differences see key above.

Description. ***Holotype***, ♀; length of body in lateral view 3.3 mm (Fig. 3A), length of antenna 6.1 mm and length of fore wing 3.6 mm.

Colour. Head (Fig. 3D) black; antenna orange (third and fourth antennal segments yellow); mandible orange brown. First tergite dark brown and mesonotum entirely reddish brown, area around of medio-posterior depression orangish brown.

Head. Width 1.9 times median length in dorsal view. Antenna (Fig. 3B) twice as long as body, 39 segmented. Fourth segment 1.5 times longer than third segment and 1.3 times longer than fifth; third and fourth segments robust. Eye slightly oval, 1.3 times as long as wide in lateral view. Width of face (Fig. 3E) 1.6 times its height from ventral rim of antennal sockets to upper margin of clypeus. Eye in dorsal view 2.6 times as long as temple. Ocello-ocular line 4.1 times longer than diameter of anterior ocellus;

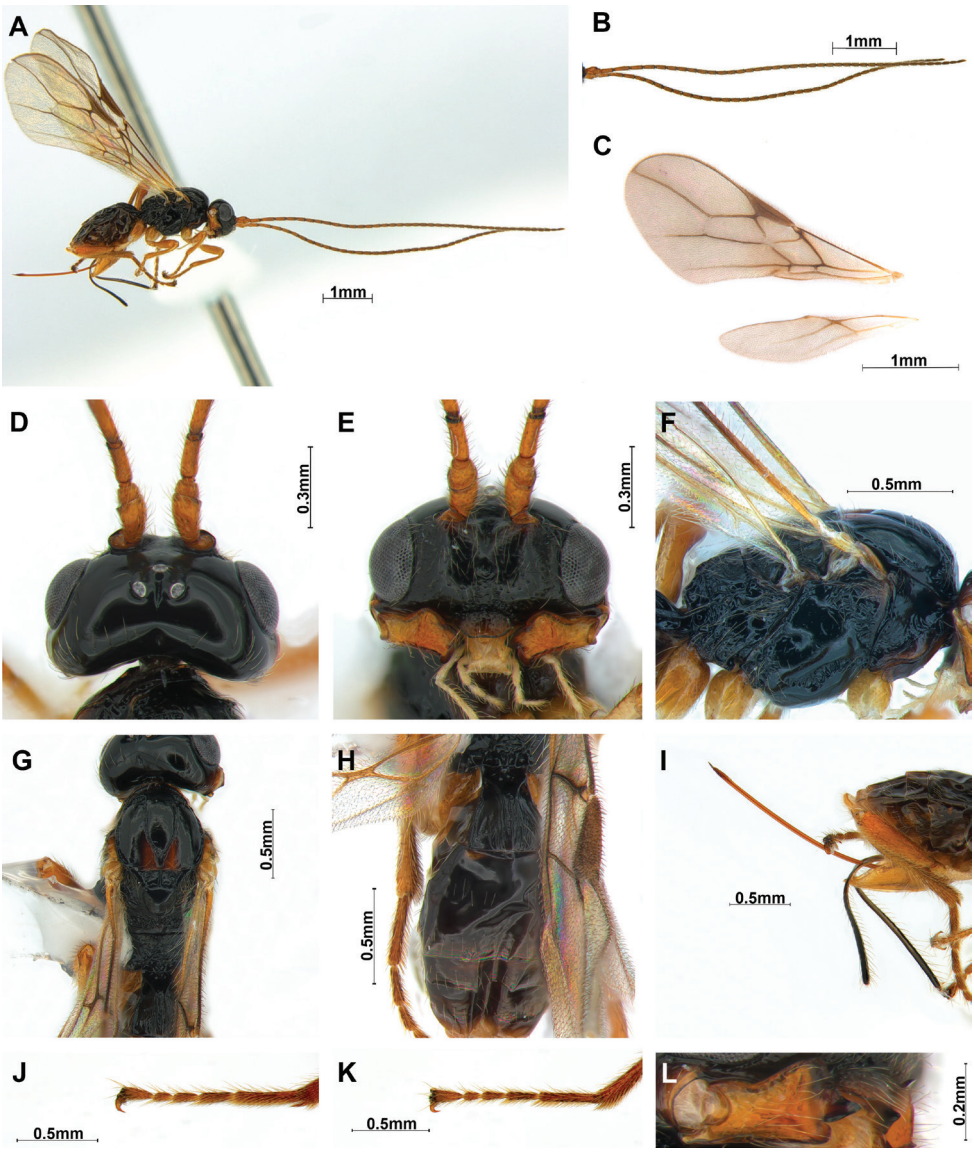

Figure 3. *Phaenocarpa lobata* sp. nov., ♀ **A** body **B** antennae **C** wings **D** head, dorsal **E** head, anterior **F** mesosoma, lateral **G** mesosoma, dorsal **H** propodeum and metasoma, dorsal **I** ovipositor and its sheaths, lateral **J** tarsus, lateral **K** tarsus, dorsal **L** mandible, lateral.

OOL:AOL:POL = 25:6:9. Stemmaticum concave. Vertex smooth, glossy. Mandible with three teeth and first tooth separated from second tooth by incision (Fig. 3L); middle tooth of mandible widened dorsally, with black tip. Labrum 2.0 times longer than wide. Maxillary palp 0.8 times longer than mesosoma.

Mesosoma. Mesosoma (Fig. 3G) 1.8 times longer than wide in dorsal view. Notauli comparatively coarsely crenulate near middle of mesoscutum and reaching

medio-posterior depression; medio-posterior depression nearly reaching transscutal articulation; scutellar sulcus with two carinae; metanotum obtuse dorsally in lateral view; small bump on hind coxa adjacent to metapleuron; in lateral view metapleuron with distinct setae. Anterior half of propodeum less sloping; propodeum bent in lateral view; precoxal sulcus (Fig. 3F) deep and distinct, with about eight crenulae. Fore wing (Fig. 3C) 2.4 times as long as wide; pterostigma long and narrow, 5.5 times longer than wide; vein r of fore wing 1.5 times longer than wide; vein 2-SR slightly bent; vein r-m not sclerotized; vein 2-SR:vein r:vein 3-SR = 11:2:16; first subdiscal cell of fore wing ca 0.9 times longer than wide.

Leg. Hind coxa compressed, grooved and 1.2 times longer than hind trochanter; hind femur 0.6 times longer than hind tibia; hind tibia 1.2 times longer than hind tarsus; tarsal claws robust.

Metasoma. First tergite very robust, 1.2 times longer than its apical width; T1:T2 = 44:54. Setose part of ovipositor sheath (Fig. 3I) 1.2 times longer than mesosoma, as long as hind tibia and with long setae (Fig. 3I).

Male. Unknown.

Distribution. South Korea.

Etymology. From "lobus" (Latin for lobe), because of the lobe-shaped third mandibular tooth.

Phaenocarpa fidelis **Fischer, 1970**
Figure 4A–L

Examined material. 1♀ (KNA), **South Korea**, DMZ Botanical Garden, Mandae-ri, Haean-myeon, Yanggu-gun, Gangwon-do, 38°15'09.3"N, 128°06'40.6"E, 20.VI.–4.VII.2017, H.T. Shin, S.J. Kim. GenBank accession no. MZ318083 for the barcoding sequence of the COI region.

Description. ♀; length of body in lateral view 2.9 mm (Fig. 4A), length of antenna 4.7 mm, length of fore wing 3.1 mm.

Colour. Head (Fig. 4D) entirely black; mandible yellowish brown. Antenna entirely brown (first and second segments orangish brown). First tergite dark brown.

Head. Width 1.9 times median length in dorsal view. Antenna (Fig. 4B) 1.6 times longer than body, 28 segmented. Fourth segment 1.6 times longer than third segment, 1.1 times longer than fifth. Eye slightly oval, 1.2 times longer than wide in lateral view. Width of face (Fig. 4E) 1.3 times its height from ventral rim of antennal sockets to upper margin of clypeus. Face with dense setae. Eye in dorsal view 2.6 times longer than temple. Ocello-ocular line 2.6 times longer than diameter of anterior ocellus; OOL:AOL:POL = 17:5:7. Stemmaticum concave. Mandible robust with three teeth (Fig. 4L) and first tooth gradually connected to second tooth, forming a straight or arcuate connection. Labrum 1.8 times longer than wide. Maxillary palp 0.7 times longer than mesosoma.

Mesosoma. Mesosoma (Fig. 4G) 2.3 times longer than wide in dorsal view, with medio-posterior depression and setae near it; notauli narrowly crenulate near middle

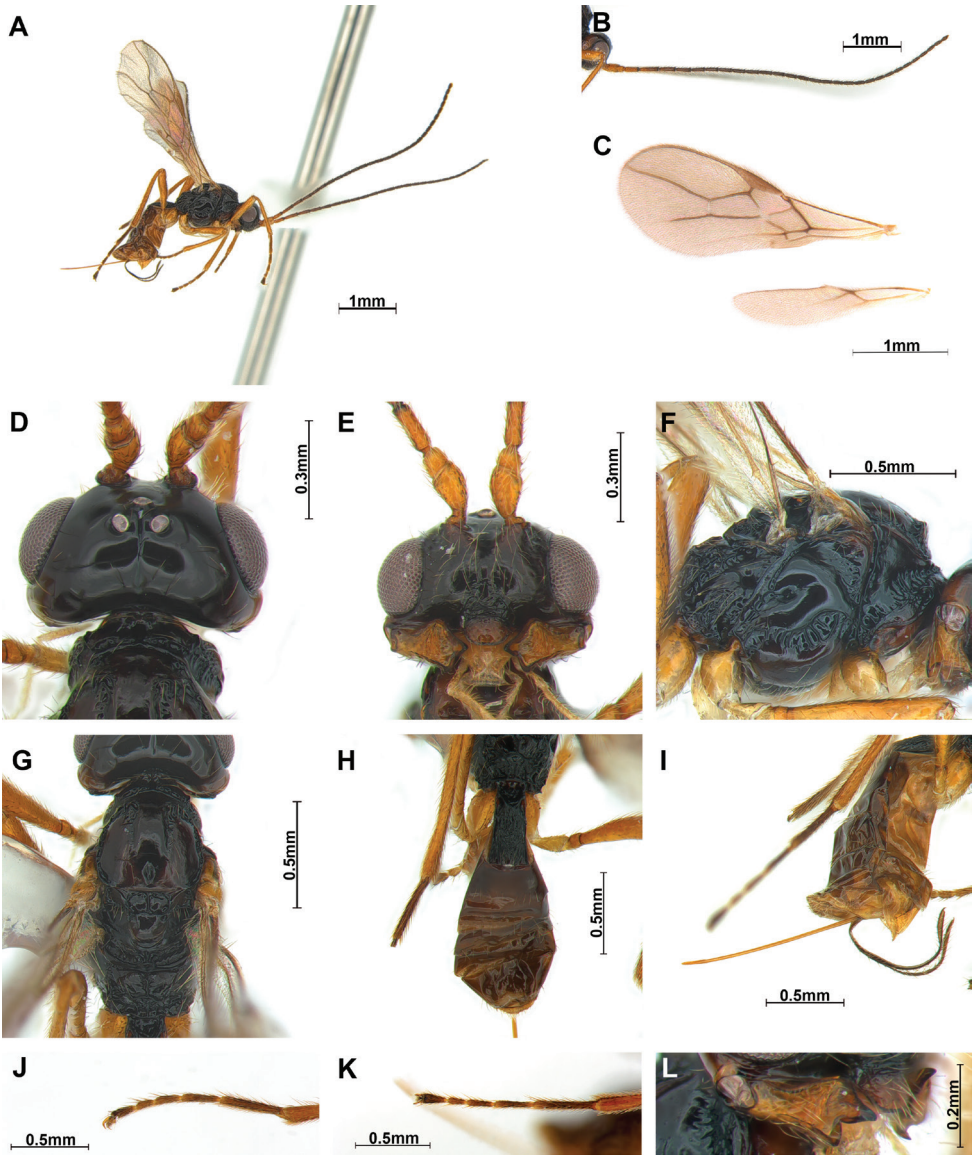

Figure 4. *Phaenocarpa fidelis* Fischer, 1970, ♀ **A** body **B** antenna **C** wings **D** head, dorsal **E** head, anterior **F** mesosoma, lateral **G** mesosoma, dorsal **H** propodeum and metasoma, dorsal **I** metasoma, ovipositor and its sheaths, lateral **J** tarsus, lateral **K** tarsus, dorsal **L** mandible, lateral.

of mesoscutum, not reaching medio-posterior depression; scutellar sulcus with two carinae, 2.4 times wider than long medially; metanotum sculptured; with small bump on hind coxa adjacent to metapleuron; metapleuron with long setae; in lateral view mesoscutum with anterior bump. Propodeum (Fig. 4H) extensively rugose medially and in lateral view not bent; precoxal sulcus (Fig. 4F) complete and with 12 crenulae;

scutellum with setae partially. Fore wing (Fig. 4C) 2.4 times longer than wide; pterostigma long and narrow, 4.3 times longer than wide; vein r of fore wing 2.3 times longer than wide; vein 2-SR slightly bent; vein r-m not sclerotized; vein 2-SR:vein r:vein 3-SR = 9:2:15; first subdiscal cell of fore wing ca 1.1 times longer than wide; second submarginal cell robust.

Leg. Hind coxa compressed, grooved and 1.1 times longer than hind trochanter; hind femur 0.7 times longer than hind tibia; hind tibia 0.9 times longer than hind tarsus.

Metasoma. First metasomal tergite subparallel-sided (Fig. 4H), 2.0 times longer than apical width; T1:T2 = 50:24. Setose part of ovipositor sheath (Fig. 4I) 0.5 times as long as mesosoma, 0.4 times as long as hind tibia and with long setae.

Male. Unknown.

Distribution. Eastern Palaearctic, Western Palaearctic, Europe; South Korea (new record).

Phaenocarpa masha Belokobylskij, 1998

Figure 5A–L

Examined material. 1♀ (KNA), **South Korea**, DMZ Botanical Garden, Mandae-ri, Haean-myeon, Yanggu-gun, Gangwon-do, 38°15'09.3"N, 128°06'40.6"E, 20.VI.–4.VII.2017, H.T. Shin, S.J. Kim. GenBank accession no. MW376066 for the barcoding sequence of the COI region.

Description. ♀; length of body in lateral view 2.8 mm (Fig. 5A), length of antenna 4.7 mm and length of fore wing 3.3 mm.

Colour. Head (Fig. 5D) entirely black; mandible orangish brown. Antenna entirely brown (third and fourth segments dark brown). First tergite reddish brown and mesonotum orangish brown.

Head. Width 1.7 times median length in dorsal view. Antenna (Fig. 5B) 1.6 times longer than body, 27-segmented. Fourth segment 1.6 times longer than third segment and 1.2 times longer than fifth, third and fourth segments dark brown and slender. Eye slightly oval, 1.2 times as long as wide in lateral view. Width of face (Fig. 5E) 1.5 times its height from ventral rim of antennal sockets to upper margin of clypeus. Face with dense setae. Eye in dorsal view 3.0 times as long as temple. Ocello-ocular line 4.1 times longer than diameter of anterior ocellus; OOL:AOL:POL = 21:5:7. Stemmaticum concave. Mandible with three teeth (Fig. 5L) and first tooth separated from second tooth by incision; third tooth bent outside, middle tooth not widened dorsally. Labrum 2.4 times longer than wide. Maxillary palp 0.9 times longer than mesosoma.

Mesosoma. Mesosoma (Fig. 5G) 1.9 times longer than wide in dorsal view, with medio-posterior depression and setae near it; notauli line-shape, reaching medio-posterior depression; scutellar sulcus with two carinae; metanotum more or less tooth-shaped protruding dorsally in lateral view; small bump on hind coxa adjacent to

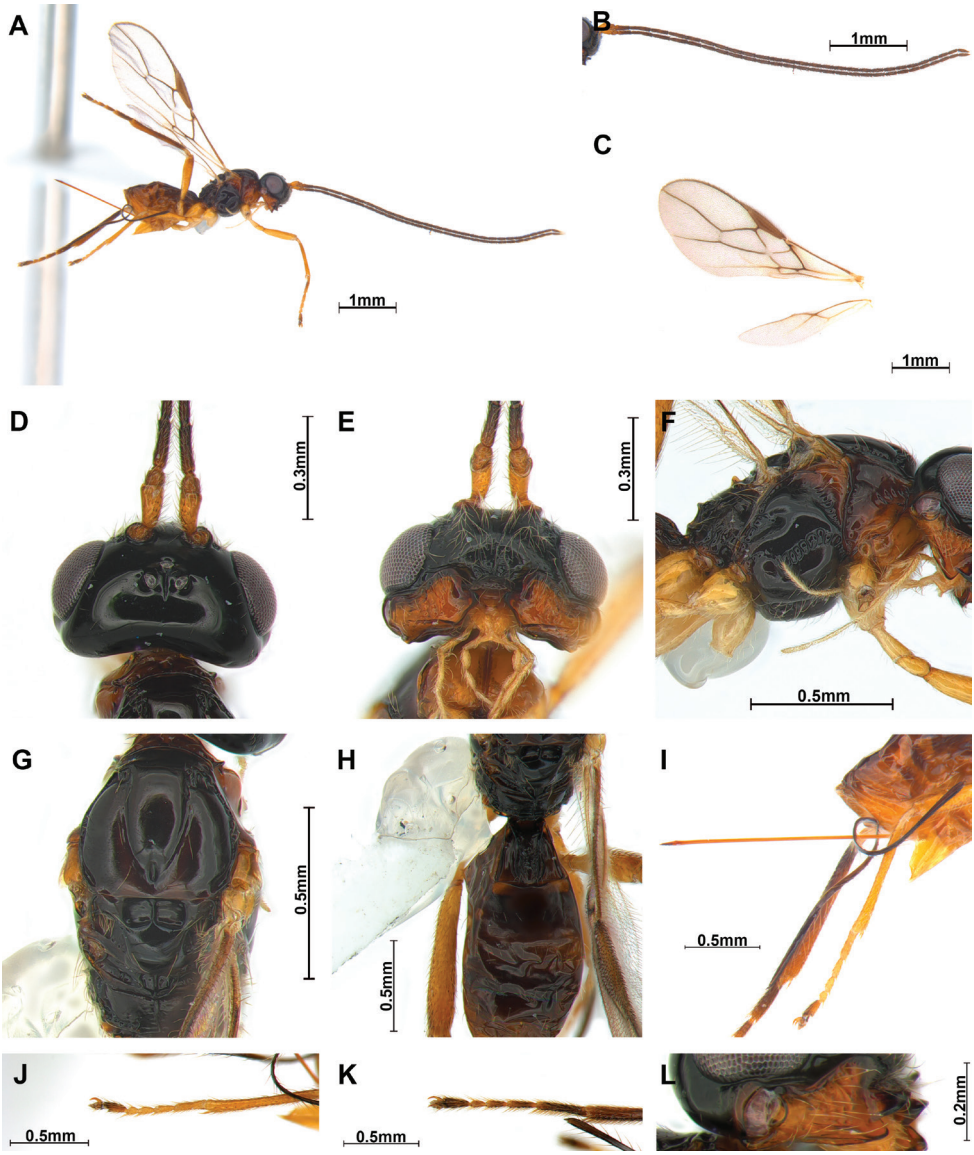

Figure 5. *Phaenocarpa masha* Belokobylskij, 1998, ♀ **A** body **B** antennae **C** wings **D** head, dorsal **E** head, anterior **F** mesosoma, lateral **G** mesosoma, dorsal **H** propodeum and T1 to T3, dorsal **I** metasoma, ovipositor and its sheaths, lateral **J** tarsus, lateral **K** tarsus, dorsal **L** mandible, lateral.

metapleuron. Propodeum (Fig. 5H) 0.7 times longer than width, more extensively rugose medially; lateral view of propodeum not bent; precoxal sulcus (Fig. 5F) completed with 11 crenulae; scutellum with setae partially. Fore wing (Fig. 5C) 2.5 times as long as wide; pterostigma long and narrow, 4.2 times longer than wide; vein r of fore wing 3.0 times longer than wide; vein r-m not sclerotized; vein 2-SR:vein r:vein 3-SR = 10:2:14; first subdiscal cell of fore wing ca 0.7 times longer than wide; second submarginal cell robust.

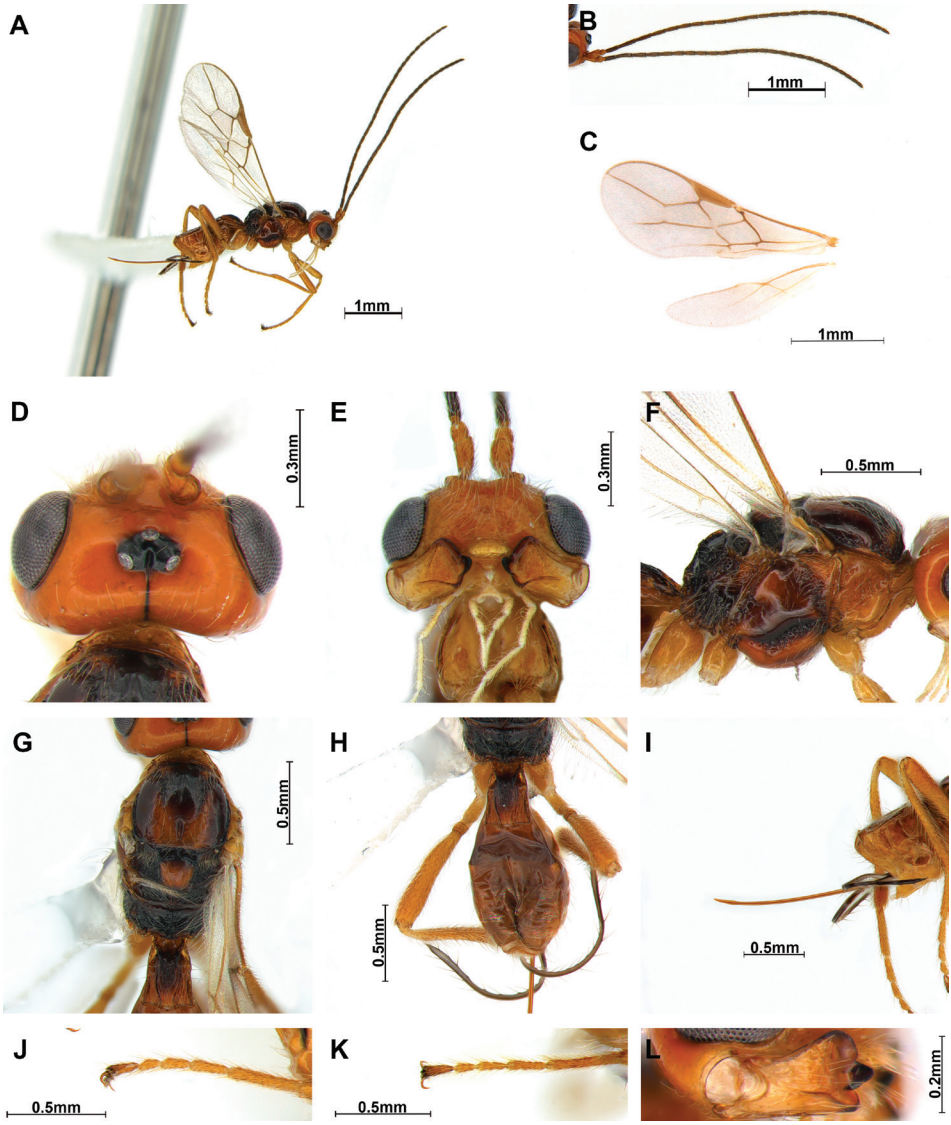

Figure 6. *Phaenocarpa ruficeps* (Nees, 1812), ♀ **A** body **B** antennae **C** wings **D** head, dorsal **E** head, anterior **F** mesosoma, lateral **G** mesosoma, dorsal **H** propodeum and metasoma, dorsal **I** metasoma,ovipositor and its sheaths, lateral **J** tarsus, lateral **K** tarsus, dorsal **L** mandible, lateral.

Leg. Hind coxa compressed, grooved and 1.4 times longer than hind trochanter; hind femur 0.6 times longer than hind tibia; hind tibia 1.2 times longer than hind tarsus; tarsal claws slender.

Metasoma. First tergite robust, widened posteriorly, 1.2 times longer than apical width; T1:T2 = 32:30. Setose part of ovipositor sheath (Fig. 5I) 1.2 times longer than mesosoma, 1.1 times longer than hind tibia and with long setae.

Male. Unknown.

Distribution. Eastern Palaearctic; South Korea (new record).

Acknowledgements

This work was supported by the Korean National Arboretum (KNA1-1-20) and a grant from the National Institute of Biological Resources (NIBR), funded by the Ministry of Environment (MOE) of the Republic of Korea (NIBR202130203). This work was supported by a grant from the National Institute of Biological Resources (NIBR), funded by the Ministry of Environment (MOE) of the Republic of Korea (NIBR202102204).

References

Ashmead WH (1900) Classification of the Ichneumon flies, or the superfamily Ichneumonoidea. Proceedings of the United States National Museum 23(1206): 1–220. https://doi.org/10.5479/si.00963801.23-1206.1

Abd-Rabou S (2006) Biological control of the leafminer, *Liriomyza trifolii* by introduction, releasing, evaluation of the parasitoids *Diglyphus isaea* and *Dacnusa sibirica* on vegetables crops in greenhouses in Egypt. Archives of Phytopathology and Plant Protection 39: 439–443. https://doi.org/10.1080/03235400500356079

Belokobylskij SA (1998) Tribe Alysiini. In: Ler PA (Ed.) Key to the Insects of Russian Far East. Dal'nauka, Vladivostok, 163–298. [In Russian]

Cameron P (1910) On some Asiatic species of the Braconid subfamilies Rhogadinae, Agathinae, and Macrocentrinae and of the Alysiidae. Wiener Entomologische Zeitschrift 29: 1–10. https://doi.org/10.5962/bhl.part.23337

Chen JH, Wu ZS (1994) The Alysiini of China: (Hymenoptera: Braconidae: Alysiinae). China Agricultural Press, Fuzhou, 218 pp. [In Chinese, with summary in English]

Favret C (2005) New non-destructive DNA extraction and specimen clearing technique for aphids (Hemiptera). Proceedings of the Entomological Society of Washington 107: 469–470.

Fischer M (1970) Zur Kenntnis der europäischen *Phaenocarpa*-Arten mit besonderer Berücksichtigung der Fauna Niederösterreichs (Hymenoptera, Braconidae, Alysiinae). Zeitschrift für Angewandte Zoologie 57: 409–498.

Foerster A (1863) Synopsis der Familien und Gattungen der Braconiden. Verhandlungen des Naturhistorischen Vereins der Preussischen Rheinlande und Westfalens 19: 225–288.

Haliday AH (1838) Essay on parasitic Hymenoptera. Entomological Magazine 5(3): 209–249.

Kumar S, Stecher G, Tamura K (2016) MEGA7: Molecular Evolutionary Genetics Analysis version 7.0 for bigger datasets. Molecular, Biology and Evolution. 33: 1870–1874. https://doi.org/10.1093/molbev/msw054

NIBR (2019) National List of Species of Korea. National Institute of Biological Resources. http://kbr.go.kr [accessed on 11/08/08]

Papp J (1968) A survey of the *Phaenocarpa* Foerster species of the Carpathian Basin, Central Europe (Hymenoptera, Braconidae: Alysiinae). Beiträge zur Entomologie 18(5/6): 569–603.

Papp J (1994) Braconidae (Hymenoptera) from Korea, XV. Acta Zoologica Academiae Scientiarum Hungaricae 40(2): 133–156.

Provancher L (1886) Additions et corrections au Volume II de la Faune Entomologique du Canada. Traitant des Hyménoptères. Québec, 475 pp.

Shenefelt RD (1974) Braconidae 7. Alysiinae. Hymenopterorum Catalogus. Pars 11: 985–1113.

Shaw MR, Huddleston T (1991) Classification and biology of Braconid wasps (Hymenoptera: Braconidae). Handbooks for the identification of British Insects 7(11): 1–126.

Stelfox AW (1941) Descriptions of five new species of Alysiidae (Hymenoptera) and notes on some others. Proceedings of the Royal Irish Academy 47(B): 1–16.

van Achterberg C (1993) Illustrated key to the subfamilies of the Braconidae (Hymenoptera: Ichneumonoidea). Zoologische Verhandelingen Leiden 283: 1–189.

van Achterberg C (1998) *Bobekoides* gen. n. (Hymenoptera: Braconidae: Alysiinae) from South Africa. Zoologische Mededelingen, Leiden 72(9): 105–111.

van Achterberg C (2009) A new species of the genus *Phaenocarpa* Foerster from Madagascar (Hymenoptera: Braconidae: Alysiinae). Zoologische Mededelingen, Leiden 83(3): 667–671.

Wharton RA (1980) Review of the Nearctic Alysiini (Hymenoptera, Braconidae): with discussion of generic relationships within the tribe. University of California Press, Berkeley, 112 pp.

Wharton RA (1984) Biology of the Alysiini (Hymenoptera: Braconidae), parasitoids of cyclorrhaphous Diptera. Texas Agricultural Experimental Station. Technical Monograph 11: 1–39.

Wharton RA, Marsh P, Sharkey M (1997) Manual of the New World Genera of the Family Braconidae (Hymenoptera). The International Society of Hymenopterists, Washington DC, 439 pp.

Wharton RA (2002) Revision of the Australian Alysiini (Hymenoptera:Braconidae). Invertebrate Systematics 16: 7–105. https://doi.org/10.1071/IT01012

Yaakop S, van Achterberg C, Idris AB (2009) Heratemis Walker (Hymenoptera: Braconidae: Alysiinae: Alysiini): revision and reconstruction of the phylogeny combining molecular data and morphology. Tijdschrift voor Entomologie 152: 1–64. https://doi.org/10.1163/22119434-900000268

Yu DSK, van Achterberg C, Horstmann K (2016) Taxapad 2016, Ichneumonoidea 2015. Database on flash-drive, Nepean, Ontario. www.taxapad.com

Zhu J-C, van Achterberg C, Chen X-X (2017) An illustrated key to the genera and subgenera of the Alysiini (Hymenoptera, Braconidae, Alysiinae), with three genera new for China. ZooKeys 722: 37–79. https://doi.org/10.3897/zookeys.722.14799

JHR 86: 19–45 (2021)
doi: 10.3897/jhr.86.71225
https://jhr.pensoft.net

RESEARCH ARTICLE

JOURNAL OF Hymenoptera RESEARCH
A peer-reviewed open-access journal
The International Society of Hymenopterists

Stars in subtropical Japan: a new gregarious *Meteorus* species (Hymenoptera, Braconidae, Euphorinae) constructs enigmatic star-shaped pendulous communal cocoons

Shunpei Fujie[1], So Shimizu[2,3], Koichi Tone[4], Kazunori Matsuo[5], Kaoru Maeto[2]

1 *Osaka Museum of Natural History, Nagaikoen 1–23, Higashisumiyoshi, Osaka 546–0034, Japan* **2** *Laboratory of Insect Biodiversity and Ecosystem Science, Graduate School of Agricultural Science, Kobe University, Rokkodaicho 1–1, Nada, Kobe, Hyogo 657–8501, Japan* **3** *Research Fellow (DC1), Japan Society for the Promotion of Science, Tokyo, Japan* **4** *Okinawa Municipal Museum, Uechi 2–19–6, Okinawa 904–0031, Japan* **5** *Faculty of Social and Cultural Studies, Kyushu University, Motooka 744, Nishi, Fukuoka 819–0395, Japan*

Corresponding author: Shunpei Fujie (shunpei.fujie@gmail.com)

Academic editor: Jose Fernandez-Triana | Received 20 July 2021 | Accepted 3 October 2021 | Published 29 October 2021

http://zoobank.org/4C11898D-A5A4-44BD-89C2-D049E6B991B4

Citation: Fujie S, Shimizu S, Tone K, Matsuo K, Maeto K (2021) Stars in subtropical Japan: a new gregarious *Meteorus* species (Hymenoptera, Braconidae, Euphorinae) constructs enigmatic star-shaped pendulous communal cocoons. Journal of Hymenoptera Research 86: 19–45. https://doi.org/10.3897/jhr.86.71225

Abstract

A new gregarious braconid parasitoid wasp of Euphorinae, *Meteorus stellatus* Fujie, Shimizu & Maeto **sp. nov.**, is described from the Ryukyu Islands in Japan, based on an integrative taxonomic framework. The phylogenetic position of the new species within the Meteorini was analyzed based on DNA fragments of the mitochondrial cytochrome c oxidase 1 (CO1) and the nuclear 28S rDNA genes. The new species was recovered as a member of the *versicolor* complex of the *versicolor* + *rubens* subclade within the *pulchricornis* clade. The new species is a gregarious parasitoid of two *Macroglossum* species (Lepidoptera: Sphingidae) and constructs single or several unique star-shaped cocoon masses separately suspended by very long threads. The evolution of gregariousness and spherical cocoon masses is discussed.

Keywords

Endoparasitoid, female-biased sex ratio, integrative taxonomy, Lepidoptera, *Macroglossum*, phylogeny, species delimitation, Sphingidae

Copyright *Shunpei Fujie et al.* This is an open access article distributed under the terms of the Creative Commons Attribution License (CC BY 4.0), which permits unrestricted use, distribution, and reproduction in any medium, provided the original author and source are credited.

Introduction

The pupae of parasitoid wasps cannot actively escape various risks, such as predation, parasitism, pathogenesis, and environmental stresses. Therefore, cocoons and mummies play important roles in protecting soft and exarate pupae from such risks (Gauld and Bolton 1988; Shaw and Huddleston 1991; Maeto 2018).

Members of Braconidae, one of the most diverse hymenopteran families, form various types of cocoons and mummies to adapt to various natural enemies and environmental threats. Many gregarious braconids produce communal cocoon masses, while discrete cocoons for each individual are also constructed (Shaw and Huddleston 1991). Final-instar braconid larvae emerge from host organisms and then spin a cocoon using silk from the labial glands (e.g., Shaw and Huddleston 1991; Quicke 2015). In some gregarious species, wasp larvae not only spin individual cocoons but also cooperate to construct massive communal cocoons (Zitani and Shaw 2002).

The cosmopolitan braconid genus *Meteorus* Haliday consists of more than 300 valid species (Yu et al. 2016). As the genus *Zele* Curtis is apparently nested within the *Meteorus* species tree, *Meteorus* is a paraphyletic group and its rearrangement into several monophyletic genera is pending (Maeto 1990b; Stigenberg and Ronquist 2011). Maeto (1990b) has divided the *Meteorus* species into seven morphologically and biologically defined species groups, while monophyly has been supported partially (Stigenberg and Ronquist 2011).

Meteorus species are solitary or gregarious koinobiont endoparasitoids of Lepidoptera or Coleoptera larvae (Huddleston 1980; Stigenberg and Ronquist 2011; Maeto 2018). Their cocoons are either suspended (pendulous) or not, and the cocoon suspension is one of diagnostic characters to identify the *pulchricornis* group (Maeto 1989a). The gregarious species construct either independent (e.g., *M. acerbiavorus* Belokobylskij, Stigenberg & Vikberg, *M. heliophilus* Fischer, and *M. rubens* Nees) or communal cocoons (e.g., *M. congregatus* Muesebeck, *M. komensis* Wilkinson, *M. kurokoi* Maeto, and *M. townsendi* Muesebeck) (Maeto 1989b; Zitani and Shaw 2002; Zitani 2003; Stigenberg et al. 2011). The latest molecular phylogeny has suggested that the gregariousness is a derived character in the *pulchricornis* + *rubens* group complex (Stibenberg and Ronquist 2011). So far, six types of cocoon architectures have been observed in the gregarious species of *Meteorus*, as is shown in Table 1. However, the evolution of gregariousness and cocoon architectures within the genus *Meteorus* has been poorly studied, and more bionomical and phylogenetic information is thus needed.

Although the cocoon structure of *Meteorus* is quite mysterious, larval behavior associated with cocoon formation has received little attention, with only a few reports examining it (Askari et al. 1977; Zitani and Shaw 2002; Maeto 2018). Recently, unique star-shaped cocoon masses of an undescribed gregarious species of *Meteorus* have been observed in subtropical Japan (Mitamura 2013). Therefore, this study aims to describe that gregarious species of *Meteorus* based on integrative morphological and molecular evidence and observe its cocoon-mass formation behavior. The phylogenetic position of the new species and evolution of gregariousness and cocoon masses are also discussed.

Table 1. The types of cocoon masses in gregarious *Meteorus*.

Types	Characteristics	Species	References
A	loosely clumped within a host pupal chamber	**Palearctic species**	
		M. acerbiavorus	Stigenberg et al. 2011.
		M. heliophilus	Maeto 1990a
		M. rubens	Maeto 1990a
B	individually suspended from host plant by a thread	**Neotropical species**	
		M. oviedoi	Shaw and Nishida 2005
		M. papiliovorus	Zitani and Shaw 2002
C	sparsely arranged and suspended by a common cable	**Palearctic species**	
		M. kurokoi	Maeto 1989b
		Neotropical species	
		M. restionis	Barrantes et al. 2011
D	loosely clumped and suspended by a common cable	**Neotropical species**	
		M. cecavorum	Aguirre and Shaw 2014
		M. juliae	Aguirre and Shaw 2014
E	congregated and directly attached to host plant without a cable	**Neotropical species**	
		M. congregatus	Zitani and Shaw 2002
F	communal and suspended by a common cable	**Afrotropical species**	
		M. komensis	Zitani and Shaw 2002
		Neotropical species	
		M. townsendi	Zitani and Shaw 2002
		undescribed species	Sobczak et al. 2012
		Oriental species	
		M. stellatus sp. nov.	Present study

Materials and methods

Study fields

The field collection of host moth larvae to observe the cocoon formation behavior of emerged larvae of wasps was conducted at Okinawa Municipal Museum, Okinawa City, Okinawa-hontô, Okinawa Prefecture, Japan. Some materials were also collected within Okinawa-hontô (Okinawa Prefecture) and Amami-ôshima (Kagoshima Prefecture), Japan. All materials were from the middle part of the Ryukyu Islands, the subtropical Oriental region in Japan.

Morphological observation and terms

Morphological observation was conducted with a stereoscopic microscope (SMZ800N, Nikon, Tokyo, Japan). Specimens and cocoons were photographed using a Digital Microscope (VHX-1000, Keyence, Osaka, Japan) with a 10–130× lens. Multi-focus photographs were stacked in the software associated with the Keyence System. Multi-focus photographs of cocoon masses were taken using a single lens reflex camera (α7II, Sony, Tokyo, Japan) with a micro-lens (A FE 50 mm F2.8 Macro SEL50M28, Sony). The RAW format photographs were developed using Adobe Lightroom CC v.2.2.1 (Adobe Systems Inc., San Jose, CA, USA), and stacked using Zerene Stacker v.1.04 (Zerene Systems LLC., Richland, WA, USA). The holotype of *M. komensis*, deposited in the Natural History Museum, London, UK was also examined by the second author

using a stereoscopic microscope (SMZ1500, Nikon). Multi-focus photographs were taken using an α7II camera with micro-lenses (LAOWA 25 mm F2.8 2.5–5× ULTRA MACRO, Anhui Changgeng Optics Technology Co., Ltd, Hefei, China). The captured RAW format photographs were developed and stacked as per the aforementioned photo technique used for the cocoon masses. The figures were edited in Microsoft PowerPoint 2019.

The description style mostly follows that of Stigenberg and Ronquist (2011). The morphological terms and measurements follow those of Richards (1977) and van Achterberg (1988). The following abbreviations are used: **OOL** = ocelli-ocular line, **OD** = ocelli diameter of a posterior ocellus, and **POL** = posterior ocellar line.

The abbreviations for repositories are listed below:

CNC Canadian National Collection of Insects, Ottawa, Canada;
ELKU Entomological Laboratory, Faculty of Agriculture, Kyushu University, Fukuoka, Japan;
EMUS Utah State University Insect Collection (= American Entomological Institute: AEI), Department of Biology, Utah State University, Logan, Utah, USA;
EUM Ehime University Museum, Matsuyama, Japan;
KPMNH Kanagawa Prefectural Museum of Natural History, Odawara, Japan;
MNHA Museum of Nature and Human Activities, Sanda, Japan;
NARO Institute for Agro-Environmental Sciences, NARO (= NIAES: National Institute for Agro-Environmental Sciences), Tsukuba, Japan;
NHMUK Natural History Museum, London, United Kingdom (formerly BMNH);
NSMT National Museum of Nature and Science, Tsukuba, Japan;
OMM Okinawa Municipal Museum, Okinawa, Japan;
OMNH Osaka Museum of Natural History, Osaka, Japan;
RUM Ryukyu University Museum, Okinawa, Japan;
SEHU the Laboratory of Systematic Entomology, Faculty of Agriculture, Hokkaido University, Sapporo, Japan;
TARI Taiwan Agricultural Research Institute Council of Agriculture, Executive Yuan, Taichung, Taiwan;
ZISP Zoological Institute, Russian Academy of Sciences, St Petersburg, Russia.

Secondary sex ratio

To investigate the secondary sex ratio of wasps, the number of males and females of all enclosed wasps that emerged from each host larva was counted for 11 host larvae (Suppl. material 1: Table S1). Cocoon masses with hyper-parasitoids were excluded, and the number of dead cocoons was not counted. The effect of the number of total wasps on the proportion of males was analyzed using a generalized linear model (GLM). A logit link function and binomial error distribution were employed. The mean proportion of males was estimated from the average number of total wasps. The analysis was performed in IBM SPSS Statistics for Windows, v. 25.0 (IBM Corp., Armonk, NY, USA).

Observation of cocoon formation behavior

The cocoon formation behavior of wasp larvae was observed at a laboratory of OMM, in June 2019 by the third author. It was recorded with video cameras (Sony Handycam, HDR-CX470 and HDR-XR150, Sony). The suspended larvae were blown with air currents created by breathing, as there was no wind, which would enhance the merging of each individually suspended larva in the laboratory as it would in natural conditions. A single silk thread spun by an individual larva is called a "thread", and intertwined threads are called a "cable" as in Barrantes et al. (2011). A short movie showing the cocoon formation behavior is available on YouTube (https://www.youtube.com/watch?v=AuHarLHolPM).

Molecular analysis

Gene selection

To delimit a species, fragments of a mitochondrial protein encoding gene, cytochrome c oxidase 1 (CO1), were selected, because its evolutionary rate is more or less rapid and it is one of the most common genes used for population to species level phylogenetic analysis (this is well-known as the DNA barcoding gene). To infer the phylogenetic relationships among species of Meteorini (*Meteorus* and *Zele*), CO1 and a nuclear noncoding gene, 28S rRNA (28S), were selected. 28S is a gene that has evolved more slowly than CO1 and is usually used for species-groups or higher-level phylogeny; therefore, the combined CO1 and 28S analysis can provide a higher resolution of species phylogeny.

Taxon sampling and outgroups

A total of 44 species of *Meteorus* including five morphospecies were sampled as ingroups. Five species of *Zele* were also sampled as ingroups because *Zele* is deeply nested within the *Meteorus* tree (Stigenberg and Ronquist 2011). Three species from different tribes of euphorine genera were sampled as outgroups (*Syrrhizus* Förster, *Syntretus* Förster, and *Peristenus* Förster). A total of 177 sequences of CO1 and 172 of 28S were compiled from GenBank. Sequences obtained from databases sometimes contain unreliable information (e.g., Klimov et al. 2019; Shimizu et al. 2020), and an evaluation of such sequences is always strongly recommended to ensure that the analysis is accurate. In the present study, the sequences used by Stigenberg and Ronquist (2011) and several additional sequences were considered as reliable sources. The complete information of the sampled taxa and sequences is available in the Suppl. material 2: Table S2.

DNA extraction, amplification, and sequencing

Table 2. Primer information for PCR.

Target	Primer name	Sequence (5' to 3')	References
CO1	CO1 lco hym	CAA ATC ATA AAG ATA TTG G	Schulmeister (2003)
	CO1 hco extB*	CCT ATT GAW ARA ACA TAR TGA AAA TG	Schulmeister (2003)
28S	28SD1F	ACC CGC TGA ATT TAA GCA TAT	Harry et al. (1997)
	28SD5R*	CCC ACA GCG CCA GTT CTG CTT ACC	Schulmeister (2003)

The newly collected samples from Okinawa were stored in 99.9% ethanol for DNA extraction. DNA was extracted from a right mid or/and hind leg. The protocols followed from PCR to sequencing were according to the work of Shimizu et al. (2020), except for the primers in Table 2, for which the PCR conditions were as follows: CO1: initial denaturation (2'00") at 95 °C, 35 cycles of denaturation (0'30") at 95 °C, annealing (0'30") at 48 °C, an extension (1'00") at 72 °C, and a final extension (10'00") at 72 °C; 28S: 1'00" at 95 °C, 40 cycles of 0'30" at 95 °C, 0'30" at 48 °C, 1'30" at 72 °C, and 5'00" at 72 °C.

Species delimitation

Partial fragments of CO1 were used for species delineation. A total of 189 sequences were used for analysis (Suppl. material 2: Table S2). To obtain an accurate multiple sequence alignment (MSA), MSA was conducted using MEGA v.10.0.5 (Kumar et al. 2018) based on amino acids. First, the codon positions of all nucleotide sequences were adjusted, the nucleotide sequences were translated to amino acids, the amino acid sequences were aligned by CLUSTAL W (Thompson et al. 1994) implemented in MEGA with default settings, the amino acid alignment was checked by eye, and finally the aligned amino acid sequences were retranslated to nucleotides. The final dataset was 657 bp without indels.

To delimit the species, both distance- and topology-based methods were employed as below. Using both methods, three types of datasets were analyzed: (1) *Meteorus* + *Zele* + outgroups, (2) *Meteorus* + *Zele*, and (3) *Meteorus*. Prior to the analysis, identical haplotypes were removed from the datasets on the web server of ALTER (Glez-Peña et al. 2010) (available at: http://sing.ei.uvigo.es/ALTER/).

Distance-based method (ABGD)

The barcoding gap based analysis, Automatic Barcode Gap Discovery (ABGD) (Puillandre et al. 2012), was ran on the graphic web version of ABGD (available at: http://wwwabi.snv.jussieu.fr/public/abgd/abgdweb.html), with the following parameters: Pmin = 0.001, Pmax = 0.1, Steps = 10, X (relative gap width) = 1.0, model = Kimura (K80) (TS / TV = 2.0), and Nb bins (for distance distribution) = 20.

Topology-based method (GMYC)

The General Mixed Yule Coalescent (GMYC) analysis was employed. GMYC analysis requires an ultrametric tree (UTree) as an input. To construct the UTree, the model and parameters was selected on a web server of the smart model selection (SMS) (Lefort et al.

2017) (available at: http://www.atgc-montpellier.fr/phyml-sms/): the GTR+G+I model was selected as the best fit model under the Bayesian information criterion (BIC). The UTree was generated using BEAST v.2.6.3 (Bouckaert et al. 2019), with a random starting tree, the uncorrelated lognormal relaxed clock model, and the coalescent tree prior. A Bayesian Markov chain Monte Carlo (MCMC) was run for 40,000,000 generations, with trees sampled every 5,000 generations, and a burnin of anterior 25%. The convergence of run was assessed using Tracer v.1.6 (Rambaut and Drummond 2007): run reached a stationary distribution and all effective sample sizes (ESS) were greater than 200. A majority-rule consensus ultrametric tree was finally generated using TreeAnnotator v.2.6.3 (Bouckaert et al. 2019). GMYC analysis was run using the GMYC function of the R-package Splits (Fujisawa and Barraclough 2013) (available at: http://r-forge.r-project.org/projects/splits/) using R v.3.6.3 (R Core Development Team 2020).

Phylogenetic analysis

The phylogeny of Meteorini species was inferred with both the Bayesian Inference (BI) and maximum likelihood (ML) approaches using a concatenated CO1 and 28S fragments.

MSA

Although the MSA of CO1 was already performed in the species delimitation, MSA for 28S was conducted in the MAFFT online service (Katoh et al. 2019), using the Q-INS-i algorithm, which is the structural alignment method for RNA (Katoh and Toh 2008; Katoh and Standley 2013). Ambiguously aligned regions were automatically removed from the dataset using trimAl v.1.2 (Capella-Gutíerrez et al. 2009), with default parameters. The final datasets were 657 (CO1) and 560 (28S) bp in length: the concatenated CO1 and 28S dataset was 1,217 bp.

Terminal species selection

In order to exclude the taxon sampling bias, a single sequence for each species was selected based on the conservative results of the species delimitation analysis by ABGD: sequences of 61 *Meteorus* species, six *Zele* species, and three outgroup species were finally selected (Table 3).

Model selection

Each codon position within the CO1 fragment was treated as a different data block, but not for noncoding 28S. The best-fit substitution model was determined using PartitionFinder v.2.1.1 (Lanfear et al. 2017) with the greedy search algorithm under the corrected Akaike information criterion (AICc): the selected model was the GTR+I+Γ model for the first and second codon position of CO1 and 28S, and GTR+Γ for the third codon position of CO1.

Table 3. Nomenclature systems for Meteorini species. The following abbreviations are used: *pulchri.* = *pulchricornis*.

Species	Present study	Stigenberg et al. (2011)	Maeto (1990)
	clade / subclade / complex	Clade	group / subgroup
Meteorus ictericus A, B	*ictericus* / – / –	I	*ictericus* / –
M. ruficeps	*ictericus* / – / –	I	*ictericus* / –
M. aff. *ruficeps*	*ictericus* / – / –	I	*ictericus* / –
Meteorus sp.	*ictericus* / – / –	–	–
M. artocercus	*pulchri.* / *colon* / –	IIA	–
M. cinctellus	*pulchri.* / *colon* / –	IIA	*pulchri.* / *colon*
M. colon	*pulchri.* / *colon* / –	IIA	*pulchri.* / *colon*
M. stenomastax	*pulchri.* / *colon* / –	IIA	–
M. tenellus A–C	*pulchri.* / *colon* / –	IIA	–
M. pendulus A–C	*pulchri.* / *pendulus* / –	IIB	*pulchri.* / *gyrator*
M. abscissus	*pulchri.* / *pulchri.* / –	IIB	–
M. limbatus	*pulchri.* / *pulchri.* / –	IIB	*pulchri.* / *gyrator*
M. pulchricornis	*pulchri.* / *pulchri.* / –	IIB	*pulchri.* / *pulchri.*
Meteorus sp.	*pulchri.* / *pulchri.* / –	–	–
M. acerbiavorus	*pulchri.* / *rubens-versicolor* / *rubens*	IIB	–
M. rubens A–C	*pulchri.* / *rubens-versicolor* / *rubens*	IIB	*rubens* / –
M. aff. *versicolor* A, B	*pulchri.* / *rubens-versicolor* / *versicolor*	–	*pulchri.* / *versicolor*
M. arizonensis	*pulchri.* / *rubens-versicolor* / *versicolor*	–	–
M. obsoletus	*pulchri.* / *rubens-versicolor* / *versicolor*	IIB	*pulchri.* / *versicolor*
M. tarius	*pulchri.* / *rubens-versicolor* / *versicolor*	–	–
M. stellatus sp. nov.	*pulchri.* / *rubens-versicolor* / *versicolor*	–	–
M. versicolor	*pulchri.* / *rubens-versicolor* / *versicolor*	IIB	*pulchri.* / *versicolor*
M. micropterus	*micropterus* / – / –	IIC	*micropterus* / –
M. abdominator A, B	Unresolved	III	–
M. affinis A–D	Unresolved	III	–
M. cespitator A, B	Unresolved	III	*hirsutipes* / –
M. cis A, B	Unresolved	III	*hirsutipes* / –
M. consimilis	Unresolved	III	–
M. densipilosus	Unresolved	III	–
M. eklundi	Unresolved	III	–
M. filator A, B	Unresolved	III	–
M. gigas	Unresolved	–	–
M. hirsutipes	Unresolved	III	*hirsutipes* / –
M. jaculator	Unresolved	III	–
M. kyushuensis	Unresolved	III	*hirsutipes* / –
M. longicaudis	Unresolved	III	–
M. obfuscatus	Unresolved	III	–
M. aff. *obfuscatus*	Unresolved	III	–
M. oculatus	Unresolved	III	–
M. sibyllae	Unresolved	III	–
Meteorus sp.	Unresolved	–	–
Meteorus sp.	Unresolved	–	–
M. sulcatus	Unresolved	III	*corax* / –
M. tabidus	Unresolved	III	–
M. vexator	Unresolved	III	–
Zela albiditarsus	*Zele*	IV	*Zele* / –
Z. caligatus	*Zele*	IV	*Zele* / –
Z. chlorophthalmus	*Zele*	IV	*Zele* / –
Z. deceptor	*Zele*	IV	*Zele* / –
Z. niveitarsis	*Zele*	–	*Zele* / –
Zela sp.	*Zele*	–	–

Analysis

The BI analyses were conducted using MrBayes v.3.2.2 (Ronquist et al. 2012). A Bayesian MCMC analysis was ran with the following settings: four independent runs, 20

chains each, heating 0.05, random starting trees, and trees sampled every 1,000th generation for 10,000,000 generations. The convergence of the MCMC runs was checked by the average standard deviation of split frequencies (ASDSF) in MrBayes (i.e., ASDSF < 0.01) (Ronquist and Huelsenbeck 2003) and chain stationarity in Tracer v.1.6 (Rambaut and Drummond 2007). Then, we discarded the anterior 25% of the generations as burn-in, obtained estimates for the harmonic means of the likelihood scores from the remaining 75% of the generations using the sump command, and conducted a final check of the convergence of the runs by the value of a potential scale reduction factor (PSRF); if the runs were convergent enough, PSRF was less than 5% divergent from 1.0. Finally, a consensus tree with the Bayesian inference posterior probabilities was obtained using the sumt command in MrBayes. The ML analysis was conducted in IQ-TREE v.2.1.2 (Minh et al. 2020) with a Shimodaira-Hasegawa-like approximate likelihood ratio test (SH-aLRT) (Guindon et al. 2010) and ultrafast likelihood bootstrap replicates (UFBoot2) (Minh et al. 2013; Hoang et al. 2018) for 10,000 replicates. The trees were edited in FigTree v.1.4.3 (Rambaut 2006–2016), Adobe Illustrator CC v.23.0.2, and Photoshop CC v.20.0.4 (Adobe Systems Inc., San Jose, CA, USA).

Results

Species identification

Although the molecular species delimitation was conducted using (1) whole datasets (i.e., *Meteorus* plus *Zele* plus outgroups), (2) *Meteorus* plus *Zele* datasets, and (3) *Meteorus* datasets, the results were congruent among all datasets in both the ABGD and GMYC methods. The number of recognized species was higher in the GMYC than in the ABGD method (Fig. 1). However, all results indicated that *Meteorus stellatus* sp. nov. was a single species.

Baded on morphological data, *M. stellatus* sp. nov. ran to the *versicolor* subgroup of the *pulchricornis* group based on Maeto's (1989a, b) criteria, but it could not be identified as any described species of *Meteorus* (see also Differential diagnosis).

Taxonomic account

Meteorus stellatus **Fujie, Shimizu & Maeto, sp. nov.**
http://zoobank.org/D8785F79-E874-4854-95D7-5C0A928914CA
[Japanese name: Hoshigata-haraboso-komayubachi]
Figs 2, 3

Etymology. The specific name is a masculine Latin word, "stellatus", meaning "starry", which is derived from the unique shape of the cocoon masses.

Type series. 41♀♀ 40♂♂ (all from Japan). ***Holotype*** ♀ (OMNH): "Japan: Okinawa Is., Okinawa City, Goya / Kitanakagusuku Vil., Shimabukuro, Okinawa Kodomono-kuni, 3. VI. 2019 cocoon masses), K. TONE et al. leg." "9. VI. 2019 emerged".

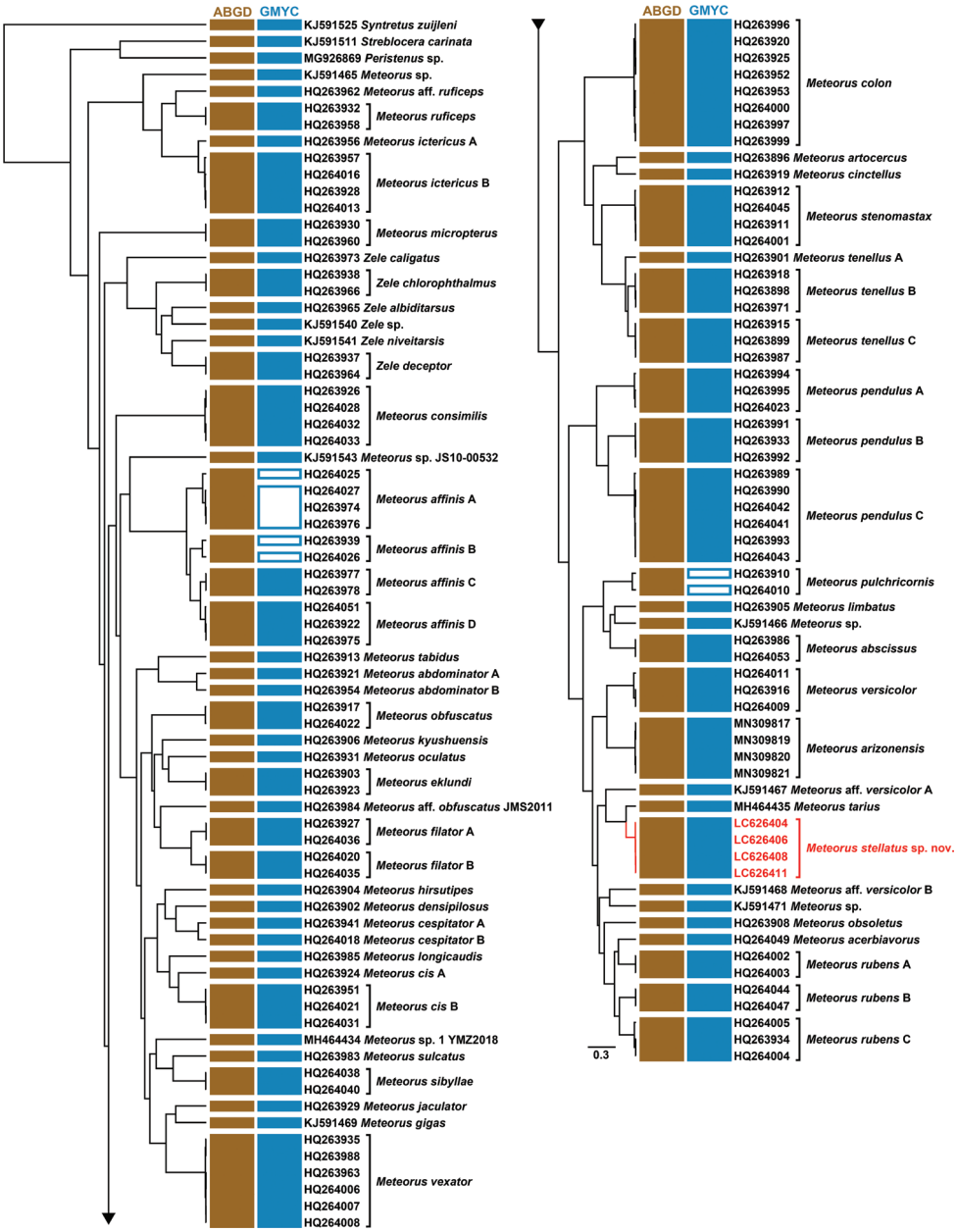

Figure 1. Species delimitation of *Meteorus* plus *Zele* plus closely related outgroups based on ABGD and GMYC methods, shown using a Bayesian consensus ultrametric tree generated using BEAST. Although the species delimitation was conducted using (1) *Meteorus* plus *Zele* plus outgroups, (2) *Meteorus* plus *Zele*, and (3) *Meteorus* sequences or topologies, all results were congruent; therefore, all results are shown as a summarized unit for each method.

***Paratypes*:** 1♀2♂♂ (OMM), same as holotype; 2♀♀2♂♂ (OMM), Okinawa-kodomonokuni, Goya, Okinawa City /Shimabukuro, Kitanakagusuku Vil, Okinawa-hontô Is., collected as cocoon masses on 13.V.2019 and emerged on 19.V.2019, Koichi Tone et. al leg.; 2♀♀2♂♂ (OMNH), Nago City, Okinawa-hontô Is., collected as cocoon masses on *Morinda umbellata* and emerged on 23–24.V.2011, Masashi Sugimoto leg.; 4♀♀4♂♂ (OMNH), Nago City, Okinawa-hontô Is., collected as host larva of *Macroglossum passalus passalus*, and adult wasps emerged on XII.2010 (2♀♀2♂♂) and I.2011 (2♀♀2♂♂), Masashi Sugimoto leg.; 2♀♀2♂♂ (RUM), Hentona, Kunigami Vil., Okinawa-hontô Is., collected as cocoon masses on 14.IV.2011 and emerged on 19.IV.2011, Koichi Sugino leg.; 2♀♀2♂♂ (ZISP), Hentona, Kunigami Vil., Okinawa-hontô Is., collected as cocoon masses on 30.X.2010 and emerged on 7.XI.2010, Kozue Miyagi leg.; 2♀♀2♂♂ (NARO), Aha, Kunigami Vil., Okinawa-hontô Is., collected as cocoon masses on 23.X.2010 and emerged on 25.X.2010, Yasuji Kakazu leg.; 2♀♀2♂♂ (OMNH), Okinawa-kodomonokuni, Goya, Okinawa City, Okinawa-hontô Is., collected as host larva of *Macroglossum pyrrhosticta* feeding *Paederia scandens* on 3.VI.2019, cocoon masses formed on 9.VI.2019, and emerged on 17.VI.2019, Yu Erh Chen leg.; 2♀♀2♂♂ (CNC), Ryukyu University, Nishihara Town, Okinawa-hontô Is., collected as cocoon masses on 22.VI.2005 and emerged on 25–29.VI.2005, Kazuo Minato leg.; 20♀♀20♂♂ (ELKU, EMUS, EUM, KPMNH, MNHA, NHMUK, NSMT, OMM, SEHU and TARI with 2♀♀2♂♂ each), Yoshihara, Chatan Town, Okinawa-hontô Is., collected as cocoon masses on 4.VI.2020 and emerged on 9–11.VI.2020, Tamami Gushiken leg.; 1♀ (OMNH), Chuo-rindo, Amami City, Amami-ôshima Is., 5.VII.2013, Shunpei Fujie leg.

Non-types. 323♀♀228♂♂ adults; 29 cocoon masses (see Suppl. material 1: Table S1).

Distribution. Japan (Ryukyus: Okinawa-hontô Island and Amami-ôshima Island).

Differential diagnosis. *Meteorus stellatus* sp. nov. is most similar to *M. komensis* (Fig. 4) but can be distinguished from the latter by the following combination of characters: the comparatively larger posterior ocelli (in *M. stellatus* sp. nov., OOL/OD = 1.2–1.6, while 1.7 in *M. komensis* (Fig. 4C)), the medially longitudinally strigose first metasomal tergite (Figs 2J, 3F) (fairly striate in *M. komensis*, as is shown in Fig. 4E, F). *Meteorus stellatus* sp. nov. is also very similar to *M. kurokoi* but can be distinguished from *M. kurokoi* by the face width (1.5–1.8× its height in *M. stellatus* sp. nov. (Figs 2E, 3B), while 1.2–1.3× in *M. kurokoi*) and the sculpture of frons (frons with a median longitudinal or a pair of carinae in *M. stellatus* sp. nov. (Fig. 2G), but smooth without any carinae in *M. kurokoi*).

In the key to species of *Meteorus* from the West Palaearctic region (Stigenberg and Ronquist 2011) and China (Chen et al. 2004), *M. stellatus* sp. nov. would run to *M. versicolor* (Wesmael), but can be distinguished from *M. versicolor* by the face width (1.5–1.8× its height in *M. stellatus* sp. nov. (Figs 2E, 3B), while 1.0–1.2× in *M. versicolor*), the sculpture of frons (with a median longitudinal or a pair of carinae in *M. stellatus* sp. nov. (Fig. 2G), but smooth in *M. versicolor*), and the shape of temple (Figs 2C, 3C) (roundly narrowed in *M. stellatus* sp. nov. (Figs 2C, 3C), but directly narrowed in *M. versicolor*).

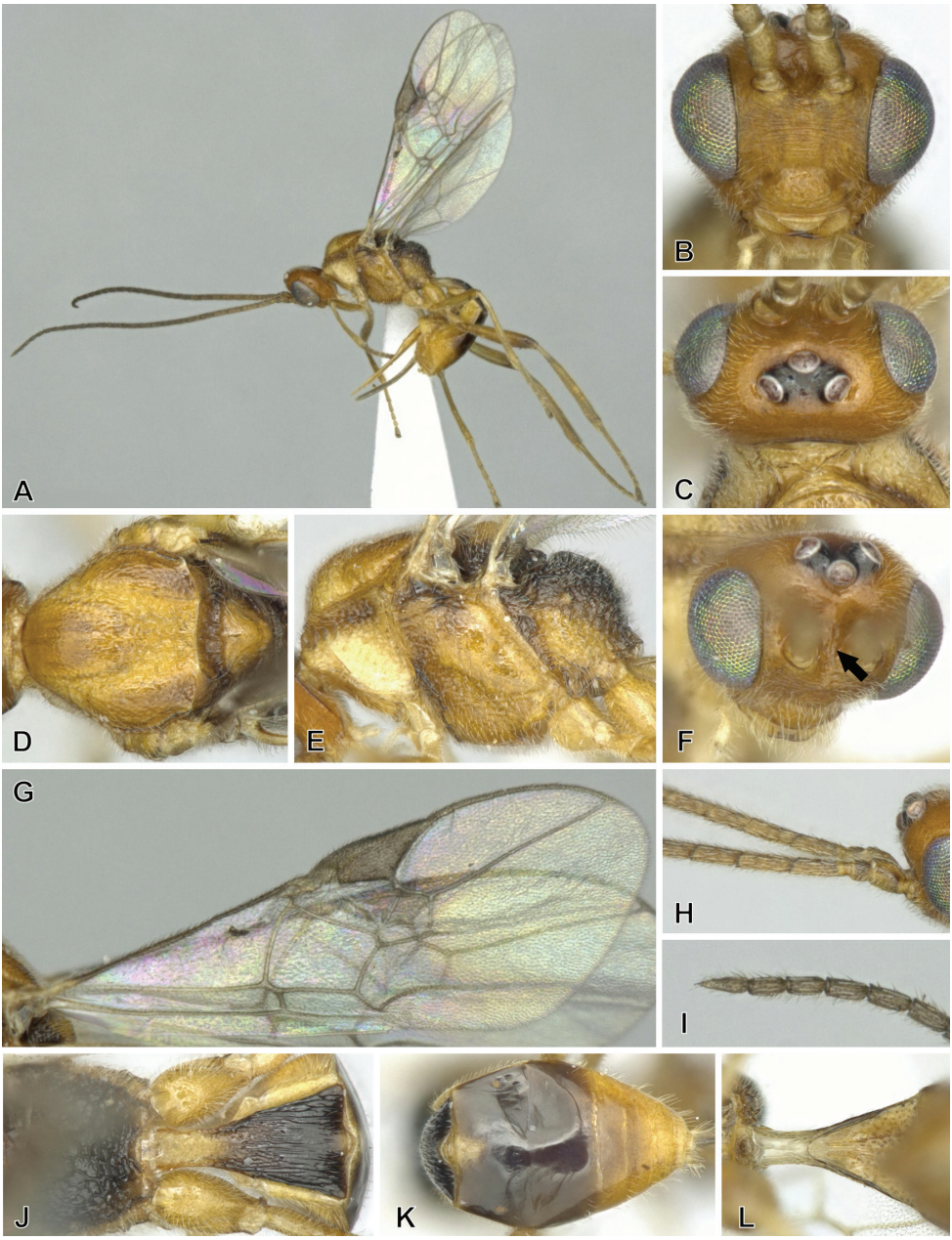

Figure 2. *Meteorus stellatus* sp. nov., ♀ holotype (exceptionally L is a paratype) **A** habitus **B** head, frontal view **C** head, dorsal view **D** mesopleuron and scutellum, dorsal view **E** mesosoma, lateral view **F** head, dorso-lateral view **G** forewing **H** basal antennal segments **I** apical antennal segments **J** propodeum and T1, dorsal view **K** T2 and following tergites, dorsal view **L** T1, ventral view.

The results of a GenBank BLAST search showed that the CO1 sequences of *M. stellatus* sp. nov. were closest to those of *M. arizonensis* Muesebeck and *M. tarius* Huddleston. However, *M. stellatus* sp. nov. can be distinguished from *M. arizonensis*

by its smaller body (the body lengths of *M. stellatus* sp. nov. and *M. arizonensis* are 2.9–3.9 mm and 4.6–5.5 mm, respectively), the longer malar space (the malar space length 1.0–1.4× the basal mandibular width in *M. stellatus* sp. nov. whereas 0.6–0.7× in *M. arizonensis*), the shorter ovipositor sheaths (the ovipositor sheath length 1.1–1.2× length of the first tergite in *M. stellatus* sp. nov. and 1.6–1.9× in *M. arizonensis*); the species can be distinguished from *M. tarius* by its broader face (the face width 1.5–1.7× its height in *M. stellatus* sp. nov. whereas approximately 1.0× in *M. tarius*) and the position of the forewing vein m-cu (slightly antefurcal to interstitial in *M. stellatus* sp. nov.**,** but far antefurcal in *M. tarius*).

Description. Female (holotype; Fig. 2). Body length 3.6 mm.

Head (Fig. 2B, C, F, H, I). Width of head 1.7× median height. Length of eye 1.7× length of temple in dorsal view. Temple roundly narrowed posteriorly. Eyes large and moderately convergent ventrally. Face with width 1.6× height; distinctly and densely transversely striate with fine granulation. Clypeus as wide as face, distinctly separated from face, and punctate-rugose. OOL / OD = 1.2. POL / OD = 1.4. Frons widely smooth, anteriorly with a pair of obscure carinae. Vertex and temple almost smooth. Length of malar space 1.1× basal mandibular width. Antennae with 26 segments; 4th segment 3.1× longer than wide; and penultimate one 1.9× longer than wide.

Mesosoma (Fig. 2D, E, J). Mesosoma length 1.4× height. Mesoscutum entirely covered with short and dense pale setae; median lobe weakly punctulate in anterior 0.6 and mostly rugose reticulate in posterior 0.4; lateral lobes weakly punctulate. Notauli shallow, wide, complete, coarsely rugose-reticulate. Prescutellar depression deep, almost straight, with often five rather fine carinae. Scutellum smooth and distinctly convex. Mesopleuron mostly punctulate, and rugose reticulate anterodorsally. Precoxal sulcus shallow and widely rugose-reticulate. Propodeum entirely coarsely rugose reticulate without median longitudinal carina.

Wings (Fig. 2G). Fore wing with 3.1 mm in length, length of pterostigma 2.9× maximum width, 3-SR / r = 1.2, m-cu distinctly (left) to slightly (right) postfurcal, cu-a far postfurcal, 1-CU1 / cu-a = 0.8. Hind wing with 1M / cu-a = 0.8, 1M / 1r-m = 0.6.

Legs. Tarsal claws with a distinct submedial lobe. Hind leg: outer surface of coxa punctate; femur 4.7× longer than wide, and distinctly and densely punctate.

Metasoma (Fig. 2J, K, L). 1st tergite 1.6× longer than apical width; dorsopes absent; mostly smooth anteriorly, longitudinally strigose with some rugosity medially, densely striate in posterior 0.3; ventral borders jointed from the base of segment to about middle point. Remaining terga smooth. Ovipositor slightly down-curved; length of ovipositor sheath 0.7× C+SC+R, 0.3× fore wing, and 1.2× 1st tergite.

Color (Fig. 2A). Brownish yellow, except for following parts infuscate: stemmaticum, apical segments of antennae, dorsal part of propleuron, side of scutellum, metanotum, propodeum, apex of hind femur and tibia, posterior half of 1st tergite, 2nd tergite (often except for anteromedially), 3rd tergite and ovipositor sheath; and palpi pale yellow. Wing membrane hyaline; pterostigma light brown, faintly paler basally.

Variation. Body length 2.9–3.9 mm. Width of head 1.6–1.8× median height. Length of eye 1.5–1.7× length of temple in dorsal view. Face with width 1.5–1.7× height. OOL / OD = 1.2–1.6. POL / OD = 1.3–1.7. Frons with a longitudinal carina

Figure 3. *Meteorus stellatus* sp. nov., ♂ paratype **A** habitus **B** head, frontal view **C** head and mesonotum, dorsal view **D** basal antennal segments **E** apical antennal segments **F** propodeum and T1, dorsal view **G** T2 and following tergites, dorsal view.

or a pair of obscure carinae. Length of malar space 1.0–1.4× basal mandibular width. Antennae with 26–31 segments; 4th segment 2.9–3.6× longer than wide; and penultimate one 1.7–2.0× longer than wide. Mesosoma length 1.4–1.5× height. Fore wing length 2.7–3.5 mm with length of pterostigma 2.8–3.3× maximum width, 3-SR / r = 0.8–1.4, m-cu distinctly postfurcal to interstitial, 1-CU1 / cu-a = 0.6–1.1. Hind wing with 1M / cu-a = 0.6–1.0, 1M / 1r-m = 0.5–0.7. Hind femur 4.6–4.9× longer than wide. 1st metasomal tergite 1.5–1.8× longer than apical width; longitudinally strigose with often some rugosity medially; length of ovipositor sheath 0.6–0.8× C+SC+R and

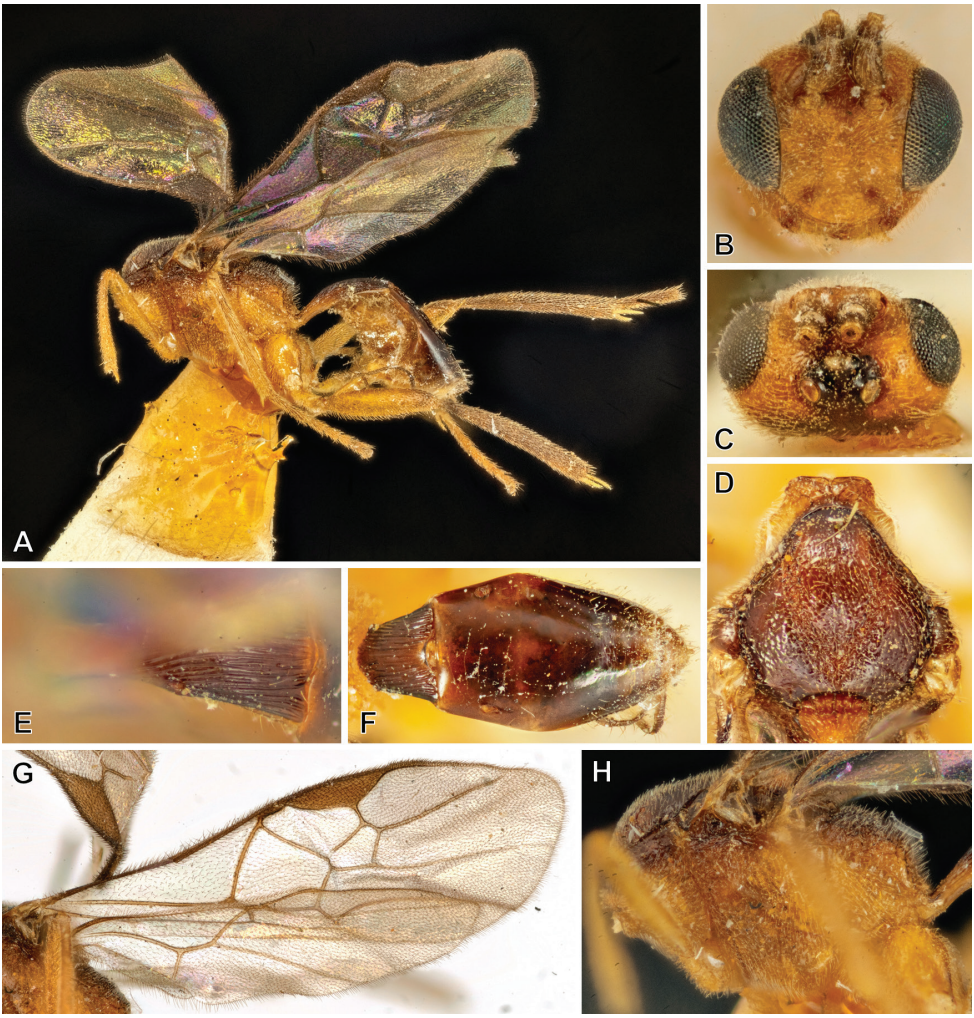

Figure 4. *Meteorus komensis* Wilkinson, ♀ holotype **A** habitus **B** head, frontal view **C** head, dorsal view **D** mesoscutum, dorso-lateral view **E** T1, dorsal view **F** T2 and following tergites, dorsal view **G** forewing **H** mesosoma, lateral view.

1.1–1.2× 1st tergite. 2nd tergite brownish yellow to infuscate anteromedially. Pterostigma unicolored or faintly paler basally.

Males (Fig. 3). Similar to females, except for length of eye 1.6–1.9× length of temple in dorsal view; width of face 1.6–1.8× height; OOL / OD = 1.1–1.4; POL / OD = 1.4–1.8; length of malar space 1.1–1.7× basal mandibular width; antennae with 27–31 segments; penultimate segments of antenna 2.2–2.8× longer than wide; hind femur 4.6–5.1× longer than wide; 1st metasomal tergite 1.6–1.9× long than apical width; propleuron not darkened dorsally.

Hosts and host plants. Two species of Sphingidae (Lepidoptera) were identified as hosts of *M. stellatus* sp. nov.: *Macroglossum passalus* (Drury) feeding on

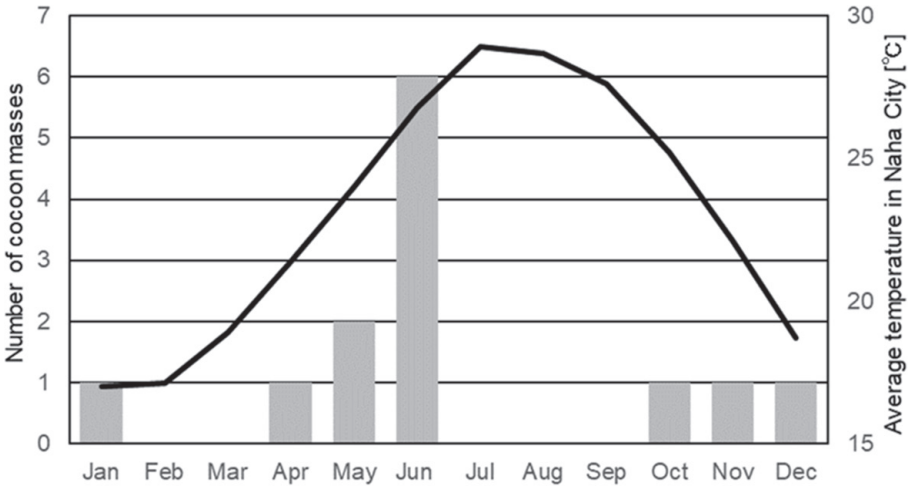

Figure 5. Seasonal changes in the adult emergence of *Meteorus stellatus* sp. nov. (bars indicating the number of cocoon masses) and in the monthly average temperature in Naha City, Okinawa-hontô Island (a solid line).

Daphniphyllum glaucescens Blume (Daphniphyllaceae) and *M. pyrrhosticta* Butler feeding on *Paederia foetida* Linnaeus [= *P. scandens* (Lour.) Merr.] (Rubiaceae). All wasp larvae of *M. stellatus* sp. nov. emerged from mature larvae of the host sphingids.

Hyper-parasitoids. Some hymenopteran hyper-parasitoids emerged from the cocoon masses after the emergence of *M. stellatus* sp. nov. adults. The following three species were identified as morphospecies at the generic level: *Tetrastichus* sp. (Eulophidae), *Eurytoma* sp. (Eurytomidae), and *Aphanogmus* sp. (Ceraphronidae) (Suppl. material 2: Table S2).

Habitats. Despite the multiple field collection sessions at primary forest areas in the Okinawa-hontô and Amami-ôshima Islands, only one specimen of *M. stellatus* sp. nov. was sampled from a secondary evergreen forest in the latter island. Most other specimens of *M. stellatus* sp. nov. were collected from a campus of the University of the Ryukyus, urban parks, and back yards in Okinawa-hontô Island, by finding suspended cocoon masses or rearing host larvae. As the host sphingids and their host plants are abundant in or around the edges of sparse forests, *M. stellatus* sp. nov. likely prefers rather open forests.

Phenology. The emergence of adult wasps occurred from April to June and from October to January, but not during the hottest season from July to September (Fig. 5).

Secondary sex ratio. The proportion of males (secondary sex ratio) ranged from 0.20 to 0.64, showing a gradual increase with the total number of wasps per host larva (Fig. 6). The positive effect of the total number of wasps on the sexual ratio was significant (B = 0.010, Wald Chi-Square = 18.129, df = 1, $p < 0.001$). The estimated mean of the proportion of males was 0.36 (95% confidence interval = 0.31–0.42, significantly less than 0.50) in the average number of total wasps (50.5), indicating an overall female-biased sex ratio.

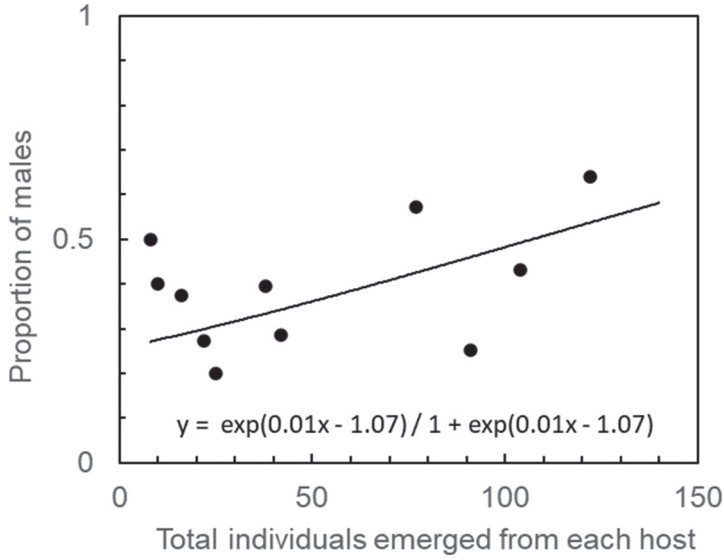

Figure 6. Sex ratios of emerged adults of *Meteorus stellatus* sp. nov. in relation to the number of individuals per host larva.

Cocoon mass formation. The third author observed a case of larval emergence and subsequent cocoon formation in the laboratory. At approximately 1:30 p.m. on June 9, 2019, approximately 100 larvae of *M. stellatus* sp. nov. emerged from the abdomen of a matured larva of *M. pyrrhosticta* on the vine of *P. foetida* by chewing holes (Fig. 7A). The larvae commenced hanging down from the host plant substance with their own suspensory threads as soon as they emerged (Fig. 7B). The larvae began to cluster by actively rotating, twisting, swaying, and horizontally stretching (Fig. 7C). When the larvae found the threads of other individuals, they actively went down, intertwined with said threads, and eventually merged together. Once they formed a large mass, the mass did not descend any more (Fig. 7D). In rare cases, several larvae moved from the upper mass to the lower mass as the cable of the former intertwined with that of the latter, owing to the blowing wind. No further larval transfer was observed after approximately 70 min of the emergence of the larvae. Initially, the shape of the larval masses was irregular (Fig. 7E), but gradually the larvae adopted a spherical shape (Fig. 7F, G). The larvae twisted their upper bodies and spun the thread at the posterior of their body, namely inside the cocoon mass. The silk walling action lasted approximately 40 min, along with the spinning of their own individual cocoons (Fig. 7H, I). Finally, three cocoon masses were completed approximately 2 h after larval emergence (Fig. 7J). A video of the entire process of cocoon mass formation is available at the following address: https://www.youtube.com/watch?v=AuHarLHolPM.

The host sphingid died on the following day after wondering. The color of the cocoons gradually darkened over a few days. After 8 days, 68 females and 23 males of *M. stellatus* sp. nov. emerged from these three cocoon masses. The wasps emerged simultaneously, cutting the tip of each cocoon.

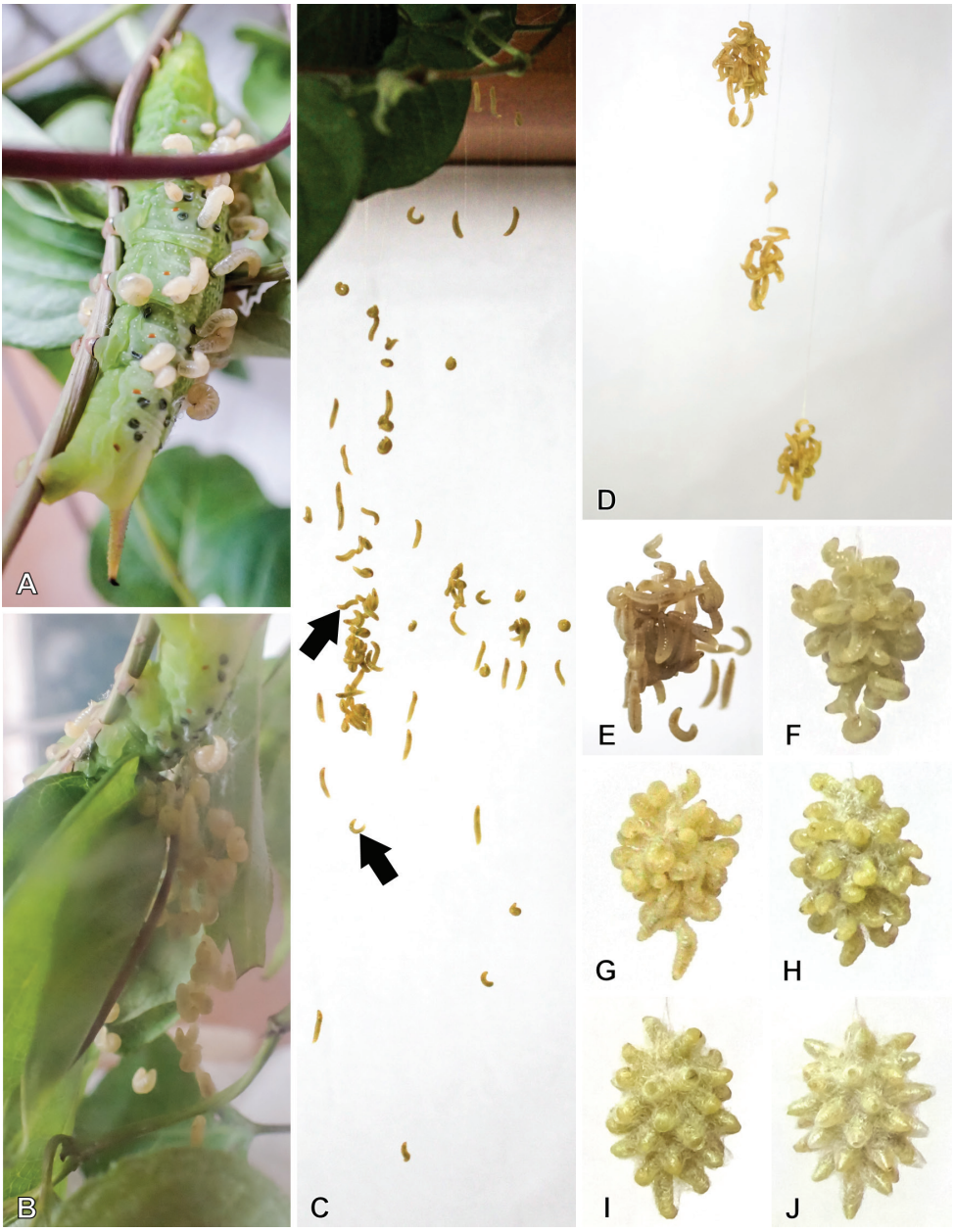

Figure 7. Cocoon forming behavior of *Meteorus stellatus* sp. nov. **A** emerging from a host larva (start time) **B** hanging down from the host plant substance (2 min) **C** intertwining with threads: arrows show larvae looking for other threads (39 min) **D** almost merging into three masses (57 min) **E–J** forming spherical cocoon masses (**E** 30 min **F** 65 min **G** 69 min **H** 84 min **I** 105 min **J** 139 min).

Characteristics of the cocoon masses. The cocoon masses of *M. stellatus* sp. nov. (Fig. 8) were light brown to brown, 7–14 mm in width, 9–23 mm in length, and regularly spherical to ovoid with minimally 12 (Fig. 8D) to maximally over 100 cocoons

(Fig. 8C). Exceptionally, approximately 200 cocoons formed a collapsed large mass in an artificial breeding case (Fig. 8B). Each cocoon mass was suspended by a single thick cable. The cable was 12–100 cm in length. Although most larvae constructed such cocoon masses, sometimes a few single larvae formed their own cocoons on the cable (Fig. 8F). The cable consisted of individual threads, which were tightly intertwined, like a rope (Fig. 8G). The anterior third to half of individual cocoons was exposed outward and fairly distributed on the spherical or ovoid surface. The posterior half of individual cocoons was invisible under the dense silk wall. Adults emerged by opening an anterior outside cocoon cap, which was circular shaped and tapering (Fig. 8F). Cocoons with such a regular cap are typical of the *pulchricornis* clade of *Meteorus* (Askari et al. 1977; Maeto 1989a, b, 1990a).

Phylogeny of Meteorini and affinity of *M. stellatus* sp. nov. The Meteorini phylogeny is illustrated in Fig. 9. The Meteorini classification was also revised based on our phylogeny and those of Maeto (1990b) and Stigenberg et al. (2011) (Table 3). Although our topology was poorly resolved at the species level, it was mostly congruent with that of Stigenberg and Ronquist (2011). Meteorini was recovered as a monophyletic group. Meteorini species were divided into five clades (Fig. 9; Table 3). *Zele* was recovered as a robustly supported monophyletic clade and nested within *Meteorus* species. Monophyly was robustly supported for the *ictericus* and *pulchricornis* clades but not for the unresolved clade. The *pulchricornis* clade was divided into four internal subclades (the *colon*, *pendulus*, *pulchricornis*, and *rubens* subclades).

Meteorus stellatus sp. nov. was recovered as an ingroup of the *versicolor* complex of the *rubens* subclade within the *pulchricornis* clade and sister to *M. tarius*.

Discussion

Our observation of *M. stellatus* sp. nov. shows that gregarious cocoon masses were constructed by the highly elaborated cooperation of larvae. The larvae never merged immediately after emergence from their host, but initially just descended. This seems to reinforce the idea that the suspended cocoon makes the pupating wasp inaccessible to some potential enemies (Shaw and Huddleston 1991; Quicke et al. 2006; Zitani 2003; Shirai and Maeto 2009; Maeto 2018). It seems that predators, like ants, seldom encounter suspended larvae because the threads of larvae are attached to the plant subtract only by a small area.

The cable of gregarious *Meteorus* is thought to be very resistant to breaking and highly tolerant to environmental stress (Barrantes et al. 2011). A cable of *M. stellatus* sp. nov. consists of a lot of individual threads and seems to be very strong, pretty much like that of *M. restionis* Shaw & Jones (Barrantes et al. 2011). Interestingly, cocoon masses of *M. townsendi* are suspended by a fairly long cable, the length of which is approximately 3.0 m (Zitani and Shaw 2002; Zitani 2003), while the longest cable of *M. stellatus* sp. nov. is approximately 1.0 m. According to our observation, the long individual threads and the adequate wind during the hanging period seem to make it easier for the larvae of *M. stellatus* sp. nov. to merge with each other. The larvae continue to spin thread until they are able to merge into a cocoon mass, and in most cases, they never go down unnecessarily after that.

Figure 8. Cocoon masses of *Meteorus stellatus* sp. nov. **A** habitus, medium-sized **B** habitus, exceptionally large-sized and somewhat collapsed in an artificial condition **C** a medium-sized cocoon mass **D, E** small-sized cocoon masses **F** independent cocoons near a cocoon mass **G** a part of suspending thread, consisting of individual cable.

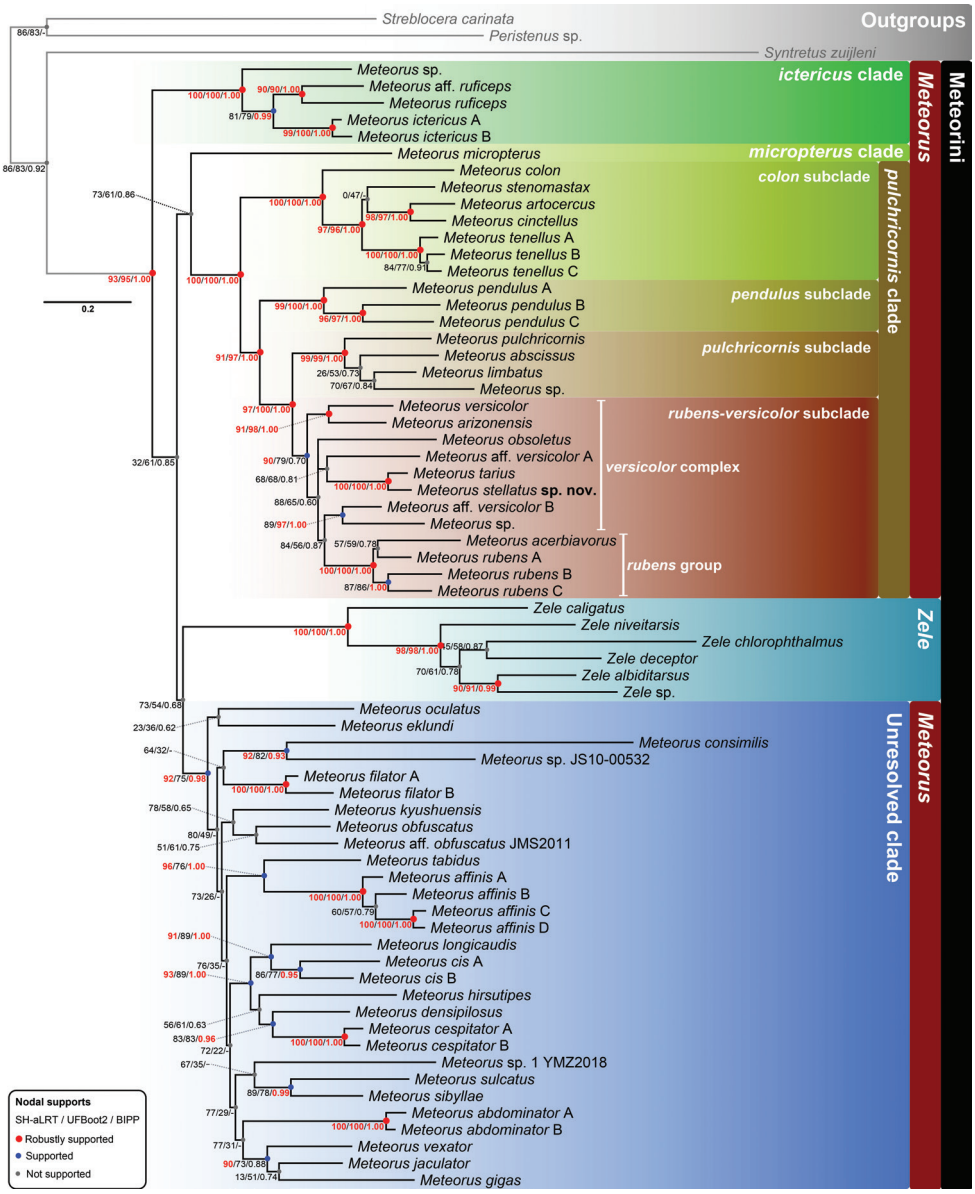

Figure 9. Maximum likelihood tree of Meteorini generated using IQ-TREE (BIPP, Bayesian inference posterior probabilities; SH-aLRT, a Shimodaira-Hasegawa-like approximate likelihood ratio test; UF-Boot2, ultrafast likelihood bootstrap replicates).

The star-shaped cocoon masses of *M. stellatus* sp. nov. can reduce the risk of hyperparasitism, because the exposed area of each individual cocoon is apparently smaller than the solitary cocoon or non-star-shaped cocoon masses, as suggested by the spherical cocoons of *M. komensis* (Zitani 2003). The outer cocoons of non-circular cocoon masses of gregarious *Cotesia glomerata* (Linnaeus) (Braconidae, Microgastrinae) are actually more easily parasitized than the inner ones (Tagawa and Fukushima 1993;

Tanaka and Ohsaki 2006). Therefore, the evolution of gregariousness and spherical cocoon masses seems reasonable.

The sex ratio has been studied in gregarious species of *Meteorus*, while a similar pattern of female-biased sex ratio has been shown in *Macrostomion sumatranum* (Enderlein) (Braconidae, Rogadinae), which is also a gregarious parasitoid of matured sphingid larvae (Maeto and Arakaki 2005). Both in the gregarious parasitoid category, the number of wasps emerged from each host varies widely (8–122 in *M. stellatus* sp. nov. and 26–160 in *Ma. sumatranum*) and the proportion of males increases with it. The female-biased sex ratio could be a result of the local mate competition, as expected in inbreeding gregarious parasitoids (Hamilton 1967; Godfray 1994; Smart and Mayhew 2009), in which the increase of the male proportion may be caused by the oviposition of multiple females on a single host larva (Werren 1983). This prediction will be tested by the examination of mating systems, oviposition behavior, and primary sex ratio.

The *pulchricornis* and *rubens* species-groups belong to the monophyletic lineage of *pulchricornis* clade (Fig. 10), in which both solitary and gregarious species are included and cocoons are usually suspended by a spun thread (Maeto 1990b; Stigenberg and Ronquist 2011). It is thus likely that communal cocoon masses of type F have evolved through individually or sparsely suspended gregarious cocoons of type B and C, and subsequently loosely clumped and suspended gregarious cocoons of type D, from suspended solitary cocoons within the *versicolor* complex. However, the evolutionary pathways are not yet clarified because only a few gre-

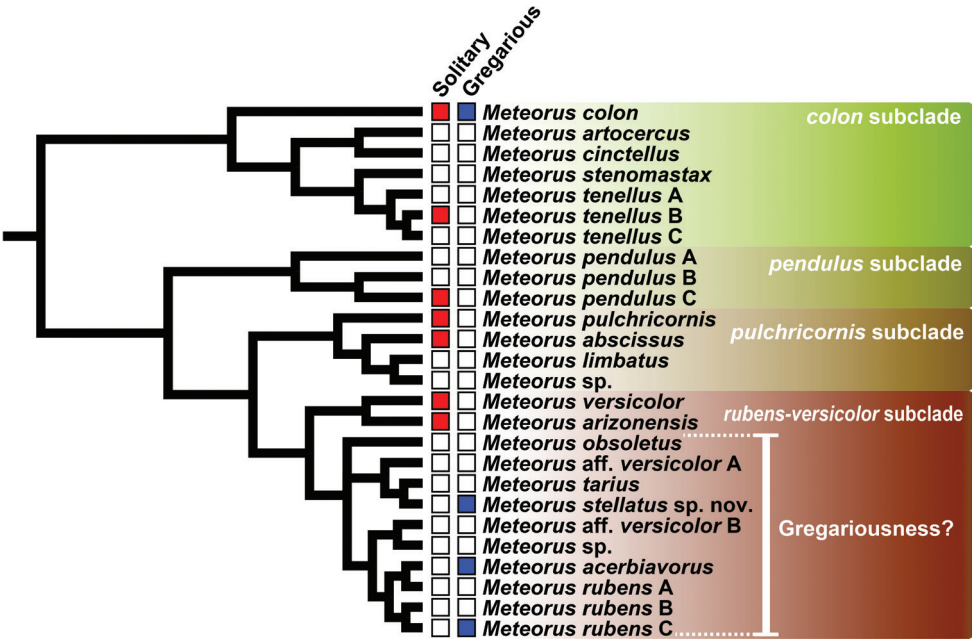

Figure 10. Phylogenetic relationships among the species of *pulchricornis* clade and their lifestyle.

garious species are placed in the present phylogram. Further and comprehensive analyses including more gregarious species are necessary to confirm and expand this evolutionary scenario.

Acknowledgements

We are grateful to Yu Erh Chen, Tamami Gushiken, Kazuo Minato, Toshimasa Mitamura, Kozue Miyagi, Masashi Sugimoto, Koichi Sugino, Nakatada Wachi, Masako Yafuso, and research volunteers of Okinawa Zoo and Museum for collecting and offering the materials; to Kota Sakagami for identifying the host sphingid; to Kees van Achterberg and Jose Fernandez-Triana for variable suggestions on the manuscript; to Gavin Broad (NHMUK) for supporting at NHMUK.

This research is partially supported by the Grants-in-Aid for JSPS KAKENHI (Grant numbers 19H00942) to KM and the Grant-in-Aid for JSPS Fellows (Grant Number 18J20333) to SS from the Japan Society for the Promotion of Science. The JSPS Overseas Challenge Program for Young Researchers enabled SS to carry out research at NHMUK.

References

Aguirre H, Shaw SR (2014) Neotropical species of *Meteorus* Haliday (Hymenoptera: Braconidae: Meteorinae) parasitizing Arctiinae (Lepidoptera: Noctuoidea: Erebidae). Zootaxa 3779: 353–367. https://doi.org/10.11646/zootaxa.3779.3.3

Askari A, Mertins JW, Coppel HC (1977) Developmental biology and immature stages of *Meteorus pulchricornis* in the laboratory. Annals of the Entomological Society of America 70: 655–659. https://doi.org/10.1093/aesa/70.5.655

Barrantes G, Triana E, Shaw SR, Jones GZ (2011) Characteristics of the cocoon and natural history of the gregarious *Meteorus restionis* sp. n. (Hymenoptera, Braconidae, Meteorinae) from Costa Rica. Journal of Hymenoptera Research 20: 9–21. https://doi.org/10.3897/jhr.29.867

Bouckaert R, Vaughan TG, Barido-Sottani J, Duchêne S, Fourment M, Gavryushkina A, Heled J, Jones G, Kühnert D, De Maio N, Matschiner M, Mendes FK, Müller NF, Ogilvie HA, du Plessis L, Popinga A, Rambaut A, Rasmussen D, Siveroni I, Suchard MA, Wu C-H, Xie D, Zhang C, Stadler T, Drummond AJ (2019) BEAST 2.5: An advanced software platform for Bayesian evolutionary analysis. PLoS Computational Biology 15: e1006650. https://doi.org/10.1371/journal.pcbi.1006650

Capella-Gutiérrez S, Silla-Martínez JM, Gabaldón T (2009) trimAl: a tool for automated alignment trimming in large-scale phylogenetic analyses. Bioinformatics 25: 1972–1973. https://doi.org/10.1093/bioinformatics/btp348

Chen X-X, He J-H, Ma Y (2004) Fauna Sinica. Insecta Vol. 37. Hymenoptera. Braconidae (II). Science Press, Beijing, 581 pp.

Fujisawa T, Barraclough TG (2013) Delimiting species using single-locus data and the Generalized Mixed Yule Coalescent approach: a revised method and evaluation on simulated data sets. Systematic Biology 62: 707–724. https://doi.org/10.1093/sysbio/syt033

Gauld ID, Bolton B [Eds] (1988) The Hymenoptera. Oxford University Press, Oxford and The Natural History Museum, London, 332 pp.

Glez-Peña D, Gómez-Blanco D, Reboiro-Jato M, Fdez-Riverola F, Posada D (2010) ALTER: program-oriented format conversion of DNA and protein alignments. Nucleic Acids Research 38: W14–W18. https://doi.org/10.1093/nar/gkq321

Godfray HCJ (1994) Parasitoids: Behavioral and Evolutionary Ecology. Princeton University Press, Princeton, 473 pp. https://doi.org/10.1515/9780691207025

Guindon S, Dufayard JF, Lefort V, Anisimova M, Hordijk W, Gascuel O (2010) New algorithms and methods to estimate maximum-likelihood phylogenies: assessing the performance of PhyML 3.0. Systematic Biology 59: 307–321. https://doi.org/10.1093/sysbio/syq010

Hamilton WD (1967) Extraordinary sex ratios. Science 156: 477–488. https://doi.org/10.1126/science.156.3774.477

Harry M, Solignac M, Lachaise D, (1996) Adaptive radiation in the Afrotropical region of the Paleotropical genus *Lissocephala* (Drosophilidae) on the pantropical genus *Ficus* (Moraceae). Journal of Biogeography 23: 543–552. https://doi.org/10.1111/j.1365-2699.1996.tb00016.x

Hoang DT, Chernomor O, von Haeseler A, Minh BQ, Le SV (2018) UFBoot2: improving the ultrafast bootstrap approximation. Molecular Biology and Evolution 35: 518–522. https://doi.org/10.1093/molbev/msx281

Huddleston T (1980) A revision of the western Palaearctic species of the genus *Meteorus* (Hymenoptera: Braconidae). Bulletin of the British Museum (Natural History), Entomology series 41: 1–58.

Katoh K, Rozewicki J, Yamada KD (2019) MAFFT online service: multiple sequence alignment, interactive sequence choice and visualization. Briefings in Bioinformatics 20: 1160–1166. https://doi.org/10.1093/bib/bbx108

Katoh K, Toh H, (2008) Improved accuracy of multiple ncRNA alignment by incorporating structural information into a MAFFT-based framework. BMC Bioinformatics 9: 212. https://doi.org/10.1186/1471-2105-9-212

Katoh K, Standley DM (2013) MAFFT multiple sequence alignment software version 7: improvements in performance and usability. Molecular Biology and Evolution 30: 772–780. https://doi.org/10.1093/molbev/mst010

Klimov PB, Skoracki M, Bochkov AV (2019) Cox1 barcoding versus multilocus species delimitation: validation of two mite species with contrasting effective population sizes. Parasites Vectors 12: e8. https://doi.org/10.1186/s13071-018-3242-5

Kumar S, Stecher G, Li M, Knyaz C, Tamura K (2018) MEGA X: molecular evolutionary genetics analysis across computing platforms. Molecular Biology and Evolution 35: 1547–1549. https://doi.org/10.1093/molbev/msy096

Lanfear R, Frandsen PB, Wright AM, Senfeld T, Calcott B (2017) PartitionFinder 2: new methods for selecting partitioned models of evolution for molecular and morphological phylogenetic analyses. Molecular Biology and Evolution 34: 772–773. https://doi.org/10.1093/molbev/msw260

Lefort V, Longueville J-E, Gascuel O (2017) SMS: smart model selection in PhyML. Molecular Biology and Evolution 34: 2422–2424. https://doi.org/10.1093/molbev/msx149

Maeto K (1989a) Systematic studies on the tribe Meteorini from Japan (Hymenoptera, Braconide) V. The *pulchricornis* group of the genus *Meteorus* (1). Japanese Journal of Entomology 57: 581–595.

Maeto K (1989b) Systematic studies on the tribe Meteorini (Hymenoptera: Braconidae) from Japan. VI. The *pulchricornis* group of the genus *Meteorus* Haliday (2). Japanese Journal of Entomology 57: 768–777.

Maeto K (1990a) Systematic studies on the tribe Meteorini (Hymenoptera: Braconidae) from Japan. VII. The group of *Meteorus ictericus* and *M. rubens*. Japanese Journal of Entomology 58: 81–94.

Maeto K (1990b) Phylogenetic relationships and host associations of the subfamily Meteorinae Cresson (Hymenoptera, Braconidae). Japanese Journal of Entomology 58: 383–396.

Maeto K (2018) Polyphagous koinobiosis: the biology and biocontrol potential of a braconid endoparasitoid of exophytic caterpillars. Applied Entomology and Zoology 53: 433–446. https://doi.org/10.1007/s13355-018-0581-9

Maeto K, Arakaki N (2005) Gregarious emergence of *Macrostomion sumatranum* (Hymenoptera: Braconidae; Rogadinae) from the mummified, full-grown larvae of *Theretra silhetensis* (Lepidoptera: Sphingidae). Entomological Science 8: 131–132. https://doi.org/10.1111/j.1479-8298.2005.00107.x

Minh BQ, Nguyen MAT, von Haeseler A (2013) Ultrafast approximation for phylogenetic bootstrap. Molecular Biology and Evolution 30: 1188–1195. https://doi.org/10.1093/molbev/mst024

Minh BQ, Schmidt HA, Chernomor O, Schrempf D, Woodhams MD, von Haeseler A, Lanfear R (2020) IQ-TREE 2: new models and efficient methods for phylogenetic inference in the genomic era. Molecular Biology and Evolution 37: 1530–1534. https://doi.org/10.1093/molbev/msaa015

Mitamura T (2013) The Handbook of Japanese Cocoon. Bun-ichi (Tokyo): 1–112. [in Japanese]

Puillandre N, Lambert A, Brouillet S, Achaz G (2012) ABGD, automatic barcode gap discovery for primary species delimitation. Molecular Ecology 21: 1864–1877. https://doi.org/10.1111/j.1365-294X.2011.05239.x

Quicke DLJ (2015) The Braconid and Ichneumonid Parasitoid Wasps. Biology, systematics, evolution and ecology. John Wiley & Sons, Ltd., Hoboken, 681 pp. https://doi.org/10.1002/9781118907085

Quicke DLJ, Mori M, Zaldivar-Riverón A, Laurenne NM, Shaw MR (2006) Suspended mummies in *Aleiodes* species (Hymenoptera: Braconidae: Rogadinae) with descriptions of six new species from western Uganda based largely on DNA sequence data. Journal of Natural History 40: 2663–2680. https://doi.org/10.1080/00222930601121288

R Core Development Team (2020) R: a language and environment for statistical computing. https://www.R-project.org/

Rambaut A (2006–2016) Tree Figure Drawing Tool, version 1.4.3, Institute of Evolutionary Biology, University of Edinburgh. http://tree.bio.ed.ac.uk/software/figtree/

Rambaut A, Drummond AJ (2007) Tracer: MCMC trace analysis tool v1.4.1. http://tree.bio.ed.ac.uk/software/tracer?/

Richards OW (1977) Hymenoptera. Introduction and key to families. Handbooks for the Identification of British Insects, 2nd edn. 6: 1–100.

Ronquist F, Huelsenbeck JP (2003) MrBayes 3: Bayesian phylogenetic inference under mixed models. Bioinformatics 19: 1572–1574. https://doi.org/10.1093/bioinformatics/btg180

Ronquist F, Teslenko M, van der Mark P, Ayres DL, Darling A, Höhna S, Larget B, Liu L, Suchard MA, Huelsenbeck JP (2012) MrBayes 3.2: efficient Bayesian phylogenetic inference and model choice across a large model space. Systematic Biology 61: 539–542. https://doi.org/10.1093/sysbio/sys029

Schulmeister S (2003) Simultaneous analysis of basal Hymenoptera (Insecta): introducing robust-choice sensitivity analysis. Biological Journal of Linnean Society 79: 245–275. https://doi.org/10.1046/j.1095-8312.2003.00233.x

Shaw MR, Huddleston T (1991) Classification and biology of Braconid wasps (Hymenoptera: Braconidae). Handbooks for the Identification of British Insects 7(11): 1–126.

Shaw SR, Nishida K (2005) A new species of gregarious *Meteorus* (Hymenoptera: Braconidae) reared from caterpillars of *Venadicodia caneti* (Lepidoptera: Limacodidae) in Costa Rica. Zootaxa 1028: 49–60. https://doi.org/10.11646/zootaxa.1028.1.4

Shimizu S, Broad GR, Maeto K (2020) Integrative taxonomy and analysis of species richness patterns of nocturnal Darwin wasps of the genus *Enicospilus* Stephens (Hymenoptera, Ichneumonidae, Ophioninae) in Japan. ZooKeys 990: 1–144. https://doi.org/10.3897/zookeys.990.55542

Shirai S, Maeto K (2009) Suspending cocoons to evade ant predation in *Meteorus pulchricornis*, a braconid parasitoid of exposed- living lepidopteran larvae. Entomological Science 12: 107–109. https://doi.org/10.1111/j.1479-8298.2009.00301.x

Sobczak JF, Maia DP, Moura JCMS, Costa VA, Vasconcellos-Neto J (2012) Natural history of interaction between *Meteorus* sp. Haliday, 1835 (Hymenoptera: Braconidae) and its hyperparasitoid *Toxeumella albipes* Girault, 1913 (Hymenoptera: Pteromalidae). Brazilian Journal of Biology 72: 211–214. https://doi.org/10.1590/S1519-69842012000100026

Stigenberg J, Ronquist F (2011) Revision of the Western Palearctic Meteorini (Hymenoptera, Braconidae), with a molecular characterization of hidden Fennoscandian species diversity. Zootaxa 3084: 1–95. https://doi.org/10.11646/zootaxa.3084.1.1

Stigenberg J, Vikberg V, Belokobylskij SA (2011) *Meteorus acerbiavorus* sp. nov. (Hymenoptera, Braconidae), a gregarious parasitoid of *Acerbia alpina* (Quensel) (Lepidoptera, Arctiidae) in North Finland. Journal of Natural History 45: 1275–1294. https://doi.org/10.1080/00222933.2011.552807

Tagawa J, Fukushima H (1993) Effects of host age and cocoon position on attack rate by the hyperparasitoid, *Eurytoma* sp. (Hym.: Eurytomidae), on cocoons of the parasitoid, *Cotesia* (= *Apanteles*) *glomerata* (Hym.: Braconidae). Entomophaga 38: 69–77. https://doi.org/10.1007/BF02373141

Tanaka S, Ohsaki N (2006) Behavioral manipulation of host caterpillars by the primary parasitoid wasp *Cotesia glomerata* (L.) to construct defensive webs against hyperparasitism. Ecological Research 21: 570–577. https://doi.org/10.1007/s11284-006-0153-2

Thompson JD, Higgins DG, Gibson TJ (1994) CLUSTAL W: improving the sensitivity of progressive multiple sequence alignment through sequence weighting, position-specific gap penalties and weight matrix choice. Nucleic Acids Research 22: 4673–4680. https://doi.org/10.1093/nar/22.22.4673

Werren JH (1983) Sex ratio evolution under local mate competition in a parasitic wasp. Evolution 37: 116–124. https://doi.org/10.1111/j.1558-5646.1983.tb05520.x

Yu DSK, van Achterberg C, Horstmann K (2016) Taxapad 2016, Ichneumonoidea 2015 Database on flash-drive. Nepean, Ontario. www.taxapad.com

van Achterberg C (1988) Revision of the subfamily Blacinae Foerster (Hymenoptera, Braconidae). Zoologische Verhandelingen Leiden 249: 1–324.

Zitani NM (2003) The evolution and adaptive significance of silk use in the Meteorinae (Hymenoptera, Braconidae). PHD Thesis. University of Wyoming, Laramie.

Zitani NM, Shaw RS (2002) From *Meteorus* to death star. Variations on a silk thread (Hymenoptera: Braconidae: Meteorinae). American Entomologist 48: 228–235. https://doi.org/10.1093/ae/48.4.228

Supplementary material 1

Table S1

Authors: Shunpei Fujie, So Shimizu, Koichi Tone, Kazunori Matsuo, Kaoru Maeto

Data type: excel (.xslx) file

Explanation note: Table S1. Examined materials *Meteorus stellatus* sp. nov.

Copyright notice: This dataset is made available under the Open Database License (http://opendatacommons.org/licenses/odbl/1.0/). The Open Database License (ODbL) is a license agreement intended to allow users to freely share, modify, and use this Dataset while maintaining this same freedom for others, provided that the original source and author(s) are credited.

Link: https://doi.org/10.3897/jhr.86.71225.suppl1

Supplementary material 2

Table S2

Authors: Shunpei Fujie, So Shimizu, Koichi Tone, Kazunori Matsuo, Kaoru Maeto

Data type: excel (.xslx) file

Explanation note: Table S2. Gene bank accession numbers for the sampled taxa in the analyses.

Copyright notice: This dataset is made available under the Open Database License (http://opendatacommons.org/licenses/odbl/1.0/). The Open Database License (ODbL) is a license agreement intended to allow users to freely share, modify, and use this Dataset while maintaining this same freedom for others, provided that the original source and author(s) are credited.

Link: https://doi.org/10.3897/jhr.86.71225.suppl2

JHR 86: 47–61 (2021)
doi: 10.3897/jhr.86.72690
https://jhr.pensoft.net

RESEARCH ARTICLE

JOURNAL OF Hymenoptera RESEARCH
A peer-reviewed open-access journal
The International Society of Hymenopterists

Revision of the genus *Schoenlandella* (Hymenoptera, Braconidae, Cardiochilinae) in the New World, with a potential biological control agent for a lepidopteran pest of bitter gourd (*Momordica charantia* L.)

Ilgoo Kang[1], Michael J. Sharkey[2], Rodrigo Diaz[1]

1 *Department of Entomology, Louisiana State University Agricultural Center, 404 Life Sciences Building, Baton Rouge, LA, 70803, USA* **2** *The Hymenoptera Institute, 116 Franklin Ave., Redlands, CA, 92373, USA*

Corresponding author: Ilgoo Kang (ikang1@lsu.edu)

Academic editor: Jose Fernandez-Triana | Received 6 August 2021 | Accepted 21 September 2021 | Published 29 October 2021

http://zoobank.org/5617D391-3973-4570-9722-E67A3EDF477E

Citation: Kang I, Sharkey MJ, Diaz R (2021) Revision of the genus *Schoenlandella* (Hymenoptera, Braconidae, Cardiochilinae) in the New World, with a potential biological control agent for a lepidopteran pest of bitter gourd (*Momordica charantia* L.). Journal of Hymenoptera Research 86: 47–61. https://doi.org/10.3897/jhr.86.72690

Abstract

Schoenlandella Cameron, 1905 is the second largest genus of Cardiochilinae. Most members are recorded from the Old World, with a small number of species in the New World. Herein, the New World species of *Schoenlandella* are revised based on morphological data. This work entails a description of a new species: *S. montserratensis* Kang, **sp. nov.** and potential lepidopteran host information of the new species associated with bitter gourds on the Caribbean Island of Montserrat. *Schoenlandella diaphaniae* (Marsh, 1986) and *S. gloriosa* Mercado & Wharton, 2003 are re-described, and a key to species of New World *Schoenlandella* is provided. The taxonomic status of *Schoenlandella* is discussed.

Keywords

Caribbean Islands, Crambidae, melonworm moth, Neotropical region, parasitoid wasp

Introduction

Schoenlandella Cameron, 1905 is the second largest genus of the subfamily Cardiochilinae (Yu et al. 2016). All the members of the genus, which host data are available, are solitary endoparasitoids of exposed-feeding lepidopteran larvae such as

Copyright *Ilgoo Kang et al.* This is an open access article distributed under the terms of the Creative Commons Attribution License (CC BY 4.0), which permits unrestricted use, distribution, and reproduction in any medium, provided the original author and source are credited.

Chrysodeixis includens (Walker, 1858) (Soybean looper; Noctuidae) and *Chloridea virescens* (Fabricius, 1777) (Tobacco budworm; Noctuidae). Fifty-four species have been included in the genus worldwide, and most members are recorded from the Old World, especially from the Afrotropical and Australian regions (Dangerfield et al. 1999; Mercado and Wharton 2003; Yu et al. 2016). Three species have been recorded from the New World: *S. diaphaniae* (Marsh, 1986), *S. gloriosa* Mercado & Wharton, 2003, and *S. longimala* (Mao, 1945).

Herein, the New World species of *Schoenlandella* are revised. This includes a new species description, potential host information of *S. montserratensis* Kang sp. nov., and a key to species of New World *Schoenlandella*. Previously described species of New World *Schoenlandella* are re-described.

Material and methods

Specimen information

During 2019, braconid wasps collected from a bitter gourd field in Montserrat by Dr Chris Malumphy's team (Fera Science Ltd.) were shipped to the first author (IK). Two specimens were identified as a new species of *Schoenlandella* based on morphological data, and potential lepidopteran hosts were identified.

Specimens were borrowed from the following institutions:

- Fera Sciences Ltd (London, UK);
- Hungarian Natural History Museum (**HNHM**: Budapest, Hungary);
- Illinois Natural History Survey (**INHS**: Champaign, Illinois, USA);
- Museo de Insectos, University of Costa Rica (**MICR**: San José, Costa Rica);
- Texas A&M University Insect Collection (**TAMU**: College Station, Texas, USA).

The holotype and sole paratype of *S. montserratensis* Kang sp. nov. will be deposited in the Natural History Museum in London (**NHML**: London, UK).

Morphological analysis

A Leica MZ75 stereomicroscope was used to examine specimens. Morphological terminology used in this review are mostly based on Dangerfield et al. (1999) and Sharkey and Wharton (1997), supplemented by terms on the Hymenoptera Anatomy Consortium website (http://portal.hymao.org/projects/32/public/ontology/, accessed in September 2020). Terms for surface sculpture follow Harris (1979). The following acronyms are used for morphological terms: T1: first metasomal tergite; T2: second metasomal tergite; T3: third metasomal tergite; T4: forth metasomal tergite; T6: sixth metasomal tergite. Color images were taken with a Visionary Digital BK Plus imaging system (Dun, Inc.) equipped with a Canon EOS

5DS DSLR camera. Multiple images were stacked using Zerene Stacker v.1.04 (Zerene Systems LLC.) and edited in Adobe Photoshop CS 6 and Photoshop CC (Adobe Systems, Inc). Body parts were measured also via Adobe Photoshop CS 6 and Photoshop CC. Each number in parentheses in species descriptions indicate 0.01× the actual size of each body part. The unit of length is mm. For example, 12 and 123 in parentheses (12:123) indicate 0.12 mm and 1.23 mm, respectively. The distribution map of the new species was generated using QGIS 3.10.0 (QGIS Development Team 2019). The Google terrain map was downloaded using QuickMapServices plugin.

Results

Taxonomy

Schoenlandella Cameron, 1905

Schoenlandella Cameron, 1905 (Cameron 1905a). Type Species: *Schoenlandella nigromaculata* Cameron, 1905 (Cameron 1905a) by subsequent designation by Viereck, 1914 (synonymized with *Cardiochiles* Nees, 1819 by Szépligeti, 1911). Removed from synonymy by Whitfield & Dangerfield, 1997.

Ernestiella Cameron, 1905 (Cameron 1905b) synonymized with *Schoenlandella* Viereck, 1914. Type species: *Ernestiella nigromaculata* Cameron 1905 (Cameron 1905b).

Diagnosis (based on Dangerfield et al. (1999) with additions and modifications). Diagnostic characters of *Schoenlandella* were described in Dangerfield et al. (1999), based mostly on Old World species. The following are diagnostic features based on both Old World and New World members.

Members of *Schoenlandella* can be distinguished from species of other cardiochiline genera by the following characters: ***Head*:** possessing 32–44-segmented antenna; densely setose eye (Figs 2C, 4C); two clypeal tubercles with sharp or smooth apical margin (Fig. 1C); short to elongate malar space; bidentate mandible; six-segmented maxillary palpus; four-segmented labial palpus; absence of occipital carina; elongate galea, at least as long as malar space in lateral view (Note: narrower than galeae of members of *Cardiochiles* Nees, 1819) (Figs 1A, 2A, 4A); glossa elongate and deeply bilobed if entirely spread (Fig. 4A). ***Mesosoma*:** notaulus finely crenulate; scutellar sulcus crenulate; posterior scutellum without cup-like pit; pronotum mostly smooth; mesopleuron mostly smooth; epicnemial carina absent; metapleuron rugulose; mesosternal sulcus crenulate; propodeum rugulose; propodeum with completely developed areola. ***Wings*:** stigma of forewing moderate to broad; (RS+M)a of forewing present; 1r of forewing absent; spectral 3r of forewing reaching at basal fifth to half, if absent, examine characters of mouthparts and hypopygium; RS vein of forewing angled or curved (Fig. 4F); 1a of forewing absent

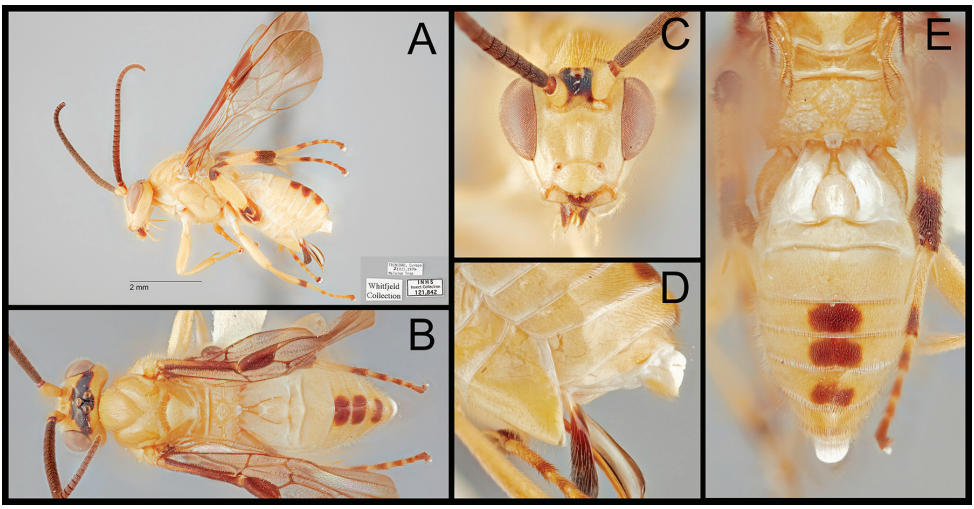

Figure 1. *Schoenlandella diaphaniae*, non-type **A** lateral habitus **B** dorsal habitus **C** anterior head **D** ventro-lateral metasoma **E** dorsal propodeum and mesonotum.

(Note: if present, the vein is nebulous); 2–1A of hind wing usually absent. ***Legs*:** tarsal claw pectinate with sharp or obtuse apical tooth; hind basitarsus cylindrical (Fig. 1A) or slightly expanded (Fig. 4A) (Note: not nearly as expanded as in *Hartemita* Cameron, 1910); ***Metasoma*:** lateral suture of T1 absent posteriorly; T2 and T3 entirely smooth; hypopygium apically acute in lateral view (Fig. 1D); hypopygium uniformly sclerotized (Fig. 1D); median longitudinal fold of hypopygium absent (Fig. 1D) (Note: if present, the fold is entirely sclerotized or only slightly desclerotized (Figs 2D, 4D)); ovipositor slightly downcurved (Figs 1A, 2D); ovipositor sheath < ~0.6 × length of hind tibia.

Key to species of the genus *Schoenlandella* of the Neotropical region

1 **A.** Body mostly melanic..... ***S. longimala* (Mao, 1945)** Note: Based on images of the holotype on the NMNH website (https://collections.nmnh.si.edu/search/ento/?ark=ark:/65665/3a9805bdd51964c16838984ab0e197ed9, accessed September 2021)

– **B.** Body mostly orange or yellow pale **2**

2 **A.** Malar space < ~0.33 × longer than eye height in anterior view, **AA.** forewing entirely infuscate ..... ***S. montserratensis* Kang, sp. nov.**

– **B.** Malar space about ~0.50 × longer than eye height in anterior view, **BB.** forewing apically infuscate **3**

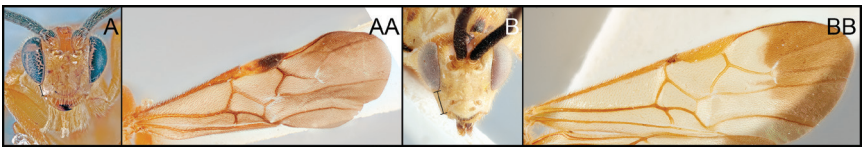

3 **A.** Forewing basally hyaline, and stigma entirely melanic, **AA.** apex of clypeal tubercle sharply angled ..... ***S. diaphaniae*** **(Marsh, 1986)**

– **B.** Forewing basally pale yellow, and stigma entirely pale, **BB.** apex of clypeal tubercle relatively smooth ..... ***S. gloriosa*** **Mercado & Wharton, 2003**

Schoenlandella diaphaniae **(Marsh, 1986)**
Fig. 1A–E

Cardiochiles diaphaniae Marsh, 1986 (Marsh 1986)
Schoenlandella diaphaniae (Marsh, 1986) (Dangerfield et al. 1999)

Material examined. ***Non-type specimen*:** Trinidad and Tobago • 1♀; Curepe, Trinidad and Tobago; 21 Jul. 1978. Malaise Trap. Deposited in INHS.

Diagnosis. Members of *S. diaphaniae* are distinguished from members of *S. gloriosa* by having shorter lower face and malar space (Fig. 1C); basally hyaline forewing (Fig. 1A); stigma entirely melanic (Fig. 1A).

Description. Marsh (1986) described color of the species and some morphological characters in his species description. Here, the species is re-described based on a specimen collected in Trinidad and Tobago.

Body length 4.5–5.8 mm (Marsh 1986). Antenna length: ~4.2 mm. Forewing length: ~5.5 mm. ***Head*:** Antenna 34-segmented. Eye length ~0.45 × longer than its height (40:89). Dorsal width of lower face as long as its height (81:81); Malar space ~0.40 × longer than height of eye in anterior view (32:80), ~2.13 × longer than basal width of mandible (32:15) (Fig. 1C). Clypeus ~1.53 × longer than its width (49:32); clypeal tubercles with sharp margins (Fig. 1C). Galea as long as malar length in lateral view (32:32), with curved apical margin (Fig. 1A). ***Mesosoma*:** Scutellar sulcus with five to six crenulae. Postscutellar depression present. Propodeum rugulose; median areola of propodeum diamond-shaped, median length as long as its width; propodeum with median transverse carina reaching lateral margin. Pronotum mostly smooth with incomplete posteroventral carina reaching posterior margin. Mesopleuron mostly smooth and polished; precoxal sulcus medially present with five crenulae. Metapleuron rugulose. Mesosternal sulcus crenulate. ***Legs*:** Basal spur on mid tibia ~0.83 × mid-basitarsus (49:59). Hind femur medially ~0.33 × broader than its length (45:137). Basal spur on hind tibia ~0.66 × longer than hind basitarsus (60:90). Hind basitarsus cylindrical. Hind tarsal claw pectinate with five teeth; apical tooth basally rounded and apically angled; basal four teeth sharp. ***Wings*:** Forewing second submarginal cell its maximum width ~2.87 × longer than its maximum length (89:31); 3r absent; Rs broken basally and angled at a basal sixth; stigma about ~3.44 × longer than width medially (93:27).

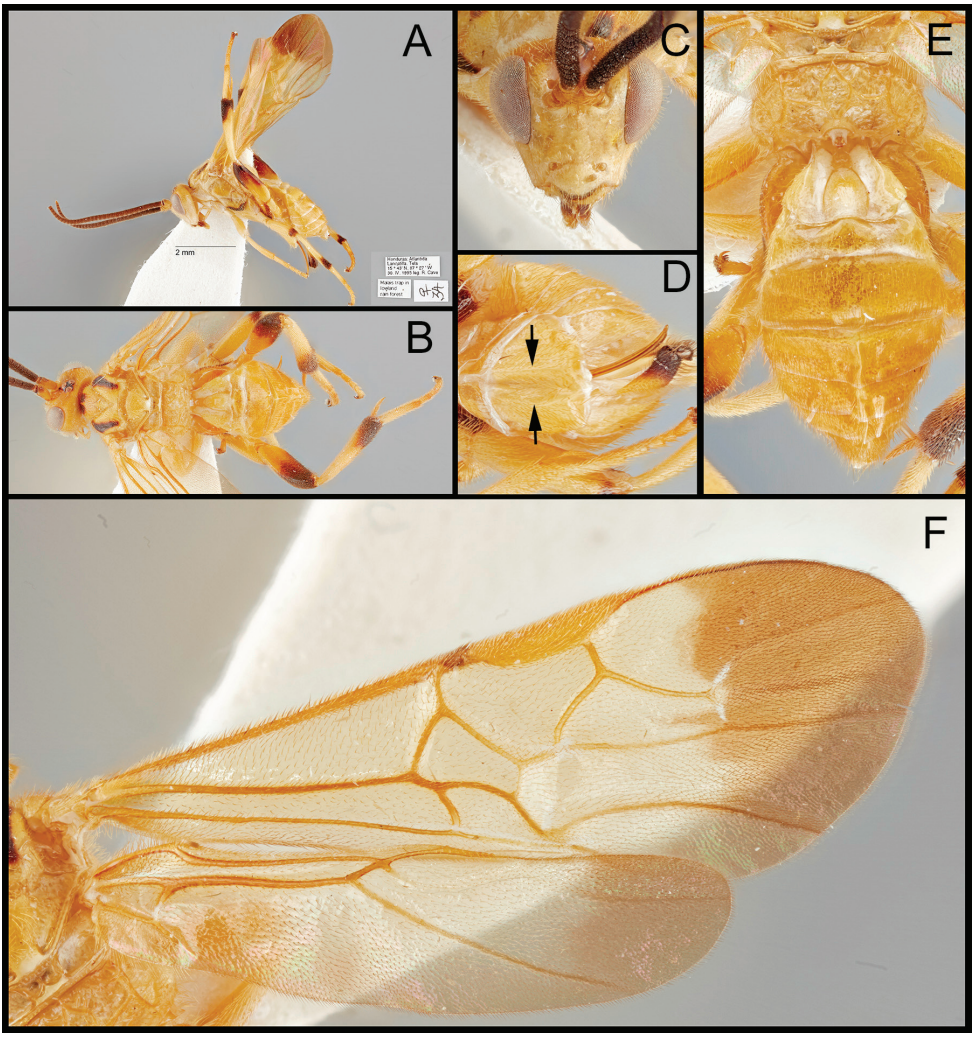

Figure 2. *Schoenlandella gloriosa*, non-type Honduras **A** lateral habitus **B** dorsal habitus **C** anterior head **D** ventral metasoma; arrow: median invagination on hypopygium **E** dorsal propodeum and mesonotum **F** wings.

Hind wing 2–1A present at basal third (Fig. 1A). ***Metasoma*:** Medial length of T1 ~2.59 × longer than medial length of T2 (75:29). Medial length of T2 ~0.22 × longer than its apical width (29:129). T3 about ~1.66 × longer than T2 medially (48:29). Hypopygium entirely sclerotized, medially with shallow area, without median longitudinal fold (Fig. 1D). Ovipositor moderately downcurved. Protruded ovipositor sheath moderately downcurved, ~0.57 × longer than hind tibia (101:176), slightly broadened apically, anterior 2/5 depilous and posterior 3/5 pilose apically with long setae.

Color. Body mostly bright yellow; the following areas melanic: flagellomeres, pedicel mostly, outer scape; ocellary field and frons dorsally, labrum, apical mandible, galea mostly, mid tibia apically, hind coxa apically, hind trochanter and trochantellus, hind

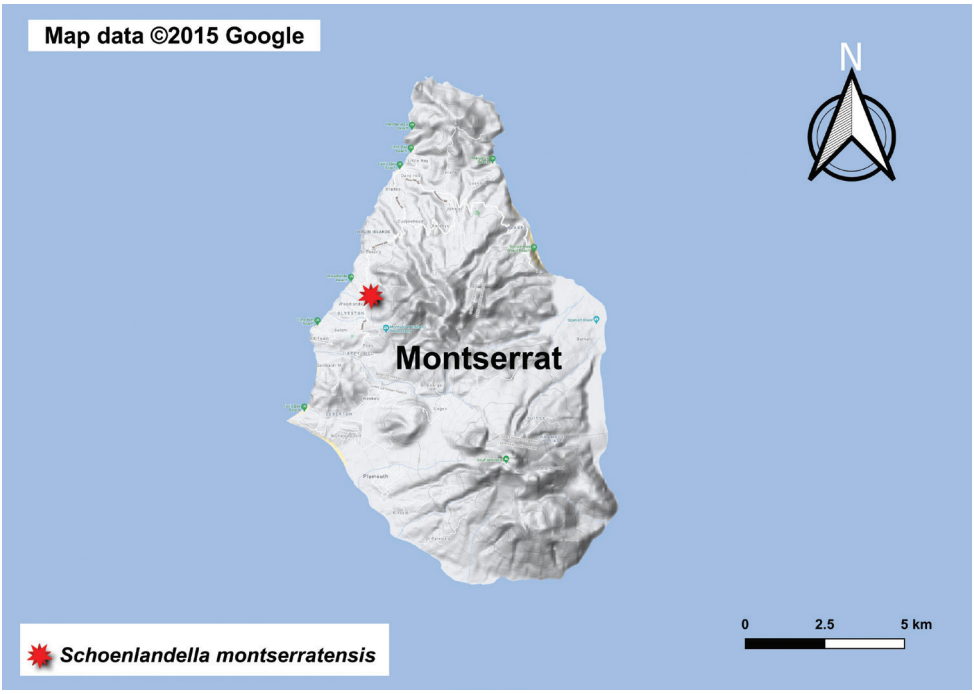

Figure 3. Distribution map of *S. montserratensis* sp. nov. in Montserrat.

femur basally and apically, hind tibia apically, hind tarsomeres apically, entire ovipositor sheath. T4–T6 medially (Fig. 1E). Wings basally hyaline and apically infuscate, C+SC+R vein in forewing mostly melanic, stigma mostly melanic.

Male. See Marsh (1986).

Hosts. *Diaphania nitidalis* (Stall) and *D. hyalinata* (L.) (Marsh 1986).

Distribution. Colombia, Venezuela, and Trinidad and Tobago.

Schoenlandella gloriosa Mercado & Wharton, 2003

Fig. 2A–F

Material examined. ***Paratypes*:** Mexico • 1♀; 3 mi E Papantla, Veracruz, Mexico; 7 Jun. 1965; leg. Burke, Meyer, Schaffner • 1♀; 2 mi SE Tecpan de Galeana, Guerrero, Mexico; 14 Jul. 1966; leg. P.M and P.K Wagner • 2♂; Hotel Covandonga, 12 km S Valles, Ruta 85, San Luis Potosi, Mexico; 27–29 Jun. 1981; leg. C. Porter, L. Stange. Deposited in TAMU. ***Non-type material*:** Costa Rica • 1♀; 10 km NW Cañas, Mojica, Guanacaste, Costa Rica; 26 Sep.–10 Oct. 2011; leg. P. Hanson. Deposited in MICR. Honduras • 1♀; Tela, Lancetilla, Atlántida, Honduras; 15°43'N, 87°27'W; 30 Apr. 1995; leg. R. Cave. 1♀; same as previous except for the collecting date, 15 May. 1995. 1♂; same as previous except the collecting date, 31 Aug. 1995. Deposited in HNHM.

Diagnosis. Members of the *S. gloriosa* are nearly identical to *S. diaphaniae*. The following combination of characters differentiate *S. gloriosa* from *S. diaphaniae*: face

concave; malar space relatively elongate (~0.50 × longer than height of eye in anterior view) (Fig. 2C); two clypeal tubercles with smooth margins (Fig. 2C); forewing basally yellow and apically infuscate; stigma entirely pale; forewing with junction of angled Rs not swollen (Fig. 2F).

Description. Modified from Mercado and Wharton (2003), including additional characters.

Body 5.5–8.0 mm. ***Head*:** Antenna 32–34-segmented. Eye length ~0.41 × longer than its height (35:85) in lateral view. Dorsal width of lower face ~1.05 × longer than height of lower face (79:75). Clypeus 1.20–1.53 × longer than its width, two clypeal tubercles with smooth margin (Fig. 2C). Malar space 0.47–0.50 × longer than height of eye in anterior view (35:75–40:80), 2.75–3.42 × longer than basal width of mandible (33:12–41:12). Galea 1.30–1.40 × longer than malar length as viewed laterally (43:33–56:40) (Fig. 2A). ***Mesosoma*:** Scutellar sulcus with 5–7 crenulae. Propodeum with median transverse carina reaching lateral margin. Pronotum weakly carinate medially. Mesopleuron mostly smooth; precoxal sulcus smooth, not reaching posterior margin. ***Legs*:** Basal spur on mid tibia 0.83–0.90 × mid-basitarsus length. Hind femur medially 0.31–0.32 × broader than its length (52:164–48:155). ***Wings*:** Forewing: maximum width of second submarginal cell ~2.26× longer than maximum length (113:50); 3r absent; Rs vein angled at basal fourth (Fig. 2F). Hind wing 2–1A present as basal stump (Fig. 2F). ***Metasoma*:** Medial length of T1 2.00–2.47 × longer than medial length of T2 (78:39–75:30). Medial length of T2 0.21–0.26 × longer than its apical width (30:140–39:149). T3 about 1.46–1.60 × longer than T2 medially (57:39–48:30). Hypopygium evenly sclerotized, median longitudinal fold absent (Note: A weakly depressed medial longitudinal area is present in females collected in Honduras, but never membranous and folded) (Fig. 2D). Ovipositor moderately downcurved. Protruded ovipositor sheaths moderately downcurved, 0.45–0.50 × longer than hind tibia, broadened apically, anteriorly depilous and moderately pilose apically with long setae.

Color. See Mercado and Wharton (2003). Melanic areas of the Costa Rican specimen (female) and Mexican specimens are slightly darker than specimens collected in Honduras.

Male. See Mercado and Wharton (2003).

Host. Unknown.

Distribution. Costa Rica, Honduras, and Mexico.

Schoenlandella longimala **(Mao, 1945)**

Cardiochiles longimala Mao, 1945 (Mao 1945)
Schoenlandella longimala (Mao, 1945) (Dangerfield et al. 1999)

Type material. ***Holotype*:** Mexico • ♂, Guadalajara, Mexico; 2 Aug. 1914; Deposited in NMNH.

Diagnosis (based on images of the holotype on the NMNH website). Body mostly black except for legs. Malar space shorter than basal width of mandible. Mouthparts moderately elongated. Scutellar sulcus with six crenulae. Lateral side of scutellum mostly rugulose. Pronotum medially rugose, with median areola anteriorly angled. Forewing entirely infuscate; stigma entirely melanic; 3r vein absent; 1a present as a nebulous vein.

Description. See Mao (1945).

Host. Unknown.

Distribution. Mexico.

Schoenlandella montserratensis **Kang, sp. nov.**
http://zoobank.org/D22783D0-15B6-422E-9989-34760DA85579
Fig. 4A–F

Material examined. ***Holotype*****:** Montserrat • ♀; 16°45'34.19"N, 62°13'1.58"W; leg. Elvis Gerald (Ref. CM-Mt-2019–41) woodlands, private farm. Single adult on *Momordica charantia* L. (bitter melon), hand caught in a plastic pot. ***Paratype*** same data as for holotype.

Diagnosis. Members of *Schoenlandella montserratensis* sp. nov. are distinguished from other New World *Schoenlandella* species by having shorter malar space (Fig. 4C); longer mouthparts (Fig. 4C); stigma basally pale and apically melanic (Fig. 4F); 3r vein of forewing present at basal half (Fig. 4F).

Description. Body 4.21–4.40 mm. Forewing length: ~4.45 mm (holotype). Antenna length: ~3.25 mm (paratype). ***Head*****:** Antenna 34-segmented (paratype). Eye length ~0.52 × longer than its height (31:60). Malar space slightly shorter than basal width of mandible. Clypeus ~2.08 × longer than its width (50:23); two clypeal tubercles with smooth margins. Galea ~2.12 × longer than malar space in lateral view (36:17), apically narrowed. ***Mesosoma*****:** Scutellar sulcus with five crenulae. Propodeal median transverse carina reaching lateral margin. Pronotum medially crenulate, ventrally costate. Mesopleuron mostly smooth; precoxal sulcus strongly crenulate with ~10 crenulae, not reaching posterior margin. ***Legs*****:** Basal spur on mid tibia ~0.88 × mid-basitarsus (30:34). Basal spur on hind tibia ~0.68 × longer than hind basitarsus (36:53). Hind basitarsus laterally broaden. Tarsal claw pectinate with five teeth; apical tooth obtuse, other remaining teeth sharp. ***Wings*****:** Forewing second submarginal cell width ~2.79 × longer than height (78:28); 3r apparently present at basal half and slightly curved; Rs angled at basal two-fifths; stigma about ~3.36 × longer than wide medially (74:22); 1a absent (Fig. 4F). Hind wing 2–1A absent (Fig. 4F). ***Metasoma*****:** Medial length of T1 ~2.68 × longer than medial length of T2 (59:22). Medial length of T2 ~0.20 × longer than its apical width (22:110). T3 entirely smooth, ~1.27 × longer than T2 medially (28:22). Hypopygium surface entirely sclerotized with a distinct median longitudinal fold (Fig. 4D). Ovipositor slightly downcurved; protruded ovipositor sheath ~0.40 × longer than hind tarsus, broadened apically.

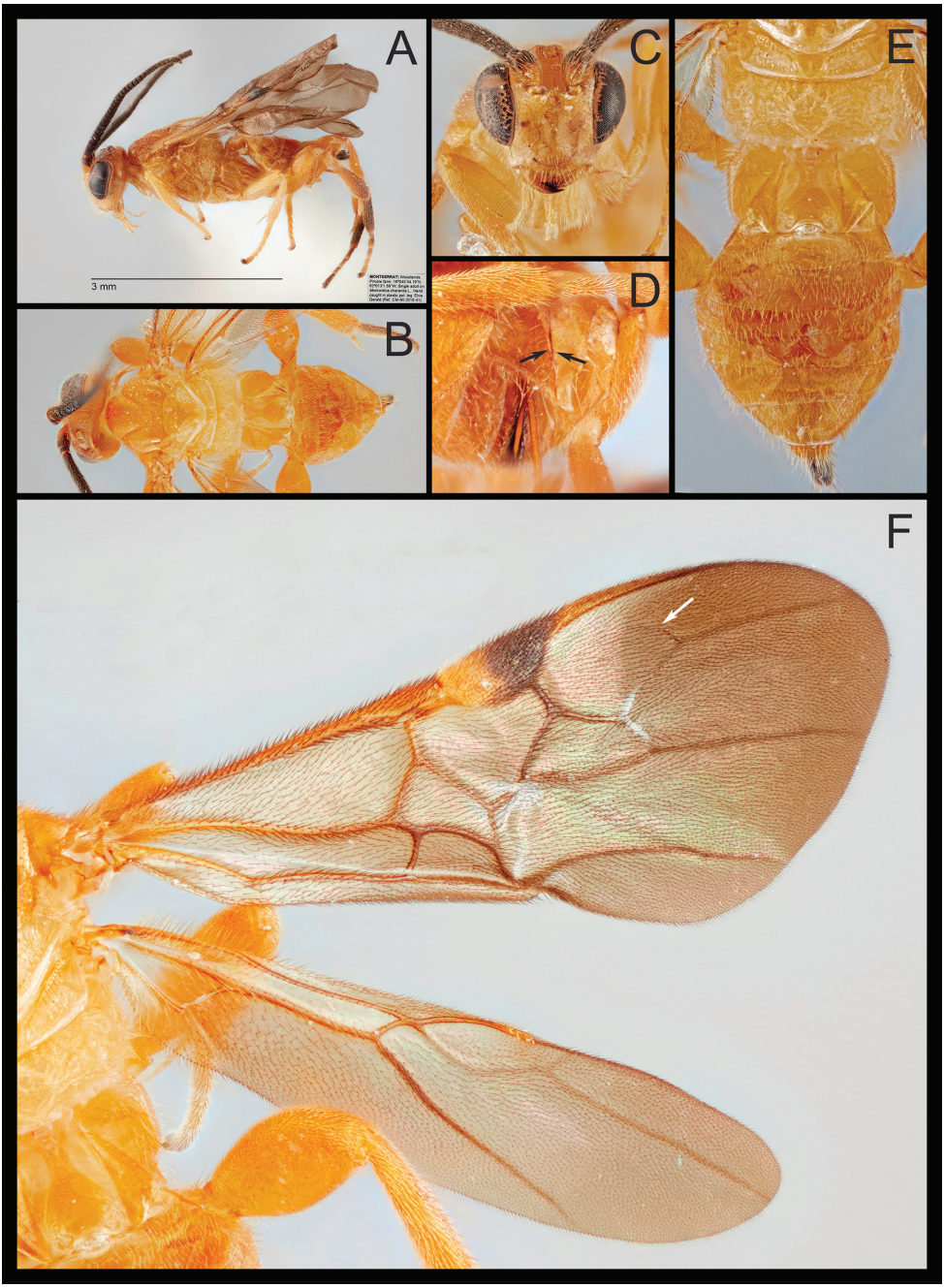

Figure 4. *Schoenlandella montserratensis*, sp. nov. **A** lateral habitus **B** dorsal habitus **C** anterior head **D** ventral metasoma; arrow: median fold on hypopygium **E** dorsal propodeum and mesonotum **F** wings; arrow: 3r vein on forewing.

Color. Body mostly pale orange; the following areas melanic: apical scape, pedicel, flagellomere, apical mandible, hind tarsus, external ovipositor sheaths. Wings entirely lightly infuscate, stigma dark brown at apical half.

Etymology. This species is named after the collecting site, "Montserrat", a volcanic Caribbean Island.

Host. Unknown but see details in the following discussion section.

Distribution. *Schoenlandella montserratensis* sp. nov. is only known from Montserrat (Fig. 3).

Discussion

Taxonomic status of *Schoenlandella* and character discussion

The validity of the taxonomic status of *Schoenlandella* Cameron has fluctuated several times before the current work. Dangerfield et al. (1999) indicated that species of *Schoenlandella* could be easily distinguished from all other cardiochiline genera based on the following five characters: conspicuously setose eyes; long and deeply bilobed glossa; elongate blade-like galea; presence of spectral 3r of forewing (if absent, members of the genus have relatively short mouthparts); evenly sclerotized hypopygium (if a median longitudinal fold is present, the surface is not membranous). The genus was resolved as a monophyletic group in the phylogeny in Dangerfield et al. (1999) based on morphological data. However, Mercado and Wharton (2003) and Papp (2014) indicated difficulty in distinguishing members of *Schoenlandella* from those of *Cardiochiles* Nees. Dangerfield et al. (1999) and Mercado and Wharton (2003) retained *Schoenlandella* as a valid genus, and the latter author subsumed the genus into *Cardiochiles* as a subgenus. Edmardash et al. (2018) treated *Schoenlandella* as a valid genus.

Only one study partially indicated genus-level relationships of Cardiochilinae. Murphy et al. (2008) presented three phylogenies based on seven genes. Even though the phylogenies focused on subfamily-level relationships of microgastroid subfamilies, genus-level relationships of five cardiochiline genera were included. *Cardiochiles* and *Schoenlandella* were resolved as polyphyletic in a clade with a rare Australian genus, *Gwenia* Dangerfield, Austin & Whitfield in their Maximum Parsimony phylogeny. However, the other two phylogenies resulting from Maximum Likelihood and Bayesian phylogenetic analyses using the same molecular data indicated that members of each genus were well-clustered even though they were recovered as paraphyletic. It should be noted that Murphy et al. (2008) treated *C. minutus* (Cresson) as a member of *Schoenlandella* and indicated *Cardiochiles* and *Schoenlandella* were polyphyletic. We treat *S. minuta* in Murphy et al. (2008) as *C. minutus* (Cresson) since Mercado and Wharton (2003) transferred the species to *Cardiochiles*.

In the current work, we examined specimens of both New World and Old World *Schoenlandella* species. Old World members mostly possess and share the five diagnostic characters defined by Dangerfield et al. (1999). We confirmed that specimens of

S. montserratensis sp. nov. collected in Montserrat are the first New World species having the five diagnostic characters. Of the other three New World species, specimens of *S. diaphaniae* and *S. gloriosa* were examined, and morphological characters of *S. longimala* were confirmed based on descriptions of Mao (1945) and images of the holotype on the NMNH website (https://collections.nmnh.si.edu/search/ento/, accessed September 2020). All New World species have dense eye setae consistent with Old World members. Dangerfield et al. (1999) indicated that most *Schoenlandella* members possess elongate mouthparts. Tucker et al. (2012) discussed two hypotheses regarding the elongation of mouthparts of the Afrotropical agathidine genus *Camptothlipsis* Enderlein and preferred the hypothesis that the members with elongate mouthparts are specialized nectar feeders, dependent on flowers that their host caterpillars feed on. This has been confirmed in the case of *Agathis malvacearum* Latreille (Juhala 1967). Most other cardiochilines as well as members of *Heteropteron* Brullé, which was resolved as the most ancestral cardiochiline genus (Dangerfield et al. 1999; Murphy et al. 2008) possess short mouthparts. The elongate mouthparts most likely evolved independently in *Schoenlandella*. Some Old World members and the three New World species in the current work possess relatively shorter mouthparts than most *Schoenlandella* species (but narrower and longer than the typical mouthparts of *Cardiochiles*). This seems to be a secondary loss due to environmental changes like host flower traits. In addition, IK confirmed that females of *S. diaphaniae* and *S. gloriosa* do not possess the median membranous fold or area in the hypopygium. The hypopygial character of *S. longimala* could not be confirmed because the holotype is male. Additionally, most *Schoenlandella* members possess an angled RS vein in the forewing, which is not present in *Cardiochiles*. They also have relatively longer second submarginal cells than members of *Cardiochiles*. Despite the contradictory opinions of Papp (2014) and Murphy et al. (2008), we treat *Schoenlandella* as a valid genus as in Dangerfield (1999) and Mercado and Wharton (2003) and place the New World species in the genus. IK is conducting molecular analysis to generate a phylogeny to determine genus-level relationships of cardiochilines based on a larger taxon sample than previous research. We expect that the phylogeny will help resolve the taxonomic issue in the near future and predict that *Schoenlandella* will be confirmed as a valid genus with support of shared morphological characters such as elongate mouthparts, angled Rs vein and elongated submarginal cell of the forewing, and evenly sclerotized surface of the hypopygium.

Potential host information of *S. montserratensis* sp. nov.

Female adults of *S. montserratensis* sp. nov. were collected in a bitter gourd field in Montserrat in 2019. Four potential lepidopteran host species were collected in the same location in the same period: *Diaphania hyalinata* (L., 1767) (Melonworm moth; Crambidae); *Plutella xylostella* (L. 1758) (Diamondback moth; Plutellidae); *Calpodes ethlius* (Larger canna leafroller; Hesperiidae), and unidentified bagworm (Psychidae) (Dr Chris Malumphy pers. comm.). Among these species, the melonworm moth caterpillars were the most serious pests in the field. Because other *Schoenlandella* species chiefly attack caterpillars of Crambidae and Noctuidae (Ta-

Table 1. Host information of each *Schoenlandella* species prior to the current study.

***Schoenlandella* species**	**Lepidopteran host**	**Source(s)**
S. diaphaniae (Marsh, 1986)	*Diaphania hyalinata* (L., 1767) (Crambidae)	(Marsh 1986)
S. fulva (Cameron, 1907)	*Omiodes indicata* (F., 1775) (Crambidae), *Spoladea recurvalis* (F., 1775) (Crambidae), *Pramadea lunalis* (Guenée, 1854) (Crambidae)	(Odak and Dhamdhere 1968)
S. goosei (Dangerfield & Austin, 1995)	*Crocidolomia pavonana* (F., 1794) (Crambidae)	(Dangerfield and Austin 1995)
S. hymeniae (Fischer & Parshad, 1968)	*Spoladea recurvalis* (F., 1775) (Crambidae)	(Fischer and Parshad 1968)
S. nigromaculata Cameron, 1905	*Helicoverpa armigera* (Hübner, 1808) (Noctuidae)	(Nyiira 1970)
S. sahelensis (Huddleston & Walker, 1988)	*Heliocheilus albipunctella* (de Joannis, 1925) (Noctuidae)	(Bhatnagar 1988) (Huddleston and Walker 1988)
S. trimaculata Cameron, 1905	*Helicoverpa armigera* (Hübner, 1808) (Noctuidae)	(Coaker 1959) (Risbec 1960)
S. uniformis (Turner, 1918)	*Helicoverpa sp.* (Noctuidae)	(Chadwick and Nikitin 1976) (Dangerfield and Austin 1995)
S. variegata (Szépligeti, 1913)	*Helicoverpa armigera* (Hübner, 1808) (Noctuidae)	(Bhatnagar 1988) (Huddleston and Walker 1988)

ble 1), the melonworm moth caterpillar may be the preferred host of *S. montserratensis* sp. nov. If females of the new species are host specific and attack the melonworm moth caterpillars as expected, females of *S. montserratensis* sp. nov. should be developed as effective biological control agents for the melonworm moth. Detailed biology of *S. montserratensis* sp. nov. and its host range will need to be confirmed in further investigations (i.e., rearing caterpillars and collecting parasitoids of the host caterpillars). Future studies should investigate the effectiveness of *S. montserratensis* sp. nov. to parasitize the melonworm moth and determine its potential as a biological control agent against melonworm moth.

Acknowledgements

Thanks to Dr Chris Malumphy (Fera Science Ltd.) who led the collecting team in Montserrat as well as Mr Rob Deady (Fera Science Ltd.) who sent the specimens of *S. montserratensis* sp. nov. We are also grateful to LSU AgCenter for financial support and Dr Karen Wright in TAMU, Dr Paul Hanson in the MICR, Dr Tommy McElrath in the INHS, and Dr Zoltan Vas in the HNHS for the loans of specimens. We also thank Dr James Whitfield who donated cardiochiline specimens to INHS, Dr Michael Stout for his support, and Mr Josh Snook for reviewing the manuscript. In particular, IK would like to acknowledge Dr Chris Carlton and Ms Victoria Bayless for their encouragement and supports.

References

Ashmead WH (1894) Report upon the parasitic Hymenoptera of the island of St. Vincent. Linnean Society 25: 56–254.

Ashmead WH (1900) Report upon the Aculeate Hymenoptera of the islands of St. Vincent and Grenada, with additions to the parasitic Hymenoptera and a list of the described Hy-

menoptera of the West Indies. Transactions of the Entomological Society of London 48: 207–367. https://doi.org/10.1111/j.1365-2311.1900.tb02379.x

Bhatnagar VS (1988) New records of Cardiochiles (Braconidae: Hymenoptera) on *Heliothis armigera* (Hb.) and *Raghuva albipunctella* de Joannis in the Sahel. Current Science 57(16): 904–905.

Brullé GA (1846) Suites á Buffon: histoire naturelle des insects: hyménoptéres. Paris Roret 4: 1–689. https://doi.org/10.5962/bhl.title.9005

Cameron P (1905a) On the Hymenoptera of the Albany Museum, Grahamstown, South Africa (First paper). Record of the Albany Museum 1: 161–175.

Cameron P (1905b) On the phytophagous and parasitic Hymenoptera collected by Mr. E. Green in Ceylon. Spolia zeylanica 3: 67–143.

Cameron P (1907) Descriptions of two new genera and four new species of Indian parasitic Hymenoptera. Zeitschrift für Systematische Hymenopterologie und Dipterologie 7: 462–466.

Coaker TH (1959) Investigations on *Heliothis armigera* (Hb.) in Uganda. Bulletin of Entomological Research 50(3): 487–506. https://doi.org/10.1017/S0007485300053062

Cresson, E. (1873). Descriptions of North American Hymenoptera, No. 5. The Canadian Entomologist 5(3): 51–54. https://doi.org/10.4039/Ent551-3

Dangerfield PC, Austin AD (1995) Revision of the Australasian species of Cardiochilinae (Hymenoptera: Braconidae). Invertebrate Systematics 9(3): 387–445.

Dangerfield PC, Austin AD, Whitfield JB (1999) Systematics of the world genera of Cardiochilinae (Hymenoptera: Braconidae). Invertebrate Systematics 13(6): 917–976. https://doi.org/10.1071/IT98020

Edmardash YA, Gadallah NS, Sharkey MJ (2018) Revision of the subfamily Cardiochilinae Ashmead, 1900 (Hymenoptera: Braconidae) in Egypt, with new records and a new species. Journal of Natural History 52(5–6): 269–297. https://doi.org/10.1080/00222933.2017.1420834

Enderlein G (1920) Zur Kenntnis aussereuropäischer Braconiden. Archiv für Naturgeschichte (A) 84: 51–224. https://doi.org/10.5962/bhl.part.13627

Fischer M, Parshad B (1968) A new reared braconid-fly (Hymenoptera) from India. Polskie Pismo Entomologiczne 38: 807–810.

Harris RA (1979) Glossary of surface sculpturing. Occasional Papers in Entomology 28: 1–31.

Huddleston T, Walker AK (1988) *Cardiochiles* (Hymenoptera: Braconidae), a parasitoid of lepidopterous larvae, in the Sahel of Africa, with a review of the biology and host relationships of the genus. Bulletin of Entomological Research 78(3): 435–461. https://doi.org/10.1017/S0007485300013201

Juhala C (1967) Notes on parasitic Hymenoptera associated with a Gelechiid moth, *Metzneria lappella*, in the Common Burdock, and description of a new species of *Agathis* (Braconidae). Annals of the Entomological Society of America 60(1): 95–97.

Latreille PA (1805) Histoire naturelle generale et particulière des crustacés et des insectes 13. F. Dufart, Paris, 432 pp. https://doi.org/10.5962/bhl.title.15764

Mao YT (1945) Synopsis of the Mexican species of *Cardiochiles* Nees (Hymenoptera: Braconidae). Pan-Pacific Entomologist 21(4): 125–134.

Marsh PM (1986) A new species of Cardiochiles (Hymenoptera: Braconidae) introduced into Florida to control *Diaphania* spp. (Lepidoptera: Pyralidae). Proceedings of the Entomological Society of Washington 88(1): 131–133.

Mercado I, Wharton RA (2003) Mexican cardiochiline genera (Hymenoptera: Braconidae), including a preliminary assessment of species-groups in *Toxoneuron* Say and *Retusigaster* Dangerfield, Austin and Whitfield. Journal of Natural History 37(7): 845–902. https://doi.org/10.1080/00222930110097167

Nees von Esenbeck CG (1819) Appendix ad JLC Gravenhorst conspectum generum et familiarum Ichneumonidum, genera et familias Ichneumonidum adscitorum exhibens. Nova Acta Leopid. Carol. 9: 299–310.

Nyiira ZM (1970) A note on the natural enemies of lepidopterous larvae in cotton bolls in Uganda. Annals of the Entomological Society of America 63(5): 1461–1462. https://doi.org/10.1093/aesa/63.5.1461

Odak SC, Dhamdhere SV (1970) New record of Hymenopterous parasites of *Sylepta lunalis* Guen (Lepidoptera: Pyralidae), a pest of grapevines. Indian Journal of Entomology 32(4): e395.

Papp J (2014) A revisional study on Szépligeti's cardiochiline type specimens deposited in the Hungarian Natural History Museum, Budapest (Hymenoptera, Braconidae: Cardiochilinae). Annales Historico-Naturales Musei Nationalis Hungarici 106: 169–214.

QGIS Development Team (2019) QGIS Geographic Information System. Open Source Geospatial Foundation Project. http://qgis.osgeo.org

Risbec J (1960) Les parasites des insectes d'importance économique en Afrique tropicale et à Madagascar. Agronomie Tropicale 15: 624–655.

Say T (1836) Descriptions of new species of North American Hymenoptera, and observation on some already described. Boston Journal of Natural History 1(3): 209–305.

Sharkey MJ, Wharton RA (1997) Morphology and terminology. In: Wharton RA, Marsh PM, Sharkey MJ (Eds) Manual of the New World genera of the family Braconidae (Hymenoptera). Special Publication of the International Society of Hymenopterists, No 1, Washington DC, 19–37.

Szépligeti V (1911) Braconidae der I. Zentral-Afrika-Expedition. Wissenschaftliche Ergebnisse der Deutschen Zentral-Afrika Expedition 1907–1908 3: 393–418.

Szépligeti V (1913) Neue afrikanische Braconiden aus der Ungarischen National-Museums. Annales historico-naturales Musei Nationalis Hungarici 11: 592–608.

Tucker ET, Sharkey MJ, Stoelb SAC (2012) A new species-group of *Camptothlipsis* (Braconidae, Agathidinae) from South Africa, with notes on the evolution of long mouthparts. Journal of Hymenoptera Research 24: 59–74. https://doi.org/10.3897/JHR.24.1909

Turner RE (1918) VII. – Notes on the Braconidæ in the British Museum. – II. On the Australian species of Cardiochilinae and Doryctinae. Annals and Magazine of Natural History 1(1): 49–57. https://doi.org/10.1080/00222931808562286

Viereck HL (1914) Type species of the genera of ichneumon flies. US Government Printing Office 83: 1–186. https://doi.org/10.5479/si.03629236.83.1

Whitfield JB, Dangerfield PC (1997) Subfamily Cardiochilinae. In: Wharton RA, Marsh PM, Sharkey MJ (Eds) Manual of the New World genera of the family Braconidae (Hymenoptera). International Society of Hymenopterists, Washington DC 1: 176–183.

Yu DS, van Achterberg CV, Horstmann K (2016) Taxapad 2016, Ichneumonoidea 2015. Database on flash-drive. Ottawa, Ontario.

JHR 86: 63–77 (2021)
doi: 10.3897/jhr.86.70767
https://jhr.pensoft.net

RESEARCH ARTICLE

JOURNAL OF Hymenoptera RESEARCH
A peer-reviewed open-access journal
The International Society of Hymenopterists

Three new species of the genus *Aphidius* (Hymenoptera, Braconidae, Aphidiinae) from South Korea

Sangjin Kim[1*], Željko Tomanović[2*], Yeonghyeok Yu[1], JuHyeong Sohn[1], Yunjong Han[1], Gyeonghyeon Lee[1], Hyojoong Kim[1]

1 *Animal Systematics Laboratory, Department of Biology, Kunsan National University, Gunsan 54150, Republic of Korea* **2** *University of Belgrade, Faculty of Biology, Institute of Zoology, Studentski trg 16, 11000 Belgrade, Serbia*

Corresponding author: Hyojoong Kim (hkim@kunsan.ac.kr)

Academic editor: Jose Fernandez-Triana | Received 29 June 2021 | Accepted 17 September 2021 | Published 29 October 2021

http://zoobank.org/E2D51361-BE76-445E-92AA-22F6ED8C80F8

Citation: Kim S, Tomanović Ž, Yu Y, Sohn JH, Han Y, Lee G, Kim H (2021) Three new species of the genus *Aphidius* (Hymenoptera, Braconidae, Aphidiinae) from South Korea. Journal of Hymenoptera Research 86: 63–77. https://doi.org/10.3897/jhr.86.70767

Abstract

Several species of the genus *Aphidius* are well known as commercial biocontrol agents of pest aphids, and more than 130 species of the genus have been recorded worldwide. To date, only 15 *Aphidius* species have been recorded in South Korea. Using the DNA barcode region (ca. 658 bp) of mitochondrial cytochrome c oxidase subunit I (COI), we amplified sequences of 15 *Aphidius* Korean species, aligned them in combination with 23 reference species retrieved from GenBank for comparison and identification, and then reconstructed a barcode phylogeny by the neighbour-joining method. As a result, three *Aphidius* species were found to be new to Science. Descriptions and illustrations of the three species new to Science – *Aphidius longicarpus* **sp. nov.**, *A. longistigmus* **sp. nov.**, and *A. asiaticus* **sp. nov.** – are provided, together with their phylogenetic position within the genus *Aphidius*. In addition, a redescription of *A. areolatus*, a parasitoid of maple aphids (*Peryphillus* spp.), is also given.

Keywords

DNA barcoding, natural enemy, parasitoid wasps, systematics, taxonomy

* These authors contributed equally to this work.

Copyright *Sangjin Kim et al.* This is an open access article distributed under the terms of the Creative Commons Attribution License (CC BY 4.0), which permits unrestricted use, distribution, and reproduction in any medium, provided the original author and source are credited.

Introduction

The genus *Aphidius* consists of more than 130 species around the world and belongs to the subfamily Aphidiinae, which includes approximately 63 genera and 650 species (Yu et al. 2016). All *Aphidius* species are solitary koinobiont endoparasitoids of aphids, and many of them (e.g. *A. colemani*, *A. gifuensis*) are commercially used and produced as biocontrol agents against pest aphids worldwide (Hågvar and Hofsvang 1991; Blackman and Eastop 2000). As a species-rich genus with a huge diversity of host aphids, many new species have been discovered and described in recent studies (Tomanović et al. 2007; Davidian and Gavrilyuk 2010; Petrović et al. 2020).

Members of the genus *Aphidius* are medium-sized wasps, only 15 species of which have been recorded in South Korea (Starý and Choi 2000; Yu et al. 2016; Hwang et al. 2018; NIBR 2019; Kim et al. 2020). Since *Aphidius* species such as *A. colemani* and *A. ervi* are used as imported biocontrol agents against pest aphids worldwide, especially in agriculture and horticulture (Sequeira and Mackauer 1992; Henter and Via 1995; Fernandez and Nentwig 1997; Takada 1998), it is important to explore indigenous *Aphidius* species and to confirm their diversity in South Korea and surrounding regions.

In this study, we describe and diagnose three new *Aphidius* species and present their phylogenetic relationships with other congenerics. We also confirm the presence of *A. areolatus*, which was poorly known and often misidentified, in South Korea and redescribe it.

Materials and methods

Samples were borrowed from the Korean National Arboretum (Pocheon, South Korea). All of them were obtained with Malaise traps in South Korea. They are stored in 95% ethyl alcohol at -19 °C.

Specimen morphological identification was based on Shaw and Huddleston 1991; Wharton et al. 1997; Yu et al. 2016; and Rakhshani et al. 2019. We first performed morphological sorting of similar phenotypes and labeling of these samples using a dissecting microscope (OLYMPUS SZX16, Leica M205C, NIKON SMZ 1500), after which DNA extraction was performed. Total genetic DNA extraction was performed using a LaboPass Tissue Kit (COSMOgenetech, Korea) following the manufacturer's protocol. For DNA extraction, samples consisted of single or several individuals from the same colony.

The target site for molecular identification was the front partial region of mitochondrial COI, viz., a 658-bp fragment, amplified using primers LCO1490 (forward) 5'-GGTCAACAAATCATAAAGATATTGG-3' and HCO2198 (reverse) 5'-TAAACTTCAGGGTGACCAAAAAATCA-3' (Folmer et al. 1994) and AccuPower PCR PreMix (Bioneer Corp., Daejeon, Korea). Polymerase chain reaction (PCR) amplification was conducted with 20 µl of a reaction mixture consisting of 3 µl of DNA extract, 2 µl of primer, and 15 µl of H_2O. It was carried out as follows: denaturation for 5 min at 95 °C; 38 cycles of 20 s at 95 °C, 30 s at 45 °C, and 40 s

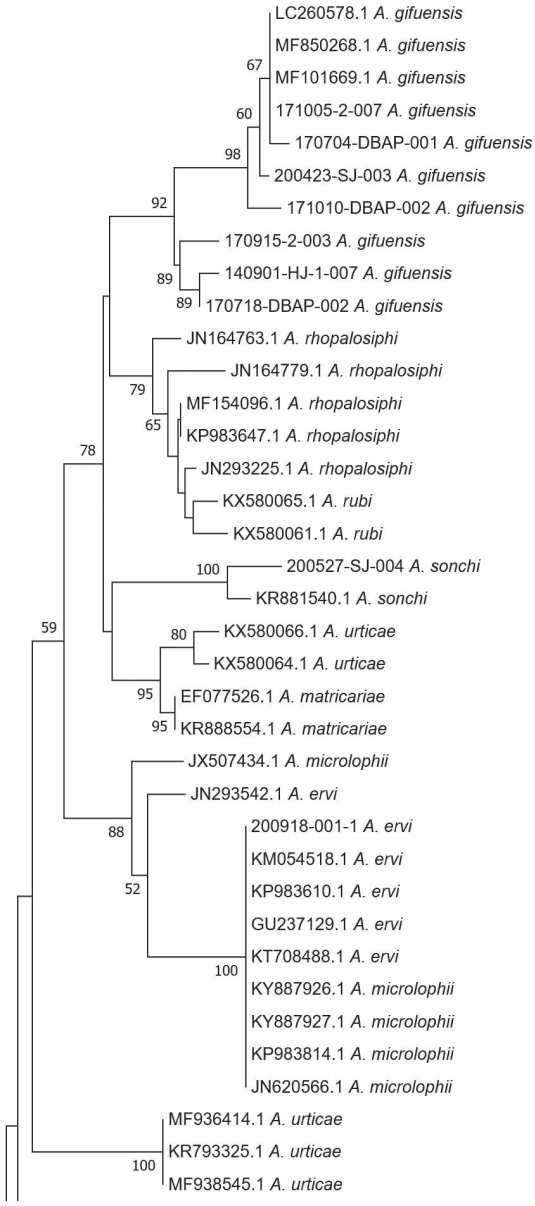

Figure 1. Neighbour-joining tree of 28 *Aphidius* spp. from South Korea based on their COI DNA barcode. *Diaeretiella rapae* was used for an outgroup.

at 72 °C; and final extension at 72 °C for 5 min. PCR products were tested by electrophoresis on agar gel and if a band existed, we commissioned Bionics (Korea) for analysis and purification.

Sequences were aligned using Clustal W default setting and their frame-shifts were checked to avoid pseudogenes. Alignments were translated to amino acids using

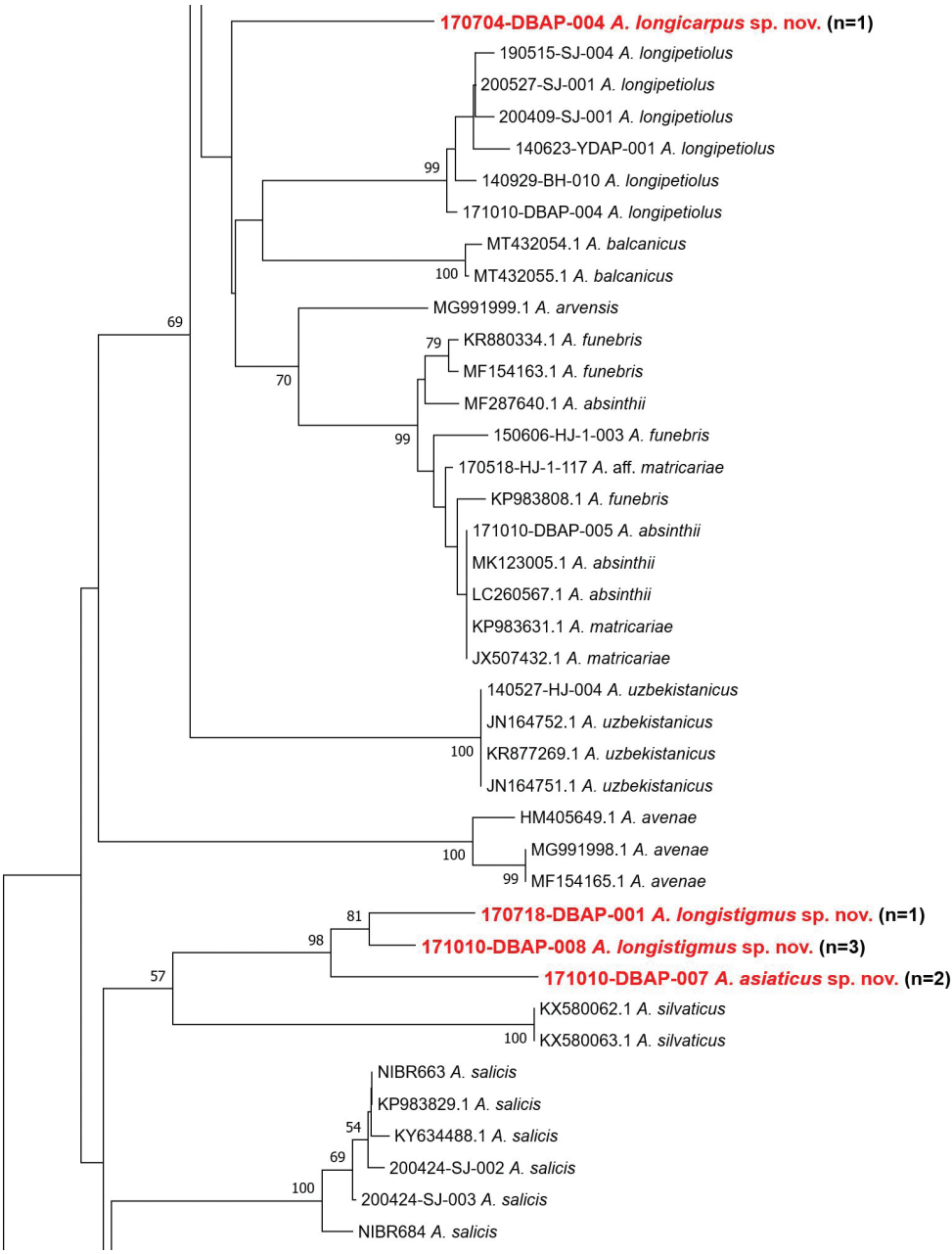

Figure 1. Continued.

MEGA, version 7.0. We calculated sequence divergences using the '*p*-distance' model commonly employed to analyze *COI* barcoding data. A phylogeny tree was constructed using the neighbor-joining method with 1,000 bootstrapping replications and complete deletion in data gaps.

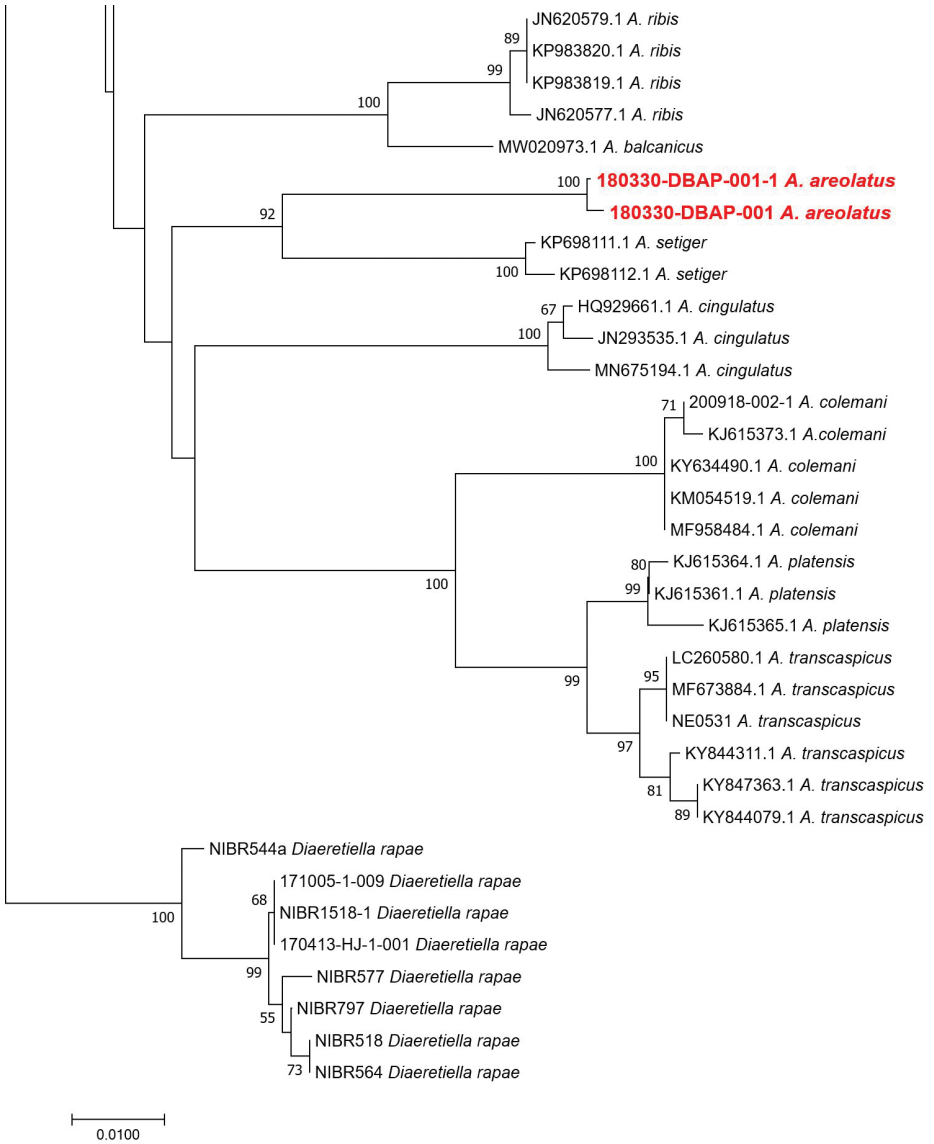

Figure 1. Continued.

After morphological and molecular identification, measurements of the new species were carried out. A LEICA DMC2900 digital camera and a LEICA M205 C microscope (Leica Geosystems AG) were used for photography and characterization, several pictures being taken for each height using multifocusing technology. LAS V4.11 (Leica Geosystems AG) and HeliconFocus 7 (Helicon Soft) software were used for stacking work. After stacking work, illustrations were created using Adobe Photoshop CS6. LAS V4.11 (Leica Geosystems AG) was used to ascertain the shape of specimens (Berkovitch et al. 2009; Arias-Penna et al. 2013).

Results

A total of 110 COI MOTUs (≥525) of 28 species, including the outgroup, were used to establish the phylogenetic tree. Fourteen species recorded in South Korea (but not *A. pleotricophori* because of a lack of sequence data) were used in phylogenetic analysis. Altogether, sequences of 28 species containing 72 reference sequences of 22 *Aphidius* species from GenBank (Suppl. material 1: Table S1), were used to explore the phylogenetic position of the three newly described species. *Diaeretiella rapae* was used as an outgroup.

Aphidius longistigmus sp. nov. contains two MOTUs (molecular operational taxonomic units), 171010-DBAP-008 in three specimens and 170718-DBAP-001 in one specimen. *Aphidius asiaticus* sp. nov. is clustered with *Aphidius longistigmus* sp. nov. and is present with two specimens (171010-DBAP-007). Genetic divergence between *Aphidius asiaticus* sp. nov. and *Aphidius longistigmus* sp. nov. is in the range of 3.1–3.9%, as compared with the two MOTUs in *Aphidius longistigmus* sp. nov., whose average genetic divergence is 1.6%.

Systematic accounts (description on the basis of females)

***Aphidius longicarpus* Kim & Tomanović, sp. nov.**
http://zoobank.org/D82A1BC5-37CE-44FB-A78C-F6D6CAA643A4
Fig. 2A–G

Diagnosis. In some morphological characters (shape of the first flagellomere and antennae, number of antennal segments, shape of the pterostigma, and number of maxillary and labial palps), *Aphidius longicarpus* sp. nov. is similar to *A. funebris* and *A. balcanicus*. However, it clearly differs from *A. balcanicus* in having a shorter R1 vein (the R1 vein is subequal to pterostigma length in *Aphidius longicarpus* sp. nov., while in *A. balcanicus* the ratio of pterostigma length to R1 vein length is 1.4–2.0). It differs from *A. funebris* in possessing a more elongate pterostigma (the pterostigma length/width ratio is 4.06 in *Aphidius longicarpus* sp. nov., vs. 3.0–3.5 in *A. funebris*) and a more elongate petiole (the petiole length/width ratio at the spiracle level is about 3.14 in *Aphidius longicarpus* sp. nov., vs. 2.5–2.9 in *A. funebris*). The new species is distinguished from all other congeneric *Aphidius* species by a combination of the following characters: 16-segmented antennae, short first flagellomere (length/width ratio of about 2.6), and subequal length of the R1 vein and pterostigma.

Description. Female. Length of body about 2.26 mm (Fig. 2A). Length of forewing 2.06 mm (Fig. 2B).

Head. Tentorial index 0.53 (Fig. 2D). Malar space 0.29 × longitudinal eye diameter. Antenna 16-segmented (Fig. 2C). F1 slightly shorter than F2. F1 and F2 2.61 and 3.35 times as long as their width at the middle, respectively. F1 and F2 with three and four longitudinal placodes, respectively. Maxillary palp with four palpomeres, labial palp with three palpomeres. Ratio of eye to temple in dorsal view 1.40. Face width/height ratio 1.25 (Fig. 2D).

Mesosoma. Propodeum areolated, areola length/width ratio 2.00 (Fig. 2E). Pterostigma 4.06 times as long as wide. Ratio of pterostigma length to R1 vein (=metacarpus) length 1.14 (Fig. 2B).

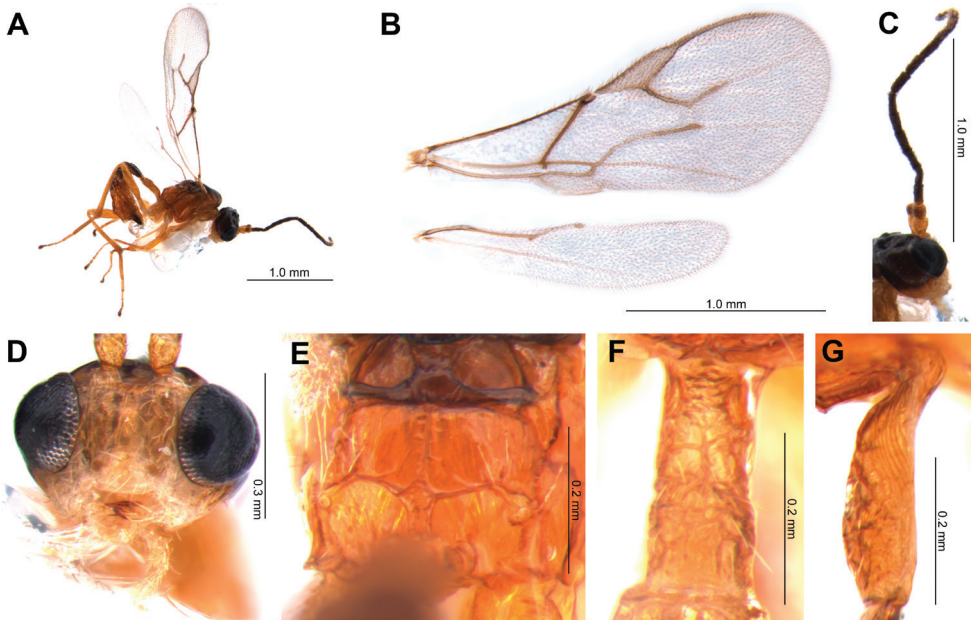

Figure 2. *Aphidius longicarpus* Kim & Tomanović, sp. nov., female **A** body **B** wing **C** antennae **D** head **E** propodeum **F** dorsal view of petiole **G** lateral view of petiole.

Metasoma. Petiole 3.14 times as long as wide at spiracles (Fig. 2F, G), with eight curved costulae in the anterolateral area (Fig. 2G). Petiole rugose on dorsal side, with prominent dorsal carina (Fig. 2F).

Colour. Antenna black; scape yellowish-brown; pedicel brown to black from base to apex. Head black. Face brown, clypeus with mouthparts yellowish-brown. Dorsal side of mesoscutum and metasoma dark brown, except yellowish brown propodeum and petiole. Legs yellowish-brown with dark apices.

Etymology. The name of the new species refers to the very long fore wing R1 vein (=metacarpus).

Specimen examined. ***Holotype*:** Korea, 1 ♀; DMZ Botanical Garden, Mandae-ri, Haean-myeon, Yanggu-gun, Gangwon-do, collected by Malaise trap: 20.VI.–04.VII.2017, leg. H.T. Shin, S.J. Kim. Holotype deposited in the Korean National Arboretum, Gyeonggi-do, Republic of Korea.

Aphidius longistigmus Kim & Tomanović, sp. nov.

http://zoobank.org/720E0253-F2D9-4F99-AFBF-6635FBB2DBA8
Fig. 3A–G

Diagnosis. On the basis of the number of maxillary (three) and labial (two) palpomeres, number of antennal segments, and possession of an elongate pterostigma, the new species is morphologically related to *A. matricariae*. However, it differs clearly from *A. matricariae* in having a very elongate fore wing pterostigma (fore wing pterostigma

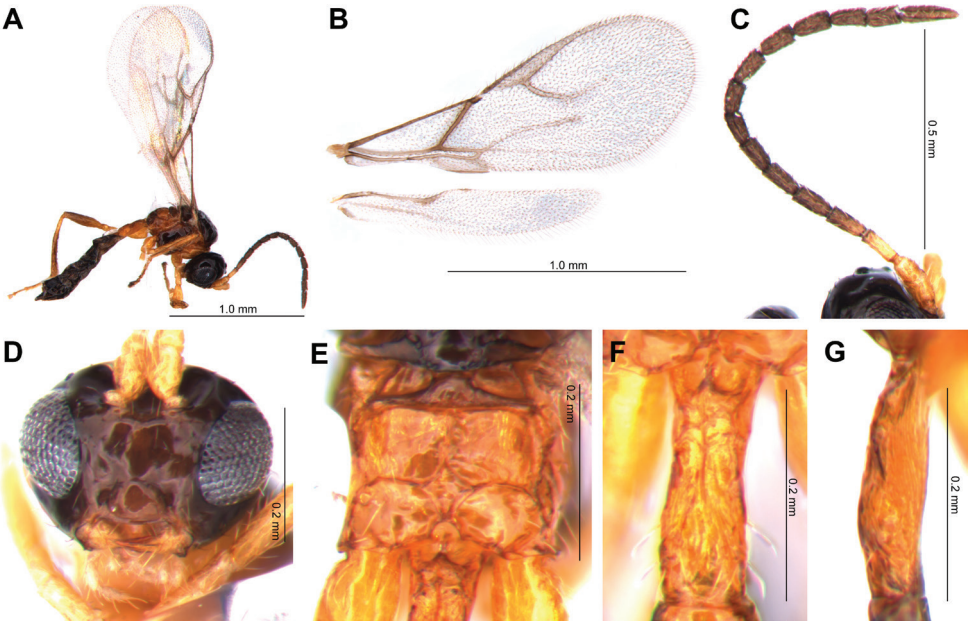

Figure 3. *Aphidius longistigmus* Kim & Tomanović, sp. nov., female **A** body **B** wing **C** antennae **D** head **E** propodeum **F** dorsal view of petiole **G** lateral view of petiole.

length/width ratio of 4.96–5.46 in *Aphidius longistigmus* sp. nov., vs. 3.50–4.00 in *A. matricariae*) and shorter flagellomere 1 (F1 length/width ratio of 2.11–2.52 in *Aphidius longistigmus* sp. nov., vs. 2.50–3.00 in *A. matricariae*).

Description. Female. Length of body about 1.85 mm (Fig. 3A). Length of fore wing 1.45 mm (Fig. 3B).

Head. Tentorial index 0.39–0.50 (Fig. 3D). Malar space 0.26–0.30 times longitudinal eye diameter. Antenna 13–15-segmented (Fig. 3C). F1 slightly shorter than F2. F1 and F2 2.11–2.52 and 1.93–2.28 times as long as their width at the middle, respectively. F1 with 2–3 and F2 with 3–4 longitudinal placodes. Maxillary palp with three palpomeres, labial palp with two palpomeres. Ratio of eye to temple in dorsal view 0.98–1.13. Face width/height ratio 1.43–1.51 (Fig. 3D).

Mesosoma. Propodeum with clearly defined central areola, areola length/ width ratio 1.00 (Fig. 3E). Pterostigma 4.96–5.46 times as long as wide. Ratio of pterostigma length to R1 vein (=metacarpus) length 1.00–1.34 (Fig. 3B).

Metasoma. Petiole 3.09–3.29 times as long as wide at spiracles (Fig. 3F, G), with about 10 curved costulae in anterolateral area (Fig. 3G). Petiole with prominent dorsal carina (Fig. 3F).

Colour. Antenna dark-brown; scape, pedicel, and flagellomere 1 yellowish–brown, partly dark-brown. Head black. Face with clypeus dark-brown, mouth parts yellowish-brown. Dorsal side of mesoscutum and metasoma dark–brown, except for propodeum with petiole. Legs yellowish-brown with dark apices.

Etymology. The name of the new species refers to the very long fore wing pterostigma.

Specimens examined. ***Holotype*:** Korea, 1 ♀; DMZ Botanical Garden, Mandae-ri, Haean-myeon, Yanggu-gun, Gangwon-do, collected by Malaise trap: 05.IX. – 19.IX.2017, leg. H.T. Shin, S.J. Kim. Holotype deposited in the Korean National Arboretum, Gyeonggi-do, Republic of Korea.

***Paratypes*:** Korea, 3 ♀; 1 ♀, DMZ Botanical Garden, Mandae-ri, Haean-myeon, Yanggu-gun, Gangwon-do, collected by Malaise trap: 04.VII.–18.VII.2017, leg. H.T. Shin, S.J. Kim. 2 ♀, same locality, collected by Malaise trap: 19.IX.–10.X.2017, leg. H.T. Shin, S.J. Kim. Paratype specimens deposited as dry and immersion-mounted in the Korean National Arboretum, Gyeonggi-do, Republic of Korea.

***Aphidius asiaticus* Kim & Tomanović, sp. nov.**
http://zoobank.org/D381A6F3-D58F-4799-A2AE-F9C58A1610E4
Fig. 4A–G

Diagnosis. On the basis of the number of antennal segments and wing venation pattern, the new species is morphologically related to *A. matricariae* and *Aphidius longistigmus* sp. nov.. However, it differs clearly from *A. matricariae* in having a more elongate fore wing pterostigma (the fore wing pterostigma length/width ratio is 4.62–4.79 in *Aphidius asiaticus* sp. nov., vs. 3.50–4.00 in *A. matricariae*) and a shorter flagellomere 1 (The F1 length/width ratio is 2.23–2.49 in *Aphidius asiaticus* sp. nov., vs. 2.50–3.00 in *A. matricariae*). *Aphidius asiaticus* sp. nov. differs from *Aphidius longistigmus* sp. nov.

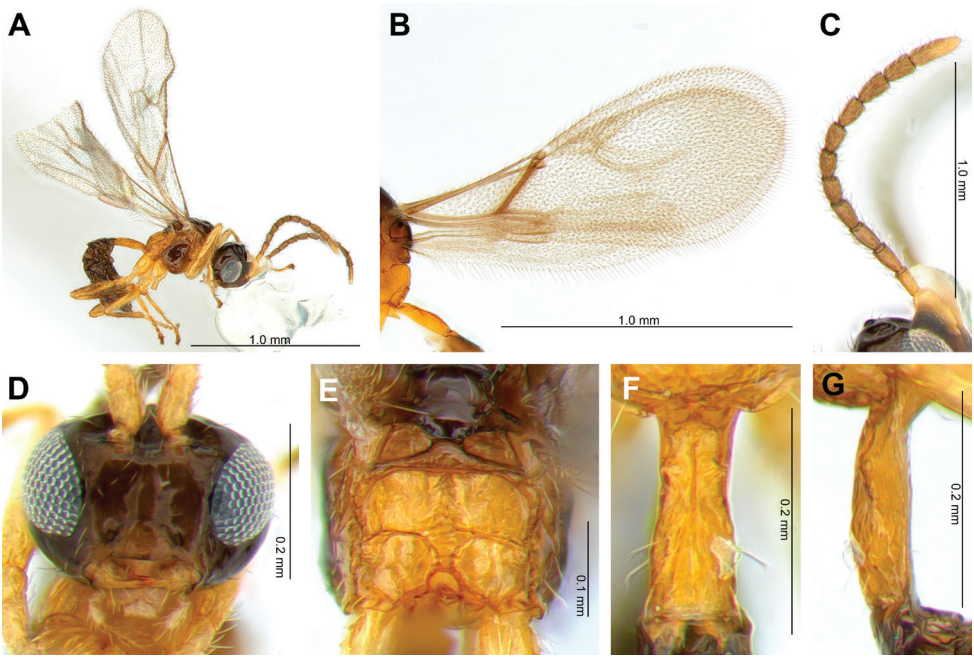

Figure 4. *Aphidius asiaticus* Kim & Tomanović, sp. nov., female **A** body **B** wing **C** antennae **D** head **E** propodeum **F** dorsal view of petiole **G** lateral view of petiole.

in having a less elongate pterostigma (the pterostigma length/width ratio is 4.62–4.79 in *A. asiaticus* sp. nov., vs. 4.96–5.46 in *Aphidius longistigmus* sp. nov.). Additionally, *A. asiaticus* sp. nov. has four maxillary palpomeres (or three when the last one is very long and undivided), while *A. longistigmus* sp. nov. has three maxillary palpomeres.

Description. Female. Length of body about 1.85 mm (Fig. 4A). Length of fore wing 1.45 mm (Fig. 4B).

Head. Tentorial index 0.47–0.50 (Fig. 4D). Malar space 0.28–0.31 times longitudinal eye diameter. Antenna 13–15-segmented (Fig. 4C), thickened at apex. F1 slightly shorter than F2. F1 and F2 2.23–2.49 and 2.11–2.14 times as long as their width at the middle, respectively. F1 with 0–3 and F2 with 1–3 longitudinal placodes. Maxillary palps with four or three palpomeres (in the latter case, the last palpomere is long and undivided), labial palp with two palpomeres. Ratio of eye to temple in dorsal view ca. 1.00. Face width/ height ratio 1.44–1.54 (Fig. 4D).

Mesosoma. Propodeum with clearly defined central areola, areola length/ width ratio 1.18–1.20 (Fig. 4E). Pterostigma 4.62–4.79 times as long as wide. Ratio of pterostigma length to R1 vein (metacarpus) length 1.26–1.32 (Fig. 4B).

Metasoma. Petiole 3.08–3.12 times as long as wide at spiracles (Fig. 4F, G), with about 10 curved costulae in anterolateral area (Fig. 4G). Mediodorsal carina of petiole well developed (Fig. 4F).

Colour. Antennal scape, pedicel, and flagellomere 1 yellow, flagellomere 2 yellow at the base, remaining parts of antennae yellowish to light-brown. Head black. Face with clypeus dark-brown, mouth parts yellow. Dorsal side of mesoscutum and metasoma dark-brown except for the yellow to light-brown propodeum (propodeum sometimes dark-brown) with yellow petiole. Legs yellow with dark apices.

Etymology. The name of the new species is derived from its known geographic distribution.

Specimens examined. ***Holotype*:** Korea, 1 ♀; DMZ Botanical Garden, Mandae-ri, Haean-myeon, Yanggu-gun, Gangwon-do, collected by Malaise trap: 19.IX.–10.X.2017, leg. H.T. Shin, S.J. Kim. Holotype deposited in the Korean National Arboretum, Gyeonggi-do, Republic of Korea.

***Paratypes*:** Korea, 1 ♀; DMZ Botanical Garden, Mandae-ri, Haean-myeon, Yanggu-gun, Gangwon-do, 15.VII.2014, leg. H.T. Shin. Paratype specimen deposited as fluid- mounted in the Korean National Arboretum, Gyeonggi-do, Republic of Korea.

Aphidius areolatus Ashmead, 1906

Fig. 5A–G

Aphidius areolatus Ashmead, 1906; Starý and Schlinger 1967; Chang and Youn 1983; Starý and Choi 2000.

Redescription. Female. Length of body 2.93 mm (Fig. 5A). Length of fore wing 2.63 mm (Fig. 5B).

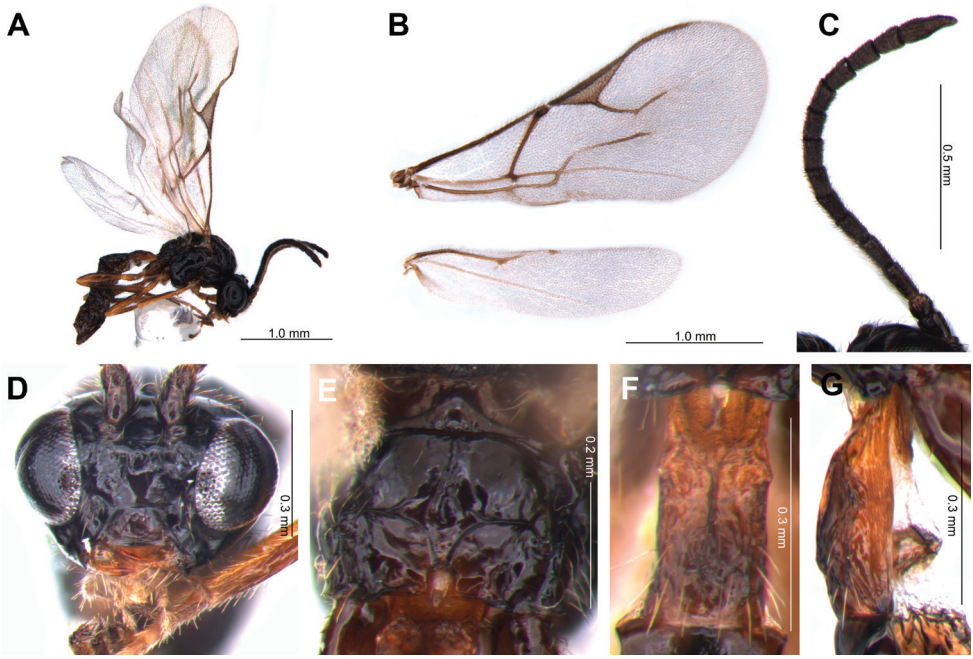

Figure 5. *Aphidius areolatus* Ashmead, female **A** body **B** wing **C** antennae **D** head **E** propodeum **F** dorsal view of petiole **G** lateral view of petiole.

Head. Tentorial index 0.35–0.39 (Fig. 5D). Malar space 0.27–0.30 times longitudinal eye diameter. Antenna 14-segmented, thickened at apex with short antennal segments (Fig. 5C). F1 slightly longer than F2. F1 and F2 2.12–2.14 and 1.63–1.76 times as long as their width at the middle, respectively. Maxillary palp with four palpomeres, labial palp with three palpomeres. Ratio of eye to temple in dorsal view 1.42. Face width/height ratio 1.46–1.57 (Fig. 5D).

Mesosoma. Propodeum areolated, areola length/width ratio ca. 1.53 (Fig. 5E). Pterostigma 3.61 times as long as wide. Ratio of pterostigma length to R1 vein length ca. 1.14 (Fig. 5B).

Metasoma. Petiole 2.17 times as long as wide at spiracles (Fig. 5F, G), with about 10 straight costulae in anterolateral area (Fig. 5G).

Colour. Antenna black. Head black. Face with clypeus black, mouth parts light-brown. Mesoscutum and metasoma black, except for brown petiole. Legs brown with dark apices.

Male. Antenna 19–20-segmented. Maxillary palp with four palpomeres, labial palp with three palpomeres.

Specimens examined. Korea, 2 ♀, 6 ♂; Korean National Arboretum, Gwangneung Forest, Soheul-eup, Pocheon-si, Gyeonggi-do, collected by Malaise trap: 19.III.–30.III.2018, leg. M.H. Kim, M.C. Kim, S.W. Jo, O. Ki.

Remarks. Morphologically, the examined specimens exhibited more variability than was known before (Starý and Schlinger 1967). The pterostigma is more

triangular and the petiole more quadrate than in the original description. Chang and Youn (1983) reported *A. areolatus* from South Korea (one male specimen), but their record of this endemic Japanese species is doubtful. Due to misidentification (Chang and Youn 1983), *Aphidius areolatus* should be deleted from the previously known Korean parasitoid fauna (personal communication with Prof. Paik). It follows that *A. areolatus* is recorded from South Korea for the first time in the present study.

Discussion

It is well known that parasitoids, as a hyperdiverse and understudied group of organisms, generally are characterized by cryptic speciation (Derocles et al. 2012). Important biocontrol agents, aphidiine parasitoids in particular remain a largely unexplored group. In the last decades, through an integrative approach including DNA barcoding, there has been a rapid increase of knowledge about aphidiine diversity and cryptic species (Tomanović et al. 2018; Čkrkić et al. 2019; Kocić et al. 2020).

Here, we use DNA barcoding to describe three new *Aphidius* species from the Korean Peninsula, an area with a poorly known aphidiine fauna that includes only 58 known species (Starý and Choi 2000; Starý et al. 2001; Yu et al. 2016; Choi et al. 2017; Choi and Kim 2018; Hwang et al. 2018; Kim et al. 2020), which is not consistent with their economic and ecological importance. *Aphidius longicarpus* sp. nov. is a sister species to the *A. absinthii* – *A. funebris* – *A. longipetiolus* clade, with a long and narrow pterostigma as a clear apomorphic character, along with a short flagellomere 1 and long R1 vein as clear plesiomorphies. *Aphidius longistigmus* sp. nov. and *Aphidius asiaticus* sp. nov. are clustered with *A. silvaticus*, a member of the *A. urticae* group (Jamhour et al. 2016). Both species share a long and narrow pterostigma, along with three maxillary and two labial palpomeres in *A. asiaticus* sp. nov. as apomorphies and a short flagellomere 1 as a plesiomorphic character. In addition, we here redescribe *A. areolatus*, an interesting species related to *Periphyllus* aphids as hosts in the Far East (Starý and Schlinger 1967). This species is morphologically similar to the European and Central Asian *A. setiger*, replacing it in the forest type of habitats in the Far East, where it parasitizes *Periphyllus* aphids on *Acer* spp. Correspondingly, in our phylogeny, *A. areolatus* is clustered with *A. setiger* and *A. cingulatus*, both parasitoids of aphids on *Acer* spp. (*Periphyllus* spp. and *Pterocomma* spp., respectively).

We presume that the Korean parasitoid fauna is extremely rich due to habitat and plant diversity (NIE 2017a, 2017b; NIBR 2019). This group is very important because most of its members are already being used or are tentatively applicable as biological control agents. Further research should therefore be conducted to explore this rich parasitoid biodiversity and detect tritrophic (host plant-aphid-parasitoid) interactions.

Acknowledgements

This work was supported by the Korean National Arboretum (KNA1-1-20), and a grant from the National Institute of Biological Resources (NIBR), funded by the Ministry of Environment (MOE) of the Republic of Korea (NIBR202102204), This work was supported by a grant from the National Institute of Biological Resources (NIBR), funded by the Ministry of Environment (MOE) of the Republic of Korea (NIBR202130203). The contribution of ŽT was supported by the Serbian Ministry of Science and Education (grant No. 451-03-9/2021-14/ 200178).

References

Arias-Penna DC, Whitfield JB, Janzen DH, Hallwachs W (2013) Three new species in the genus *Wilkinsonellus* (Braconidae, Microgastrinae) from the Neotropics, and the first host record for the genus. ZooKeys 302: 79–95. https://doi.org/10.3897/zookeys.302.4962

Berkovitch A, Belfer I, Hassin Y, Landa E (2009) Diffraction imaging by multifocusing. Geophysics 74: WCA75–WCA81. https://doi.org/10.1190/1.3198210

Blackman RL, Eastop VF (2000) Aphids on the world's crops: an identification and information guide. John Wiley & Sons Ltd., Chichester, 466 pp.

Chang YD, Youn YN (1983) On four-species of Aphididae (Hym.) from Korea. Res. Rep. Env. Sci. Tech. Chungnam Univ 1(2): 16–22.

Choi S, Ku DS, Kim H (2017) New record of the genus *Taxares* Haliday (Hymenoptera: Braconidae: Aphidiinae) from Korea. Journal of Asia-Pacific Biodiversity 10(4): 596–598. https://doi.org/10.1016/j.japb.2017.07.004

Choi S, Kim H (2018) Three new records of the subfamily Aphidiinae (Hymenoptera: Braconidae) from Korea. Journal of Asia-Pacific Entomology 21(4): 1198–1202. https://doi.org/10.1016/j.aspen.2018.09.003

Čkrkić J, Petrović A, Kocić K, Kavallieratos NG, Hebert PDN, Starý P, Tomanović Ž (2019) Review of the world *Monoctonina* Mackauer 1961 (Hymenoptera, Braconidae, Aphidiinae): key for their identification and descriptions of five new species. Zootaxa 4691(4): 359–385. https://doi.org/10.11646/zootaxa.4691.4.3

Davidian EM, Gavrilyuk AV (2010) A new species of the genus *Aphidius* Nees (Hymenoptera: Aphidiidae) from Western Siberia. Russian Entomological Journal 19(2): 119–121. https://doi.org/10.15298/rusentj.19.2.05

Fernandez C, Nentwig W (1997) Quality control of the parasitoid *Aphidius colemani* (Hym., Aphidiidae) used for biological control in greenhouses. Journal of Applied Entomology 121: 447–456. https://doi.org/10.1111/j.1439-0418.1997.tb01433.x

Folmer O, Black M, Hoeh W, Lutz R, Vrijenhoek R (1994) DNA primers for amplification of mitochondrial cytochrome c oxidase subunit I from diverse metazoan invertebrates. Molecular Marine Biology and Biotechnology 3: 294–299.

Hågvar EB, Hofsvang T (1991) Aphid parasitoids (Hymenoptera, Aphidiidae): biology, host selection and use in biological control. Biocontrol news and Information 12(1): 13–42.

Henter HJ, Via S (1995) The potential for coevolution in a host-parasitoid system. I. Genetic variation within an aphid population in susceptibility to a parasitic wasp. Evolution 49(3): 427–438. https://doi.org/10.1111/j.1558-5646.1995.tb02275.x

Hwang HS, Jung DO, Kim JW, Lee KY (2018) Molecular identification of *Aphidius transcaspicus* (Hymenoptera: Braconidae: Aphidiinae), a closely associated species of *Aphidius colemani*, in Korea. Journal of Asia-Pacific Entomology 21: 1246–1252. https://doi.org/10.1016/j.aspen.2018.09.009

Jamhour A, Mitrović M, Petrović A, Starý P, Tomanović Ž (2016) Re-visiting the *Aphidius urticae* s. str. group: re-description of *Aphidius rubi* Starý and *A. silvaticus* Starý (Hymenoptera: Braconidae: Aphidiinae). Zootaxa 4178(2): 278–288. https://doi.org/10.11646/zootaxa.4178.2.6

Kim S, Yu Y, Lee Y, Han HW, Kim H (2020) COI DNA barcoding for molecular identification of the genus *Aphidius* (Braconidae: Aphidiinae) in South Korea, with diagnoses of two newly recorded species. Journal of Asia-Pacific Entomology 23(4): 1202–1207. https://doi.org/10.1016/j.aspen.2020.09.017

Kocić K, Petrović A, Čkrkić J, Kavallieratos NG, Rakhshani E, Arnó J, Aparicio J, Hebert PDN, Tomanović Ž (2020) Resolving the taxonomic status of potential biocontrol agents belonging to the neglected genus *Lipolexis* Förster (Hymenoptera, Braconidae, Aphidiinae) with descriptions of six new species. Insects 11(10): e667. https://doi.org/10.3390/insects11100667

NIBR (2019) National List of Species of Korea. National Institute of Biological Resources. http://kbr.go.kr

NIE (2017a) Natural Environment Survey 30 years. National Institute of Ecology. http://www.nie.re.kr

NIE (2017b) Data Book of National Ecosystem Survey. National Institute of Ecology. http://www.nie.re.kr

Petrović A, Pérez Hidalgo N, Michelena Saval J, Tomanović Ž (2020) A new *Aphidius* Nees species (Hymenoptera, Braconidae), a parasitoid of *Acyrthosiphon malvae* (Mosley, 1841) in Europe. Phytoparasitica 49: 93–101. https://doi.org/10.1007/s12600-020-00860-1

Rakhshani E, Barahoei H, Ahmad Z, Starý P, Ghafouri-Moghaddam M, Mehrparvar M, Kavallieratos NG, Čkrkić J, Tomanović Ž (2019) Review of Aphidiinae parasitoids (Hymenoptera: Braconidae) of the Middle East and North Africa: key to species and host associations. European Journal of Taxonomy 552: 1–132. https://doi.org/10.5852/ejt.2019.552

Sequeira R, Mackauer M (1992) Nutritional ecology of an insect host-parasitoid association: the pea aphid-*Aphidius ervi* system. Ecology 73: 183–189. https://doi.org/10.2307/1938730

Shaw M, Huddleston T (1991) Classification and biology of braconid wasps. Handbooks for the Identification of British Insects (London) 7(11): 1–126.

Starý P, Schlinger EI (1967) A revision of the far east Asian Aphidiidae (Hymenoptera). Springer Science & Business Media (The Hague) 3: 15–17. https://doi.org/10.1007/978-94-017-6337-0_2

Starý P, Choi JY (2000) An annotated review of tritrophic associations of aphid parasitoids (Hymenoptera, Braconidae, Aphidiinae) in Korea. Insecta Koreana 17(1–2): 91–109.

Starý P, Havelka J, Choi J (2001) New parasitoid species of Cinara-aphids on conifers from Korea (Hymenoptera, Braconidae, Aphidiinae). Insecta Koreana 18(2): 163–169.

Takada H (1998) A review of *Aphidius colemani* (Hymenoptera: Braconidae; Aphidiinae) and closely related species indigenous to Japan. Applied Entomology and Zoology 33: 59–66. https://doi.org/10.1303/aez.33.59

Tomanović Ž, Rakhshani E, Starý P, Kavallieratos NG, Stanisavljević LŽ, Žikić V, Athanassiou CG (2007) Phylogenetic relationships between the genera *Aphidius* and *Lysaphidus* (Hymenoptera: Braconidae: Aphidiinae) with description of *Aphidius iranicus* sp. nov. The Canadian Entomologist 139(3): 297–307. https://doi.org/10.4039/n06-007

Tomanović Ž, Mitrović M, Petrović A, Kavallieratos NG, Žikić V, Ivanović A, Rakhshani E, Starý P, Vorburger C (2018) Revision of the European *Lysiphlebus* species (Hymenoptera: Braconidae: Aphidiinae) on the basis of COI and 28SD2 molecular markers and morphology. Arthropod Systematics & Phylogeny 76(2): 179–213.

Wharton RA, Marsh PM, Sharkey MJ (1997) Manual of the New World genera of the family Braconidae (Hymenoptera). The International Society of Hymenopterists (Washington DC): 118–131.

Yu D, Van Achterberg C, Horstmann K (2016) Taxapad 2016. Ichneumonoidea 2015 (biological and taxonomical information), Taxapad Interactive Catalogue Database on Flash-drive (Nepean). www.taxapad.com

Supplementary material 1

Table S1

Authors: Sangjin Kim, Željko Tomanović, Yeonghyeok Yu, JuHyeong Sohn, Yunjong Han, Gyeonghyeon Lee, Hyojoong Kim

Data type: table

Explanation note: List of 72 reference sequences of 22 *Aphidius* spp. retrieved from GenBank * nine *Aphidius* spp. are not recorded in South Korea but included for molecular identification.

Copyright notice: This dataset is made available under the Open Database License (http://opendatacommons.org/licenses/odbl/1.0/). The Open Database License (ODbL) is a license agreement intended to allow users to freely share, modify, and use this Dataset while maintaining this same freedom for others, provided that the original source and author(s) are credited.

Link: https://doi.org/10.3897/jhr.86.70767.suppl1

JHR 86: 79–92 (2021)
doi: 10.3897/jhr.86.70971
https://jhr.pensoft.net

RESEARCH ARTICLE

JOURNAL OF Hymenoptera RESEARCH
A peer-reviewed open-access journal
The International Society of Hymenopterists

A new species of the genus *Pseudocyanopterus* van Achterberg, Cao & Yang (Hymenoptera, Braconidae, Braconinae) from China

Konstantin Samartsev[1], De-Jun Hao[2], Tao Li[3]

1 *Zoological Institute, Russian Academy of Sciences, St Petersburg 199034, Russia* **2** *Co-Innovation Center for the Sustainable Forestry in Southern China, College of Forestry, Nanjing Forestry University, 159 Longpan Road, Nanjing 210037, China* **3** *General Station of Forest and Grassland Pest Management, National Forestry and Grassland Administration, 58 Huanghe North Street, Shenyang 110034, China*

Corresponding author: Konstantin Samartsev (k.samartsev@gmail.com)

Academic editor: Jose Fernandez-Triana | Received 2 July 2021 | Accepted 14 September 2021 | Published 29 October 2021

http://zoobank.org/DE157D0A-92B9-44F3-9210-423380BDB6F0

Citation: Samartsev K, Hao D-J, Li T (2021) A new species of the genus *Pseudocyanopterus* van Achterberg, Cao & Yang (Hymenoptera, Braconidae, Braconinae) from China. Journal of Hymenoptera Research 86: 79–92. https://doi.org/10.3897/jhr.86.70971

Abstract

A new species, *Pseudocyanopterus pagiophloeusis* Samartsev & Li, **sp. nov.**, is described from Shanghai, China. Illustrated diagnoses to distinguish the new species from its closest relative and the members of related genera are presented. New combinations are proposed for five species previously considered in the genus *Cyanopterus* Haliday, 1835, *Bracomorpha hinoemataensis* (Belokobylskij, 2000), **comb. nov.**, *B. kusarensis* (Abdinbekova, 1973), **comb. nov.**, *B. praecinctus* (Shestakov, 1936), **comb. nov.**, *Parallobracon oriens* (Belokobylskij, 2000), **comb. nov.**, and *P. tzymbali* (Belokobylskij, 2000), **comb. nov.**

Keywords

Cinnamomum camphora, *Pagiophloeus tsushimanus*, parasitoid, taxonomy

Introduction

In recent decades, China has undergone major forest management reforms (Ji et al. 2011), which significantly slowed down forest loss (Ahrends et al. 2017). Modern forestry programs turn to new forest management methods particularly directed on

Copyright *Konstantin Samartsev et al.* This is an open access article distributed under the terms of the Creative Commons Attribution License (CC BY 4.0), which permits unrestricted use, distribution, and reproduction in any medium, provided the original author and source are credited.

prevention and natural control of pests (Ji et al. 2011). Studying entomophages (e.g. parasitoid wasps) is required for the development of ecologically sustainable measures of dangerous pest control in China (Wang et al. 2019).

One of the forest pests recently attracted attention in China is *Pagiophloeus tsushimanus* Morimoto, a monophagous curculionid beetle that causes serious damage to the camphor tree *Cinnamomum camphora* (L.) J. Presl (Zhang et al. 2017; Chen et al. 2020). The knowledge on biology and ecological relations of this pest will provide guidance for its managing (Chen et al. 2020). The current article reports the discovery of a new parasitoid species attacking *P. tsushimanus*.

The new species belongs to the recently described genus *Pseudocyanopterus* of the subfamily Braconinae Nees. It belongs to a broad group of genera comprising in China also *Bracomorpha* Papp, *Campyloneurus* Szépligeti, *Cyanopterus* Haliday, *Indabracon* van Achterberg, and *Parallobracon* Li, van Achterberg & Chen. The fauna of these genera in China was actively studied in recent years, when 25 out of 31 currently known Chinese species have been described (Li et al. 2017, 2020a, 2020b, 2021; Cao et al. 2020). Morphological peculiarity of the new taxa considerably complicated the classification of the group of genera. For example, some species of *Campyloneurus* have extraordinarily broadened and lacking dorsal nodus apex of ovipositor (Li et al. 2020c), *Parallobracon* has unusual ovipositor length, and *Pseudocyanopterus* is characterised by an exceptional shape of scape. We expect that the fauna of the genera related to *Pseudocyanopterus* is far from being fully discovered in China and further findings would help to clarify the statuses of questionable taxa. Thus, the revealing diversity of the braconine wasps of China provides not only an important information for forest pest forecasting and control, but also a useful material for elaboration of the systematics of this subfamily.

Material and methods

The insects were dissected from the trunks of *Cinnamomum camphora* (L.) J. Presl (Lauraceae) (Fig. 1A). Parasitized hosts (4th instar larvae of *P. tsushimanus*) were obtained from Maogang, Songjiang District, Shanghai, on 12 June 2018 (14 host larvae) and 24 June 2021 (two host larvae). There were usually four parasitoids per host (Fig. 1B, C). Larvae were brought to the laboratory and maintained in an incubator at the temperature 26±1 °C and relative humidity 60±5%. The emerged insects collected daily. The host was identified by Dr. Jun-Hao Huang (Zhengjiang A & F University, Hangzhou, Zhejiang).

Description, measurements and photographs of the new species were made under a Leica M205A stereomicroscope with a Leica Microsystem DFC550 digital camera. Photographs were combined using Leica Application Suite (Version 4.5.0). Type specimens are deposited in the Insect Museum, General Station of Forest and Grassland Pest Management, National Forestry and Grassland Administration (Shenyang, P. R. China).

Morphological nomenclature follows Quicke (1987) and van Achterberg (1993). The length of fifth segment of hind tarsus is measured without its pretarsus; first metasomal tergite is measured from its articulating condyle [term applied after Vilhelmsen et al. (2010)].

Abbreviations of morphological terms

OD maximum diameter of lateral ocellus;
OOL ocular-ocellar distance;
POL postocellar distance.

Collection acronyms for specimen deposition

GSFGPM General Station of Forest and Grassland Pest Management, National Forestry and Grassland Administration (Shenyang, P. R. China);
HNHM Hungarian Natural History Museum (Budapest, Hungary);
MIIZ Museum and Institute of Zoology, Polish Academy of Sciences (Warszawa, Poland);
NIBR National Institute of Biological Resources (Incheon, South Korea);
SMNE Science Museum of Natural Enemies (Geochang, South Korea);
ZISP Zoological Institute of the Russian Academy of Sciences (Saint Petersburg, Russia).

Material of related taxa used in diagnoses and illustrations

Bracomorpha hinoemataensis (Belokobylskij, 2000), comb. nov. Japan • 1 ♀ (paratype); Fukushima Prefecture, Hinoemata; 16–18 Aug. 1999; S.A. Belokobylskij leg.; ZISP.

Bracomorpha kusarensis (Abdinbekova, 1973), comb. nov. Belarus • 1 ♀; Khoyniki; 29 Jun. – 5 Oct. 1994; A.M. Tereshkin leg.; Malaise trap; ZISP. – Russia • 1 ♀; Krasnodar Territory, Sochi, Lazarevskoye; 14 May 1973; V.I. Tobias leg.; terrace slopes, forest; ZISP.

Bracomorpha praecinctus (Shestakov, 1936), comb. nov. Russia • 1 ♀; Primorskiy Territory, Yakovlevka, 7 Jun. 1926; Dyakonov & Filipiev leg.; ZISP • 1 ♀; Sakhalin Province, Kunashir Island, near Alekhino; 31 Aug. 1962; Krivolutskaya leg.; from galleries of *Xylosandrus germanus* (Blandford, 1894) (Curculionidae) in ash tree; ZISP.

Bracomorpha tricolor (Ivanov, 1896). Russia • 1 ♀; Primorskiy Territory, 30 km S of Slavyanka; 3 Aug. 1985; S.A. Belokobylskij leg.; oak forest, hazel grove; ZISP • 1 ♀; Primorskiy Territory, Spassk-Dalny; 17–21 Jun. 1996; S.A. Belokobylskij leg.; shrubs, forest; ZISP • 1 ♀; Primorskiy Territory, Tarasovka; 24 Jul. 1972; L. Kulikova leg.; flowers, soybean, wheat; ZISP.

Campyloneurus abnormis (Belokobylskij, 2000). Russia • 1 ♀ (holotype); Primorskiy Territory, 20 km SE of Ussuriysk; 4 Aug. 1991; S.A. Belokobylskij leg.; forest,

Figure 1. The larva of *Pagiophloeus tsushimanus* Morimoto, 1982 dissected from the trunks of *Cinnamomum camphora* (L.) J. Presl (**A**) and parasitised by *Pseudocyanopterus pagiophloeusis* sp. nov. (**B, C**).

clearings; ZISP • 1 ♂; Primorskiy Territory, Evseevka, 25 km SE of Spassk-Dalny; 23 Jul. 2013; S.A. Belokobylskij leg.; forest; ZISP.

Campyloneurus angulosus (Enderlein, 1920). Indonesia • 1 ♀ (lectotype); Sumatra, "Soekaranda"; H. Dohrn leg.; MIIZ.

Campyloneurus bicolor Szépligeti,1900. Papua New Guinea • 1 ♀ (lectotype); Astrolabe Bay; S. Fenichel leg.; HNHM 153455.

Campyloneurus pachypus Li, van Achterberg & Chen, 2020. Russia • 1 ♀; Primorskiy Territory, 20 km SW of Nakhodka, Dushkino; 1 Aug. 2013; A. Lelej leg.; forest, glades; ZISP. – South Korea • 1 ♀; Gangwon-do, Hongcheon-gun, Duchon-myeon; 11 Oct. 1995; J.Y. Choi leg.; NIBR.

Campyloneurus penini (Belokobylskij, 2000). Russia • 1 ♀ (holotype); Primorskiy Territory, 20 km SW of Putsilovka, Monakino; 24–28 Jun. 1993; S.A. Belokobylskij leg.; forest, glades; ZISP. – South Korea • 1 ♀; Gangwon-do, Hongcheon-gun, Naechon-myeon, Waya-ri, Baegamsan Mountain; 1 Sep.–18 Oct. 2002; D.-S. Ku leg.; Malaise trap; SMNE 526.

Cyanopterus (*Cyanopterus*) *anuphrievi* (Tobias & Abdinbekova, 1973). Russia • 1 ♀; Jewish Autonomous Region, Lesser Khingan Range, Radde, Amur River bank; 12–15 Jul. 2003; S.A. Belokobylskij leg.; forest, forest edges; ZISP.

Cyanopterus (*Cyanopterus*) *nigrator* (Zetterstedt, 1838). Russia • 1 ♀; Saratov Province, 5 km W of Dyakovka; 27 Jun. 2012; K. Samartsev leg.; forest (aspen, birch); ZISP

• 1 ♀; Samara Province, SE of Bakhilova Polyana; 13 Jul. 2010; K. Samartsev leg.; birch forest; ZISP.

Parallobracon oriens (Belokobylskij, 2000), comb. nov. Russia • 1 ♀ (paratype); Primorskiy Territory, 10 km E of Kavalerovo; 2 Aug. 1979; S.A. Belokobylskij leg.; forest; ZISP • 1 ♀ (paratype); Primorskiy Territory, 20 km SE of Spassk-Dalny; 31 Jul. 1998; S.A. Belokobylskij leg.; forest, forest edges and glades; ZISP.

Parallobracon tzymbali (Belokobylskij, 2000), comb. nov. Russia • 1 ♀ (paratype); Khabarovskiy Territory, Khekhtsir Range, Korfovskoe forestry; 22 Jul. 1981; D.R. Kasparyan leg.; ZISP • 1 ♀ (paratype); Primorskiy Territory, 15 km NW of Partizansk; 16 Aug. 1985; S.A. Belokobylskij leg.; forest; ZISP.

Results

Genus *Pseudocyanopterus* van Achterberg, Cao & Yang, 2020

Pseudocyanopterus van Achterberg, Cao & Yang, 2020 in Cao et al. 2020: 113 (type species: *Pseudocyanopterus raddeivorus* Cao, van Achterberg & Yang, 2020).

Diagnosis. *Pseudocyanopterus* is very similar to the genera *Bracomorpha* Papp, 1971 and the recently described *Parallobracon* Li, van Achterberg & Chen, 2021. The three taxa are associated by the following character states. Malar space more or less impressed, but malar suture not developed; metasoma with five visible tergites, their apical margins thick; second metasomal tergite with large anterolateral triangular areas delineated by anterolateral posteriorly diverging grooves and sublateral S-shaped grooves; median area of second metasomal tergite large, triangular; ovipositor apically acute, with weak nodus located somewhat distant from its apex and with weak serration (both structures become easily obliterated during oviposition and were not found in some species of *Bracomorpha*). The members of these genera are known to be parasitoids of xylophagous insects. Species of the genus *Bracomorpha* attack beetles from the families Cerambycidae and Curculionidae and lepidopterans of the family Tortricidae (Yu et al. 2016), *Pseudocyanopterus raddeivorus* Cao, van Achterberg & Yang is recorded from the oak longhorn beetle *Massicus raddei* (Blessig & Solsky) on *Quercus liaotungensis* Koidzumi (Cao et al. 2020); the biology of *Parallobracon* is unknown, but possibly also associated with xylophages.

Pseudocyanopterus, *Bracomorpha*, and *Parallobracon* run to the couplet 121 (*Campyloneurus* Szépligeti, 1900) in the key to the Old World genera of Braconinae (Quicke 1987). The genus *Campyloneurus* differs from all three genera by the absence of anterolateral posteriorly diverging grooves on second metasomal tergite. The differences between three related genera are presented in the key below (the characters additionally defining taxa under a certain paragraph of a key couplet, but variable in an alternative paragraph, are listed after a dash).

1 Dorsal side of scape (lateral view) longer than its ventral side, laterally straight or only slightly concave (Fig. 4B). Vein 3-SR 0.3–0.4× as long as vein SR1 (Figs 2B, 4A). Ovipositor sheath at least 2.6× as long as hind tibia, 0.85–1.40× as long as fore wing (Figs 2A, 3A). Malar space very weakly impressed. – Hind wing membrane basally evenly (but sometimes sparsely) setose (Fig. 4A, C) . ..... ***Pseudocyanopterus* van Achterberg, Cao & Yang**

– Dorsal side of scape (lateral view) as long as its ventral side or shorter, laterally concave (Fig. 2F). Vein 3-SR 0.5–0.8× as long as vein SR1 (Fig. 2E, H). Ovipositor sheath at most 0.9–2.4× as long as hind tibia, 0.2–0.7× as long as fore wing (Fig. 2D, G). Malar space distinctly impressed **2**

2 Ovipositor sheath 2.1–2.4× as long as hind tibia, 0.5–0.7× as long as fore wing (Fig. 2G) ..... ***Parallobracon* Li, van Achterberg & Chen**

– Ovipositor sheath 0.9–1.6× as long as hind tibia, 0.20–0.45× as long as fore wing (Fig. 2D) ..... ***Bracomorpha* Papp**

Remarks. The members of *Cyanopterus* with developed anterolateral areas on second metasomal tergite are considered here within *Bracomorpha* after Li et al. (2021), which included the latter taxon in *Cyanopterus* as a subgenus. In *Cyanopterus*, third–seventh metasomal tergites are equally sclerotised, with thin posterior margins, while in *Bracomorpha* five basal tergites are much coarser than the following and conceal them. Because this difference exceeds the subgeneric level, *Bracomorpha* is considered here a valid genus. The recently described genus *Parallobracon* differs from *Bracomorpha* mainly by the length of ovipositor and thus is likely to be considered a subgenus of the latter. However, a separate revision involving much more genera (e.g. *Bicarinibracon* Quicke & Walker and *Indabracon* van Achterberg, *Campyloneurus* Szépligeti, *Chelonogastra* group of genera, *Cyanopterus* Haliday, and others) is required in order to redefine their taxonomic statuses. Two species from the Russian Far East previously described in the genus *Cyanopterus* belong to *Parallobracon*, *P. oriens* (Belokobylskij, 2000), comb. nov. and *P. tzymbali* (Belokobylskij, 2000), comb. nov. The ovipositor sheath is equally long in these two species, 0.6–0.7 times as long as the fore wing, while in the type species *Parallobracon prolatus* Li, van Achterberg & Chen, 2021 it is 0.5–0.6 times as long as the fore wing (Li et al. 2021: 154).

***Pseudocyanopterus pagiophloeusis* Samartsev & Li, sp. nov.**
http://zoobank.org/139D82E0-05AD-46DF-A278-DB21A549BC21
Figs 3, 4

Type material. ***Holotype.*** China • ♀; Shanghai, Songjiang District, Maogang; 12 Jun. 2018; Cong Chen & Shou-Yin Li leg.; pupated 18 Jun. and reared 26 Jun. 2018 from *Pagiophloeus tsushimanus* Morimoto; GSFGPM.

Paratypes. China • 4 ♀♀; same data as for holotype (but reared from different host larvae); GSFGPM • 1 ♂; same data as for preceding; GSFGPM • 2 ♀♀; same

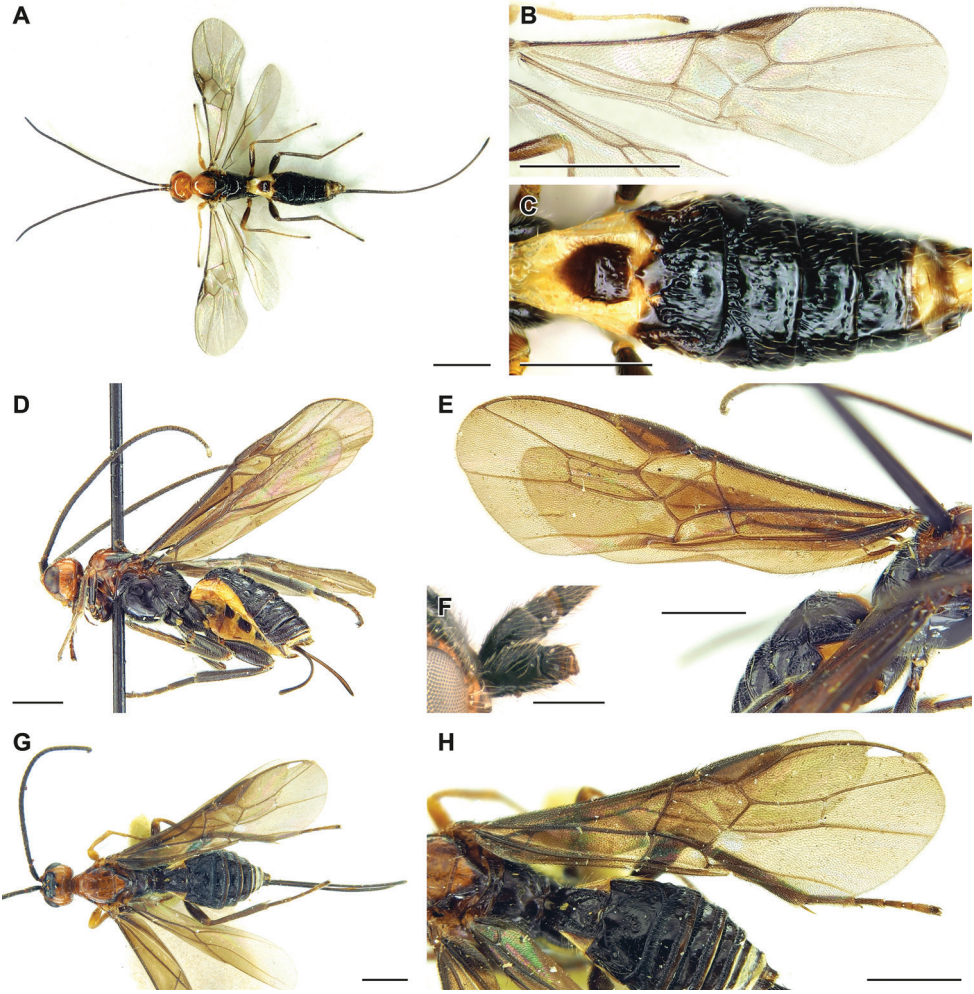

Figure 2. *Pseudocyanopterus raddeivorus* Cao, van Achterberg & Yang, 2020 (**A–C** holotype, female), *Bracomorpha praecinctus* (Shestakov, 1936) (**D–F** female), and *Parallobracon oriens* (Belokobylskij, 2000) (**G, H** paratype, female) **A, G** habitus, dorsal view **D** habitus, lateral view **B, E, H** fore wing **C** metasoma, dorsal view **F** scape, lateral view. Scale bars: 1 mm (**A, B, D, E, G, H**), 0.5 mm (**C**), 0.25 mm (**F**).

data as for preceding; 24 Jun. 2021; De-Jun Hao & Tao Li leg.; pupated 28 Jun. and reared 10 Jul. 2021; GSFGPM • 3 ♂♂; same data as for preceding; GSFGPM.

Etymology. The name of the new species is derived from the host's genus name.

Description. Female. Body length 5.8–6.2 mm; fore wing length 4.5–5.1 mm.

Head. Width of head (dorsal view) 1.5–1.7× its median length. Transverse diameter of eye (dorsal view) 1.6–1.9× as long as temple. Eyes with sparse short setae. OOL 2.4× OD; POL 0.85–0.98× OD; OOL 2.45–2.85× POL. Frons with deep mid-longitudinal groove. Longitudinal diameter of eye (lateral view) 1.2–1.3× its transverse diameter. Transverse diameter of eye (lateral view) 1.8–2.0× minimum width of

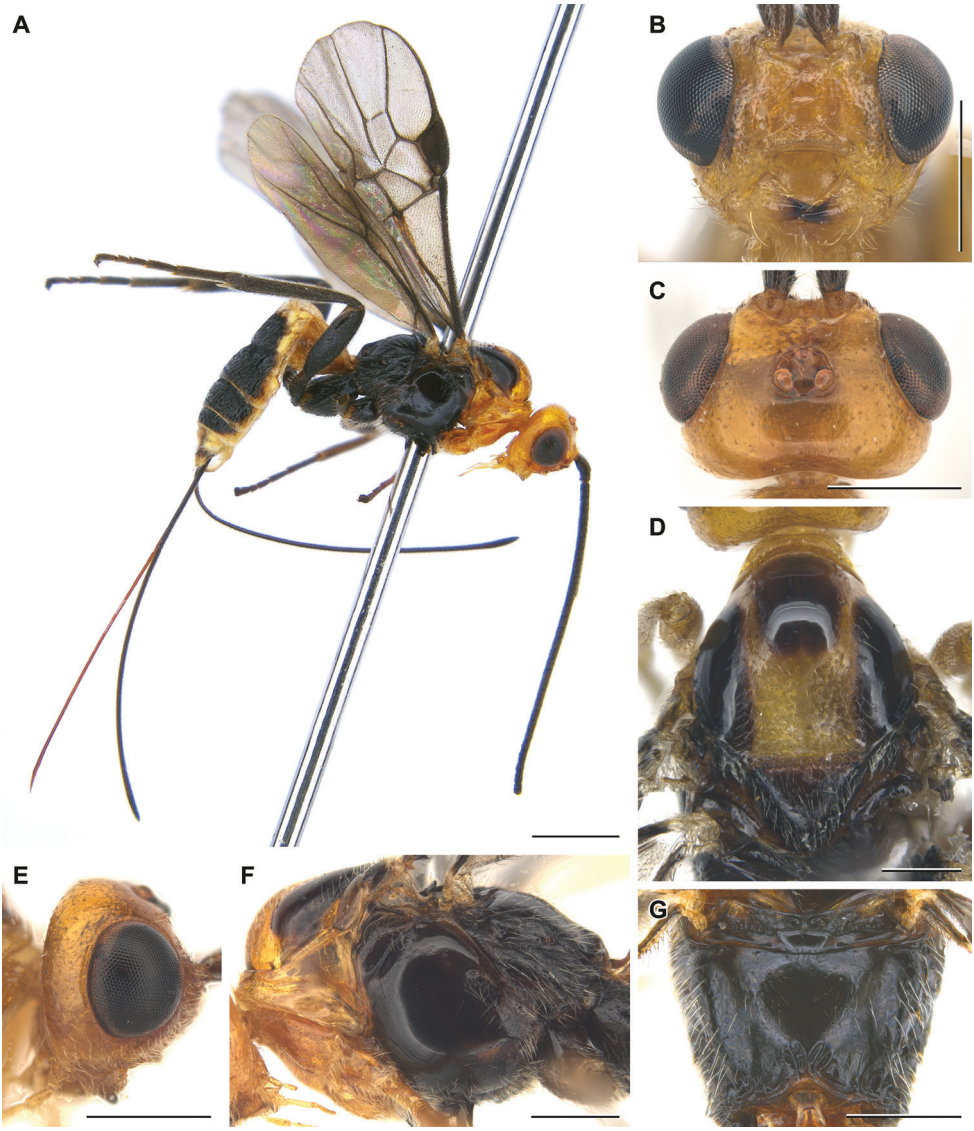

Figure 3. *Pseudocyanopterus pagiophloeusis* sp. nov. (female, **A, C, E-G** holotype **B, D** paratype) **A** habitus, lateral view **B** head, anterior view **C** head, dorsal view **D** mesoscutum and scutellum, dorsal view **E** head, lateral view **F** mesosoma, lateral view **G** propodeum, dorsal view. Scale bars: 1 mm (**A**), 0.5 mm (**B–G**).

temple, hind margins of eye and temple parallel or slightly broadened upwards. Face width 1.6× combined height of face and clypeus; 1.90–1.95× width of hypoclypeal depression. Longitudinal diameter of eye 2.7–2.9× as long as malar space (anterior view); malar space length 0.70–0.95× base of mandible. Malar space shallowly impressed. Width of hypoclypeal depression 1.50–1.55× distance from depression to eye. Clypeus separated from face by dorsal carina; clypeal sulcus impressed; clypeus flattened, with

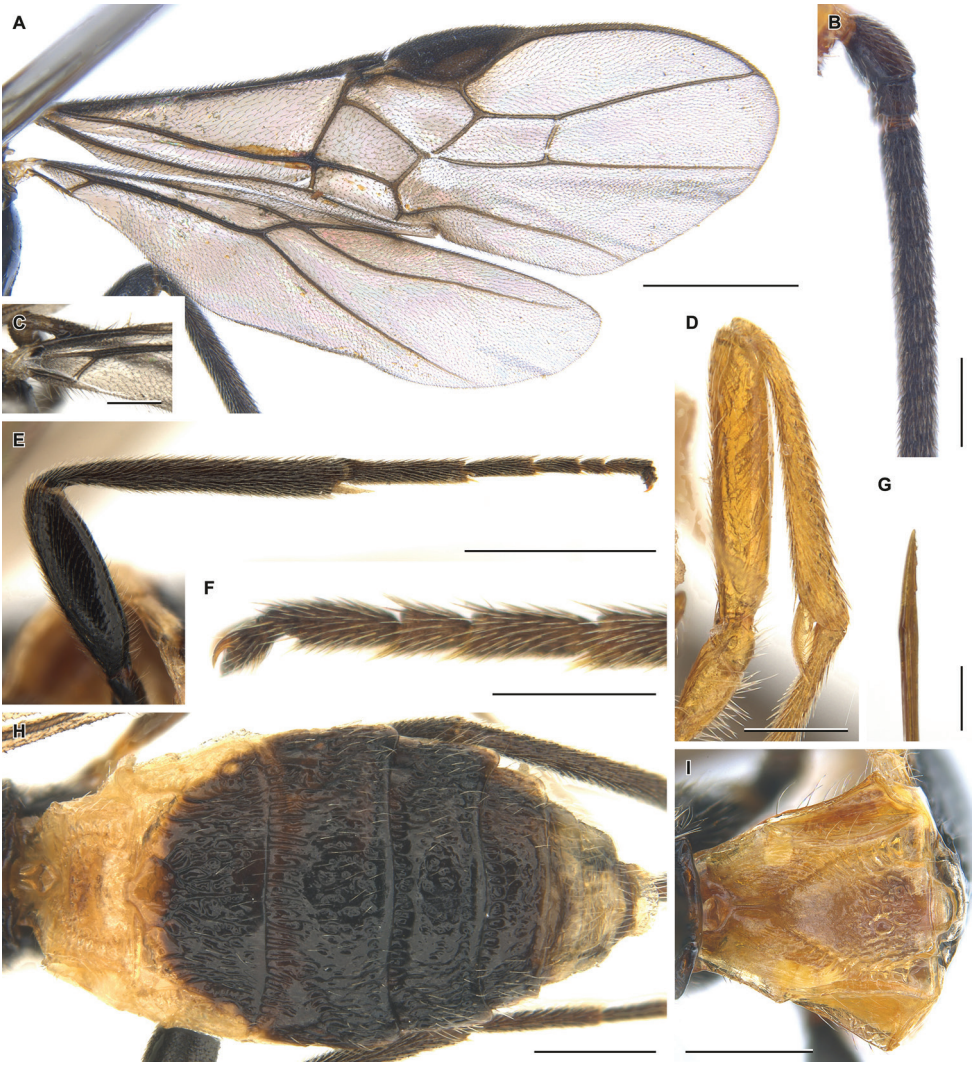

Figure 4. *Pseudocyanopterus pagiophloeusis* sp. nov. (female, **A, B, E, F, I** holotype **C, D, G, H** paratype) **A** wings **B** base of antenna, lateral view **C** base of hind wing **D** fore femur and tibia **E** hind leg **F** hind leg claw **G** apex of ovipositor **H** metasoma, dorsal view **I** first metasomal tergite, dorsal view. Scale bars: 1 mm (**A, E**), 0.5 mm (**C, H, I**), 0.25 mm (**B, D, F, G**).

protruding ventral rim, height of clypeus 0.25–0.30× width of hypoclypeal depression. Maxillary palp as long as eye.

Antenna with 32–38 antennomeres (incomplete in holotype, with 35 antennomeres left). Scape (lateral view) with somewhat protruding ventral margin, but its dorsal side as long as its ventral side. First flagellomere 2.2–2.4× as long as its apical width, 1.25–1.40× as long as second flagellomere. Middle flagellomeres 1.45–1.70× as long as wide. Penultimate flagellomere 1.7–1.9× as long as wide and 0.8–1.0× as long as apical flagellomere.

Mesosoma 1.75–1.85× as long as its maximum height. Transverse pronotal sulcus deep and crenulate anteriorly and smooth and shallow posteriorly. Notauli weakly impressed, united posteriorly. Mesoscutum widely glabrous, setose only on notaulic area and medioposteriorly. Scutellar sulcus crenulate, 0.12–0.13× as long as scutellum. Mesepimeral and metapleural sulci smooth. Mesopleural pit deep and wide, separated from mesepimeral sulcus.

Wings. Pterostigma 2.6–2.9× as long as wide. Vein 1-R1 1.30–1.55× as long as pterostigma. Marginal cell 5.5–5.6× as long as distance from its apex to apex of wing. Vein 3-SR 2.3–2.6×, 0.35–0.40×, and 1.30–1.35× as long as veins r, SR1 and 2-SR, respectively. Vein 1-M 0.65–0.70× and 1.55–1.70× as long as veins 1-SR+M and m-cu, respectively. Vein 1-SR+M weakly curved anteriorly in proximal part. Vein cu-a weakly postfurcal. Hind wing membrane proximally with more or less sparsed setosity (Fig. 4A, C); vein 1-1A 1.4–1.7× as long as cu-a; vein 2-1A absent.

Legs. Fore tibia widely with sparse long thick setae. Hind femur 3.35–3.45× as long as wide, with subapical transverse row of thick setae. Hind tibia 1.50–1.55× as long as hind femur, its inner spur 0.33–0.37× as long as hind basitarsus. Hind tarsus 0.95–1.00× as long as hind tibia. Fifth segment of hind tarsus 0.35–0.40× and 0.7–0.8× as long as hind basitarsus and second segment, respectively. Basal lobes of claws large, rectangular, but not protruding.

Metasoma with five coarsely sclerotised tergites, about 1.6× as long as mesosoma. Median length of first tergite 0.70–0.85× as large as its apical width. Dorsolateral carinae of first metasomal tergite developed. Median area of first tergite separated by crenulate furrow. Second tergite medially 1.05–1.10× as long as third tergite, its basal width 1.75–1.80× its median length. Second metasomal tergite with short (only delineating anterolateral areas) sublateral posteriorly converging furrows and with anterolateral, posteriorly diverging, crenulate grooves; anterolateral areas elongate-triangle, smooth, with sharp crenulate margins; median area strongly elevated, wide, triangular, with crenulate margin. Suture between second and third tergites deep and wide, weakly curved and crenulate. Third metasomal tergite anterolaterally with wide areas separated by crenulate suture. Apical margins of third to fifth tergites thick, with foveate transverse subapical grooves. Ovipositor sheath 2.55–2.60× as long as hind tibia and 0.85–0.90× as long as fore wing. Apex of ovipositor with developed dorsal nodus and ventral serration.

Sculpture. Head and mesosoma mainly smooth. Face medially smooth, laterally punctate. Malar space granulate. Propleuron smooth. Mesopleuron medially weakly granulate. Propodeum smooth with short rugae apicomedially. First metasomal tergite laterally weakly rugulose, its median area rugose posteriorly. Second metasomal tergite areolate-rugose, third–fifth tergites foveolate-rugose.

Colour. Head, pronotum, propleuron, fore coxa and mesoscutum along notauli (or its median lobe entirely) reddish yellow. First metasomal tergite, anterolateral parts of second tergite, sixth and seventh tergites and sternites pale yellow. The rest of body brownish black. Wing membrane weakly darkened, pterostigma and wing veins brown; tegulae dark brown.

Male. Body length 4.8 mm; fore wing length 3.7 mm. Face width 1.7× combined height of face and clypeus. Longitudinal diameter of eye 3.1× as long as malar space (anterior view); malar space length 0.7× base of mandible. Antenna with 28–32 antennomeres. First, middle and penultimate flagellomeres 2.5×, 2.2×, and 2.1× as long as wide, respectively. Median length of first metasomal tergite 1.3× its apical width; second tergite medially 1.1× as long as third tergite, its basal width 1.5× its median length. First metasomal tergite and anterolateral parts of second tergite and pale yellow; the rest of metasoma brownish black. Otherwise similar to female.

Distribution. China (Shanghai).

Biology. Gregarious ectoparasitoid. Host: *Pagiophloeus tsushimanus* Morimoto, 1982 (Coleoptera: Curculionidae: Molytinae). Host plant: *Cinnamomum camphora* (L.) J. Presl (Lauraceae).

Diagnosis. The differences between two known species of *Pseudocyanopterus* are presented in the dichotomy below.

1 Median length of first metasomal tergite 0.70–0.85× its apical width (Fig. 4I). Ovipositor sheath 0.85–0.90× as long as fore wing. First flagellomere 2.2–2.4× as long as apically wide (Fig. 4B). Median area of first metasomal tergite apically rugose (Fig. 4I). Second metasomal tergite with weakly proximally curved dorsolateral impressions, areolate-rugose (Fig. 4H); third–fifth tergites areolate-rugose to foveolate-rugose, their apical margins with deep, complete and foveate transverse subapical grooves..... ..... ***Pseudocyanopterus pagiophloeusis*** **Samartsev & Li, sp. nov.**

– Median length of first metasomal tergite 1.3–1.4× its apical width (Fig. 2C). Ovipositor sheath 1.3–1.4× as long as fore wing (Fig. 2A). First flagellomere about 2.7× as long as apically wide. Median area of first metasomal tergite apically weakly foveate (Fig. 2C). Second metasomal tergite with S-shaped dorsolateral impressions, longitudinally rugose anteriorly, smooth posteriorly; third–fifth tergites almost smooth, their apical margins with incomplete, weak and weakly crenulate transverse subapical grooves ....***Pseudocyanopterus raddeivorus*** **Cao, van Achterberg & Yang**

Additional taxonomic treatments

Genus *Bracomorpha* Papp, 1971

Bracomorpha Papp, 1971: 276 (type species: *Bracomorpha torkai* Papp, 1971). Tobias and Abdinbekova 1973: 431 (synonymised with *Ipobracon* Thomson, 1892); Shenefelt 1978: 1808 (as a synonym of *Ipobracon*); Quicke 1984: 358 (as a valid genus); 1987: 93 (in key), 104; Li et al. 2021: 116 (in key; as a subgenus of *Cyanopterus* Haliday).

***Bracomorpha hinoemataensis* (Belokobylskij, 2000), comb. nov.**

Cyanopterus hinoemataensis Belokobylskij, 2000 in Belokobylskij and Tobias 2000: 175.

***Bracomorpha kusarensis* (Abdinbekova, 1973), comb. nov.**

Ipobracon kusarensis Abdinbekova, 1973 in Tobias and Abdinbekova 1973: 437; Shenefelt 1978: 1822; Tobias 1986: 105.

***Bracomorpha praecinctus* (Shestakov, 1936), comb. nov.**

Ipobracon praecinctus Shestakov 1936 in Telenga 1936: 96; Shestakov 1940: 2; Shenefelt 1978: 1828; Tobias and Abdinbekova 1973: 437; Belokobylskij and Tobias 2000: 175 (as *Cyanopterus praecinctus*).

Genus *Parallobracon* Li, van Achterberg & Chen, 2021

Parallobracon Li, van Achterberg & Chen, 2021: 150 (type species: *Parallobracon prolatus* Li, van Achterberg & Chen, 2021).

***Parallobracon oriens* (Belokobylskij, 2000), comb. nov.**

Cyanopterus oriens Belokobylskij, 2000 in Belokobylskij and Tobias 2000: 173.

***Parallobracon tzymbali* (Belokobylskij, 2000), comb. nov.**

Cyanopterus tzymbali Belokobylskij, 2000 in Belokobylskij and Tobias 2000: 173.

Acknowledgements

We are deeply thankful to Cong Chen and Shou-Yin Li (Nanjing Forestry University, Nanjing, China) for rearing the insects, Jun-Hao Huang (Zhejiang A & F University, Hangzhou, China) for identification of the hosts, Liang-Ming Cao (Research Institute of Forest Ecology, Environmental and Protection CAF, Beijing, China) for the pictures of *Pseudocyanopterus raddeivorus*, and to Mao-Ling Sheng (General Station of Forest and Grassland Pest Management, National Forestry and Grassland Administration, Shenyang, China) for organizing the work on this article and introducing the authors

to each other. We are indebted to Sergey A. Belokobylskij (ZISP, MIIZ), Deok-Seo Ku (SMNE), and Zoltán Vas (HNHM) for the opportunities to study the necessary type and additional material. Finally, we would like to thank Hyojoong Kim (Kunsan National University, South Korea) and two other, anonymous reviewers for careful examination of the article and helpful corrections. This research was supported by the National Natural Science Foundation of China (NSFC, No 31870639), Science and Technology Commission of Shanghai Municipality (No 18391903200). Participation of KS was performed in the frames of the state research project No AAAA-A19-119020690101-6 and supported by the Russian Foundation for Basic Research (grant No 19-04-00027).

References

Ahrends A, Hollingsworth PM, Beckschäfer P, Chen H, Zomer RJ, Zhang L, Wang M, Xu J (2017) China's fight to halt tree cover loss. Proceedings of the Royal Society B: Biological Sciences 284: 20162559. https://doi.org/10.1098/rspb.2016.2559

Belokobylskij SA, Tobias VI (2000) Fam. Braconidae. In: Lehr PA (Ed.) Key to the Insects of the Russian Far East. Neuropteroidea, Mecoptera, Hymenoptera. Vol. IV, pt 4. Dal'nauka, Vladivostok, 8–571. [In Russian]

Cao L-M, van Achterberg C, Tang Y-L, Wang X-Y, Yang Z-Q (2020) Revision of parasitoids of *Massicus raddei* (Blessig & Solsky) (Coleoptera, Cerambycidae) in China, with one new species and genus. Zootaxa 4881(1): 104–130. https://doi.org/10.11646/zootaxa.4881.1.7

Chen C, Zhang C, Li S, Zhu H, Fan B, Wang Y, Su P, Han Y, Hao D (2020) Biological traits and life history of *Pagiophloeus tsushimanus* (Coleoptera: Curculionidae), a weevil pest on camphor trees in China. Journal of Forestry Research 32: 1979–1988. https://doi.org/10.1007/s11676-020-01227-2

Ji L, Wang Z, Wang X, An L (2011) Forest Insect Pest Management and Forest Management in China: An Overview. Environmental Management 48(6): 1107–1121. https://doi.org/10.1007/s00267-011-9697-1

Li Y, van Achterberg C, Chen X-X (2017) Review of the genus *Craspedolcus* Enderlein sensu lato in China, with the description of a new genus and four new species (Hymenoptera, Braconidae, Braconinae). ZooKeys 647: 37–65. https://doi.org/10.3897/zookeys.647.11247

Li Y, He J-H, Chen X-X (2020a) Review of six genera of Braconinae Nees (Hymenoptera, Braconidae) in China, with the description of eleven new species. Zootaxa 4818(1): 1–74. https://doi.org/10.11646/zootaxa.4818.1.1

Li Y, Tang P, Chen X-X (2020b) The genus *Indabracon* van Achterberg (Hymenoptera, Braconidae, Braconinae) in China, with description of four new species. Journal of Hymenoptera Research 76: 39–56. https://doi.org/10.3897/jhr.76.50794

Li Y, van Achterberg C, Chen X-X (2020c) Two genera *Campyloneurus* Szépligeti and *Iphiaulax* Foerster in China, with the descriptions of fourteen new species (Hymenoptera, Braconidae, Braconinae). Zootaxa 4884(1): 1–67. https://doi.org/10.11646/zootaxa.4884.1.1

Li Y, van Achterberg C, Chen X-X (2021) A new genus and eight newly recorded genera of Braconinae Nees (Hymenoptera, Braconidae) from China, with descriptions of fourteen new species. ZooKeys 1038: 105–178. https://doi.org/10.3897/zookeys.1038.55258

Papp J (1971) *Bracomorpha torkai* gen. et sp. n. und Mitteilungen über einige *Bracon* Fabr.-Arten von Ratzeburg, Schmiedeknecht und Fahringer (Hymenoptera, Braconidae). Reichenbachia 13: 275–292.

Quicke DLJ (1984) Redescription of *Craspedolcus* with notes on included species and related genera (Hymenoptera: Braconidae). Oriental Insects 18: 354–360. https://doi.org/10.1080/00305316.1984.10432211

Quicke DLJ (1987) The Old World genera of braconine wasps (Hymenoptera: Braconidae). Journal of Natural History 21: 43–157. https://doi.org/10.1080/00222938700770031

Shenefelt RD (1978) Pars 15. Braconidae 10. Braconinae, Gnathobraconinae, Mesostoinae, Pseudodicrogeniinae, Telengainae, Ypsistocerinae plus Braconidae in general, major groups, unplaced genera and species. In: van Achterberg C, Shenefelt RD (Eds) Hymenopterorum Catalogus. Nova Editio. Dr. W. Junk B.V., Hague, 1425–1872.

Shestakov AV (1940) Zur Kenntnis der Braconiden Ostsibiriens. Arkiv för Zoologi 32A(19): 1–21.

Telenga NA (1936) Hymenoptera. Family Braconidae. Fauna of USSR. Vol. V, pt 2. AS USSR Publishing House, Moscow–Leningrad, 404 pp.

Tobias VI (1986) Braconinae. In: Medvedev GS (Ed.) Key to Insects of the European Part of the USSR. Hymenoptera. Vol. III, pt 4. Nauka, Leningrad, 94–149.

Tobias VI, Abdinbekova AA (1973) Ichneumon flies of the genus *Ipobracon* Thomson, 1892 (Hymenoptera, Braconidae) from the fauna USSR and Mongolia. Entomologicheskoe Obozrenie 52(2): 430–438.

van Achterberg C (1993) Illustrated key to the subfamilies of the Braconidae (Hymenoptera: Ichneumonoidea). Zoologische Verhandelingen 283: 1–189.

Vilhelmsen L, Mikó I, Krogmann L (2010) Beyond the wasp-waist: structural diversity and phylogenetic significance of the mesosoma in apocritan wasps (Insecta: Hymenoptera). Zoological Journal of the Linnean Society 159(1): 22–194. https://doi.org/10.1111/j.1096-3642.2009.00576.x

Wang Z-Z, Liu Y-Q, Shi M, Huang J-H, Chen X-X (2019) Parasitoid wasps as effective biological control agents. Journal of Integrative Agriculture 18(4): 705–715. https://doi.org/10.1016/S2095-3119(18)62078-7

Yu DS, van Achterberg C, Horstmann K (2016) Taxapad 2016, Ichneumonoidea 2015. Database on flash-drive. Nepean (Ontario), Canada.

Zhang C-C, Wang M, Su P, Fan B-Q, Wang Y, Hao D-J (2017) Mating and oviposition behaviors of *Pagiophloeus tsushimanus* (Coleoptera: Curculionidae). Acta Entomologica Sinica 60: 1208–1215.

JHR 86: 93–100 (2021)
doi: 10.3897/jhr.86.71615
https://jhr.pensoft.net

RESEARCH ARTICLE

JOURNAL OF Hymenoptera RESEARCH
A peer-reviewed open-access journal
The International Society of Hymenopterists

Deducing how tropical rhyssines (Hymenoptera, Ichneumonidae) mate from body measurements

Sanna Keronen[1], Ilari E. Sääksjärvi[1], Tapani Hopkins[1]

1 *Zoological Museum, Biodiversity Unit, FI-20014 University of Turku, Finland*

Corresponding author: Sanna Keronen (samake@utu.fi)

Academic editor: Gavin Broad | Received 14 July 2021 | Accepted 6 October 2021 | Published 29 October 2021

http://zoobank.org/1F2FB9A5-D26B-41A1-B45D-82F240F90B02

Citation: Keronen S, Sääksjärvi IE, Hopkins T (2021) Deducing how tropical rhyssines (Hymenoptera, Ichneumonidae) mate from body measurements. Journal of Hymenoptera Research 86: 93–100. https://doi.org/10.3897/jhr.86.71615

Abstract

The biology of many Darwin wasp (Hymenoptera: Ichneumonidae) species is poorly known. Existing museum specimens can potentially be used to get information on e.g. how species live, what they eat, and what their life cycle is. One example of this is a 1991 study by Eggleton in which he measured some rhyssine (Ichneumonidae: Rhyssinae) species, and used the results to deduce how the species likely mate. We extend this work by measuring five tropical species. We found no evidence that the males of our species scramble for females before the females emerge, which matches what was hypothesised by Eggleton. Further measurements of more species would provide information on how other species mate, and field observations of mating rhyssines would help confirm that Eggleton's method for deducing rhyssine mating strategies gives true results.

Keywords

Amazon Malaise trapping 2000, Darwin wasps, Ichneumonidae, Rhyssinae, Uganda Malaise trapping 2014–2015

Introduction

The Darwin wasps (Hymenoptera: Ichneumonidae) are an extremely diverse but poorly known family, with possibly over 100000 species (Gauld et al. 2002) of which only about 24000–25000 are known (Yu et al. 2016; Bennet et al. 2019; Roskov et al. 2019). With so many species still undiscovered, it is scarce surprising that our

Copyright *Sanna Keronen et al.* This is an open access article distributed under the terms of the Creative Commons Attribution License (CC BY 4.0), which permits unrestricted use, distribution, and reproduction in any medium, provided the original author and source are credited.

knowledge of most described species is restricted to the mere fact that they exist. We often know nothing about the biology of species: how they live, what they eat, what their life cycle is.

Existing museum specimens can be used to deduce details of the biology of a species. Eggleton (1991), for example, measured the metasomas of male rhyssine wasps (Ichneumonidae: Rhyssinae) in the Natural History Museum (London) collections, and deduced how the different species mate. The assumption behind the measurements was that rhyssine males often emerge from their pupas before the females and that species whose males scramble for emerging females will tend to invest in long, slender and elongated male metasomas, so as to reach females before other males. Interestingly, according to Gauld (1991) the male metasomas are slender in some temperate species, while most tropical rhyssine species possess shorter and stouter metasomas.

Eggleton (1991) divided rhyssine mating strategies into three categories. These are before-emergence scramble competition (BESC), before-emergence female defence (BEFD) and after-emergence scramble competition (AESC). The first of these (BESC) involves males competing to be the first to insert the metasoma into an emerging female's burrow and inseminate her. Eggleton showed that in several species known to use this strategy, large-sized males have relatively more slender metasomas than small males. This strategy is only known in *Megarhyssa* Ashmead, 1900 and *Rhyssella* Rohwer, 1920.

Eggleton then suggested using this information to deduce the likely mating strategy of other species. Eggleton's sample sizes were very small, however, so he was unable to deduce the mating strategy of more than a few (mainly European or North American) species. Five of his species were from the genus *Epirhyssa* Cresson, 1865, a mainly tropical genus found in both the Old and New World, and one that is suspected not to be monophyletic (Hopkins et al. 2019).

After Eggleton's (1991) work, a large number of rhyssine wasps have been collected and described in Uganda (Hopkins et al. 2019) and Peruvian Amazonia (Gómez et al. 2015). These include 81 males in three Ugandan species, and 26 males in two Peruvian species, all in the genus *Epirhyssa*. This relatively large sample size allows us to use the method proposed by Eggleton to deduce the likely mating strategy of several Afrotropical and Amazonian species.

Materials and methods

Our material consisted of 107 male rhyssines in 5 species. Three of these species were collected in Uganda: *Epirhyssa ghesquierei* Seyrig, 1937 (42 males), *E. overlaeti* Seyrig, 1937 (16 males) and *E. quagga* Hopkins et al., 2019 (23 males). Two species were collected in Peru: *E. braconoides* Porter, 1978 (7 males) and *E. diatropis* Porter, 1978 (19 males). We also collected data from two non-tropical species: *Rhyssa persuasoria* (Linnaeus, 1758) (3 males), collected in Finland, and *Megarhyssa nortoni* (Cresson, 1864) (4 males) from the USA. Their sample sizes were too low to be analysed. The data on all

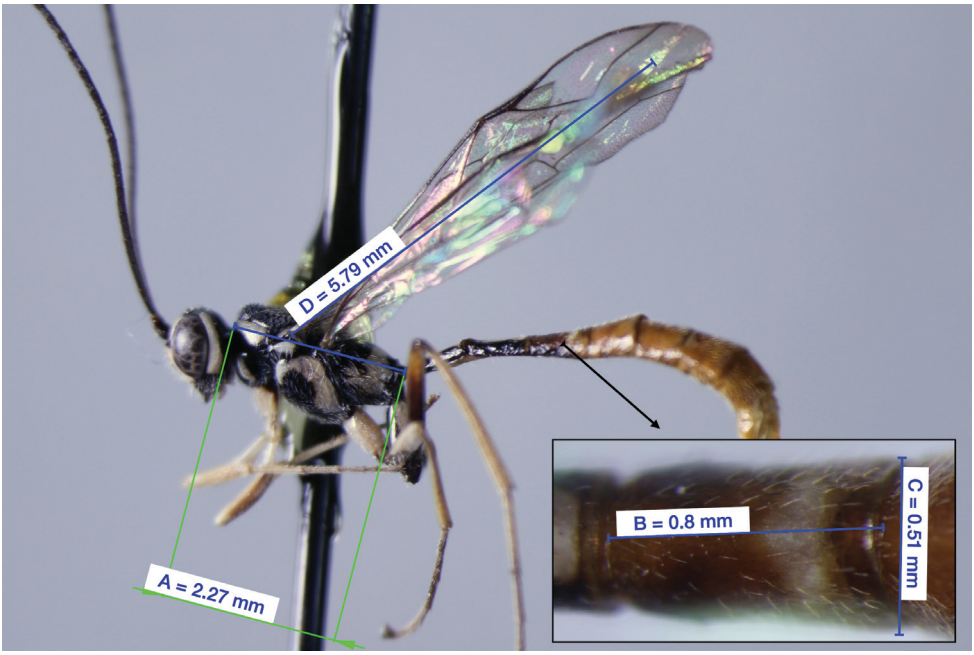

Figure 1. Measurements taken. We estimated the size of a rhyssine wasp by measuring the length of the mesosoma (**A**). We estimated the slenderness of the metasoma by measuring the length (**B**) and width (**C**) of tergite 3. The forewing (**D**) of some wasps was also measured. Note that the left forewing is blurred in this image; these measurement images were taken mainly for the purpose of future reference, so details are not always as clear as during the measurement itself.

the rhyssine individuals is available online (https://doi.org/10.5281/zenodo.5528589; Keronen et al. 2021).

To find out which mating strategy these species most likely use, we measured the length of the male mesosoma and the slenderness (length/width) of the third metasomal tergite. The former was used as a proxy for body size, and the latter as a proxy for metasoma slenderness. We measured the mesosoma from the foremost edge of the mesoscutum/pronotum to the insertion of the metasoma (Figure 1). We measured the width of the tergite at its widest point, and the length at its midline (Figure 1). All measurements were done under a microscope, and images saved for future reference.

We plotted metasoma slenderness versus body size, fitted a linear regression line to the plot, and interpreted a significantly increasing line (slenderness increase in large males) as evidence of the BESC mating strategy. For consistency with Eggleton's (1991) work, we also calculated the significance of the association between body size and tergite slenderness based on Pearson's correlation coefficient. This is otherwise mathematically equivalent to the linear regression, except that the regression uses a two-tailed test whereas the correlation coefficients are one-tailed.

We analysed the data in the R software v. 3.4.0 (R core team 2017). Digital images of the wasps were taken with a CANON DS126461 digital camera attached to

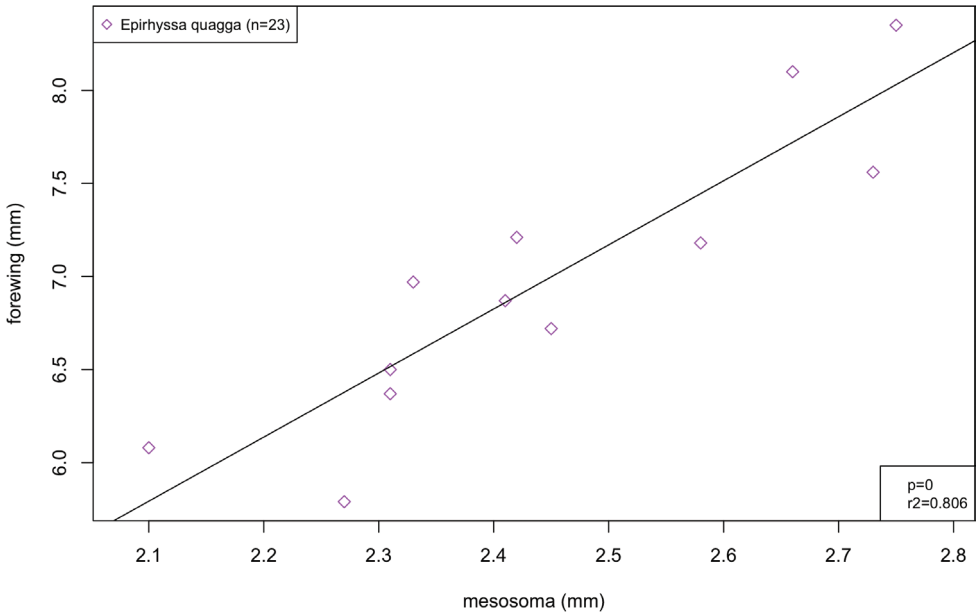

Figure 2. Mesosoma length versus forewing length of some *Epirhyssa quagga* males. Our proxy for body size (mesosoma length) matched the earlier used proxy (forewing length). We fitted a regression line that was significant and explained much of the variation (statistics in lower right corner).

an OLYMPUS SZX16 stereomicroscope. We used the software Quickphoto Micro 3.1 to take the images and to get measurements from them. The analyses and images are available online (https://doi.org/10.5281/zenodo.5528589 Keronen et al. 2021).

Our analyses differ somewhat from those of Eggleton (1991). He used forewing length as a proxy for body size, and the slenderness of the fifth tergite as a proxy for the slenderness of the metasoma. We found mesosoma length and tergite 3 easier to measure for our material. The forewings of our specimens were sometimes hard to get in focus for a reliable measurement, and were occasionally curled or otherwise unmeasurable. Tergite 5 sometimes telescoped under the previous tergite, making accurate measurements difficult. We expect all tergites to give similar results, with the choice of tergite being a compromise between easy visibility (posterior tergites) and the tergite not telescoping under other tergites (anterior tergites). To validate that forewing length and mesosoma length are sufficiently equivalent, we measured both of them for our *Epirhyssa quagga* (23 males), and fitted a linear regression between them (Figure 2).

Eggleton also used correlations, instead of linear regression, to analyse his data; again, we expect the results to be similar whichever method is used. The p-values in particular are calculated the same way, since both are based on the t-statistic; the only difference arises from Eggleton's analyses using a one-tailed test whereas the linear regressions are two-tailed. We felt that a linear regression with its corresponding plots gives a better visualisation of the results, but give the p-values of both approaches.

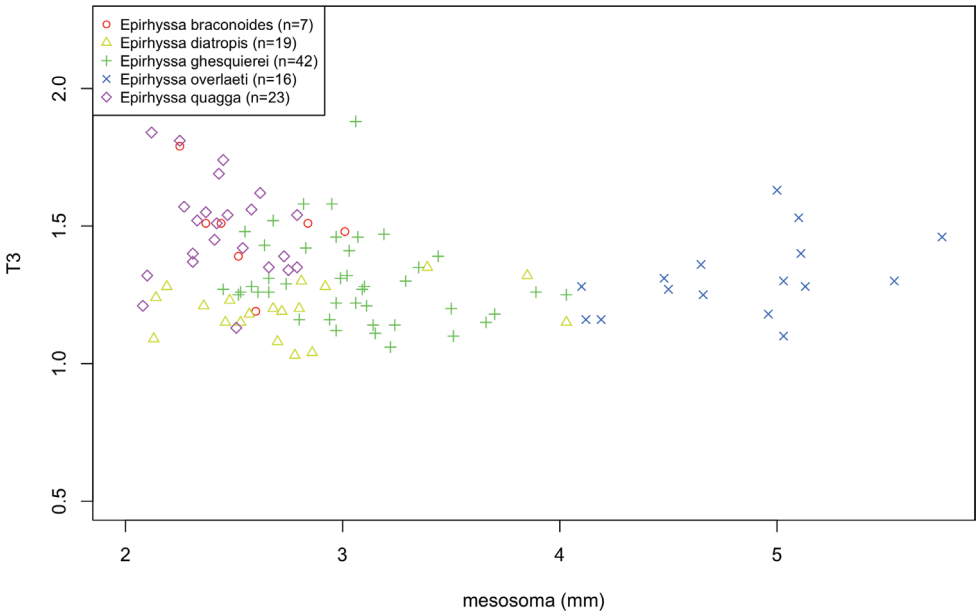

Figure 3. Mesosoma length and tergite 3 slenderness (length/width) of 107 male rhyssine wasps. Males of all species had similarly slender tergites 3, irrespective of body size. The only exception was *Epirhyssa overlaeti*, whose tergites got significantly more slender with body size when the significance was estimated by one-tailed correlation (c.f. Figure 4).

Results

Mesosoma length matched the previously used measure of body size, wing length (linear regression $p < 0.01$, $R^2 = 0.81$; Figure 2).

The slenderness of tergite 3 did not significantly vary with mesosoma length in any of our study species (linear regression, p range = 0.09–0.44, R2 range = 0.03–0.19, Figures 3, 4). However, the slenderness significantly increased (when analysed with a one-tailed correlation test) with metasoma length for one species, *Epirhyssa overlaeti* ($p = 0.047$, Figure 3). Metasomas were conspicuously similar in slenderness, irrespective of body size or species (Figure 3).

Discussion

We found (almost) no evidence that the males of our tropical study species scramble for females before the females emerge. The one exception was *Epirhyssa overlaeti* which showed a significant increase in tergite slenderness with body size, when analysed with one-tailed correlation tests instead of linear regression. We do not feel this merits too much attention, since this was only marginally significant and we would in any case expect some false positives when testing multiple species.

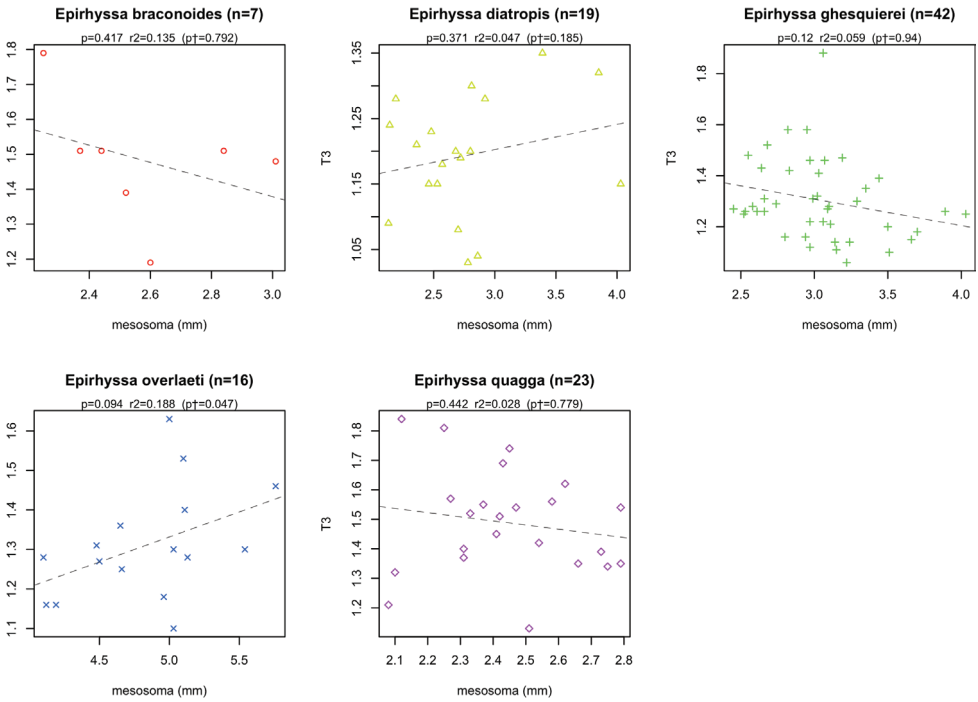

Figure 4. Mesosoma length versus tergite 3 slenderness (length/width) of 107 male rhyssine wasps. No species showed a significant increase in slenderness with body size (linear regression, statistics in top margin). This suggests the males of these species do not scramble for emerging females. The one exception was *Epirhyssa overlaeti*, whose tergites got significantly more slender with body size when the significance was estimated by one-tailed correlation (p-values marked with †) instead of linear regression.

These results fit what has been hypothesised. Eggleton (1991) suggested that scrambling for females while they emerge (the BESC mating strategy) only evolved in one rhyssine lineage (*Megarhyssa* plus *Rhyssella*), and that the males of other genera either guard a female emergence point (BEFD), or mate after the female has emerged (AESC). He also suspected that tropical rhyssines do not use the BESC strategy due to population densities being low. Gauld (1991) noted that males of most tropical rhyssine species possess stout metasomas because they are Batesian mimics of stout-bodied vespid wasps. Our results support these hypotheses. We did not find any evidence (except for the *E. overlaeti* mentioned above) of BESC mating in our tropical *Epirhyssa* species despite reasonable sample sizes.

Although our results provide some interesting insights on the biology of some rhyssine species, it remains a fact that there are over 250 rhyssine species (Hopkins et al. 2019), and that Eggleton's method for detecting BESC mating is still insufficiently tested. We recommend further measurements on more species, especially in the two genera which we measured but for which we did not get sufficient sample sizes. These are *Megarhyssa*, for which Eggleton predicted BESC mating, and *Rhyssa* Gravenhorst, 1829, for which he predicted some other mating strategy. Measurements of some la-

benine and pimpline genera (e.g. *Apechoneura* Kriechbaumer, 1890 and *Dolichomitus* Smith, 1877), which may employ similar mating strategies (Gauld and Wahl 2000: p. 310), would also be useful. Field observations of mating rhyssines would help confirm that the species whose males scramble for emerging females genuinely follow the morphological pattern proposed by Eggleton.

References

Ashmead WH (1900) Some changes in generic names in the Hymenoptera. The Canadian Entomologist 32: 368–368. https://doi.org/10.4039/Ent32368a-12

Bennett AMR, Cardinal S, Gauld ID, Wahl DB (2019) Phylogeny of the subfamilies of Ichneumonidae (Hymenoptera). Journal of Hymenoptera Research 71: 1–156. https://doi.org/10.3897/jhr.71.32375

Cresson ET (1864) Descriptions of North American Hymenoptera, in the collection of the Entomological Society of Philadelphia. Proceedings of the Entomological Society of Philadelphia 3: 257–321. https://www.biodiversitylibrary.org/page/3745740#page/273

Cresson ET (1865) On the Hymenoptera of Cuba. Proceedings of the Entomological Society of Philadelphia 4: 1–200. https://www.biodiversitylibrary.org/item/23927#page/13

Eggleton P (1991) Patterns in male mating strategies of the Rhyssini: a holophyletic group of parasitoid wasps (Hymenoptera: Ichneumonidae). Animal Behaviour 41: 829–837. https://doi.org/10.1016/S0003-3472(05)80350-1

Gauld ID (1991) The Ichneumonidae of Costa Rica, 1. Memoirs of the American Entomological Institute 47: 1–589.

Gauld ID, Wahl DB (2000) The Labeninae (Hymenoptera: Ichneumonidae): a study in phylogenetic reconstruction and evolutionary biology. Zoological Journal of the Linnean Society 129: 271–347. https://doi.org/10.1111/j.1096-3642.2000.tb00015.x

Gauld ID, Sithole R, Gomez JU, Godoy C (2002) The Ichneumonidae of Costa Rica, 4. Memoirs of the American Entomological Institute 66: 1–768.

Gómez IC, Sääksjärvi IE, Puhakka L, Castillo C, Bordera S (2015) The Peruvian Amazonian species of Epirhyssa Cresson (Hymenoptera: Ichneumonidae: Rhyssinae), with notes on tropical species richness. Zootaxa 3937: 311–336. https://doi.org/10.11646/zootaxa.3937.2.4

Gravenhorst JLC (1829) Ichneumonologia europaea (volume 1). Vratislavia (Wrocław). https://doi.org/10.5962/bhl.title.65750

Hopkins T, Roininen H, Noort S van, Broad GR, Kaunisto K, Sääksjärvi IE (2019) Extensive sampling and thorough taxonomic assessment of Afrotropical Rhyssinae (Hymenoptera, Ichneumonidae) reveals two new species and demonstrates the limitations of previous sampling efforts. ZooKeys 878: 33–71. https://doi.org/10.3897/zookeys.878.37845

Keronen S, Sääksjärvi IE, Hopkins T (2021) Measurements of male rhyssine wasps (Hymenoptera: Ichneumonidae: Rhyssinae) [Dataset]. Zenodo. https://doi.org/10.5281/zenodo.5528589

Kriechbaumer J (1890) Ichneumoniden-Studien. Neue Ichneumoniden des Wiener Museums. II. Annalen des Naturhistorischen Museums in Wien 5: 479–491. https://www.jstor.org/stable/41767720

Linnaeus C (1758) Systema Naturae (10th edn., vol. 1). Stockholm (Holmia): Lars Salvius (Laurentius Salvius). http://resolver.sub.uni-goettingen.de/purl?PPN362053006

Porter CC 1978. A revision of the genus Epirhyssa (Hymenoptera: Ichneumonidae). Studia Entomologica 20: 297–318.

R Core Team (2017) R: A Language and Environment for Statistical Computing (Versio 3.4.0). Vienna, Austria: R Foundation for Statistical Computing. https://www.R-project.org/

Rohwer SA (1920) The North American ichneumon-flies of the tribes Labenini, Rhyssini, Xoridini, Odontomerini, and Phytodietini. Proceedings of the United States National Museum 57: 405–474. https://doi.org/10.5479/si.00963801.57-2317.405

Roskov Y, Ower G, Orrell T, Nicolson D, Bailly N, Kirk PM, Penev L [Eds] (2019) Species 2000 & ITIS Catalogue of Life, 2019 Annual Checklist. Species 2000: Naturalis, Leiden, the Netherlands. http://www.catalogueoflife.org/annual-checklist/2019

Seyrig A (1937) Sur les Rhyssini de la faune éthiopienne (Hym. Ichneumonidae). Revue de Zoologie et de Botanique Africaines 30: 112–116.

Smith F (1877) Descriptions of four new species of Ichneumonidae in the collection of the British Museum. Proceedings of the Zoological Society of London 410–413. https://biostor.org/reference/70306

Yu DS, van Achterberg C, Horstmann K (2016) Taxapad 2016. Ichneumonoidea 2015 (Biological and taxonomical information), Taxapad Interactive Catalogu e Database on flashdrive. Nepean, Ottawa.

JHR 86: 101–121 (2021)
doi: 10.3897/jhr.86.71309
https://jhr.pensoft.net

RESEARCH ARTICLE

JOURNAL OF Hymenoptera RESEARCH
A peer-reviewed open-access journal
The International Society of Hymenopterists

Description of *Kavayva*, gen. nov., (Chalcidoidea, Eurytomidae) and two new species associated with *Guarea* (Meliaceae), and a review of New World eurytomids associated with seeds

Y. Miles Zhang[1], Michael W. Gates[1], Rogerio Silvestre[2,3], Manuela Scarpa[3]

1 *Systematic Entomology Laboratory, Agricultural Research Service, U.S. Department of Agriculture, c/o National Museum of Natural History, Smithsonian Institution, P.O. Box 37012, MRC-168, Washington, DC 20013-7012, USA* **2** *Hymenoptera Ecology Laboratory- Hecolab, Universidade Federal da Grande Dourados-UFGD. Rod. Dourados Itahum km 12, Cidade Universitária, 79804-970, Dourados, Mato Grosso do Sul, Brazil* **3** *Graduate Program in Entomology and Biodiversity Conservation - UFGD, Dourados, Brazil*

Corresponding author: Michael W. Gates (Michael.Gates@usda.gov)

Academic editor: Petr Janšta | Received 8 July 2021 | Accepted 3 September 2021 | Published 29 October 2021

http://zoobank.org/0B892FB9-A903-44C4-9B5D-4AF6D76E48A2

Citation: Zhang YM, Gates MW, Silvestre R, Scarpa M (2021) Description of *Kavayva*, gen. nov., (Chalcidoidea, Eurytomidae) and two new species associated with *Guarea* (Meliaceae), and a review of New World eurytomids associated with seeds. Journal of Hymenoptera Research 86: 101–121. https://doi.org/10.3897/jhr.86.71309

Abstract

Kavayva Zhang, Silvestre & Gates, **gen. nov.**, and two species are described from the Neotropics, *Kavayva bodoquenensis* Zhang, Silvestre & Gates, **sp. nov.**, and *Kavayva davidsmithi*, Zhang & Gates, **sp. nov.** Specimens of the new species were collected independently during separate research efforts in Peru and Brazil, reared from the seeds of *Guarea* F. Allam ex L. (Meliaceae), which represents a new host plant family for Eurytomidae. A differential diagnosis of the New World seed-feeding eurytomids is also provided.

Keywords

Neotropical region, Phytophagy, seed chalcids

Copyright *Y.Miles Zhang et al.* This is an open access article distributed under the terms of the Creative Commons Attribution License (CC BY 4.0), which permits unrestricted use, distribution, and reproduction in any medium, provided the original author and source are credited.

Introduction

The Eurytomidae is one of the smaller family of Chalcidoidea, and the majority of their larvae feed endophytically as seed eaters, gall formers, or as parasitoids of phytophagous insects (Lotfalizadeh et al. 2007). Most seed-feeders of cultivated plants are considered as pest insects, which can be accidentally transported to new regions given their cryptic lifestyle.

In the Neotropics, three genera have been recorded to be associated with seeds. The most commonly encountered genus is *Bephratelloides* Girault, which are known seed feeders of Annonaceae (Grissell and Schauff 1990; Grissell and Foster 1996; Chang 1998). *Bephratelloides abulus* Grissell and Foster was erroneously reported to be associated with *Diospyros digyna* Jacq. (Ebenaceae), but was later shown to be *Prodecatoma diospyri* Muesebeck (Castañeda-Vildózola et al. 2011; Ruiz-Montiel et al. 2021). Although not a major pest, *Bephratelloides* have been documented in various species of custard apple grown for human consumption, such as atemoya, cherimola and others in Florida (USA), Mexico and Brazil (Peña and Bennett 1995; Moura et al. 2006; Hernández-Fuentes et al. 2008; Castañeda-Vildózola et al. 2010). The genus is also commonly intercepted at US ports of entry and submitted to the Systematic Entomology Lab for identification, with 634 specimens submitted over the past 25 years (M. Touchet, pers. comm.). Three species of *Bephratelloides* were included in Lotfalizadeh et al. (2007) as part of the morphological phylogenetic analysis of Eurytominae, and the genus was weakly recovered by homoplastic characters including bilobed clypeus and relatively long postgenal bridge.

Prodecatoma Ashmead have been recorded from South America, Africa, and Asia, although the genus is likely not monophyletic (DalMolin et al. 2004). Lotfalizadeh et al. (2007) redefined the genus in a restricted sense to contain only the Neotropical phytophagous species, which is supported by the following morphological characteristics: lower face strigose with a median carina continued on intertorular space; intertorular space raised into a broadly laminate and discoid projection continuing dorsally on the scrobal depression; and prepectus with subventral carinae distinctly diverging anteriorly. This group now contains gall formers and inquilines on Araceae, Dipterocarpaceae, Ebenaceae, Fabaceae, Liliaceae, Myrtaceae, Meliaceae, Rubiaceae, Sabiaceae and Vitaceae (DalMolin et al. 2004; Lotfalizadeh et al. 2007; Ruiz-Montiel et al. 2021).

Paradecatoma Masi is a small genus restricted to Afrotropical region, with a single described species *Paradecatoma bannensis* Masi from the pyrene/drupe of *Cordia africana* Lam. (Boraginaceae) (Yirgu and Delvare 2019), and at least three undescribed species associated with seeds of *Combretum glutinosum* Perr. ex DC. and *Terminalia macroptera* Guill. & Perr. (Combretaceae) (Lotfalizadeh et al. 2007). All four species of *Paradecatoma* were included in the Lotfalizadeh et al. (2007) study, and the genus was weakly recovered with the following characters: narrow intertorular space and strongly raised margin on antennal toruli, lateral foraminal plate not delimited, and subforaminal bridge with vestigial median strip. *Eurytoma werauhia* Gates & Cascante-Marin (2004) is a phytophagous Neotropical species associated with floral buds of *Werauhia gladioliflora* (Wendl.) (Bromeliaceae), Lotfalizadeh et al. (2007) suggested that *E. werauhia* probably belongs to *Paradecatoma* Masi, which would greatly expand the biogeographic range of the genus. However, ongoing phylogenomic analysis suggests *E. werauhia* is actually a new genus (Zhang et al. in prep).

Table 1. Morphological comparison of comparison of New World Eurytomidae associated with seeds.

	Bephratelloides	***Prodecatoma***	***Eurytoma werauhia***	***Kavayva***
Intertorular space	minute, rounded projection with tip truncate	projection thin, long and narrow, pointy	projection thin, long and narrow, pointy	no projection
Frontal depression	wider ventrally, slightly broadening towards toruli, anterior ocellus not included	wider ventrally, slightly broadening towards toruli, anterior ocellus partially included	wider ventrally, slightly broadening towards toruli, anterior ocellus not included	wider dorsally, narrowing towards toruli, anterior ocellus not included
Ventral plaque	no	in some males	no	in all males, some females
Forewing	stigmated	not stigmated	not stigmated	thickened in males, stigmated
Procoxa	striate-rugose	striate	with oblique groove	smooth, with lamella
Propodeum	coarsely sculptured laterally, broad, median furrow present or absent	coarsely sculptured laterally, broad, no median furrow	broad, flat, median furrow areolate, slightly narrowing	broad, flat, smooth

The research presented here is based on specimens collected independently during separate research efforts in Peru, Panama, and Brazil, reared from the seeds of *Guarea* F. Allam ex L. (Meliaceae), which represents a new host plant family for Eurytomidae (Fig. 1). The goal of this study is to describe the new genus *Kavayva* and the two new species, and provide an overview of the generic concepts of New World seed-feeding eurytomids.

Materials and methods

Field collection

Guarea kunthiana A. Juss. (Meliaceae), is a perennial tree of secondary to late climax communities. Its height reaches up to 20 m and its diameter up to 60 cm, and it occurs commonly in semi-deciduous forests in Central and South American (Pennington and Clarkson 2013). The common name in Brazil is “Figo do Mato” (Lorenzi 2002). The unisexual flowers secrete nectar and are pollinated by Coleoptera and Lepidoptera, with seed dispersal by birds and rodents (Wenny 1999). Flowering occurs from November to December, but may occur sporadically throughout the year (Souza et al. 2002).

Fruits were collected in a semi-deciduous Atlantic Forest (Fig. 2) at Serra da Bodoquena, Bonito, Mato Grosso do Sul, Brazil, near the Taquaral river (21°06'56"S, 56°38'24"W), and the Boqueirão farm (21°07'31.8"S, 56°43'20.9"W), at altitudes of 582 m and 540 m above sea level, respectively. There were four seasonal samplings in May and December 2015, and in February and May 2016. The fruits were collected from trees in linear transects 1000 meters long, with a perpendicular distance of 5 meters on either side, when allowed by the topography of the area, totaling 10,000 square meters (1 ha).

The fruits were collected manually with scissors (Fig. 3), the quantity varied according to the availability on each plant. They were individually placed, where possible, in plastic pots containing sterilized sand as a substrate for pupal burial, with small holes in the lid for air circulation (Fig. 4). Pots were observed daily and parasitoids that

Figure 1. Illustration of *Kavayva davidsmithi* with its host plant, *Guarea guidonia* (Meliaceae). The upper right shows the emergence holes from the fruit. Illustrated by Taina Litwak.

emerged from the fruits kept alive six hours to fix the chromatic patterns, and then placed in ethanol and frozen.

Voucher species were incorporated into the Hymenoptera collection (HyMB) of the Museum of Biodiversity (MuBio) of the Federal University of Grande Dourados

Figure 2–6. Collection of *Kavayva bodoquenensis* **2** semi-deciduous forest along the Taquaral river, Serra da Bodoquena, Brazil **3** fruits of *Guarea kuntiana* on tree **4** individualized plastic pots with sterilized sand **5** seed damage by *K. bodoquenensis* **6** pupa of *K. bodoquenensis*. Photo **1** by Paulo Robson de Souza **3, 4** by Manuela Scarpa **5, 6** by Bhrenno Trad.

(UFGD), Dourados-MS, Brazil. For the species of trees from which fruits are sampled, vouchers were collected, and sent to the Botanic Sector of the UFGD to be identified by Dr. Zefa Valdevina Pereira and incorporated into the MuBio Herbarium.

Molecular protocol

Specimens were extracted, amplified, and sequenced at the Laboratories of Analytical Biology (LAB) at the Smithsonian Institution's National Museum of Natural History (NMNH, Washington, DC, USA). A single specimen of *K. bodoquenensis* was destructively sampled using the DNeasyTM Tissue Kit protocol (Qiagen, Valencia, CA, USA). Fragments of mtDNA COI were amplified using LCO1490 5'-GGTCAACAAATCATAAAGATATTGG-3' and HCO2198 5'-TAAACTTCAGGGTGACCAAAAAATCA-3' (Folmer et al. 1994). PCR was performed using approximately 2 µl DNA extract, 1.25 µL 10× Buffer, 1 µl dNTP, 1 µl of each primer, 1 unit of Taq DNA polymerase (TaKaRa Bio, Mountain View, CA, USA), and purified water for a final volume of 25 µl. Amplicons of COI were generated with an initial denaturation of 1 min at 95 °C, followed by 35 cycles at 95 °C for 15 s, 49 °C for 15 s and 72 °C for 45 s, and a final elongation period of 4 min at 72 °C. Sequencing was conducted using an ABI 3730xl DNA sequencer following the manufacturer's instructions. Contigs were assembled and edited using Geneious Prime v2021.1. DNA sequences were then compared with all available sequences in the Basic Local Alignment Search Tool (BLAST) for nucleotides in GenBank.

Imaging

Ethanol-preserved specimens were dehydrated through increasing concentrations of ethanol, and transferred to hexamethyldisilazane (HMDS) (Heraty and Hawks 1998) before point-mounting. MWG identified the specimens using a Leica M205C stereomicroscope with 10X oculars and a Leica LED ring light source for point-mounted specimen observation. We took scanning electron microscope (SEM) images with a Hitachi TM3000 (Tungsten source). Body parts of disarticulated specimens were adhered to a 12.7 X 3.2 mm Leica/Cambridge aluminum SEM stub by a carbon adhesive tab (Electron Microscopy Sciences, #77825–12). Stub-mounted specimens were sputter coated with gold-palladium using a Cressington Scientific 108 Auto from multiple angles to ensure complete coverage (~20–30 nm coating). Habitus images were obtained using a Visionary Digital imaging system. The system consists of a Canon EOS 5D Mark II digital SLR camera with a 65 mm macro lens. A Dynalite MP8 power pack and lights provided illumination. Image capture software was Visionary Digital's proprietary application with images saved as TIF with the RAW conversion occurring in Canon Digital Photo Professional software. Image stacks were mounted with Helicon Focus 6.2.2. Image editing was done in Adobe Photoshop and plate layout in Adobe Illustrator. The painting (Fig. 1) was made from pinned and live insect specimens, plant herbarium sheets and photographs. Additional structural details of

the insects were obtained from SEM photographs. The final image was painted using Adobe Photoshop.

All species identifications were corroborated by comparison with authoritatively identified specimens in the Smithsonian National Museum of Natural History. Terminologies used for surface sculptures follow Harris (1979), while the morphology follows Gibson (1997), Lotfalizadeh et al. (2007), and Gates and Pérez-Lachaud (2012) for adults, and Short (1952), Roskam (1982), and Henneicke et al. (1992) for larvae. Abbreviations for museums are: MUSM – Natural History Museum of the San Marcos University, UFGD, Museum of Biodiversity of the Federal University of Grande Dourados, Dourados-MS, Brazil, and USNM – United States National Museum of Natural History, Washington, D.C., USA.

Results

The *K. bodoquenensis* adults emerged between May 8–29, 2016. Twenty-eight fruits were collected with a combined weight of 584.30 g (average = 20.87 g). The fruits were soft carmine color, with fibrous texture, without pulp, containing 4–8 almond-shaped seeds (Fig. 5). On average, 25% of the seeds were parasitized. Only one hole per seed was observed to indicate emergence of wasps. A total of 32 individuals emerged from seeds in the laboratory (Fig. 6), 20 females and 12 males, with a sex ratio of 0.6 m/f. An unidentified adult female Sesiidae (Lepidoptera) emerged from one of the seeds. The *COI* sequence (676 bp, GenBank Accession # MZ483873) did not match any known species.

Kavayva Zhang, Silvestre, & Gates, gen. nov.

http://zoobank.org/E9334690-6851-4440-8244-986B9BC45405
Figs 1, 7–27

Type species. *Kavayva bodoquenensis* Zhang, Silvestre, Gates.

Diagnosis. *Kavayva* can be distinguished from other eurytomid genera by the following combination of characters – presence of ventral plaque of scape form a projection on the inner face below the attachment to pedicel in males (*Kavayva bodoquenensis*, Fig. 13) or both sexes (*Kavayva davidsmithi*, Fig. 26), F1 of antenna cylindrical and not constricted (Fig. 12), presence of deep black line along the malar sulcus (Fig. 25), middle of propodeum completely glabrous and smooth (Fig. 15), and associated with seeds of *Guarea* (Meliaceae).

Description. Female body length 6.5–10 mm, male 6.5–9.4 mm.

Color. Mostly yellow, black along malar sulcus, with brown infuscation or black bands on the dorsal mesosoma.

Head. Quadrate with rounded corners, 2.4–2.5× as wide as long in dorsal view (Figs 9, 25), areolate-rugose with setae. Lower face weakly strigose, clypeus bilobed, mandible tridentate, supraclypeal area smooth, slightly concave, extending to the toruli

Figure 7–8. Lateral habitus of *Kavayva bodoquenensis* **7** female **8** male. Photos by Cecilia Escobar.

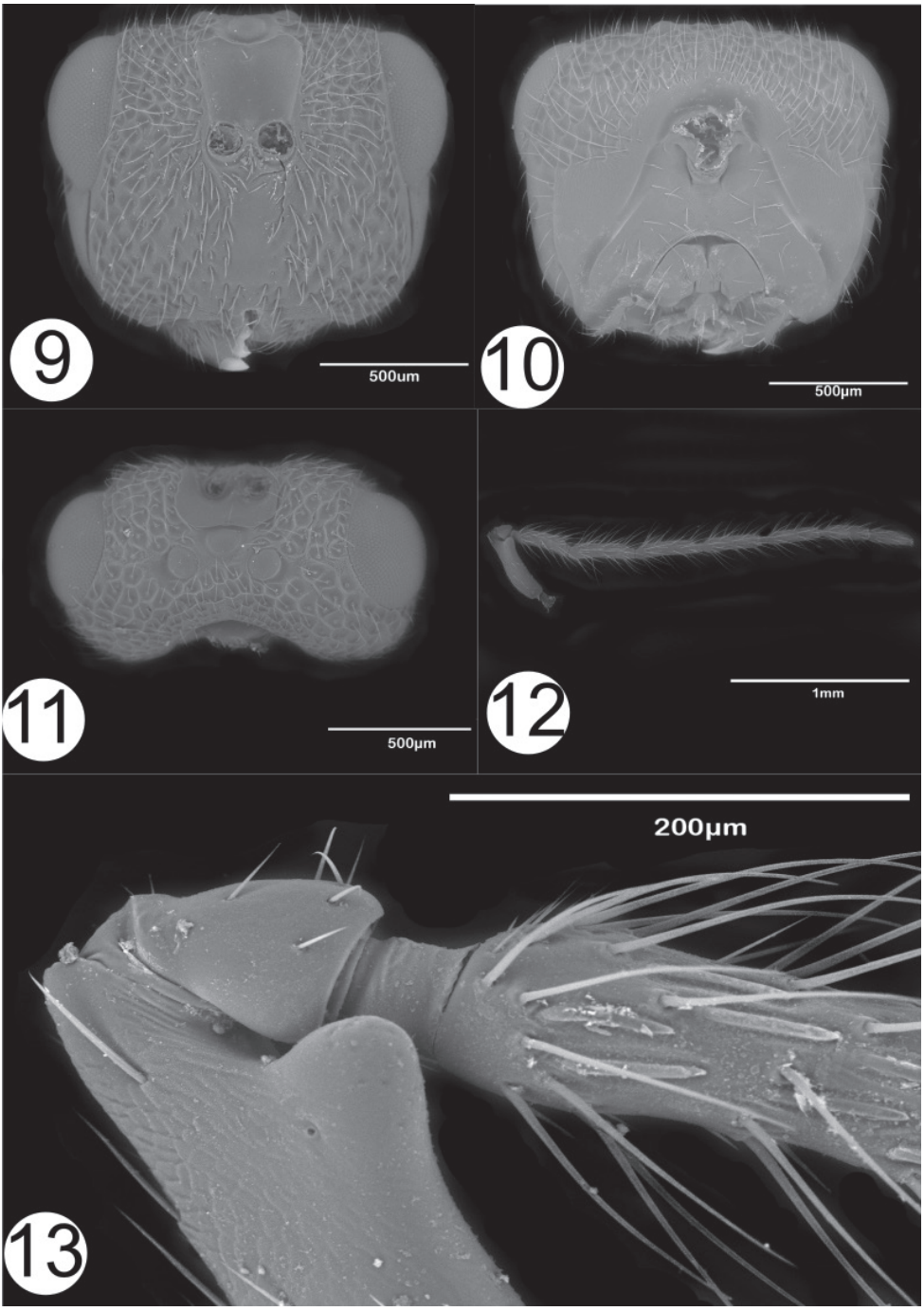

Figure 9–13. *Kavayva bodoquenensis* **9** frontal view of head **10** ventral view of head **11** dorsal view of head **12** male antenna **13** close up of ventral plaque on antennal scape.

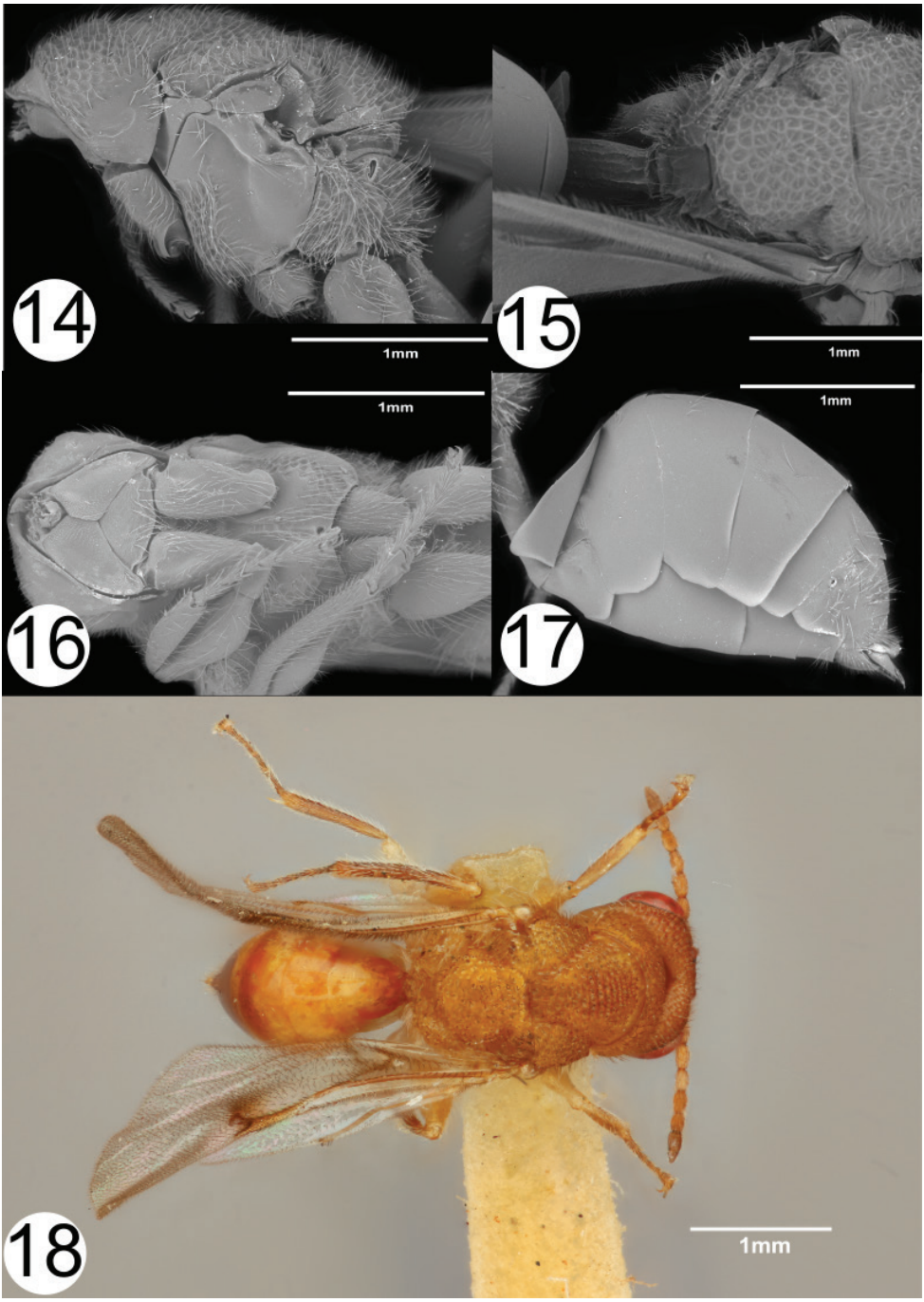

Figure 14–18. *Kavayva bodoquenensis* **14** lateral view of male mesosoma **15** dorsal view of male mesosoma **16** ventral view of mesosoma **17** ventral view of male metasoma **18** dorsal habitus of female specimen collected from Panama.

(Figs 9, 25). Malar sulcus present, incomplete, reaching about ⅔ of malar space. Malar space glabrous, smooth. Genal carina present. Toruli positioned parallel to the lower ocular line, diameter of torulus 3.3× that of the intertorular space. Intertorular space without projection between antennae (Fig. 9). Scrobal depression deeply excavated, converging ventrally in frontal view. Vertex areolate to umbilicate, anterior ocellus above scrobal depression. Scape with or without ventral plaque (females of *Kavayva bodoquenensis*). Antenna pedicel chalice-shaped, six funicular segments cylindrical with multiple irregular rows of longitudinal sensilla and whorls of setae, much shorter than its bearing segment, clava 2-segmented. Occiput concave, postgenal groove diverging, postgenal lamina present, subforaminal bridge ornamentation faint and inconspicuous (Fig. 10).

Wing. Forewing slightly infumated below marginal and stigmal vein, or forming a narrow band that curves slightly proximally and extending half way down the wing (Figs 7, 27). Costal cell, basal cell, and speculum (except for anterior edge) setose.

Mesosoma. Mesosoma umbilicate, 1.2–1.7× as long as broad. Notauli complete, shallow. Anterior pronotal carina widely interrupted. Femoral depression of mesopleuron weakly striate, mespeimeron smooth and shiny ventrally, bulging laterally (Fig. 14). Dorsellum carinae diverging. Propodeum in lateral view forming a 90° angle with mesosoma, broadly delimited by carinae forming a hexagon with raised lateral corners (Fig. 15). Median furrow of propodeum concave and smooth, bordered laterally by irregular setose cells. Forecoxa without oblique groove (Fig. 16). All femora with distal lamella, forecoxa without oblique groove. Metacoxa bare laterally, metatibia densely setose.

Metasoma. Metasoma medially compressed, smooth, Gt4–Gt6 glabrous or setose. Petiole very short and not visible while specimen is intact (Figs 7, 22). Gaster S-shaped in lateral view, ovipositor angled at about 30° dorsad of horizontal axis. Gt4 may be emarginate posteriorly in dorsal view.

Male. Color and sculpture as described similar to females. Ventral plaque on scape forming a projection on the inner face below the attachment point to pedicel (Figs 12, 13). Antennomeres with multiple rows of erect setae. Toruli positioned above the lower ocular line. Marginal vein swollen (Figs 8, 23). Gastral petiole striate dorsally, 1.5–1.7× as long as the length of metacoxa, smooth laterally.

Etymology. In the Guarani Native American language "Kavayva" means: "wasp of the fruit that gives seeds".

Key to species of *Kavayva*

1 Mesosoma uniform without black bands (Fig. 18), forewing with secondary wing band (Fig. 7), only males have ventral plaques on the scape..... ..... ***Kavayva bodoquenensis*** **sp. nov.**

– Mesosoma with black bands (Fig. 24), forewing without secondary wing band (Fig. 27), both males and females have ventral plaques on the scape (Fig. 26)..... ***Kavayva davidsmithi*** **sp. nov.**

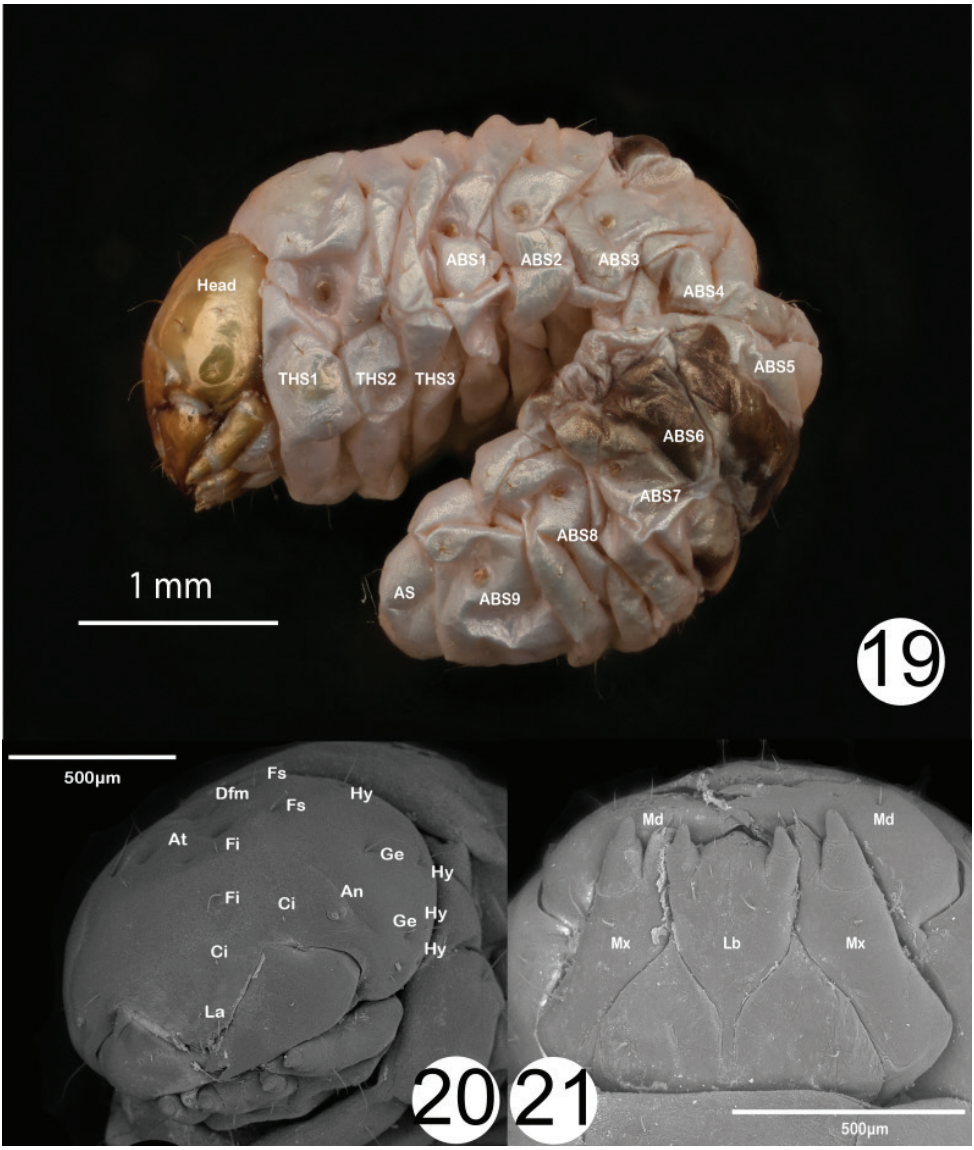

Figure 19–21. *Kavayva bodoquenensis* larva **19** lateral habitus, abdominal segment (ABS), anal segment (AS), thoracic segment (THS) **20** anterolateral view of head, antennae (An), anterior tentorial pit (At), clypeal setae (Ci), cranial depression (Dfm), interior frontal setae (Fi), superior frontal setae (Fs), anterior genal setae (Ge), hypostomal setae (Hy), labral setae (La) **21** ventral view of head, labium (Lb), mandible (Md), maxilla (Mx).

Kavayva bodoquenensis Zhang, Silvestre, & Gates, sp. nov.

http://zoobank.org/838C50D8-21F5-4092-AEDA-3E9A2675D005
Figs 7–21

Material examined. ***Holotype*** Brazil • [1F]; MS, Bonito, Serra da Bodoquena; 21°06'56"S, 56°38'24"W; 8–29 May 2016; R. Silvestre leg.; ex fruit of *Guarea kunthiana*;

USNMENT01788104. ***Paratypes*** Brazil • [9F, 9M]; same information as holotype; R. Silvestre and M. Scarpa leg.; USNMENT01788085–103 • [8F, 3M]; same information as holotype; UFGD Hymb00023-CH–00034-CH. Panama • [3F, 4M]; Arraiján; Sep. 1938; J. Zetek leg.; ex. fruit of *Guarea guarea*; No. 4279, Lot # 88–17223; USNMENT01788078–084.

Diagnosis. *Kavayva bodoquenensis* can be distinguished from *K. davidsmithi* by the lack of black bands across mesosoma in dorsal view (Fig. 18), and the lack of ventral plaque in females.

Description. ***Holotype female.*** 6.5 mm in length.

Color. Yellow except malar sulcus, supraclypeal area, Gt3-syntergum of the metasoma (except for pairs of yellow patches dorsad of Gt4 and Gt5), proximal half of femora and tibiae, wing veins, wing bands near basal setal line and marginal vein brown, edge of mandible, setae on head and mesosoma black and eyes pinkish red (Fig. 7).

Head. Quadrate with rounded corners, 1.2× as wide as high in frontal view, 2.5× as wide as long in dorsal view, areolate-rugose with setae (Fig. 11). Lower face weakly strigose, clypeus bilobed, mandible tridentate, supraclypeal area smooth, extending to the toruli. Malar sulcus present, incomplete, reaching to ⅔ of malar space. Malar space glabrous, smooth. Genal carina present, smooth. Toruli positioned above lower ocular line about 1/3 of the eye length, diameter of torulus 3.3× that of the intertorular space. Scrobal depression deeply excavated, converging ventrally in frontal view (Fig. 9). Vertex areolate-umbilicate, anterior ocellus above scrobal depression, ratios of POL:OOL:LOL 4:5:1. Scape without ventral plaque. Ratio of scape (minus radicle):pedicel:anellus:F1:F2:F3:F4:F5:F6:club as 14:3.3:1:6:6:6:5.3:4:7, pedicel chalice-shaped, funicular segments cylindrical with multiple irregular rows of longitudinal sensilla whorls of setae, much shorter than its bearing segment, clava 2-segmented. Occiput concave, postgenal groove diverging, postgenal lamina present, subforaminal bridge ornamentation faint and inconspicuous (Fig. 10).

Wing. Forewing infumated below marginal and stigmal vein, band narrow, curving slightly proximally, and extending half way down the wing. Basal and costal setal line also infumated. Ratio of marginal vein:postmarginal vein:stigmal vein as 1.5:1 (Fig. 7).

Mesosoma. Mesosoma umbilicate, 1.2× as long as broad. Notauli complete, shallow (Fig. 18). Anterior pronotal carina widely interrupted. Femoral depression of mesopleuron weakly striate, mesepisternum smooth (Fig. 14). Dorsellum carinae diverging. Propodeum in lateral view forming a 90° angle with mesosoma, concave and smooth medially, bordered laterally by irregular, ridged, setose cells (Fig. 15). All femora with distal lamella.

Metasoma. Metasoma medially compressed, smooth, Gt4-syntergum setose. Petiole very short and not visible while specimen is intact (Fig. 7). Gaster S-shaped in lateral view, ovipositor angled at about 30° dorsad to horizontal axis. Gt4 not emarginate posteriorly in dorsal view.

Male. 6.5 mm. Scrobal depression black, ventral half of body whitish-yellow, wing vein amber, otherwise color and sculpture as described for females. Ventral plaque on scape forming a projection on the inner face below the attachment point to the pedicle (Figs 12, 13). Antennomeres with multiple rows of erect setae. Gastral petiole striate dorsally, 1.5× as long as the length to metacoxa, smooth laterally (Fig. 17).

Figure 22–23. *Kavayva davidsmithi* lateral habitus **22** female **23** male. Photos by Cecilia Escobar.

Variation. Size ranges from 3.5–6.5 mm. Color ranges from mostly yellow to mostly black dorsally, mesepisternum can range from smooth to weakly striate.

Larva. Head amber-colored and body beige. Body length 4.7 mm; width 1.7 mm. Body C-shaped; 13 segmented (three thoracic, nine abdominal, and one anal segments);

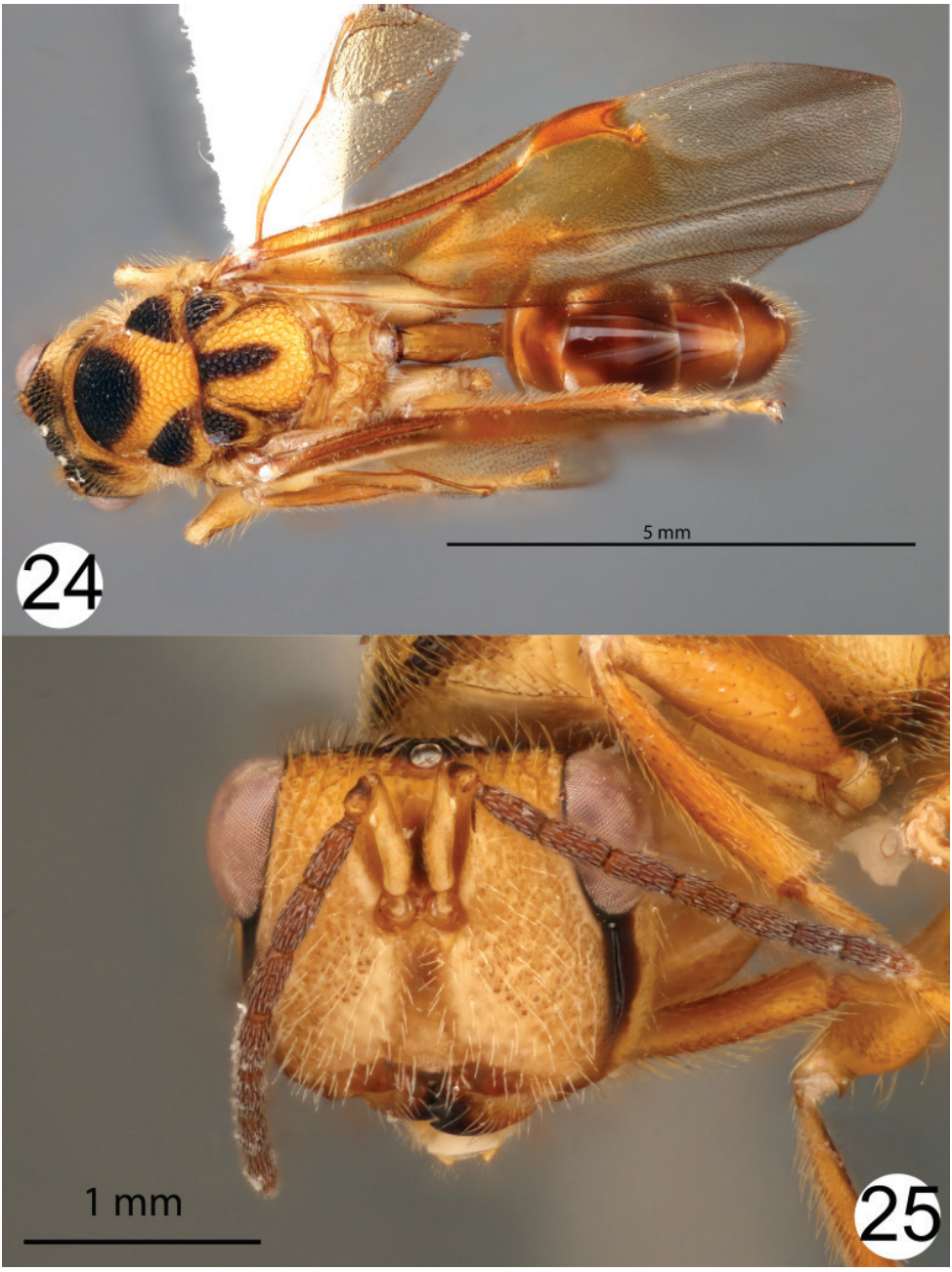

Figure 24–25. *Kavayva davidsmithi* **24** male dorsal habitus **25** frontal view of head. Photos by Cecilia Escobar.

tapering slightly posteriorly; no protuberance on body segments (Fig. 19). Head heavily sclerotized; antennae positioned ventrolaterally on the head, above the mandible, 1.29× as long as broad. Two pairs of superior frontal setae near the cranial depression, two pairs of interior frontal setae around anterior tentorial pits, two pairs of clypeal setae,

antennae low and offset laterally, two pairs of genal setae, two pairs of labral setae, and four pairs of hypostomal setae (Fig. 20). Mandible narrowing apically, bidentate, with two pairs of sensilla. Underlip complex flat, with two pairs of setae on the median lobe (labium), and one on the lateral lobe (maxilla) (Fig. 21). Thoracic segments with two dorsal setae, one pair of pleural setae, one pair of lateral setae, and one pair of ventral setae. Abdominal segments with a single pair dorsal, pleural, and ventral setae. Anal segment with one pair of dorsal terminal setae, and ventral terminal setae present.

Biology. Associated with seeds of *Guarea kunthiana* and *G. guarea* = *G. guidonia* (Meliaceae).

Distribution. Brazil, Panama.

Etymology. Named in honor of the Serra da Bodoquena National Park, an environmental conservation unit in Mato Grosso do Sul, Brazil.

Remarks. The specimens collected from Panama are slightly smaller (3.5–5.5 mm) than those from Brazil (5.5–6.5 mm), and with lighter coloration on the wings and metasoma which could be the result of specimens being older (Fig. 18). We did not find any consistent morphological differences in either sex that reliably separate the Panama specimens from those collected in Brazil. Therefore we chose to group them all within *K. bodoquenensis* until fresh material can be collected for molecular work.

Kavayva davidsmithi Zhang & Gates, sp. nov.

http://zoobank.org/50EAFCB5-FD0D-4FD5-9724-92A30E331ED8
Figs 1, 22–27

Material examined. ***Holotype*** Peru • [1F]; Manu National Park, Madre de Dios, Estación Biológica Villa Carmen; Trail 0; 14 Dec. 2013; 12°53'41"S, 71°24'13"W; 650 m a.s.l.; A. L. Norrbom leg.; ex. seed in fruit of *Guarea guidonia*; 13-PE-46; MUSM. ***Paratypes*** Peru • [1F, 1M]; same information as holotype; USNMENT01788076, 077.

Diagnosis. *Kavayva davidsmithi* can be distinguished from *K. bodoquenensis* by the light infumation of the forewing and the absence of a secondary wing band on the basal setal line, extensive black bands across mesosoma in dorsal view, and the presence of ventral plaque on both sexes.

Description. ***Holotype female.*** 10.1 mm in length.

Color. Yellow except antennomeres, supraclypeal area light brown, tip of mandible, vertex, anterior half of occiput, malar sulcus, anterior half of dorsal and lateral pronotum, anterior half of midlobe of mesoscutum, lateral lobes of mesoscutum along the notauli, axillula, mediodorsal line on scutellum, ventral prepectus black, clypeus, wing vein, forewing below submarginal and marginal vein, femur, tibia amber and –eyes pinkish red (Fig. 22).

Head. Quadrate with rounded corners, 1.2× as wide as high in frontal view, 2.4× as wide as long in dorsal view, areolate-rugose with setae (Fig. 25). Lower face weakly strigose, clypeus bilobed, mandible tridentate, supraclypeal area slightly concave and extending to the toruli. Malar sulcus present, incomplete, reaching about ⅔ of malar space. Malar space glabrous, smooth. Genal carina present. Toruli positioned above the

Figure 26–27. *Kavayva davidsmithi* **26** male head and antennae **27** female forewing. Photos by Cecilia Escobar.

lower ocular line about 1/3 of the eye length, diameter of torulus 3.3× that of the intertorular space. Scrobal depression deeply excavated. Vertex areolate, anterior ocellus above scrobal depression, ratios of POL:OOL:LOL equal to 3:4:1. Ventral plaque on scape forming a projection on the inner face below the attachment point to the pedicle. Ratio of scape (minus radicle):pedicel:anellus:F1:F2:F3:F4:F5:F6:club as 10:2.7:1:5.7:6.3:6.3:5.7:5:4.7:6.7, pedicel chalice-shaped, funicular segments with multiple irregular rows of longitudinal sensilla whorls of setae, much shorter than its bearing segment, clava 2-segmented (Fig. 25). Postgenal lamina present.

Wing. Forewing infumated half way down the wing below the submarginal and marginal vein, not exceeding stigmal vein. Ratio of marginal vein:postmarginal vein:stigmal vein as 2.3:1.2:1 (Fig. 27).

Mesosoma. Mesosoma umbilicate, 1.7× as long as broad. Notauli complete, shallow (Fig. 26). Anterior pronotal carina interrupted. Femoral depression of mesopleuron weakly striate, mesepimeron smooth and shiny ventrally, bulging laterally (Fig. 22). Dorsellum carinae diverging. Propodeum in lateral view forming a 90° angle with mesosoma, broadly delimited by carinae forming a hexagon with raised lateral corners. Median furrow of propodeum concave and smooth, bordered laterally by irregular setose cells. All femora with distal lamella.

Metasoma. Metasoma medially compressed, smooth, Gt6-syntergum setose. Gaster S-shaped in lateral view, ovipositor angled at about 30° dorsad to horizontal axis (Fig. 22). Gt4 emarginate posteriorly in dorsal view.

Male. 9.4 mm. Scrobal depression black, otherwise color and sculpture as described for female (Fig. 23). Antennomeres with multiple rows of erect setae and about 1.4× as long as width of segment (Fig. 26). Gastral petiole length in dorsal view about 2.8× as long as its greatest width, 1.7× as long as the length to metacoxa, smooth (Fig. 23).

Variation. The coloration on the vertex and occiput can be confluent or disconnected.

Biology. Associated with seeds of *Guarea guidonia* (Meliaceae).

Distribution. Manu National Park, Peru.

Etymology. Patronym honoring David Smith for his decades of devotion to Hymenoptera and improvement of the Smithsonian's National Insect Collection.

Discussion

The new genus *Kavayva* is only found associated with the seeds of Meliaceae, which represent a new plant family association within Eurytomidae, and the fourth genus associated with seeds in the Neotropics. Based on the upcoming phylogenomic study of Eurytomidae (Zhang et al., in prep.), all of these phytophagous genera are only distantly related to each other, meaning that phytophagy has evolved multiple times within Eurytomidae. While addressing the evolutionary relationships is beyond the scope of this paper, we provide a brief literature review of the morphological characters in order to distinguish these four genera (Table 1). The ventral plaque that is present in all known species of *Kavayva* is also present in some species of *Prodecatoma* (e.g., *P. diospyri*), although the latter can be easily distinguished by the presence of a large intertorular projection and the hyaline forewing. *Bephratelloides* have a stigmated wing and a minute intertorular projection similar to *Kavayva*, but lack the ventral plaque. Finally, *Eurytoma werauhia* differs from *Kavayva* in being mostly black in color, and lacks the ventral plaque.

Given the morphological conservatism within Eurytomidae, it is not surprising that a combination of morphological characters is needed to distinguish these four genera of eurytomids. We hope this study will aid in the discovery of additional *Kavayva* specimens and records, as their host plant *Guarea* can be found from northwestern Mexico down to northern Argentina (Pennington and Clarkson 2013).

Acknowledgements

We thank Bhrenno Maykon Trad, Vander Carbonari, Vinícius Marques Lopez for helping us in laboratory work/photos, and to Instituto Chico Mendes de Biodiversidade-ICMBio from Bonito MS for field collection permissions under SISBIO number 3266–1 date: Oct/06/2011. We would also like to thank Allen Norrbom for providing specimens as bycatch for the USDA Farm Bill project "Enhancement of Fruit Fly Larvae Identification and Taxonomy" (Project Coordinator G.J. Steck, ADODR Norman Barr; project numbers 3.0342 (2012) and 13–8131–0291-CA (2013). Collections in Peru were made through Asociación para la Conservación de la Cuenca Amazónica (ACCA) and its U.S. partner, the Amazon Conservation Association (ACA), with permission of Director General Forestal y de Fauna Silvestre (Resoluciones Directorales No. 0614–2011-AG-DGFFS-DGEFFS). USDA is an equal opportunity employer and provider. Mention of trade names herein is for informational purposes only and does not reflect endorsement by USDA. YMZ is supported by Oak Ridge Institute for Science and Education (ORISE) fellowship.

References

Castañeda-Vildózola A, Nava-Díaz C, Váldez-Carrasco J, Ruiz-Montiel C, Vidal-Hernández L, Barrios-Matias S (2010) Distribution and host range of *Bephratelloides cubensis* Ashmead (Hymenoptera: Eurytomidae) in México. Neotropical Entomology 39(6): 1053–1055. https://doi.org/10.1590/S1519-566X2010000600034

Castañeda-Vildózola A, Nava-Díaz C, Franco-Mora O, Lomeli-Flores JR, Peña JE (2011) *Diospyros digyna* (Ebenaceae): a new host record for *Bephratelloides ablusus* (Hymenoptera: Eurytomidae) in Mexico. Florida Entomologist 94(4): 1071–1072. https://doi.org/10.1653/024.094.0451

Chang PRA (1998) Descripción de *Bephratelloides duguetiphagus* n. sp. (Hymenoptera: Eurytomidae) criados de frutos de *Duguetia panamensis* Standl. (Annonaceae). M. Sc. Dissertation, Universidad de Panamá, Panamá.

DalMolin A, Melo GA, Perioto NW (2004) New species of *Prodecatoma* (Hymenoptera, Eurytomidae) associated to galls in fruits of two species of *Psidium* L. (Myrtaceae), with comments on *Prodecatoma spermophaga* Costa-Lima. Revista Brasileira de Entomologia 48(4): 519–528. https://doi.org/10.1590/S0085-56262004000400015

Folmer O, Black M, Hoeh W, Lutz R, Vrijenhoek R (1994) DNA primers for amplification of mitochondrial cytochrome c oxidase subunit I from diverse metazoan invertebrates. Molecular Marine Biology and Biotechnology 3: 294–299.

Gates MW, Cascante-Marin A (2004) A new phytophagous species of *Eurytoma* (Hymenoptera: Eurytomidae) attacking *Werauhia gladioliflora* (Bromeliales: Bromeliaceae). Zootaxa 512: 1–10. https://doi.org/10.11646/zootaxa.512.1.1

Gates MW, Pérez-Lachaud G (2012) Description of *Camponotophilus delvarei*, gen. nov. and sp. nov. (Hymenoptera: Chalcidoidea: Eurytomidae), with discussion of diagnostic characters. Proceedings of the Entomological Society of Washington 114: 111–124. https://doi.org/10.4289/0013-8797.114.1.111

Gibson GAP (1997) Morphology and terminology. In: Gibson GA, Huber JT, Woolley JB (Eds) Annotated keys to the genera of Nearctic Chalcidoidea (Hymenoptera). NRC Research Press, Ottawa, ON, 16–44.

Grissell EE, Schauff ME (1990) A synopsis of the seed-feeding genus *Bephratelloides* (Chalcidoidea: Eurytomidae). Proceedings of the Entomological Society of Washington 92: 177–187.

Grissell EE, Foster MS (1996) A new *Bephratelloides* (Hymenoptera: Eurytomidae) from seeds of *Cymbopetalum* (Annonaceae) in Mexico. Proceedings of the Entomological Society of Washington 98: 256–263.

Harris RA (1979) Glossary of surface sculpturing. Occasional Papers in Entomology 28: 1–31.

Henneicke K, Dawah HA, Jervis MA (1992) Taxonomy and biology of final-instar larvae of some Eurytomidae (Hymenoptera: Chalcidoidea) associated with grasses in the UK. Journal of Natural History 26(5): 1047–1087. https://doi.org/10.1080/00222939200770621

Hernández-Fuentes LM, Bautista-Martínez N, Carrillo-Sánchez JL, Sánchez Arroyo H, Urías-López MA, Salas Araiza MD (2008) Control del barrenador de las semillas, *Bephratelloides cubensis* Ashmead (Hymenoptera: Eurytomidae) en guanábana, *Annona muricata* L.(Annonales: Annonaceae). Acta Zoológica Mexicana 24(1): 199–206. https://doi.org/10.21829/azm.2008.241631

Lorenzi H (2002) Árvores brasileiras: manual de identificação e cultivo de plantas arbóreas nativas do Brasil, 2nd edn. Instituto Plantarum de Estudos da Flora Ltda, Nova Odessa, SP, Brazil, 248 pp.

Lotfalizadeh H, Delvare G, Rasplus J-Y (2007) Phylogenetic analysis of Eurytominae (Chalcidoidea: Eurytomidae) based on morphological characters. Zoological Journal of the Linnean Society 151: 441–510. https://doi.org/10.1111/j.1096-3642.2007.00308.x

Moura JIL, Sgrillo RB, Sgrillo KR, Vilela EF, Bento JMS (2006) Uso de fêmeas virgens na coleta massal de *Bephratelloides pomorum* (Fab.) (Hymenoptera: Eurytomidae) em *Annona muricata* L. (Annonaceae). Manejo Integrado de Plagas y Agroecología 77: 78–81.

Peña JE, Bennett FD (1995) Arthropods associated with *Annona* spp. in the Neotropics. Florida Entomologist 78(2): 329–349. https://doi.org/10.2307/3495906

Pennington TD, Clarkson JJ (2013) A Revision of *Guarea* (Meliaceae). Edinburgh Journal of Botany 70(2): 179–362. https://doi.org/10.1017/S0960428613000036.

Roskam JC (1982) Larval characters of some eurytomid species (Hymenoptera, Chalcidoidea). Proceedings Koninklijke Nederlandse Akademie van Wetenschappen 85: 293–305.

Ruiz-Montiel C, González-Pérez JS, Valdez-Carrasco J, Lomelí-Flores JR, Gates MW, Franco-Mora O, Castañeda-Vildózola Á (2021) Correcting the identity of a eurytomid wasp associated with Black Sapote fruits in Mexico with new distributional records and notes on its biology, Proceedings of the Entomological Society of Washington 123(2): 437–442. https://doi.org/10.4289/0013-8797.123.2.437

Short JRT (1952) The morphology of the head of larval Hymenoptera with special reference to the head of the Ichneumonoidea, including a classification of the final instar larvae of the Braconidae. Transactions of the Royal Entomological Society of London 103(2): 27–84. https://doi.org/10.1111/j.1365-2311.1952.tb02262.x

Souza LA, Moscheta IS, Mourão KSM, da Rosa SM (2002) Morfo-anatomia da flor de *Guarea kunthiana* A. Juss. e de *Guarea macrophylla* Vahl.(Meliaceae). Acta Scientiarum. Biological Sciences 24: 591–600. https://doi.org/10.4025/actascibiolsci.v24i0.2372

Wenny DG (1999) Two-stage dispersal of *Guarea glabra* and *G. kunthiana* (Meliaceae) in Monteverde, Costa Rica. Journal of Tropical Ecology 15(4): 481–496. https://doi.org/10.1017/S0266467499000966

Yirgu A, Delvare G (2019) First report of *Paradecatoma bannensis* Masi (Hymenoptera, Eurytomidae) as seed parasite of *Cordia africana* in Ethiopia. Phytoparasitica 47(5): 647–657. https://doi.org/10.1007/s12600-019-00763-w

JHR 86: 123–143 (2021)
doi: 10.3897/jhr.86.72281
https://jhr.pensoft.net

RESEARCH ARTICLE

JOURNAL OF Hymenoptera RESEARCH
A peer-reviewed open-access journal
The International Society of Hymenopterists

Notes on the genus *Dendrocerus* Ratzeburg (Hymenoptera, Megaspilidae) from China, with description of two new species

Xu Wang[1,5], Huayan Chen[2], István Mikó[3], Yixin Huang[4,5], Chaodong Zhu[5]

1 *Anhui Provincial Key Laboratory of the Conservation and Exploitation of Biological Resources, Key Laboratory of Biotic Environment and Ecological Safety in Anhui Province, College of Life Sciences, Anhui Normal University, Wuhu, Anhui 241000, China* **2** *State Key Laboratory of Biocontrol, School of Life Sciences / School of Ecology, Sun Yat-sen University, Guangzhou 510275, China* **3** *Don Chandler Entomological Collection, Department of Biological Sciences, University of New Hampshire, Spaulding Hall, Durham, NH 03824, USA* **4** *Collaborative Innovation Center of Recovery and Reconstruction of Degraded Ecosystem in Wanjiang Basin Co-founded by Anhui Province and Ministry of Education; School of Ecology and Environment, Anhui Normal University, Wuhu, Anhui 241000, China* **5** *Key Laboratory of Zoological Systematics and Evolution, Institute of Zoology, Chinese Academy of Sciences, Beijing 100000, China*

Corresponding authors: Xu Wang (wangxu0322@ahnu.edu.cn), Chaodong Zhu (zhucd@ioz.ac.cn)

Academic editor: Miles Zhang | Received 28 July 2021 | Accepted 1 September 2021 | Published 29 October 2021

http://zoobank.org/0CCED1F3-0220-4B66-AF55-72A60C54E859

Citation: Wang X, Chen H, Mikó I, Huang Y, Zhu C (2021) Notes on the genus *Dendrocerus* Ratzeburg (Hymenoptera, Megaspilidae) from China, with description of two new species. Journal of Hymenoptera Research 86: 123–143. https://doi.org/10.3897/jhr.86.72281

Abstract

Species of the genus *Dendrocerus* Ratzeburg, 1852 (Hymenoptera: Megaspilidae) from China were studied. Six species are recorded, of which two known species, *D. carpenteri* (Curtis, 1829) and *D. laticeps* (Hedicke, 1929) are re-described; and two species are described as new to science, *D. anisodontus* Wang, Chen and Mikó **sp. nov.** and *D. bellus* Wang, Chen and Mikó **sp. nov.**. Sequences of the 28S rDNA were generated to associate both sexes of the same species.

Keywords

Ceraphronoidea, DNA barcoding, hyperparasitoid, redescription, taxonomy

Copyright *Xu Wang et al.* This is an open access article distributed under the terms of the Creative Commons Attribution License (CC BY 4.0), which permits unrestricted use, distribution, and reproduction in any medium, provided the original author and source are credited.

Introduction

The family Megaspilidae comprises more than 450 species in 12 genera worldwide, whereas the Chinese fauna is still insufficiently studied (Dessart 2006; Iemma et al. 2016). *Dendrocerus* Ratzeburg, 1852 is the most economically important genus of Megaspilidae (Fergusson 1980), because they are hyperparasitoids and attack the primary parasitoids of aphids. Species of *Dendrocerus* seem to be generalists (Takada 1973; Fergusson 1980; Martens and Johnson 2018). For example, the host complex of *Dendrocerus carpenteri* (Curtis, 1829) includes at least two genera of Cynipoidea and 7 genera of Chalcidoidea (Fergusson 1980). *Dendrocerus* was erected with *D. lichtensteinii* Ratzeburg, 1852 as the type species, a synonym of *Ceraphron halidayi* Curtis, 1829. This species was later designated as a type species of *Lygocerus*, a genus proposed as new by Förster (1856). Dessart (1966) synonymised *Lygocerus* with *Dendrocerus*, and *D. lichtensteinii* with *C. halidayi*. *Dendrocerus* is a cosmopolitan genus, with 118 described species worldwide. There were only 15 *Dendrocerus* species recorded from the Oriental region (Johnson and Musetti 2004; Trietsch et al. 2018) and four species are known from China: *D. angustus* Dessart, 1999, *D. carpenteri*, *D. aphidum* (Rondani, 1877), and *D. laticeps* (Hedicke, 1929).

Based on antennal characters, Dessart (1995) proposed five species-groups for *Dendrocerus*: *halidayi*, *carpenteri*, *serricornis*, *punctipes* and *penmaricus* (Bijoy and Rajmohana 2014). Species of the *halidayi* species-group generally have ramose antennae, but the *D. mexicali* species complex have moveable branches (Burks et al. 2016). The males of the *D. halidayi* species-group are characterized by their ramose antennae, and by the long branches on proximal 4, 5 or 6 flagellomeres. There are 22 species of this group worldwide (Pezzini et al. 2014). Two new species under *D. halidayi* species-group, viz., *D. bellus* and *D. anisodontus* are hereby described and illustrated.

Materials and methods

This work is based upon the specimens in the following collections, with abbreviations used in the text: **AHNU**, Auhui Normal University, Anhui, China; **IZCAS**, Institute of Zoology, Chinese Academy of Sciences, Beijing, China; **SYSBM**, Sun Yat-sen University, The Museum of Biology, Guangzhou, China. Specimens were obtained from sweep nets, Malaise traps, and yellow pan traps.

Considering that sexual dimorphism is common in *Dendrocerus*, we sequenced the gene marker 28S rDNA to associate the female and male of the same species. Genomic DNA was extracted from a female and male of each putative species using a nondestructive DNA extraction protocol as described in Taekul et al. (2014). The primers for 28S amplification followed Zhang et al. (2008). Polymerase chain reactions (PCRs) were performed using a 25 μL system and conducted in a T100 Thermal Cycler (Bio-Rad). Thermocycling conditions were: an initial denaturing step at 94 °C for 1 min, followed by 35 cycles of 94 °C for 1 min, 50 °C for 30 s, 72 °C for 30 s and

Table 1. Detail information of sequenced samples and accession numbers.

Species	Sex	Location	GenBank accession number
D. carpenteri	male	Shandong, Yucheng	MZ340592
	female	Anhui, Chuzhou, Mingguang	MZ340590
D. laticeps	female	Anhui, Chuzhou, Mingguang	MZ340593
	female	Anhui, Chuzhou, Mingguang	MZ340624
D. bellus sp. nov.	female	Guangdong, Guangzhou	MZ344975
	male	Guangdong, Guangzhou	MZ344976
D. anisodontus sp. nov.	female	Yunnan, Menghai, Mt. Bulang	MZ344977
	male	Yunnan, Menghai, Mt. Bulang	MZ344978

an additional extension at 72 °C for 5 min. Amplicons were directly sequenced in both directions with forward and reverse primers by GENERAL BIOL (Anhui, China). Chromatograms were assembled with Sequencing Analysis 6 (ThermoFisher Scientific, Gloucester, UK). All the amplified sequences were deposited into GenBank (see Table 1). The genetic distances were calculated using the Kimura 2-parameter (K2P) model in MEGA X (Kumar et al. 2018).

All voucher specimens were then point-mounted and air-dried. Photographs were taken with a Leica M205A stereomicroscope and a Leica DFC-500 digital camera, with extended focusing software. To prepare male genitalia for study, apical metasomal segments were removed from specimens and placed in 35% H_2O_2 for 24 hours, 5% acetic acid for 24 hours, distilled water for one hour and then transferred to a droplet of glycerin on a concavity slide. Dissections were performed in glycerin by using #5 forceps and #2 insect pins.

Abbreviations and morphological terms (Table 2) follows Mikó and Deans (2009). Measurements are given in microns. Genitalia terminology follows Hymenoptera Anatomy Ontology (Yoder et al. 2010).

Results

In the present paper, we describe two new species of *Dendrocerus*: *D. anisodontus* Wang, Chen and Mikó sp. nov. and *D. bellus* Wang, Chen and Mikó sp. nov., bringing the species number of this genus to six for China. The morphological re-description and photographs are provided for *D. carpenteri* and *D. laticeps*. No Chinese specimens of *D. angustus* and *D. aphidum* are available for this study.

Eight 28S sequences of four species (length ranged from 633 to 641 bp) from China were attained and uploaded to GenBank (Table 1). The pairwise corrected genetic distances based on 28S rDNA sequences of four species, including the two new species, are shown in Table 3. Sequences of both sexes of three putative species (*D. anisodontus*, *D. bellus* and *D. carpenteri*) are 100% identical, confirming the correct association of female and male of the species. Whereas interspecific genetic distances among different *Dendrocerus* species range from 0.008 to 0.030. This will be helpful for molecular identification and the association of the female and male of the same species in this genus.

Table 2. Abbreviations and morphological terms used in text.

Abbreviations	Paraphrase
F1, F2, ..., F9	antennomere 1, 2, ..., 9
LOL	lateral ocellar length, shortest distance between inner margins of median and lateral ocelli
OOL	ocular ocellar length, minimum distance between a posterior ocellus to the eye margin
POL	posterior ocellar length, shortest distance between inner margins of posterior ocelli
HH	head height, lateral view
EHf	eye height, anterior view
HL	head length
HW	head width
IOS	interorbital space
CSB	cephalic size
T1, T2, ..., T4	metasomal tergite 1, 2, ..., 4
Prn	Pronotum
AscW	anterior mesoscutal width
PscW	posterior mesoscutal width
mms	median mesoscutal sulcus
gsp	gonostipes

Taxonomy

Dendrocerus Ratzeburg, 1852

Dendrocerus Ratzeburg, 1852: 180. Type species: *Dendrocerus lichtensteinii* Ratzeburg, by monotypy (= *Ceraphron halidayi* Curtis).

Diagnosis. Head moderately transverse; facial pit absent in most species. Males usually with an obtuse ocellar triangle (POL longer than LOL). Male flagellomeres usually asymmetrical, serrate or trapezoidal. Some species also have branched flagellomeres (*D. mexicali* group). Metapleural sulcus shape usually straight. Sternaulus never present. Medioventral conjunctiva of gonostyle-volsella complex (parossiculi fusion) absent. Wings never absent (Trietsch et al. 2020).

Dendrocerus carpenteri (Curtis, 1829)

Figs 1, 2

Ceraphron carpenteri Curtis, 1829: 249.
Cerapilron crispus Curtis, 1829: 249. Nomen nudum.
Ceraphron elegalls Curtis, 1829: 249. Nomen nudum.
Megaspilus carpenteri (Curtis) Stephens, 1829: 401.
Calliceras carpellteri (Curtis) Westwood, 1840: 77.
Ceraphroll hyalinatus Thomson, 1858: 291.
Lygocerus carpenteri (Curtis) Marshall, 1868: 158.
Coryne carpenteri (Curtis) Buckton, 1876: pl. 7.
Megaspillts niger Howard, 1890: 247.

Table 3. Genetic distance of 28S of four *Dendrocerus* species (F = female, M = male).

	1	2	3	4	5	6	7	8
1. *D. carpenteri* **M**								
2. *D. carpenteri* **F**	0.000							
3. *D. laticeps* **F**	0.008	0.008						
4. *D. laticeps* **F**	0.008	0.008	0.000					
5. *D. bellus* sp. nov. **M**	0.030	0.030	0.022	0.022				
6. *D. bellus* sp. nov. **F**	0.030	0.030	0.022	0.022	0.000			
7. *D. anisodontus* sp. nov. **M**	0.013	0.013	0.008	0.008	0.027	0.027		
8. *D. anisodontus* sp. nov. **F**	0.013	0.013	0.008	0.008	0.027	0.027	0.000	

Trichosteresis proxima Kieffer, 1907: 32.
Trichosteresis punctatipennis Kieffer, 1907: 33.
Lygocerus rlijiventrls Kieffer, 1907: 45.
Lygocerlls campestris Kieffer, 1907: 48.
Lygocerus aphidivorus Kieffer. 1907: 49.
Lygocerlls aphidivorus var. *inconspicuus* Kieffer, 1907: 50.
Lygocerus testaceimanus Kieffer, 1907: 51.
Lygocerus aphidum Kieffer, 1907: 52.
Lygocerus giraudi Kieffer, 1907: 52.
Lygocerus cameroni Kieffer, 1907: 56.
Lygocerus thomsoni Kieffer, 1907: 57.
Lygocerus inquilinus Kieffer, 1917: 349.
Trichosteresis carpenteri (Curtis) Morley, 1929: 55.
Lygocerus ambianus Dessart, 1965: 158.
Delldrocerus britannicus Dessart, 1966: 12.
Delldrocerus tischbeini Dessart, 1966: 12.
Delldrocerus carpenteri (Curtis) Dessart, 1970: 142.

Material examined. China • 1 male, 2 females; Jiangsu, Suzhou; 20.IV.2019; H. Li leg.; (AHNU) • 4 females; Shandong, Yucheng; 17.V.2019; R. Zhang leg.; (IZCAS) • 3 females; Anhui, Chuzhou, Mingguang; 28.IV.2019; H. Li leg. (SYSBM).

Redescription. Male. Body length: 1.8 mm.

***Coloration* (Fig. 1):** Cranium, mesosoma and metasoma black. Eyes, mouthparts light brown; ocelli brownish yellow. Antennae black. Legs chocolate brown with brownish-yellow joints. Syntergum dark brown to black (Fig. 1G); gaster black or brown, mostly smooth. Pterostigma, costal vein, and radial vein brown (Fig. 1F). Body pubescence white; marginal fringes of wings brown.

***Head* (Fig. 1C):** Slightly wider than mesosoma (about 1.1× wider than mesosoma). HH: EHf = 1.8–1.9. HH: HL = 1.2–1.3. HW: IOS = 1.7–1.8. HW: HH = 1.1–1.2. CSB: Mean: 550–630 μm. POL longer than OOL and ocellar triangle with broad base. OOL: LOL = 1.4–1.6. POL: OOL = 1.4–1.5. Covered with short pubescence except glabrous clypeus and adjacent areas; head concolorous below and above eye midlevel; mandibles and palps brown. Facial pit present.

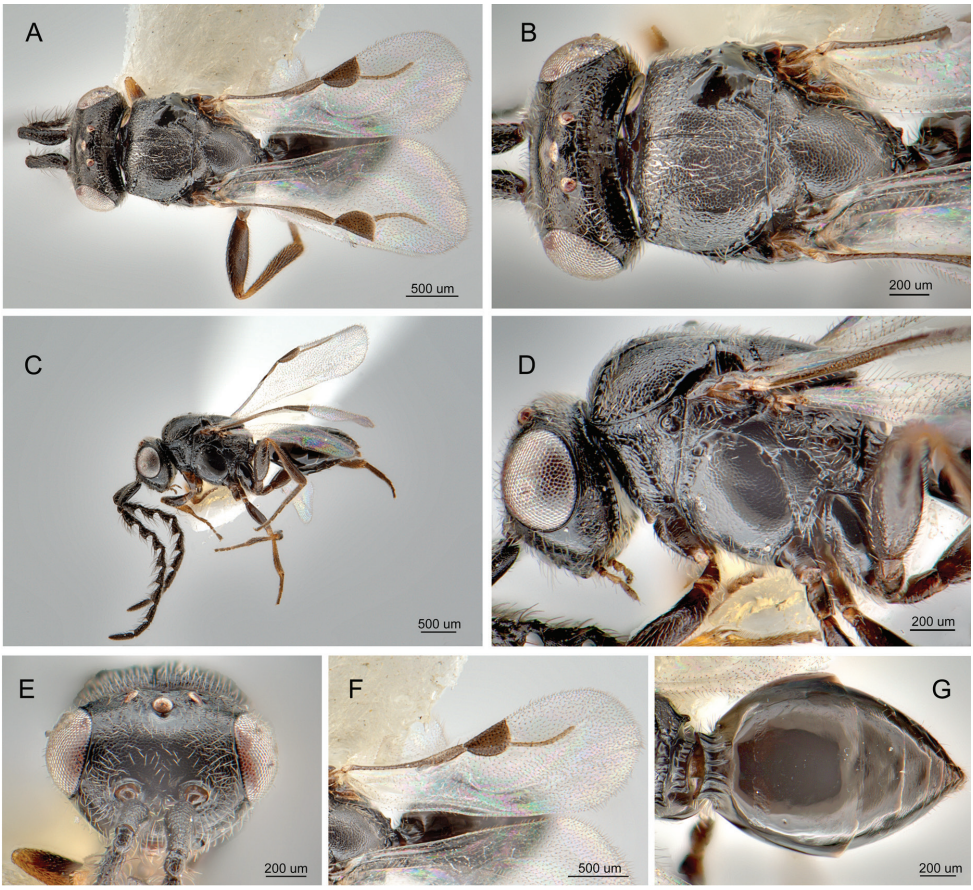

Figure 1. *Dendrocerus carpenteri* (Curtis, 1829), male **A** dorsal habitus **B** head and mesosoma, dorsal view **C** lateral habitus **D** head and mesosoma, lateral view **E** head, anterior view **F** wings **G** metasoma, dorsal view.

Intertorular carina absent. Preoccipital lunula present, more distinct and transverse in males than in females. Hyperoccipital carina present medially, not extending to eyes laterally. Preoccipital furrow present.

Antennae **(Fig. 1C):** Scape about 1.1× longer than combined length of pedicel and F1. Scape length vs. pedicel length: 3.5–4.9. Scape length vs. F1 length: 1.6–3.8. F1 length vs. pedicel length: 1.3–2.2. F1 length vs. F2 length: 1.1–1.4. Longest flagellomere: F1. Basal flagellar segments ventrally slightly concave; strongly serrate, gradually becoming less serrate distally. Flagellar pubescence long, at least as long as breadth of antennomeres.

Mesosoma **(Fig. 1B, D):** Pronotum not elongate. AscW/PscW = 0.7–0.8. Mesosoma slightly narrow (1.4× longer than wide) (Length/width/height = 770/550/550 µm); coriaceous in sculpture, densely pubescent. Mesoscutum: (Length/width = 380/490 µm); mesoscutum 1.3× wider than long, with more or less straight anterior margin. Transverse pronotal sulcus and posterior pronotal sulcus

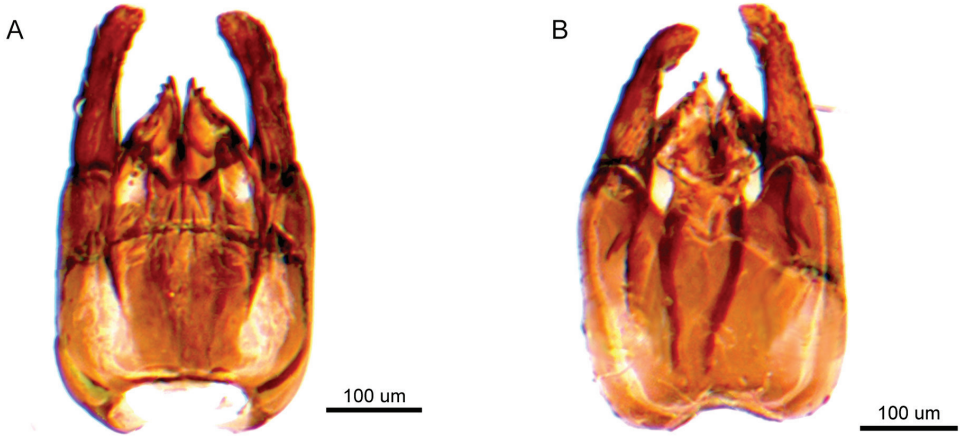

Figure 2. *Dendrocerus carpenteri* (Curtis, 1829), male, genitalia **A** dorsal view **B** ventral view.

present, distinct. Mesonotum wider than long, almost quadrate. Notauli complete, strongly angled and convergent posteriorly. Mesos scutellum broad and convex. Lateral axillar area distinctly higher than long. Mesopleural sulcus present. Propodeum medially short. Posterior propodeal carina present, more distinct laterally. Posterodorsal metapleural area trapezoid-shaped.

***Wings* (Fig. 1F):** Total wing length 1.3 mm. Hyaline, pterostigma (Length/width = 170/90 µm) nearly semicircular but distal edge almost straight. Radius (190 µm), strongly curved, often continuing distally without pigmentation.

***Metasoma* (Fig. 1G):** Metasoma concolorous with mesosoma. Metasoma 1.5× longer than wide (Length/width/height = 800/540/406 µm). Syntergum with crenulate collar, clearly with neck. Rest of metasoma smooth, but with dense punctures in middle and posterior of syntergum. Several strong transverse gastral carinae present in basal portion of metasoma; gastrocoeli not evident; posterior tergites with setae.

***Male Genitalia* (Fig. 2):** Genitalia with short cupula. Harpe median margin smooth and without tooth. Distal margin of harpe in lateral view blunt. Gonostipes longer than wide, fused dorsally; apical margin (part of gonostipes) with three teeth outward (Fig. 2A). Median notch of distodorsal margin of gonostipes square.

Female (Fig. 3): Body length: 1.8–2.1 mm. As for male except scape longer (scape about 1.3× longer than combined length of pedicel and F1). Pedicel and F1 approximately equal in length. Rest of flagellar segments short (L/B about 1.1–1.6), except F9 which is usually twice as long as broad. Flagellomeres flattened ventrally. Antenna black but distal end of pedicel sometimes lighter; weakly papillate, with short dense pubescence.

Distribution. China (Shandong, Shanghai, Anhui, Zhejiang, Jiangsu, Hubei, Jiangxi, Fujian, Taiwan, Guizhou, Yunnan); Australasian, Oceanian, Neotropical, Oriental, and Palearctic.

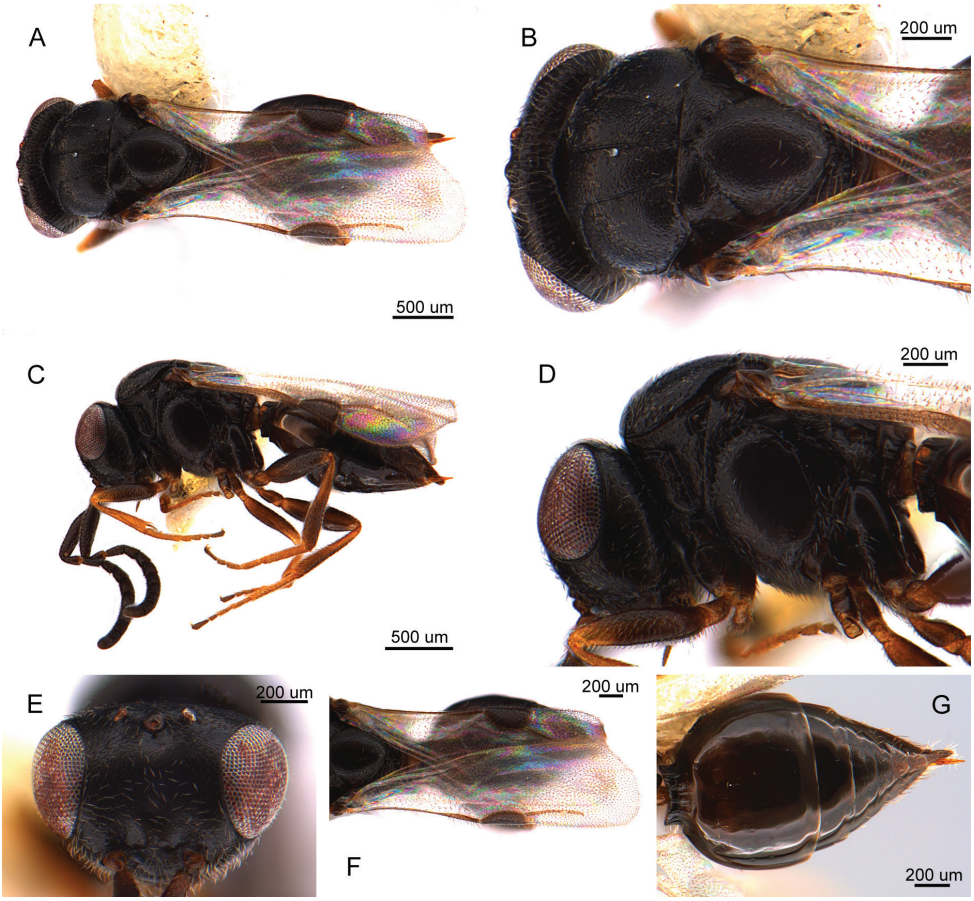

Figure 3. *Dendrocerus carpenteri* (Curtis, 1829), female **A** dorsal habitus **B** head and mesosoma, dorsal view **C** lateral habitus **D** head and mesosoma, lateral view **E** head, anterior view **F** wings **G** netasoma, dorsal view.

***Dendrocerus laticeps* (Hedicke, 1929)**
Fig. 4

Atritomellus laticeps Hedicke, 1929: 60.
Lygocerus laticeps (Hedicke) Hellen, 1966: 15.
Dendrocerus laticeps (Hedicke) Dessart, 1972: 186.

Material examined. China • 2 females; Anhui, Chuzhou, Mingguang; 28.IV.2019; H. Li leg. (AHNU).

Description. Female: Body length: 1.8–1.9 mm.

***Coloration* (Fig. 4):** Cranium and mesosoma black, metasoma alutaceous to black. Mouthparts brown or yellow; eyes light brown; ocelli brown. Flagellum black or brown. Basal scape and AIII yellow, with other antennae segments black. Legs usually

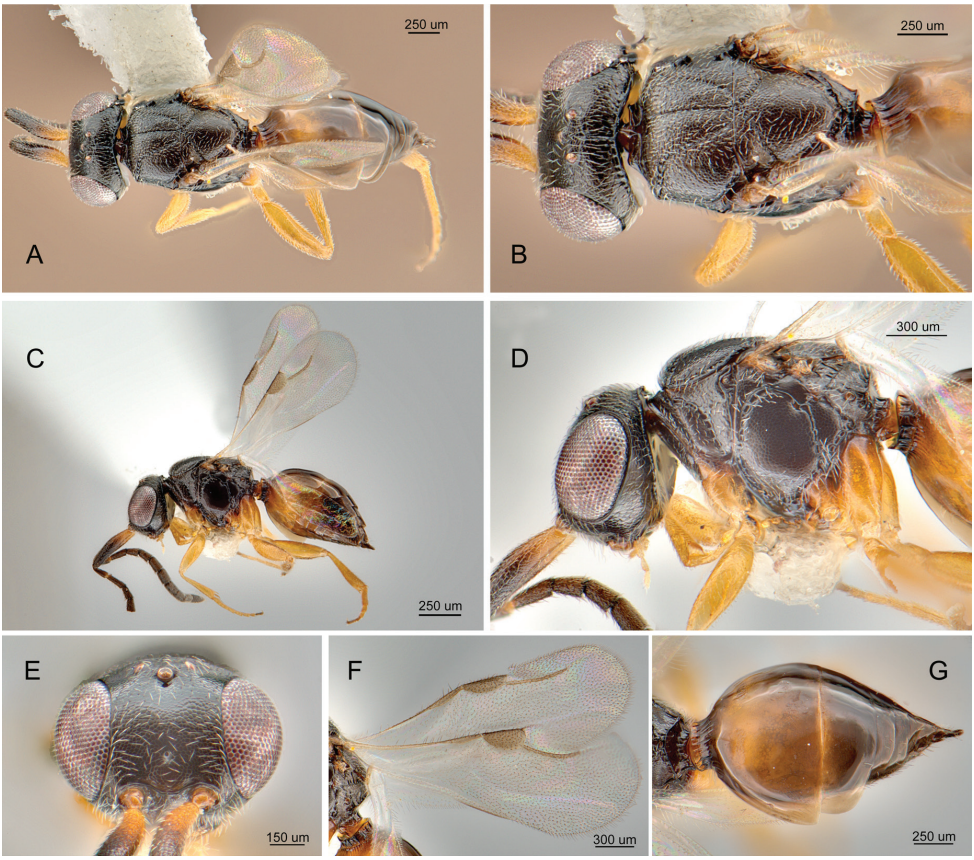

Figure 4. *Dendrocerus laticeps* (Hedicke, 1929) female **A** dorsal habitus **B** head and mesosoma, dorsal view **C** lateral habitus **D** head and mesosoma, lateral view **E** head, anterior view **F** wings **G** metasoma, dorsal view.

yellow, sometimes darkened proximally, especially on lateral side of hindlegs. Syntergum yellow to dark brown (Fig. 4G). Pterostigma, costal vein, and radial vein light brown (Fig. 4F). Body pubescence white; marginal fringes of wings brown.

***Head* (Fig. 4C):** Slightly wider than mesosoma (about 1.2× wider than mesosoma). HH: EHf = 1.8–1.9. HH: HL = 0.8–1.0. HW: IOS = 1.5–1.7. HW: HH = 0.9–1.0. CSB: Mean: 520–600 µm. POL longer than OOL and ocellar triangle with broad base. OOL: LOL = 1.6–1.8. POL: OOL = 1.1–1.2. Broad and pubescence short; head concolorous below and above eye midlevel; mandibles and palps yellow. Facial pit present. Intertorular carina distinct. Eyes usually large. Ocellus triangle broad and short lateral ocelli well separated from eyes. Preoccipital lunula present. Occipital carina strongly developed. Preoccipital furrow present.

***Antennae* (Fig. 4C):** Scape about 1.6× longer than combined lengths of pedicel and F1. Scape length vs. pedicel length: 4.1–4.8. Scape length vs. F1 length: 2.8–3.3. F1 length vs. pedicel length: 1.5–1.8. F1 length vs. F2 length: 1.2–1.5. Longest flagel-

lomere: F1. F1 longer than F2. Pedicel long. F1 long and thin, about 3 times as long as broad, distal flagellar segments broader, less elongate, with flat area ventrally. F2 sometimes slightly asymmetrical. Scape never completely dark, normally (when viewed dorsally) with distinct light-coloured basal band, but sometimes indistinct. Pubescence rather short.

Mesosoma **(Fig. 4):** Pronotum not elongate. AscW/PscW = 0.8–0.9. Mesosoma slightly narrow (1.3× longer than wide) (Length/width/height = 560/420/470 μm); coriaceous in sculpture, densely pubescent. Mesoscutum: (Length/width = 281/300 μm); mesoscutum 1.1× wider than long, with more or less straight anterior margin. Notauli very distinct but present only anteriorly, disappearing immediately after bend. Median furrow distinct. Lateral axillar area longer than high. Mesopleural sulcus present. Median projection of lateral prodeal carina present. Anterior metanotal margin with conspicuous furrow passing under apex of scutellum. Propodeum with projections posteriorly. Sparsely crenulate furrow. Median propodeal projection weakly developed. Lateral thoracic segments bordered by conspicuous foveolate or crenulate furrows. Posterodoral metapleural area trapezoid-shaped.

Wings **(Fig. 4F):** Total wing length 1.1 mm. Clear, pubescence long, fringe long and obvious. Prerostigma noticeably semioval, long and thin (Length/width = 130/80 μm). Radius (160 μm), curved a little in the middle and slightly logger (1.2×) than pterostigma; forewing densely pubescent and marginal fringes numerous; hindwing without venation.

Metasoma **(Fig. 4G):** Metasoma lighter than mesosoma. Mesosoma 1.5× longer than wide (Length/width/height = 560/420/470 μm). Syntergum with crenulate collar, clearly with neck. Rest of metasoma smooth, but with numerous pit-like punctuations in middle and posterior of T3. Several strong transverse gastral carinae present in basal portion of metasoma; gastrocoeli not evident; five terminal segments visible dorsally with numerous hairs.

Distribution. China (Shandong, Anhui, Jiangsu, Hubei, Fujian, Guangdong, Guangxi); Australasian; Oceanian; Nearctic; Palearctic; Oriental.

Dendrocerus anisodontus Wang, Chen & Mikó, sp. nov.

http://zoobank.org/8C5BDFA5-7F51-4218-B83F-6C6A81022948
Figs 5–7

Diagnosis. This new species belongs to the *D. halidayi* species-group and can be separated from other species by the following characteristics: metasoma concolorous with mesosoma and head; intertorular carina present, blunt harpe with numerous setae; distal parossiculal projection cone.

Material examined. ***Holotype*** China • male; Yunnan, Menghai, Mt. Bulang; 20.VII–21.VIII.2019; L. Ma leg. (SYSBM). ***Paratypes*** (29 males, 89 females)

China • 1 female; Hebei, Baoding, Hebei Agri. Unv. West Campus; MT; 12–19. VII.2017; F. Fan (SYSBM) • 2 females; same collection data as for preceding; 20–27.

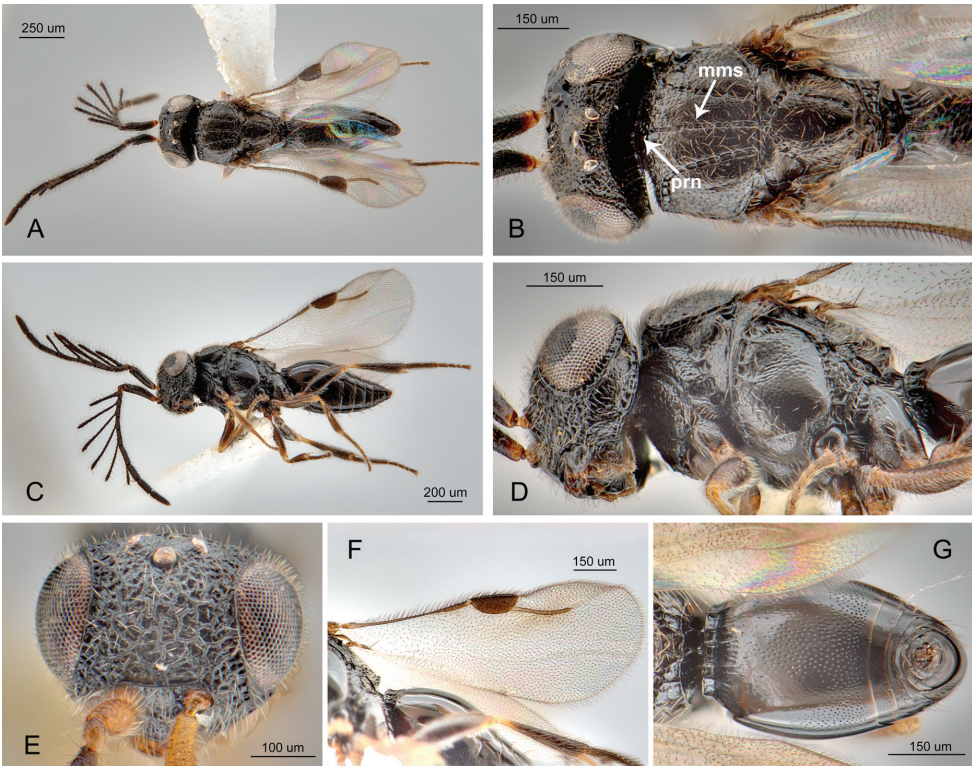

Figure 5. *Dendrocerus anisodontus* Wang, Chen and Mikó sp. nov., male, holotype **A** dorsal habitus **B** head and mesosoma, dorsal view **C** lateral habitus **D** head and mesosoma, lateral view **E** head, anterior view **F** wings **G** metasoma, dorsal view. Abbreviations: pronotum (prn), median mesoscutal sulcus (mms).

VI.2017; (IZCAS) • 4 females; same collection data as for preceding; 27.VI–4.VII.2017; (AHNU) • 1 female; Shandong, Shanghe; MT; 26.I.2018; J. Yan leg.; (SYSBM) • 4 females, same collection information as for preceding; 4–10.VIII.2018; (IZCAS) • 1 female; Zhejiang, Mt. Fengyang; 28.VII.2007; L. Zhu leg.; (AHNU); • 1 female; Zhejiang, Mt. Tianmu, 1200 m; 25–29.VII.2011; H. Chen leg.; (SYSBM) • 1 male; Zhejiang, Mt. Gutian; 5.VII.2015 • 1 female; Hunan, Mt. Mangshan; YPT; 13.VIII.2010; H. Chen leg.; (IZCAS) • 1 male; Fujian, Minqing County, Huangchulin Nature Reserve; 13–17.VII.2005; J. Liu leg.; (AHNU) • 2 males; Guangdong, Nanling National Natural Reserve; 8–17.VIII.2010• H. Chen and H. Chen leg.; (AHNU) • 1 female; Guangdong, Nanling Protection Station; YPT; 16–17.V.2011; Z. Xu leg.; (SYSBM) • 1 male; same collection information as for preceding; 1200 m; 17.V.2011; N. Wei leg.; (IZCAS) • 1 female; Guangdong, Mt. Nankun; 19.VIII.2016; Z. Xu leg.; (AHNU) • 1 male; Guangdong, Guangzhou, SYSU Bamboo Garden; 20.I–18.II.2019; H. Chen leg.; (SYSBM) • 1 male; same collection information as for preceding; 23.VII.2018–20.I.2019; H. Chen leg.; (IZCAS) • 1 female; same collection information as for preceding; 10.I–18.IV.2020; H. Chen leg.; (IZCAS) • 1 male; Guangdong, Huizhou City,

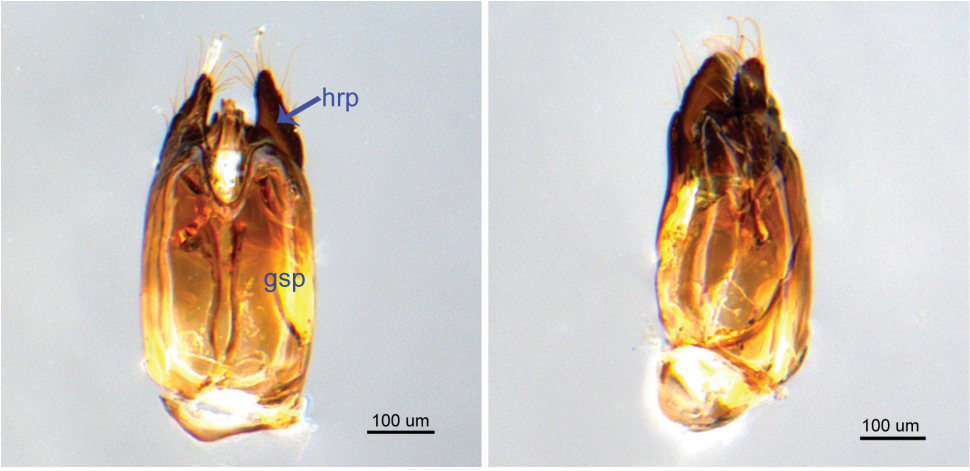

Figure 6. *Dendrocerus anisodontus* Wang, Chen and Mikó sp. nov., male, holotype, genitalia **A** dorsal view **B** lateral view. Abbreviations: harpe (hrp), gonostipes (gsp).

Mt. Gutian; 30.V–30.VI.2019; L. Chen et al. leg.; (AHNU) • 1 female; Guangdong, Qingyuan, Lian Zhou; YPT; 10–13.VI.2019; H. Chen leg.; SCAU 3049491 (AHNU) • 1 female; Guangdong, Dongguan City, Mt. Daling; 20–30.IX.2019; L. Chen et al. leg.; (IZCAS) • 1 male, 1 female; Guangdong, Guangzhou City, South China Botanical Garden; 7.II–16.III.2020; H. Huang et al. leg.; (SYSBM) • 1 male; Hainan, Baisha County, Jiujialing; 11.VII.2010; H. Chen leg.; (IZCAS) • 1 female; Hainan, Mt. Diaoluo; YPT; 12–13.VII.2010; H. Chen et al. leg.; (SYSBM) • 1 female; Hainan, Jianfengling; 14–16.VII.2010; H. Chen leg.; (AHNU) • 7 females; Hainan, Danzhou City, Institute of Environmental and Plant Protection; 20–30.VI.2019; S. Dong leg.; SCAU 3049465 (SYSBM) • 2 females, same collection information as for preceding; 4–20.VI.2019; S. Dong leg.; SCAU 3049467 (IZCAS) • 1 female; Same collection information as for preceding; 30.VI–10.VII.2019; S. Dong leg.; SCAU 3049474 (AHNU) • 2 females; Same collection information as for preceding; 30.VII–10.VIII.2019; S. Dong leg.; SCAU 3049488 (SYSBM) • 1 female; Same collection information as for preceding; 30.VII–10.VIII.2019; S. Dong leg.; SCAU 3049474 (IZCAS) • 2 females, Same collection information as for preceding; 30.VII–10.VIII.2019; S. Dong leg.; SCAU 3049489 (AHNU) • 2 females; Same collection information as for preceding; 10–20.VIII.2019; S. Dong leg.; SCAU 3049481 (SYSBM) • 5 females; Same collection information as for preceding; 20–30.VIII.2019; S. Dong leg.; SCAU 3049484 (IZCAS) • 6 females; Same collection information as for preceding; 30.VIII-10.IX.2019; S. Dong leg.; SCAU 3049480 (AHNU) • 4 females,; Same collection information as for preceding; 30.XI–30.XII.2019; S. Dong leg.; SCAU 3049487 (IZCAS) • 1 female; Same collection information as for preceding; 20–30.XI.2019, S. Dong leg.; SCAU 3049473 (AHNU) • 1 female; Same collection information as for preceding; 30.XI–30.XII.2019; S. Dong leg.; SCAU 3049469 (SYSBM) • 3 males, 5 females; Same collection information as for preceding; 20–30.IX.2019; S. Dong leg.; SCAU

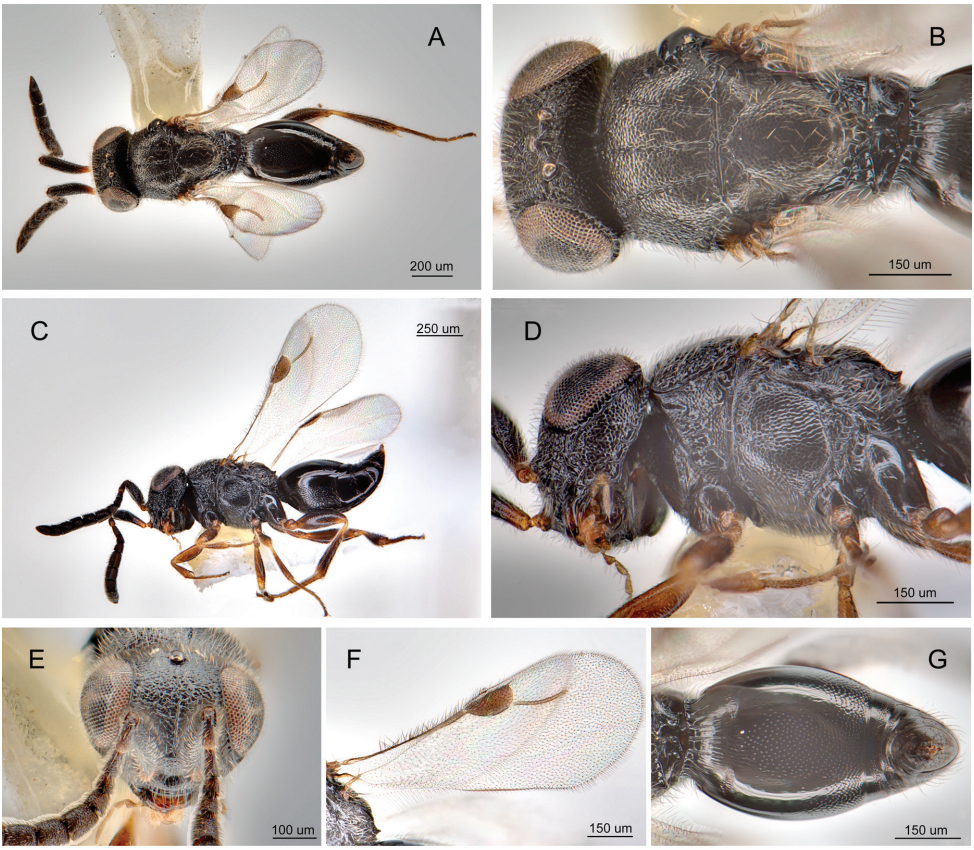

Figure 7. *Dendrocerus anisodontus* Wang, Chen and Mikó sp. nov., female, paratype **A** dorsal habitus **B** head and mesosoma, dorsal view **C** lateral habitus **D** head and mesosoma, lateral view **E** head, anterior view **F** wings **G** metasoma, dorsal view.

3049483 (IZCAS) • 2 males, 2 females; Same collection information as for preceding; 30.X-30.XI.2019; S. Dong leg.; SCAU 3049485 (SYSBM) • 1 male; Same collection information as for preceding; 10–20.X.2019, S. Dong leg.; SCAU 3049472 (IZCAS) • 2 females; Same collection information as for preceding; 20–30.VIII.2019; S. Dong leg.; SCAU 3049476 (AHNU) • 1 female; Same collection information as for preceding; 10–20.IX.2019; S. Dong leg.; SCAU 3049477 (SYSBM) • 3 females; Same collection information as for preceding; 30.VIII–10.IX.2019; S. Dong leg.; SCAU 3049471 (IZCAS) • 4 females; Same collection information as for preceding; 30.X–30.XI.2019; S. Dong leg.; SCAU 3049470 (AHNU) • 4 males, 3 females; Same collection information as for preceding; 30.IX–10.X.2019; S. Dong leg.; SCAU 3049486 (SYSBM) • 1 female; Same collection information as for preceding; 30.X–30.XI.2019; S. Dong leg.; SCAU 3049470 (IZCAS) • 1 female; Same collection information as for preceding; 30.IX–10.X.2019; S. Dong leg.; SCAU 3049486 (AHNU) • 1 male; Guangxi, Xingan County, Huajiang Village, 380 m; 26–27.VI.2011; N. Wei leg.; (SYSBM) • 2 females;

Guangxi, Nanning, Mt. Longshan, 370 m; 1–2.VII.2011; Z. Xu leg.; (IZCAS) • 1 female; Sichuan, Pingwu, Baimazhai; 25.VII.2005; H. Zhang leg.; (AHNU) • 1 male; Sichuan, Yaan City, Zhangjiashan Park; 14.VII.2006; Z. Gao leg.; (SYSBM) • 1 male; Shaanxi, Liping Forest Experiment Station; 23.VII.2004; Q. Wu leg.; (IZCAS) • 1 male; Guizhou; Leigong Mountain Forest Farm; 1.VI.2005; H. Zhang leg.; (IZCAS) • 2 females; Guizhou, Kuankuoshui Protection Center; 3.I.2010; J. Zeng leg.; (SYSBM) • 1 male, 1 female; Yunnan, Gejiu, Lüchun County; 25.VII.2003; (AHNU) • 1 female; Yunnan, Xianggelila Gaoshan Botanical Garden; 27.III.2017; J. Zeng leg.; (IZCAS) • 1 female, 1 male; Yunnan, Xishuangbanna Rainforest, 599 m; 24.IV–31.V.2017; L. Ma leg.; (SYSBM) • 1 male; Yunnan, Xianggelila, Gaoshan Botanical Garden; 27.III.2017; (AHNU) • 1 male, 2 females; Yunnan, Menghai, Mt. Bulang, 1683 m; MT; 17.V–21.VI.2018; L. Ma leg.; (SYSBM) • 1 female; Same collection information as for preceding; 21.VIII–20.IX.2019; L. Ma (IZCAS).

Description. Male: Body length: 1.8–2.1 mm.

***Coloration* (Fig. 5):** Cranium, mesosoma and metasoma black; eyes brown to black; ocelli brown; scape and basal pedicel yellow; flagellum dark brown to black; fore and mid coxa along with femur and tibia brown with brownish joints; syntergum brown (Fig. 5A); pterostigma and costal vein brown; radial vein brown (Fig. 5F); body pubescence white; marginal fringes of wings brown.

***Head* (Fig. 5C):** Slightly wider than mesosoma (about 1.1× wider than mesosoma). HH: EHf = 1.9–2.1. HH: HL = 1.2–1.6. HW: IOS = 1.8–1.9. HW: HH = 1.2–1.3. CSB: Mean: 350–470 μm. POL longer than OOL and ocellar triangle with broad base. OOL: LOL = 1.8–1.9. OOL: POL = 1.0–1.1. Head shape transverse in dorsal view, concolorous below and above eye midlevel. Preoccipital lunula absent (Fig. 5B). Facial pit absent. Intertorular carina distinct; ocular suture prominent and foveolate; frons with sparse hairs; densely pubescent at gena (Fig. 5B); Preoccipital furrow present.

***Antennae* (Fig. 5C):** Ramose with six branches; scape nearly four times longer than wide; pedicel small and almost globular. Scape length vs. pedicel length: 4.7–4.8. Scape length vs. F1 length: 3.6–3.7. F1 length vs. pedicel length: 1.3–1.5. F1 length vs. F2 length: 0.9 μm. Longest flagellomere: F9. Length of setae on flagellomere vs. flagellomere width: setae as long as or shorter than width of flagellomeres. Basal flagellar segments clearly asymmetrical, with long projections.

***Mesosoma* (Fig. 5B, D):** Pronotum not elongate. AscW/PscW = 0.7–0.8. Mesosoma slightly narrow (1.1× longer than wide) (Length/width/height = 640/600/560 μm); coriaceous in sculpture, densely pubescent. Mesoscutum: (Length/width = 350/570 μm); mesoscutum 1.6× wider than long, with more or less straight anterior margin; anterior corners of mesoscutum sharply angled; mesoscutal humeral sulcus evident; coarsely foveolate notauli angled sharply. Median mesoscutal sulcus present and complete, terminating adjacent to the transscutal articulation (Fig. 5B); scutellum 0.9× longer than wide, narrowed at apex with densely setose lateral margin; lateral scutellar carina evident; scutellum convex and highly sculptured with numerous hairs; metanotum and propodeum carinated. Posterodorsal metapleural area trapezoid-shaped. Mesopleural sulcus present.

***Wings* (Fig. 5F):** Total wing length 1.5 mm. Hyaline. Pterostigma (Length/width = 220/110 μm) elliptical, 2.0× longer than wide; distal edge of pterostigma truncated; Radius (270 μm), curved a little in the middle and slightly logger (1.2×) than pterostigma; forewing densely pubescent and marginal fringes numerous; hindwing without venation. Dark area on fore wing absent.

***Metasoma* (Fig. 5G):** Metasoma concolorous with mesosoma. Mesosoma 1.6× longer than wide (Length/width/height = 830/510/430 μm). Syntergum with crenulate collar, clearly with neck. Rest of metasoma smooth, but with numerous pit like punctuations in middle and posterior of T3. Eight strong transverse gastral carinae present in basal portion of metasoma; gastrocoeli not evident; five terminal segments visible dorsally with numerous hairs.

***Male genitalia* (Fig. 6):** Genitalia with short cupula. Harpe longer than gonostipes in lateral view; simple and not bilobed. Distal margin of harpe in lateral view blunt. Lateral setae of harpe present, but sparse (Fig. 6B). Gonostipes longer than wide, fused dorsally; apical margin (part of gonostipes) cleft medially (Fig. 6A). Median notch of distodorsal margin of gonostipes oval. Distal parossiculal projection rounded.

Females (Fig. 7): Body length: 1.9–2.1 mm. Scape about 2.6× longer than combined length of pedicel and F1. Scape length vs. pedicel length: 4.1–4.6. Scape length vs. F1 length: 2.8–3.3. F1 length vs. pedicel length: 1.5–1.7. F1 length vs. F2 length: 0.8–0.9. Longest flagellomere: F3. Other than genitalia differences and sexual dimorphism in the antennae, there are no obvious differences between males and females.

Distribution. China (Hebei, Shandong, Zhejiang, Hunan, Fujian, Guangdong, Hainan, Guangxi, Sichuan, Shaanxi, Guizhou, Yunnan).

Etymology. The species name is a Greek masculine adjective meaning "unequal tooth", signifying the irregular branches of the antennae of males.

Remarks. Like most *Dendrocerus* males, the lateral extension of the basal flagellar segments is the most notable character of *D. anisodontus* sp. nov. This is likely a device to increase the olfactory efficiency of the male, probably in its response to sex pheromones released by the female (Fergusson, 1980).

***Dendrocerus bellus* Wang, Chen & Mikó, sp. nov.**

http://zoobank.org/F0D399A4-6F74-490E-AE4B-675A5FA59F15
Figs 8–10

Diagnosis. This new species belongs to the *D. halidayi* species group, and is close to *D. caelebs* but can be distinguished by its smaller body size (only 1.1–1.2 mm), unobvious notauli, body coloration, median notch of distodorsal margin of gonostipes triangle and spatulated-shaped harpe.

Material Examined. ***Holotype*** China • male; Guangdong, Guangzhou, SYSU Bamboo Garden; 10.I–18.IV.2020; H. Chen leg.; (SYSBM) ***Paratypes*** (15 males, 17 females) China • 7 males, 1 female; Guangdong, Guangzhou, University Town 2nd Forest; 20.I–17.II.2017; H. Chen leg.; (AHNU) • 1 male, 1 female; Guangdong,

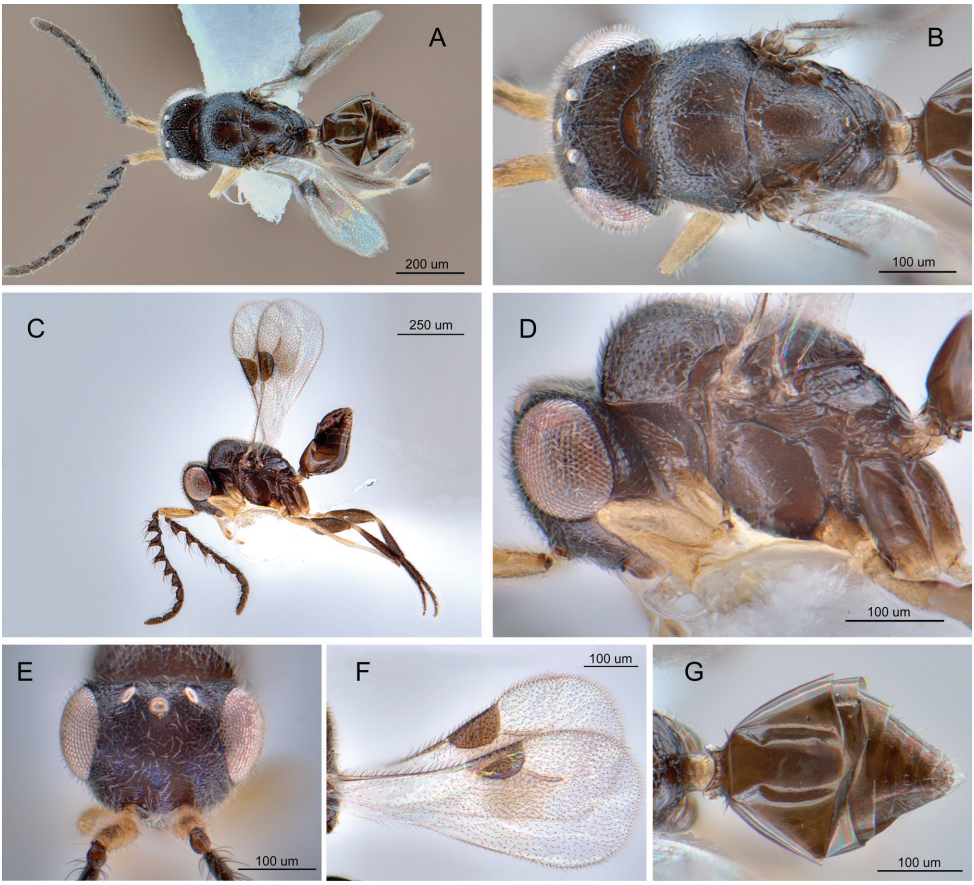

Figure 8. *Dendrocerus bellus* Wang, Chen and Mikó sp. nov., male, holotype **A** dorsal habitus **B** head and mesosoma, dorsal view **C** lateral habitus **D** head and mesosoma, lateral view **E** head, anterior view **F** wings **G** metasoma, dorsal view.

Guangzhou, University Town, 22.VII.2018–20.I.2019, H. Chen leg.; (AHNU) • 1 female; Guangdong, Dongguan, Mt. Daling, 10–20.IX.2019; L. Chen et al. leg.; (SYSBM) • 2 females; Guangdong, Guangzhou, South China Botanical Garden, 7.II–16.III.2020, H. Huang et al. leg.; (IZCAS) • 1 male; Guangdong, Huizhou, Mt. Gutian; 30.XI–30.XII.2019, L. Chen et al. leg.; (IZCAS) • 1 female; Same collection information as preceding; 20–30. IX.2019; L. Chen et al. leg.; (SYSBM) • 2 females; Guangdong, Dongguan, Mt. Daling; 30.X–30.XI.2019; L. Chen et al. leg.; (SYSBM) • 1 female; Guangdong, Mt. Dinghu; 30.XI–30.XII.2019; L. Chen et al. leg.; (IZCAS) • 4 males, 8 females; Guangdong, Guangzhou, SYSU bamboo garden; 10.I–17.IV.2020; H. Chen leg.; (IZCAS) • 1 male; Sichuan, Yaan City, Zhangjiashan Park; 14.VII.2006; Z. Gao; (AHNU) • 1 male; Yunnan, Menghai, Mt. Bulang, 1595 m; 28.V–28.VI.2019; SCAU 3049495 (AHNU).

Description. Male: Body length: 1.1–1.2 mm.

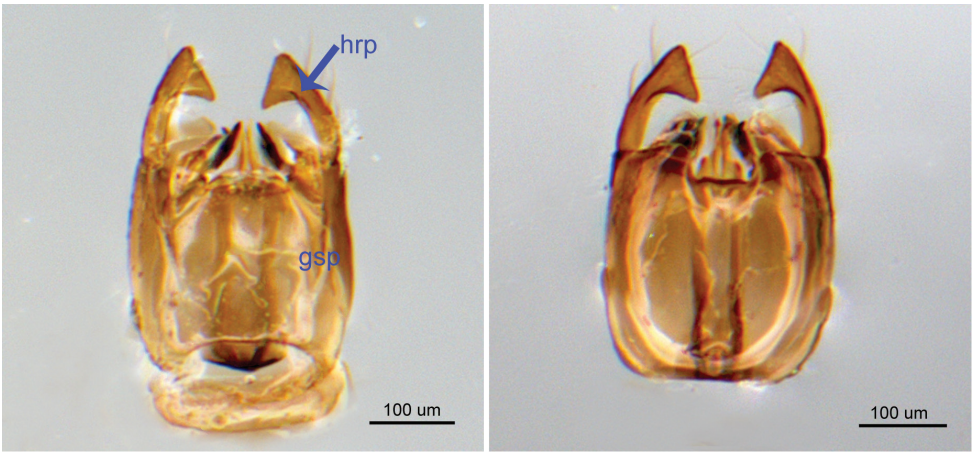

Figure 9. *Dendrocerus bellus* Wang, Chen and Mikó sp. nov., male, holotype, genitalia **A** dorsal view **B** ventral view.

***Coloration* (Fig. 8):** Cranium, mesosoma and metasoma dark brown; eyes brown; ocelli yellow. Scape yellow, pedicel and flagellum dark brown. Fore and mid coxa along with femur and tibia yellow; syntergum dark brown (Figs 8A, G); pterostigma dark brown; costal vein and radial vein brown (Fig. 8F); body pubescence white; marginal fringes of wings brown.

***Head* (Fig. 8C):** Head width, dorsal view: slightly wider than mesosoma (about 1.2× wider than mesosoma). HH: EHf = 1.7–1.9. HH: HL = 1.1–1.2. HW: IOS = 1.7. HW: HH = 1.1–1.2. CSB: Mean: 330–360 µm. POL shorter than OOL and ocellar triangle with broad base. OOL: LOL = 1.6–1.7. OOL: POL = 1.0–1.1. Head shape transverse in dorsal view; concolorous below and above eye midlevel. Preoccipital lunula absent (Fig. 8B). Facial pit absent. Intertorular carina curved; ocular suture prominent and foveolate; frons with sparse hairs; densely pubescent at gena (Fig. 8B). Facial pit present. Preoccipital furrow present.

***Antennae* (Fig. 8C):** Scape nearly five times longer than wide; pedicel small and almost globular. Scape length vs. pedicel length: 6.0–7.0. Scape length vs. F1 length: 2.7–3.2. F1 length vs. pedicel length: 2.3–2.7. F1 length vs. F2 length: 0.9–1.0. Longest flagellomere: F9. Length of setae on flagellomere vs. flagellomere width: setae as long as or shorter than width of flagellomeres. Basal flagellar segments clearly asymmetrical, strongly serrate.

***Mesosoma* (Fig. 8B, D):** Pronotum (Prn) not elongate. Anterior mesoscutal width (AscW) vs. posterior mesoscutal width (PscW): AscW/PscW = 0.7–0.8. Mesosoma slightly narrow (1.4× longer than wide) (Length/width/height = 407/350/440 µm); coriaceous in sculpture, densely pubescent. mesoscutum: (Length/width = 127/206 µm); mesoscutum 1.6X wider than long, with more or less straight anterior margin; anterior corners of mesoscutum sharply angled; mesoscutal humeral sulcus evident; notauli thin and unobvious. Median mesoscutal

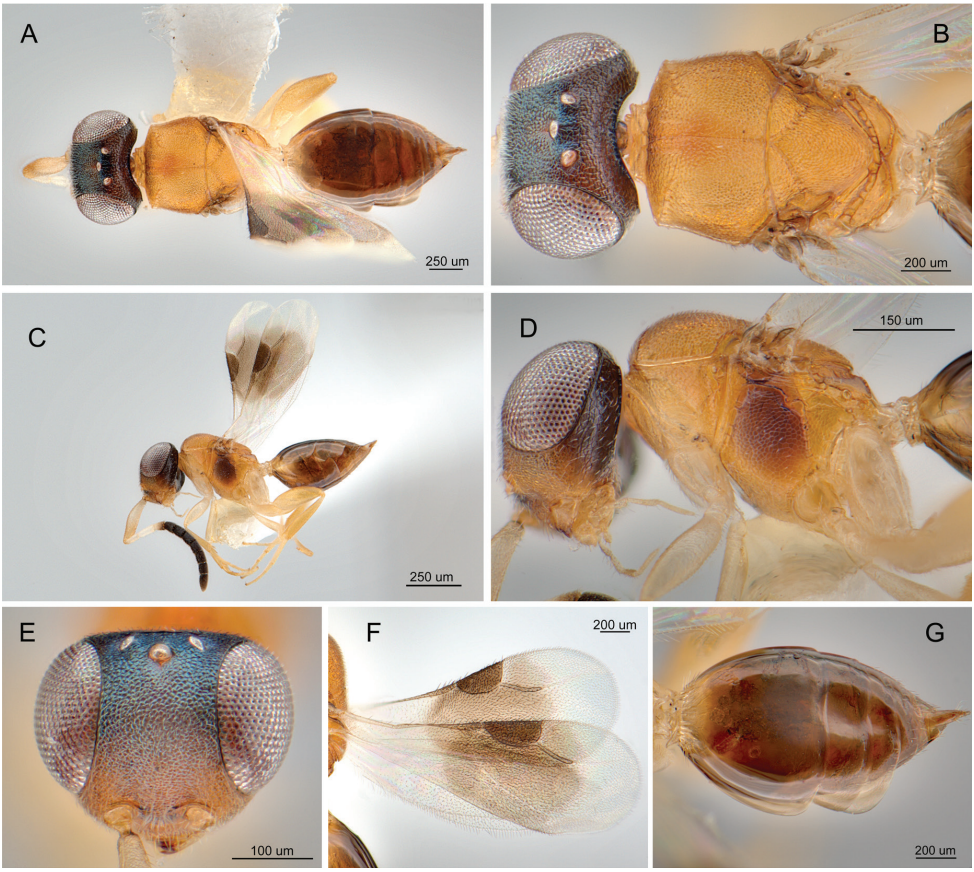

Figure 10. *Dendrocerus bellus* Wang, Chen and Mikó sp. nov., female, paratype **A** dorsal habitus **B** head and mesosoma, dorsal view **C** lateral habitus **D** head and mesosoma, lateral view **E** head, anterior view **F** wings **G** metasoma, dorsal view.

sulcus present and complete, terminating adjacent to the transscutal articulation (Fig. 8B); scutellum 0.9× longer than wide, narrowed at apex with densely setose lateral margin; lateral scutellar carina evident; scutellum convex and highly sculptured with numerous hairs; metanotum and propodeum carinated. Posterodorsal metapleural area trapezoid. Mesopleural sulcus present.

***Wing* (Fig. 8F):** Total wing length 0.9 mm. Hyaline. Pterostigma (Length/width = 180/90 μm) elliptical, 2.0× longer than wide; distal edge of pterostigma truncated; Radius (130 μm), curved a little in the middle and slightly shorter (0.7×) than pterostigma; forewing tinted with light brown, densely pubescent and marginal fringes numerous; hind wing without venation. Dark area on fore wing present.

***Metasoma* (Fig. 8G):** Metasoma lighter than mesosoma. Mesosoma 1.6× longer than wide (Length/width/height = 500/320/220 μm). Syntergum with crenulate collar, clearly with neck. Rest of metasoma smooth. Strong transverse gastral carinae pre-

sent in basal portion of metasoma; gastrocoeli not evident; five terminal segments visible dorsally with numerous hairs.

***Male genitalia* (Fig. 9):** Genitalia with short cupula. Harpe longer than gonostipes in lateral view, with numerous terminal long and slender setae; harpe shape spatulate and oriented medially. Lateral setae of harpe present, but sparse. Gonostipes longer than wide, fused dorsally; apical margin curved medially, spatulated-shaped. Volsella black, with sharped apically. Median notch of distodorsal margin of gonostipes triangle. Distal parossiculal projection pointed.

Females (Fig. 10): Body length: 1.35–1.44 mm. Head yellow below and brown above eye midlevel, mandibles and palps yellow. Mesosoma and metasoma yellowish, tinged with brown; eyes white; ocelli white to yellowish. Scape, pedicel and basal flagellar segments yellowish. Legs yellowish; syntergum light brown (Figs 10A, G). Metasoma darker than mesosoma. Flagellar segments symmetrical and cylindrical. Other characteristics similar to male.

Distribution. China (Guangdong, Hainan, Sichuan, Yunnan).

Etymology. The species name is a Latin masculine adjective meaning "beautiful and exquisite", signifying the beautiful coloration, especially in female.

Acknowledgements

This work was supported by the Major Science and Technology Projects in Anhui Province (Grant No. 202003a06020009), the Natural Science Fund of Anhui Province (Grant No. 1908085QC93), and Natural Science Foundation of Universities of Anhui Province (KJ2020A0094).

References

Bijoy C, Rajmohana K (2014) Description of a new species of *Dendrocerus halidayi* group(Hymenoptera: Ceraphronoidea: Megaspilidae) from India. Journal of Threatened Taxa 6(11): 6453–6457. https://doi.org/10.11609/JoTT.o3807.6453-7

Buckton GB (1876) Monograph of the British aphides 1: 193 pp.[, 38 pls.] London.

Burks KN, Mikó I, Deans AR (2016) *Dendrocerus mexicali* (Hymenoptera, Ceraphronoidea, Megaspilidae): novel antennal morphology, first description of female, and expansion of known range into the U.S. Zookeys 569(257): 53–69. https://doi.org/10.3897/zookeys.569.6629

Curtis J (1829) British entomology 6: fohos 242–289. London.

Dessart P (1965) Contribution à l'étude des Hymenopteres Proctotrupoidea (IX). Revision du genre *Macrostigma* Rondani 1877 (Ceraphronidae, MegaspiIinae). Redia 49: 157–163.

Dessart P (1966) Contribution a l'etude des Hymenopteres Proctotrupoidea. (XII) A propos des Ceraphronidae Megaspilinae males a antennes rameuses. Bulletin de l'Institut Royal des Sciences Naturelles de Belgique 42(32): 1–16.

Dessart P (1970) A propos de l'identite de *Ceraphron carpenteri* Curtis, 1829 (Hym. Ceraphronoidea, Megaspilidae). Bulletin & Annales de La Société Royale Entomologique de Belgique 106: 142–144.

Dessart P (1972) Revision des especes europeennes du genre *Dendrocerus* Ratzeburg, 1852 (Hymenoptera, Ceraphronoidea). Mémoires de la Société entomologique de Belgique 32: 1–310.

Dessart P (1995) A propos du genre *Dendrocerus* Ratzeburg, 1852. Les espèces du group "*penmaricus*" (Hymenoptera Ceraphronoidea Megaspilidae). Bulletin et Annales de la Société Royale Belge d'Entomologie 131: 349–382.

Dessart P (1999) Révision des *Dendrocerus* du groupe "*halidayi*" (Hymenoptera: Ceraphronoidea: Megaspilidae). Belgian Journal of Entomology 1(2): 169–265.

Dessart P (2006) Familia Megaspilidae. In: Hanson PE, Gould ID (Eds) Hymenoptera de la Región Neotropical. Memoirs of the American Entomological Institute 77: 232–236.

Fergusson NDM (1980) A revision of the British species of *Dendrocerus* Ratzeburg (Hymenoptera: Ceraphronoidea) with a review of their biology as aphid hyperparasites. Bulletin of the British Museum (Natural History). Entomology Series 41: 255–314.

Förster A (1856) Hymenopterologische Studien. II. Heft. Chalcidae und Proctotrupii. Chalcidae und Proctotrupii. Ernst ter Meer, Aachen, 152 pp.

Hedicke H (1929) *Atritomellus laticeps* sp. nov. (Hym. Callicerat.), ein neuer Parasit eines eingeschleppten Rüsselkäfers. Zeitschrift fur wissenschaftliche Insektenbiologie 24: 59–61.

Hellen W. (1966) Die Ceraphroniden Finnlands (Hymenoptera: Proctotrupoidea). Fauna Fennica 20: 1–45.

Howard LO (1890) Some new parasites of the grain plant louse. Insect Life Wash 2: 246–248.

Iemma LGR, Tavares MT, Sousa-Silva CR. (2016) First record of *Dendrocerus carpenteri* (Hymenoptera: Megaspilidae) on Aphidius ervi in alfalfa fields in Brazil. Revista Brasleira De Biologia 76: 1–2. https://doi.org/10.1590/1519-6984.07215

Johnson NF, Musetti L (2004) Catalog of the systematic literature of the superfamily Ceraphronoidea (Hymenoptera). Contributions of the American Entomological Institute 33: 1–149.

Kieffer JJ (1907) Ceraphroninae. In André, E., Species des Hyménoptères d'Europe et d'Algérie 10: 1–288.

Kieffer JJ (1917) Über neue und bekannte Microhymenopteren. Entomologiske Meddelelser 11: 341–350.

Kumar S, Stecher G, Li M, Knyaz C, Tamura K (2018) MEGA X: Molecular Evolutionary Genetics Analysis across Computing Platforms. Molecular Biology and Evolution 35(6): 1547–1549. https://doi.org/10.1093/molbev/msy096

Marshall TA (1868) Notes on some parasitic Hymenoptera, with descriptions of new species. Entomologist's mon. Mag 5: 154–160.

Martens AP, Johnson PJ (2018) Aphid-parasitoid (Insecta) diversity and trophic interactions in south Dakota. Proceedings of the South Dakota Academy of Science 97: 83–92.

Mikó I, Deans AR (2009) *Masner*, a new genus of Ceraphronidae (Hymenoptera, Ceraphronoidea) described using controlled vocabularies. Zookeys 20: 127–153. https://doi.org/10.3897/zookeys.20.119

Morley C (1929) Catalogus Oxyurarum Britannicorum. Transactions of the Suffolk Naturalists' Society 1: 39–60.

Pezzini C, Zilch KCF, Köhler A (2014) A new species of *Dendrocerus* (Hymenoptera, Megaspilidae) from southern Brazil. ZooKeys 425: 51–57. https://doi.org/10.3897/zookeys.425.7454

Ratzeburg ITC (1852) Die Jchneumonen der Forstinsecten in forstlicher und entomologischer Beziehung. Ein Anhang zur Abbildung und Beschreibung der Forstinsekten, Berlin, Dritter Band, [xviii +] 272 pp.

Rondani C (1877). Vesparia parasite no vel minus cognita observata et descripta. Bollettino de laboratorio di Entomologia Italiana 9(2): 166–213.

Stephens JF (1829) A systematic catalogue of British insects, [xxxiv + 416 +] 388 pp. London.

Taekul C, Valerio AA, Austin AD, Klompen H, Johnson NF (2014) Molecular phylogeny of telenomine egg parasitoids (Hymenoptera: Platygastridae s.l.: Telenominae): evolution of host shifts and implications for classification. Systematic Entomology 39: 24–35. https://doi.org/10.1111/syen.12032

Takada H (1973) Studies on Aphid Hyperparasites of Japan, 1. Aphid hyperparasites of the genus *Dendrocerus* Ratzeburg occurring in Japan (Hymenoptera: Ceraphronidae). Insecta Matsumurana 2: 1–37.

Trietsch C, Mikó I, Notton DG, Deans AR (2018) Unique extrication structure in a new megaspilid, *Dendrocerus scutellaris* Trietsch & Mikó (Hymenoptera: Megaspilidae). Biodiversity Data Journal 6(2): 1–14. https://doi.org/10.3897/BDJ.6.e22676

Trietsch C, Mikó I, Ezray B, Deans AR (2020) A taxonomic revision of nearctic *Conostigmus* (Hymenoptera: Ceraphronoidea: Megaspilidae). Zootaxa 4792(1): 1–155. https://doi.org/10.11646/zootaxa.4792.1.1

Thomson CG (1858) Sveriges Proctotruper. Öfversgt af Kongl. Vetenskapsakademiens forhandlingar 15: 287–358.

Westwood JO (1840) An introduction to the modern classification of insects 2: [xi + 587 +] 158 pp. London.

Yoder MJ, Mikó I, Seltmann KC, Bertone MA, Deans AR (2010) A gross anatomy ontology for Hymenoptera. PLoS ONE 5: e15991. https://doi.org/10.1371/journal.pone.0015991

Zhang YZ, Yu F, Zhu CD (2008) A preliminary phylogenetic study of *Copidosoma* spp. (Hymenoptera: Encyrtidae) associated with Noctuidae (Lepidoptera) based on 28S rDNA D2 sequence. Acta Entomologica Sinica 51: 992–996. https://doi.org/10.1016/S1005-9040(08)60003-3

JHR 86: 145–150 (2021)
doi: 10.3897/jhr.86.73837
https://jhr.pensoft.net

RESEARCH ARTICLE

JOURNAL OF Hymenoptera RESEARCH
A peer-reviewed open-access journal
The International Society of Hymenopterists

A new species of *Stilbopogon* from the Monvero dunes of California (Tiphiidae, Hymenoptera)

Lynn S. Kimsey[1]

1 *Bohart Museum of Entomology, University of California, Davis, 95616, USA*

Corresponding author: Lynn S. Kimsey (lskimsey@ucdavis.edu)

Academic editor: Michael Ohl | Received 2 September 2021 | Accepted 7 October 2021 | Published 29 October 2021

http://zoobank.org/2A1B8A78-02A1-42FC-8413-073AE3034CB6

Citation: Kimsey LS (2021) A new species of *Stilbopogon* from the Monvero dunes of California (Tiphiidae, Hymenoptera). Journal of Hymenoptera Research 86: 145–150. https://doi.org/10.3897/jhr.86.73837

Abstract

One new species in the brachycistidine tiphiid genus *Stilbopogon*, *monveroensis* is described from the Monvero Dunes in Fresno Co., California. A revised key to the species of *Stilbopogon* is included.

Keywords

Brachycistidinae, *costaricaensis*, *Quemaya*

Introduction

Brachycistidine wasps are an obscure group of generally nocturnal aculeate parasitoids. Males are winged and very different appearing than females, in much the same pattern as in the Mutillidae. However, brachycistidines lack any kind of colorful pigmentation, ranging in color from yellowish brown to nearly black. For decades there was a separate taxonomy for males versus females and no sex associations were made until Kimsey (2006). One consequence of making the sex associations was that the genus *Quemaya* Pate, 1947 (based on males) was predated by *Stilbopogon* Mickel & Krombein, 1942 (based on females). *Stilbopogon*, under the old name of *Quemaya*, was first revised by Kimsey and Wasbauer (1996).

Very little is known about the biology of the Brachycistidinae. The winged males are generally collected in blacklight traps and the wingless females in pitfall traps. Members of this group were assumed to be parasitoids much like the rest of the family.

Copyright *Lynn S. Kimsey*. This is an open access article distributed under the terms of the Creative Commons Attribution License (CC BY 4.0), which permits unrestricted use, distribution, and reproduction in any medium, provided the original author and source are credited.

The first host record for any species of Brachycistidinae was found to be a tenebrionid larvae found being attacked by a female *Stilbopogon* in the daytime (Borowiec and Kimsey 2015).

Males in the genus *Stilbopogon* exhibit a number of unusual features, even among the brachycistidines. *Stilbopogon* is the smallest bodied group in the subfamily. The largest males belong to *Stilbopogon confusa* Kimsey & Wasbauer, which reach 6 mm in length. Males in the majority of species range in length from 3–4 mm. Females are much smaller. There are also a few species of *Stilbopogon*, including *costaricaensis* Kimsey & Bohart, and the new species described below, that have proportionally small eyes and even smaller ocelli. These species are also dark brown to black in coloration. These head and coloration modifications suggest that the new species and *costaricaensis* may actually be diurnal.

Materials and methods

The new species described below was collected in Malaise traps run on the Monvero Dunes in Fresno County, California, in June and July, 2015. This is odd sand dune system is located on top of a ridge in the interior central coastal range of California, between 600 and 670 m above sea level (Fig. 1). It is considered to be the remains of an Upper Cretaceous reef (Stewart 1946). The dunes are vegetated by a combination of inner coastal range and Mojave Desert plant species, including large *Ephedra californica* plants.

Figure 1. Landscape view of Monvero Dunes looking south. Photo courtesy of Michael Powers, U.S. Bureau of Land Management.

Results

Identification key to *Stilbopogon* males

(modified from Kimsey and Wasbauer 1998)

1 Forewing with two submarginal cells **2**
– Forewing with one submarginal cell (as in Fig. 2) **5**
2 Mandible with two apical teeth; distance between midocellus and closest eye margin less than 1.5 midocellus diameters ..... ***arenicola*** **(Wasbauer)**
– Mandible with three apical teeth, one may be very small; distance between midocellus and closest eye margin more than 1.5 midocellus diameters **3**
3 Mesopleuron densely punctate, with punctures evenly dispersed over entire surface and 1–2 puncture diameters apart; propodeum coarsely sculptured with irregular demarcation between dorsal and posterior surfaces indicated by rugae ..... ***confusa*** **(Kimsey & Wasbauer)**
– Mesopleuron sparsely punctate, with punctures generally 4–6 puncture diameters apart, denser dorsally than posteroventrally, surface above midcoxa nearly impunctate; propodeum smooth, without distinct punctation or rugosities, and no demarcation between dorsal and posterior surfaces **4**
4 Midocellus separated from eye margin in front view by more than 2 midocellus diameter; epipygium apically bidentate..... ***perpunctata*** **(Cockerell)**
– Midocellus separated from eye margin in front view by less than 2 midocellus diameters; epipygium apically flat and broadly triangular..... ..... ***megalops*** **(Kimsey & Wasbauer)**
5 Gular carina with basal tooth-like projection near mandible; clypeus transversely indented, without medial projection, arcuately raised apicomedially; epipygium apex truncate..... ***inermis*** **(Malloch)**
– Gular carina simple; clypeus and epipygium various **6**
6 Flagellomeres I and II subequal in length, about twice as long as broad or longer; epipygium apex strongly convex and lip-like ..... ***marcida*** **(Bradley)**
– Flagellomeres I shorter than II, and between I.2 and 1.8× as long as broad; epipygium apex medially emarginate or truncate **7**
7 Midocellus larger, separated by 2 midocellus diameters or less from nearest eye margin; flagellomere I 1.6× as long as broad or longer..... **8**
– Midocellus small, separated by 3 or more midocellus diameters from nearest eye margin; flagellomere I 1.5× as long as broad or shorter **9**
8 Midocellus separated from nearest eye margin by 1.5 midocellus diameters or less; epipygial apex convex; clypeus with broad, blunt medial projection, bulging and strongly subtriangular in profile; forewing R1 vein strongly angulate near costal margin, marginal cell broadly parallel-sided..... ..... ***mexicana*** **(Kimsey & Wasbauer)**
– Midocellus separated from nearest eye margin by 1.8–2.0 midocellus diameters; epipygial apex bidentate; clypeus with narrow nose-like or almost

digitate medial projection; forewing R1 vein narrowly separated from stigma, curved or indistinguishable near costal margin..... ***paupercula*** **(Bradley)**

9 Midocellus five or more midocellus diameters from nearest eye margin (as in Fig. 3).....**10**

– Midocellus 3.0–3.5 midocellus diameters from nearest eye margin **11**

10 Flagellomere I 1.1–1.2× as long as broad; flagellomere II 1.4× as long as broad; propodeum coarsely sculptured, with irregular, partial transverse carina..... ***costaricaensis*** **(Kimsey & Wasbauer)**

– Flagellomere I 1.4–1.5× as long as broad; flagellomere II 1.8–1.9× as long as broad (Fig. 3); propodeum smooth without sculpturing or transverse carina (Fig. 6)..... ***monveroensis*** **Kimsey, sp. nov.**

11 Clypeus with small, sharp medial projection, apical truncation 1.5 midocellus diameters wide; epipygial apex medially emarginate, with sublateral carina..... ***eurekaensis*** **(Kimsey & Wasbauer)**

– Clypeus with broad, transverse medial projection subtended by discrete declivity, apical truncation 2 midocellus diameters wide; epipygial apex truncate.....***sonorensis*** **(Kimsey & Wasbauer)**

Systematics

Stilbopogon monveroensis **Kimsey, sp. nov.**
http://zoobank.org/56B005C7-390E-4FE8-A4B1-4C4E871D2707
Figs 2–8

Diagnosis. *Stilbopogon monveroensis* has the small ocelli (Fig. 3), single submarginal cell (Fig. 2), and short broad flagellomeres (Fig. 3) that characterize *S. costaricaensis*, and less so *S. sonorensis* and *S. eurekaensis*. The nasiform clypeus (Figs 3, 4), small eyes, and finely sculptured propodeum (Fig. 6) are diagnostic for this species.

Description. Male. ***Body*** (Figs 6, 8); length 2.5–4.4 mm. ***Head*****:** face (Fig. 3): clypeus with subrectangular medial projection, projection apex 1.0–1.1 midocellus diameter wide, appearing acute in profile (Fig. 5), apicomedial truncation 2.6–2.7 midocellus diameters wide in front view (Fig. 3); mandible with three apical teeth, preapical teeth subequal in length; gular carina simple; flagellomere I length 1.4–1.5× breadth; flagellomere II 1.9–2.0× as long as broad; interantennal distance 1.5 midocellus diameters wide; distance from midocellus to closest eye margin 5.8–6.0 midocellus diameters. ***Mesosoma*****:** mesopleuron with punctures 2–4 puncture diameters apart; forewing with one submarginal cell; marginal cell small, more than 3× as long as broad, widely separated from costal margin (Fig. 2); propodeum largely impunctate and smooth, with small medial patch of fine rugae. ***Metasoma*****:** epipygium apicomedially truncate, with two sublateral carinae, each terminating in small tooth, apical surface forming an ovoid, slightly sunken medial area (Fig. 5); paramere gently tapering, apicoventral angle obtuse (Fig. 7). ***Color*****:** body dark brown to black; antenna pale brown, slightly yellower than legs; wing veins pale brown to transparent, stigma brown; wing membrane untinted.

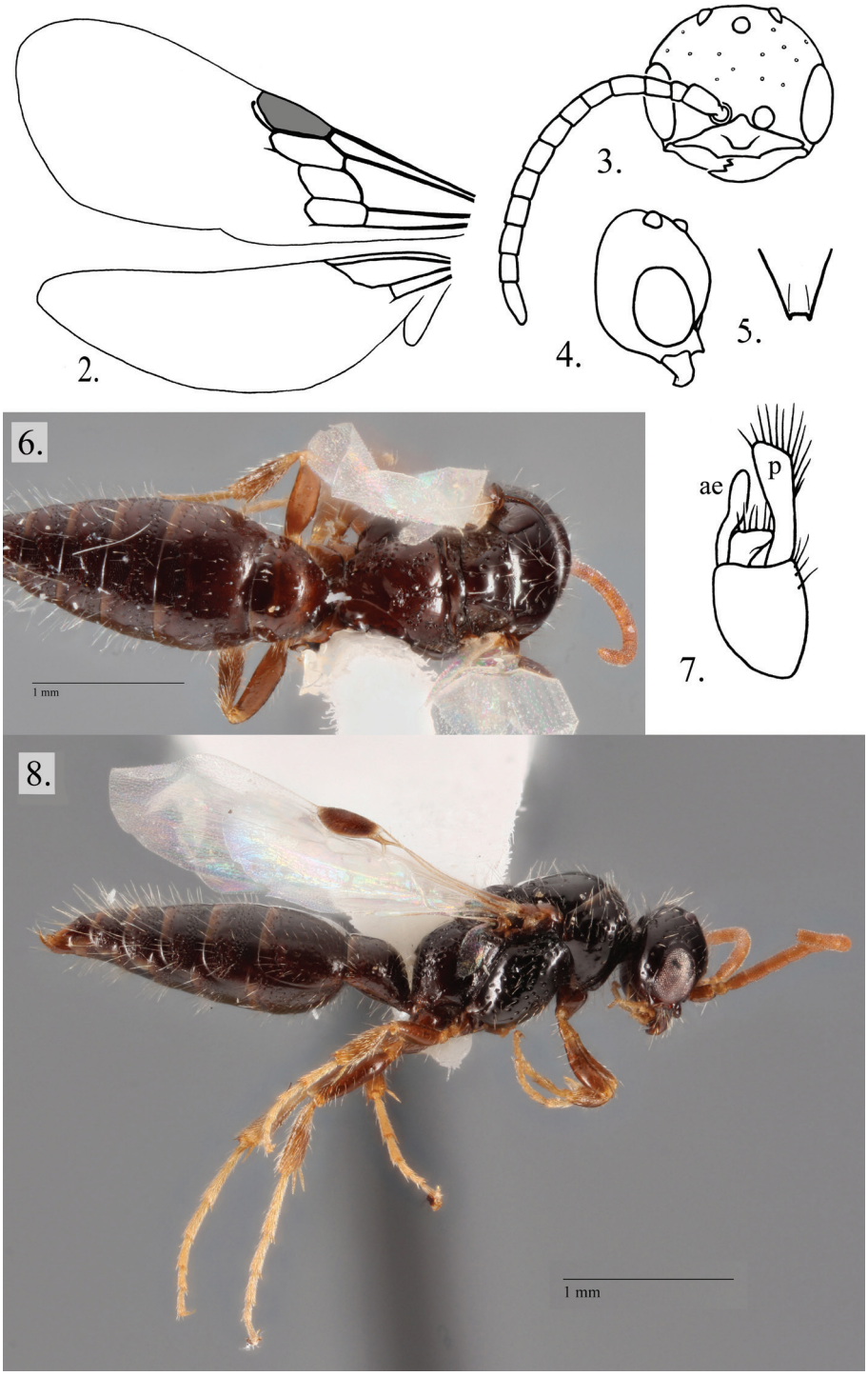

Figures 2–8. *Stilbopogon monveroensis* male **2** fore and hindwing venation **3** front view of face **4** lateral view of head **5** dorsal view of epipygium **6** dorsal view of body **7** lateral view of male genital capsule **8** lateral view of body. Abbreviations: ae = aedeagus, p = parameres.

Female. Unknown.

Etymology. This species is named after the site of collection in the Monvero Dunes.

Material examined. ***Holotype*** male; USA: California, Fresno Co., Monvero Dunes, Monocline ridge, 29 km sw Mendota,10 June 2015, 36.4974, -120.5312, 500 m, MT4 near *Ephedra californica*, M. Powers. Paratypes: 19 males: 6: same data as holotype; 6: MT1, 36°32'N, 120°33'W, 569 m, 10 June 2015, near *Ephedra*, M. Powers; 4: MT1, 36°32'N, 120°33'W, 7 July–8 August 2015, M. Powers; 1: 36.539, -120.567, 15–30 June 2015, MT1 near *Ephedra californica*, M. Powers; 3: 498 m, 17 July 2015, 498 m, 36°32'N, 120°33'W, MT2, Bohart Museum crew. All types are deposited in the Bohart Museum of Entomology, University of California, Davis.

Distribution. This species has only been found in the Monvero Dunes in Fresno Co., California.

Remarks. Most species of *Stilbopogon* appear to be quite widespread in arid and desert regions of North and Central America. *Stilbopogon monveroensis* appears to be the exception to this. However, its restricted distribution may be more the result of limited collecting than actual endemism.

Acknowledgements

This study was made possible by logistical and personnel support from the U.S. Bureau of Land Management, particularly with the assistance of Mike Powers.

References

Borowiec M, Kimsey LS (2015) The first host record for the wasp subfamily Brachycistidinae. Proceedings of the Entomological Society of Washington 117(1): 62–64. https://doi.org/10.4289/0013-8797.117.1.62

Kimsey LS (2006) Competing taxonomies: reexamination of the female-based genera of Brachycistidinae. Zootaxa 1211: 21–34. https://doi.org/10.11646/zootaxa.1211.1.2

Kimsey LS, Wasbauer MS (1996) Revision of the American tiphiid genus *Quemaya* Pate. Journal of Hymenoptera Research 7(1): 38–47.

Kimsey LS, Wasbauer MS (2006) Phylogeny and checklist of the nocturnal tiphiids of the Western Hemisphere. Journal of Hymenoptera Research 15(1): 9–25.

Stewart R (1946) Geology of Reef Ridge Coalinga District California. USDI Geological Survey Professional Paper 205-C, 52 pp. https://doi.org/10.3133/pp205C

JHR 86: 151–169 (2021)
doi: 10.3897/jhr.86.73161
https://jhr.pensoft.net

RESEARCH ARTICLE

JOURNAL OF Hymenoptera RESEARCH
A peer-reviewed open-access journal
The International Society of Hymenopterists

A new genus of anaxyelid wood wasps from the mid-Cretaceous and the phylogeny of Anaxyelidae (Hymenoptera)

Jia Gao[1], Michael S. Engel[2,3], Chungkun Shih[1,4], Dong Ren[1], Taiping Gao[1]

1 *College of Life Sciences and Academy for Multidisciplinary Studies, Capital Normal University, 105 Xisanhuanbeilu, Haidian District, Beijing 100048, China* **2** *Division of Entomology, Natural History Museum, and Department of Ecology & Evolutionary Biology, University of Kansas, 1501 Crestline Drive – Suite 140, Lawrence, Kansas, 66045-4415, USA* **3** *Division of Invertebrate Zoology, American Museum of Natural History, Central Park West at 79th Street, New York, NY, 10024-5192, USA* **4** *Department of Paleobiology, National Museum of Natural History, Smithsonian Institution, Washington, DC 20013-7012, USA*

Corresponding author: Taiping Gao (tpgao@cnu.edu.cn)

Academic editor: Michael Ohl | Received 18 August 2021 | Accepted 7 October 2021 | Published 29 October 2021

http://zoobank.org/71F5C11B-C063-474D-BC96-8085C9F43A9C

Citation: Gao J, Engel MS, Shih C, Ren D, Gao T (2021) A new genus of anaxyelid wood wasps from the mid-Cretaceous and the phylogeny of Anaxyelidae (Hymenoptera). Journal of Hymenoptera Research 86: 151–169. https://doi.org/10.3897/jhr.86.73161

Abstract

Two new species of wood wasps (Anaxyelidae), *Orthosyntexis elegans* **gen. et sp. nov.** and *Orthosyntexis thanti* **sp. nov.**, are described from mid-Cretaceous Kachin amber. *Orthosyntexis* **gen. nov.** exhibits characters and character combinations unique to the family, such as the combination of two mesotibial spurs, a length ratio of forewing 1Rs to 1M<1, a length to width ratio of forewing cell 1mcu ≥ 2, and the presence of 2M+Cu in the hind wing. The new species and morphological characters allow for an exploration of anaxyelid phylogeny. The phylogenetic results indicate that Anaxyelidae are monophyletic and it is suggested to classify the genera in two subfamilies, Syntexinae and Anaxyelinae, the latter including Kempendajinae and Dolichostigmatinae.

Keywords

Apomorphy, Kachin amber, morphological characters, phylogenetic analysis, Syntexinae, wing venation

Copyright *Jia Gao et al.* This is an open access article distributed under the terms of the Creative Commons Attribution License (CC BY 4.0), which permits unrestricted use, distribution, and reproduction in any medium, provided the original author and source are credited.

Introduction

Anaxyelidae are a small family of wood wasps, comprising a single extant species, *Syntexis libocedrii* Rohwer, 1915, commonly called the incense cedar wood wasp, which occurs in western North America (Rohwer 1915; Wickman 1967). *Syntexis libocedrii* lays eggs in the sapwood of coniferous trees, e.g., yellow juniper, giant red cedar, incense cedar, and probably Douglas fir, preferring recently burnt timber. The larvae bore through the wood, sometimes wreaking economically significant levels of damage (Wickman 1967; Smith 1979; Grimaldi and Engel 2005). While the family today consists of a single species, during the Cretaceous, particularly the Early Cretaceous, a significant diversity of anaxyelids has been documented. This diversity has been arranged into four subfamilies: Syntexinae Benson, 1935 including *S. libocedrii* and several fossil species, and three other subfamilies, i.e., Dolichostigmatinae, Kempendajinae and Anaxyelinae, known exclusively from fossils (Rasnitsyn 1968, 1969, 1980, 1990; Zhang and Rasnitsyn 2006). To date, 18 genera and 44 species of Anaxyelidae have been described (Rasnitsyn et al. 1998; Rasnitsyn and Martínez-Delclòs 2000; Zhang and Rasnitsyn 2006; Ortega-Blanco et al. 2008; Kopylov 2018, 2019; Wang et al. 2018; Kopylov et al. 2020; Wang et al. 2020: listed in Suppl. material 1). Despite this considerable compression fossil diversity, only two specimens have been described in amber, one from the Early Cretaceous of Spain (*Eosyntexis parva* Ortega-Blanco, Rasnitsyn & Delclòs, 2008) and the other from the Late Cretaceous of northern Myanmar (*Sclerosyntexis hirsuta* Wang, Ren, Kopylov & Gao, 2020). In addition, seven undescribed specimens were recorded in Zhang et al. (2018).

Most morphological studies have recovered Anaxyelidae as basal among Siricoidea (Rasnitsyn 1988; Ronquist et al. 1999). The molecular analysis of Schulmeister et al. (2002) recovered a clade Anaxyelidae + Siricidae, while Vilhelmsen et al. (2010) found the same in their analysis using implied weights. Similarly, Heraty et al. (2011) recovered Anaxyelidae as sister to Siricidae with strong support in all analyses. Most work has supported Anaxyelidae as comprising a superfamily, Siricoidea, with Siricidae, and together as the sister group to Xiphydrioidea + Euhymenoptera (i.e., Orussoidea + Apocrita) (Sharkey et al. 2012). However, all of these studies concerned only extant taxa and there have been no reports concerning the phylogenetic relationships of the many fossil anaxyelids.

Herein, we describe a new genus, with two new species, of Anaxyelidae from Kachin amber, which have a single rs-m in the fore- and hind wings and a long pedicel. *Orthosyntexis* gen. nov. is attributed to the subfamily Syntexinae based on the wider pterostigma, 1r-rs longer than 2r-rs in the forewing, and 1m-cu lacking in the hind wing. More importantly, 2M+Cu is present in the hind wing and two apical mesotibial spurs are also present in these fossils, representing new morphological features for Anaxyelidae. In addition to providing formal descriptions of the species, we present a phylogenetic analysis of living and fossil Anaxyelidae to document the placement of the fossils, explore relationships among the various fossil species and *S. libocedrii*, clarify the suprageneric classification, and explore the early evolution of the family.

Material and methods

Taxonomy

All type specimens described herein are housed in the Key Laboratory of Insect Evolution and Environmental Changes, College of Life Sciences and Academy for Multidisciplinary Studies, Capital Normal University, Beijing, China (CNUB; Curator, Dong Ren). Specimens were examined under a Leica M205C dissecting microscope, and photographed using a Nikon SMZ 25 microscope with an attached Nikon DS-Ri2 digital camera system. Line drawings were prepared in Adobe Illustrator CC and Adobe Photoshop CC . Wing venation nomenclature was modified after Rasnitsyn (1969, 1980), with the following abbreviations: A, anal vein; C, costal vein; Cu, cubital vein; M, median vein; R, radial vein; R1, first radial; Rs, radial sector; 1cu-a, crossvein between 1Cu and A; 2rs-m and 3rs-m, crossveins between Rs and M; 1m-cu and 2m-cu, crossveins between M and 1Cu.

Phylogenetic analyses

A phylogenetic analysis was undertaken using morphological characters to determine the position of the new genus *Orthosyntexis* and to clarify relationships among the subfamilies Syntexinae, Anaxyelinae, Dolichostigmatinae and Kempendajinae. Seven extant species and 19 fossil species were used in these analyses. The phylogenetic analyses include 27 taxa, with 20 ingroups and seven outgroups – *Macroxyela ferruginea* (Say 1824) (Xyelidae), *Acantholyda erythrocephala* (Linnaeus 1758) (Pamphiliidae), *Cephus nigrinus* (Thomson 1871) (Cephidae), *Sirex nigricornis* (Fabricius 1781) and *Urocerus gigas* (Linnaeus 1758) (both Siricidae), *Xiphydria camelus* (Linnaeus 1758) (Xiphydriidae), and *Orussus abietinus* (Scopoli, 1763) (Orussidae). Some of the body characters are attributable to Vilhelmsen (2001), while a subset of the wing characters is referenced in Wang et al. (2016). In addition, we made some changes to the character states based on published data and new findings, and we added new characters from the antennae and wing venation. For instance, compared with Wang et al. (2016), we designated the characters of the length ratios of forewing 1Rs to 1M as '0' for '<1', '1' for '≥ 1, < 3' and '2' for '≥ 3'; the length ratios of forewing 1m-cu to 3Cu as '0' for '≤ 1', '1' for '>1'; and the length ratios of forewing 1Cu to 1M as '0' for 'apparently<1', '1' for '≥ 1'. To make the characters of ingroups as broad as possible, we also defined forewing 1r-rs as '0' for 'always present', '1' for 'partly reduced', and '2' for 'completely reduced', and hind wing cell r as '0' for 'closed' and '1' for 'open'. A total of 63 morphological characters and their character states are presented in the Suppl. material 2. Some are clearly present in the two new species, and others are important features of representative ingroups. A character-state data matrix consisting of 27 taxa and 63 morphological characters is provided in the Suppl. material 3.

Parsimony analysis was performed using WinClada v.1.00.08 (Nixon 2002) and NONA v.2.0 (Goloboff 1997). Tree search implemented a heuristic search method,

and the options were set to hold 10,000 trees, 1000 replications, 100 starting tree replications, and a multiple TBR+TBR search strategy. All characters were treated as unordered and weighted equally. Bootstrap support values were determined in NONA with 1000 replications and are represented as numbers under the branches (in blue).

Results

Systematics

Order Hymenoptera Linnaeus, 1758
Family Anaxyelidae Martynov, 1925
Subfamily Syntexinae Benson, 1935

Genus *Orthosyntexis* J. Gao, Engel, Shih, & T. Gao, gen. nov.
http://zoobank.org/9C41FD02-F175-44C8-B69A-64D8D951E62A

Type species. *Orthosyntexis elegans* sp. nov.

Etymology. The new genus-group name is a combination of the Ancient Greek *orthós* (ὀρθός, meaning, "upright" or "erect", and geometrically "right angle"), and the genus *Syntexis* (itself from Ancient Greek *súntēxis* (σύντηξις, meaning, "colliquescence", "emaciating", or "wasting away")), type genus of the subfamily Syntexinae. Gender feminine.

Diagnosis. Female: Antenna with 16 flagellomeres, scape almost 3× as long as width and twice as long as flagellomere I, flagellomere I nearly 1.5× as long as flagellomere II. Forewing with pterostigma not enlarged, uniformly sclerotized and of normal width; 1Rs shorter than 1M; cell 1mcu length to width ratio slightly more than 2; 1r-rs and 2rs-m absent; 1Cu obviously shorter than 2Cu; 3Cu shorter than 4Cu; 2m-cu 1.5× shorter than 1m-cu in forewing; 3rs-m 2× shorter than 4M. Hind wing with abscissa 2M+Cu; 1M shorter than 2M; m-cu absent, cell r closed. Mesotibia with two apical spurs. Male: Unknown. Immatures: Unknown.

Included species. *Orthosyntexis elegans* sp. nov. and *O. thanti* sp. nov.

Remarks. *Orthosyntexis* may be differentiated from *Curiosyntexis*, in which the forewing pterostigma is desclerotized and 1r-rs is partly reduced (Kopylov 2019), and from *Dolichosyntexis*, which has an enlarged pterostigma and forewing 1Cu not obviously shorter than 2Cu (Kopylov 2019). The new genus can be separated from *Parasyntexis* by the latter's narrower pterostigma, narrower than the length of 2r-rs, and 1M longer than 2M in the hind wing (Kopylov 2019). *Orthosyntexis* can be distinguished from *Sclerosyntexis* by the latter's elongate scape, which is 3× longer than wide, and the open cell r in the hind wing (Wang et al. 2020). *Orthosyntexis* differs from the extant genus *Syntexis*, which has 3Cu longer than 4Cu and 2m-cu 1.5× longer than 1m-cu in the forewing (Rohwer 1915), and from *Daosyntexis* by 1Rs 3× being longer than 1M and 3rs-m 2× longer than 4M in the forewing (Kopylov et al. 2020). The new genus

differs from *Cretosyntexis* by 2r-rs meeting the pterostigma beyond midlength and Rs+M longer than 2M (Rasnitsyn and Martínez-Delclòs 2000), and from *Eosyntexis* in which 1RS is not shorter than 1M (Rasnitsyn and Martínez-Delclòs 2000).

Orthosyntexis elegans **J. Gao, Engel, Shih, & T. Gao, sp. nov.**
http://zoobank.org/0A3E4C6A-DB65-4FCA-83D5-E109FEAB9743
Figs 1, 2 and 3

Etymology. The specific epithet is derived from the Latin word *elegans*, meaning elegant.

Diagnosis. Antennal scape length to width ratio slightly less than 3. Forewing 1Rs subvertical to R. Meso- and metafemur shorter than associated tibiae; mesotibial apical spurs elongate and distinctly narrowed apically.

Holotype. Female, no. CNU-HYM-MA2015101 (Figs 1–3).

Type locality and horizon. The amber specimen was collected from Kachin (Hukawng Valley) in northern Myanmar, and is dated at 98.79 ± 0.62 Mya (Cruickshank and Ko 2003; Shi et al. 2012).

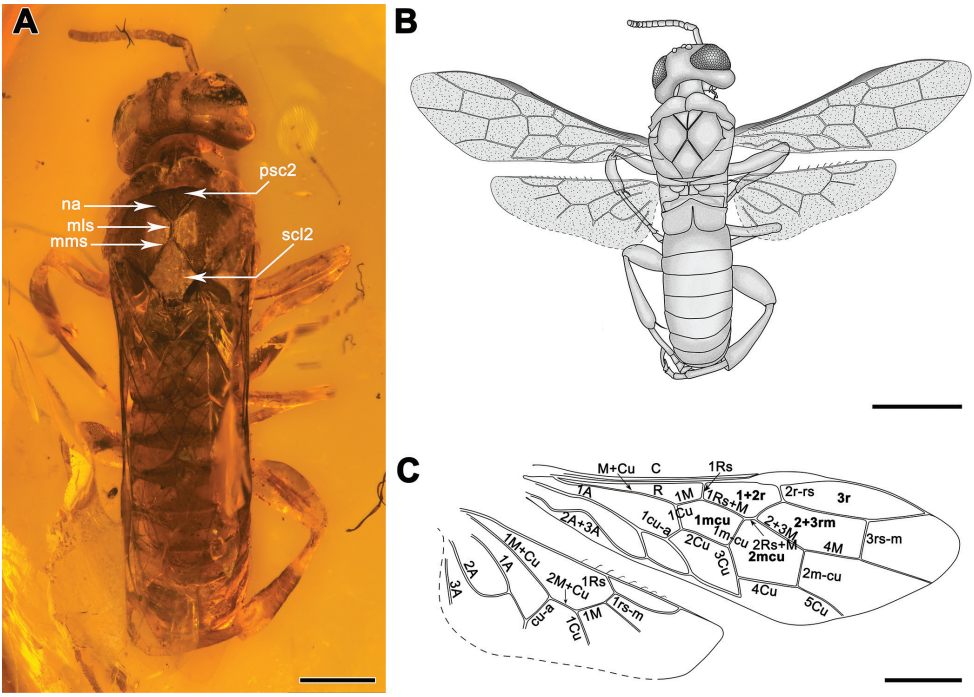

Figure 1. One photograph and two line drawings of *Orthosyntexis elegans* gen. et sp. nov., holotype (specimen CNU-HYM-MA2015101) female **A** dorsal view as preserved **B** line drawing of dorsal view with forewings and hind wings artificially extended from body **C** line drawing of forewing and hind wing. Scale bars: 1 mm (**A, C**); 2 mm (**B**). Abbreviations: mms, mesoscuto-mesoscutellar sulcus; mls, median longitudinal sulcus; na, notaulus; psc2, mesoprescutum; scl2, mesoscutellum.

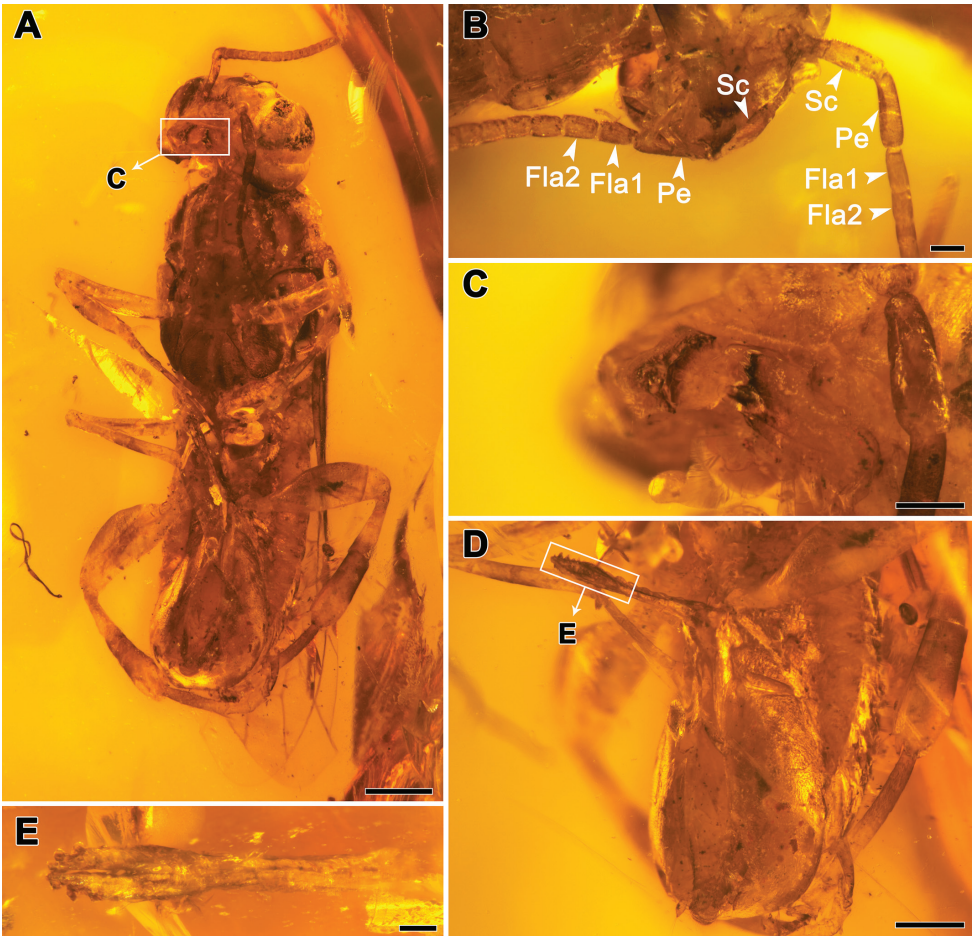

Figure 2. Photographs of *Orthosyntexis elegans* gen. et sp. nov. **A** habitus in ventral view **B** antenna in lateral view **C** mandible in ventral view **D** part of abdomen in lateral view **E** apical ovipositor in lateral view. Scale bars: 1 mm (**A**); 0.2 mm (**B, C**); 0.5 mm (**D**); 0.1 mm (**E**). Abbreviations: Fla1 and Fla2, flagellomeres I and II; Pe, pedicel; Sc, scape.

Description. Body about 8.25 mm long in dorsal view, antenna 2.73 mm long in ventral view; forewing about 5.69 mm in length, maximum width 1.74 mm; hind wing about 4.57 mm in length.

Head moderately large, narrower than thorax. Head 1.85 mm wide and 1.23 mm long, nearly quadrate. Compound eyes large and hemispherical; mandible straight, orthogonal with apical margin vertical (parallel to mandibular base) and with lowest tooth not that elongate (Fig. 2C); labial palpus with three palpomeres; maxillary palpus with at least five palpomeres; antenna with 16 flagellomeres, scape 0.40 mm long, maximum width 0.14 mm; pedicel 0.39 mm long, maximum width 0.12 mm; flagellomere I shorter than scape, 0.11 mm wide, 0.22 mm long, flagellomere II 0.10 mm wide, 0.19 mm long, as long as individual lengths of remaining flagellomeres (Fig. 2B).

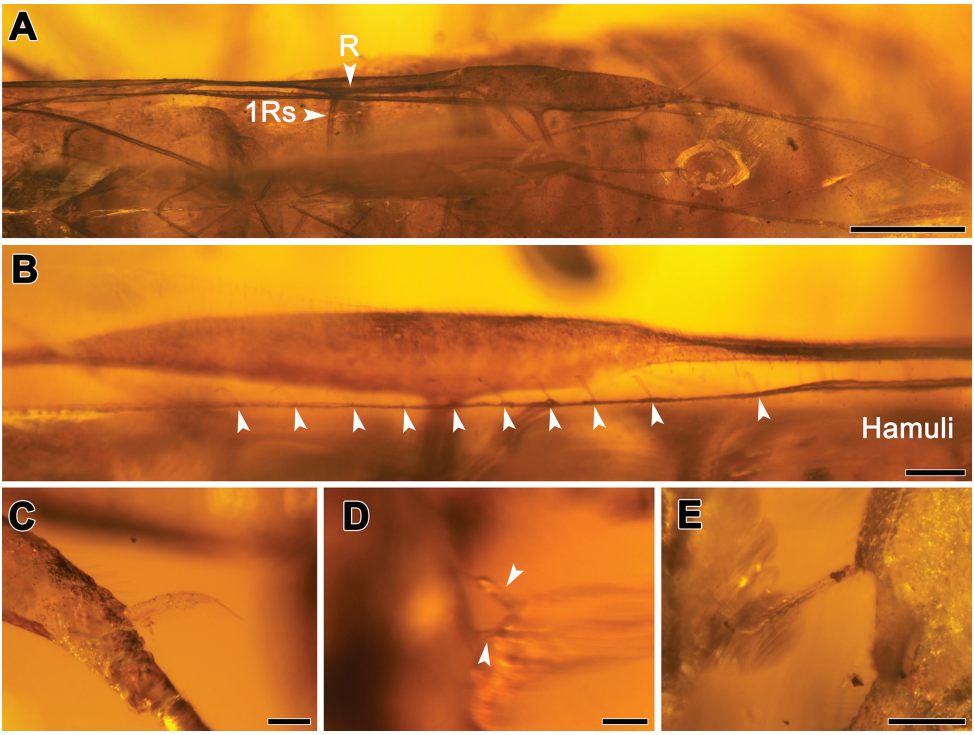

Figure 3. Photographs of *Orthosyntexis elegans* gen. et sp. nov. **A** part of left forewing **B** hind wing hamuli (white arrows) **C** right protibial spur **D** right mesotibial spurs **E** left metatibial spur. Scale bars: 0.5 mm (**A**); 0.1 mm (**B–E**).

Thorax wide, width across tegulae 1.56 mm; pronotum short, having prominent anterior notch and hind margin, with median longitudinal furrow dorsally. Mesoscutum with median longitudinal sulcus and notauli strongly impressed; mesoscutellum tapering to acute apex; ratio of lengths of prescutum, median longitudinal sulcus between notauli, and mesoscuto-mesoscutellar sulcus and mesoscutellum 2.5/1/4.5, notauli terminating close to mesoscutellum (Fig. 1A). Legs spindly, meso- and metafemora shorter than associated tibiae. Metafemur length 1.30 mm, metatibia thick subapically, length 1.65 mm. Protibia and metatibia with only one apical spur visible, mesotibia with two apical spurs (Fig. 3C, D and E); all tarsomeres with stiff apical setae; basitarsi long but shorter than remaining tarsomeres combined; tarsomere V elongate but shorter than basitarsus; pretarsal claws long, with curved apices and each with a single preapical tooth.

Abdomen only slightly narrower than mesothorax; abdominal tergum I split medially. Segments I and II slightly longer than remaining abdominal segments; ovipositor length 1.86 mm, not protruding beyond abdominal tip, strongly serrated apically (Fig. 2D and 2E)

Forewing with dense microtrichia but no coloration pattern except slightly darkened costal area. C and R thick, costal area narrower than C and R widths. Pterostigma completely sclerotized; Sc absent; 1r-rs and 2rs-m absent; 2r-rs issuing from pterostigma

at its basal 1/3; 1Rs short and subvertical to R (Fig. 3A), about 0.6× as long as 1M, meeting 1M at right angle. 2Rs+M distinct but short, 0.3× as long as 1Rs+M. 2r-rs slightly proclival. 2+3M 1.1× as long as 4M. Cell 1mcu pentagonal, about 1.9× as long as wide; cell 2mcu hexagonal, about 1.3× as long as wide. 2Cu 1.7× as long as 1Cu. 1cu-a strongly reclival, nearly 0.7× as long as 1Cu. 1m-cu nearly as long as 3Cu, 3Cu shorter than 4Cu. 2m-cu nearly 0.7× as long as 4M and 1.2× as long as 1m-cu.

Hind wing Sc absent. Cell r closed. 1Rs (about 0.28 mm in length) shorter than 1M (about 0.35 mm in length). 1rs-m (about 0.27 mm in length) reclival, nearly in line with 1M and as long as 1Rs. 1M straight; m-cu absent; 2M+Cu present (about 0.39 mm in length), free abscissa of Cu and cu-a (about 0.48 mm in length) developed, 1Cu and cu-a straight.

Orthosyntexis thanti J. Gao, Engel, Shih, & T. Gao, sp. nov.

http://zoobank.org/58143DF9-65BE-49C5-A832-FAD0BFA991E2
Figs 4, 5, 6 and 7

Etymology. The specific epithet honours 3rd Secretary General of the United Nations and Burmese diplomat U Thant (1909–1974) and his dedication to seeking peace within and between nations.

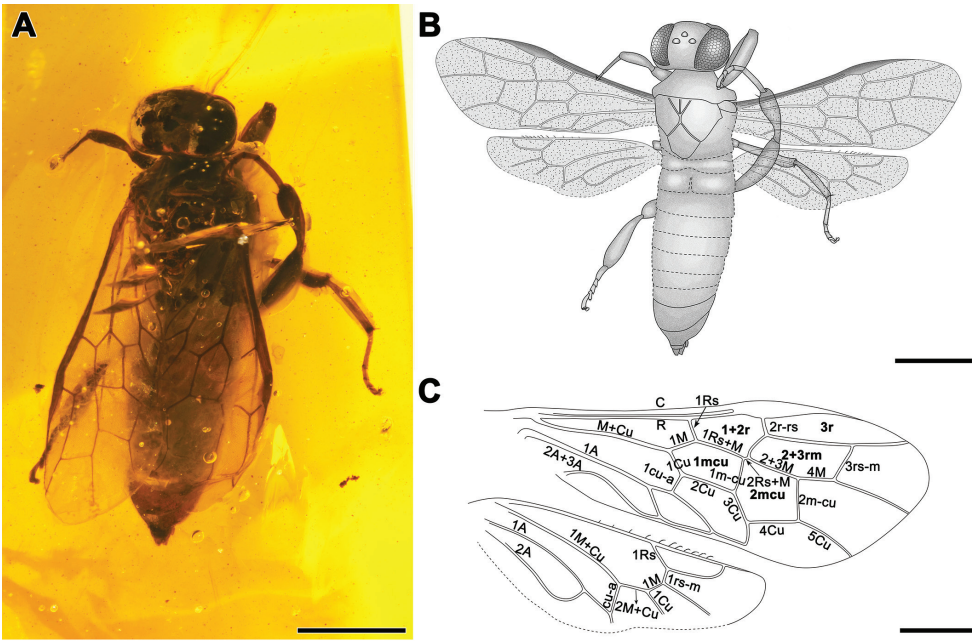

Figure 4. One photograph and two line drawings of *Orthosyntexis thanti* sp. nov., holotype (specimen CNU-HYM-MA2015102) female **A** dorsal view as preserved **B** line drawing of dorsal view with forewings and hind wings artificially extended from body **C** line drawing of forewing and hind wing. Scale bars: 2 mm (**A, B**); 1 mm (**C**).

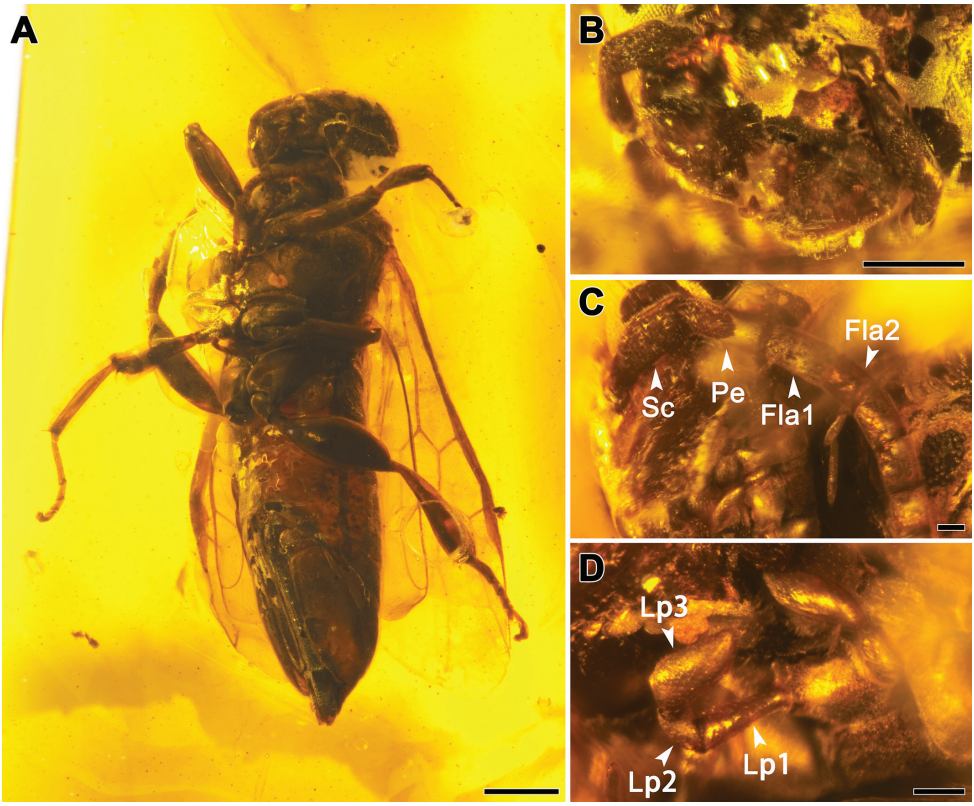

Figure 5. Photographs of *Orthosyntexis thanti* sp. nov. **A** habitus in ventral view **B** mandible in frontal view **C** part of antenna **D** labial palpus. Abbreviations: Fla1 and Fla2, flagellomeres I and II; Lp1, Lp2 and Lp3, labial palpomeres I, II and III; Pe, pedicel; Sc, scape.

Diagnosis. Antennal scape length to width ratio more than 3. Forewing 1Rs proclival to R. Mesofemur longer than mesotibia, metafemur nearly as long as metatibia; mesotibial apical spurs somewhat shortened and not narrowed apically.

Holotype. Female, no. CNU-HYM-MA2015102 (Figs 4, 5 and 6).

Paratype. Female, no. CNU-HYM-MA2015103 (Fig. 7).

Description. ***Holotype*** [paratype measurements given in parentheses]: Body about 8.61 [8.42] mm long in dorsal view, antenna 2.85 [2.62] mm long in ventral view; forewing about 5.64 [5.48] mm in length, maximum width 2.09 [1.67] mm; hind wing about 4.21 [4.42] mm in length.

Head moderately large, slightly narrower than thorax. Head 1.98 [1.77] mm wide and 1.22 [1.31] mm long, nearly quadrate. Compound eyes large and hemispherical; mandible weakly bent, with apical margin vertical (parallel to mandibular base) and with lowest tooth not that elongate (Figs 5B and 7D); labial palpus with three palpomeres (Fig. 5D); antenna with 16 flagellomeres, scape 0.55 [0.46] mm long, maximum width 0.17 [0.14] mm; pedicel 0.37 [0.41] mm long, maximum width 0.13 [0.13] mm; flagellomere I shorter than scape, 0.15 [0.11] mm wide, 0.25 [0.21] mm

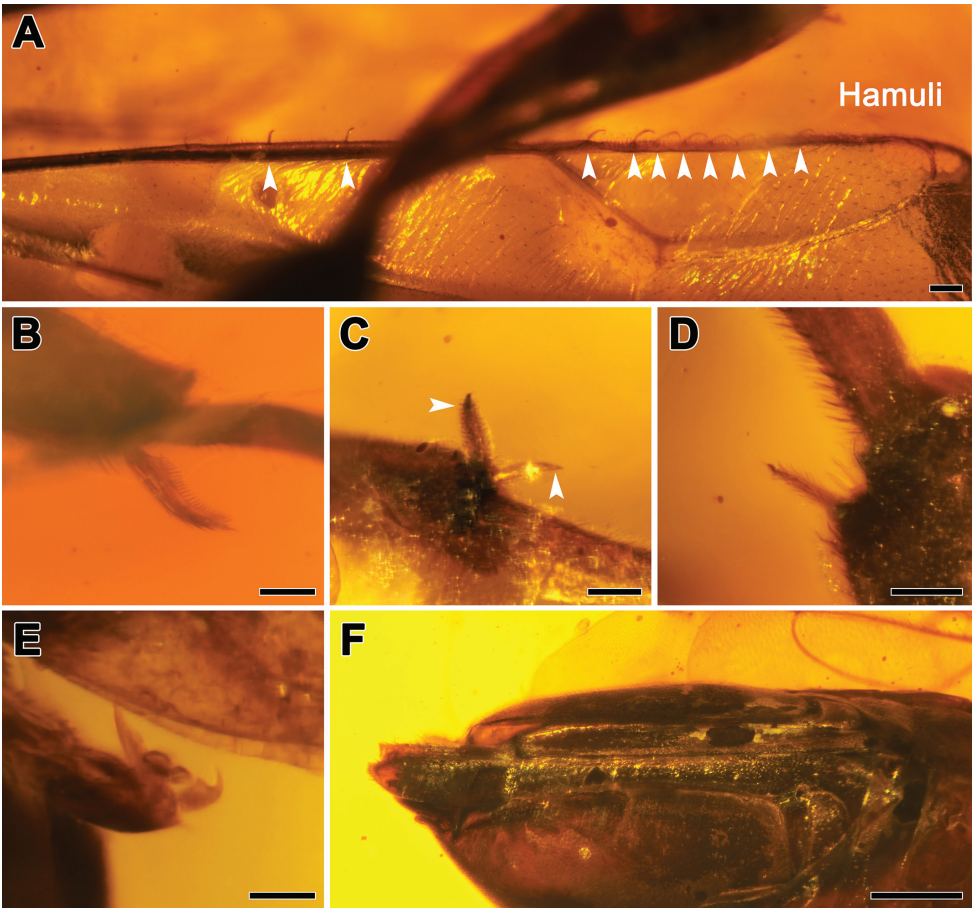

Figure 6. Photographs of *Orthosyntexis thanti* sp. nov. **A** hind wing hamuli (white arrows) **B** left protibial spur **C** right mesotibial spurs **D** left metatibial spur **E** right mesotarsal pretarsal claw **F** ovipositor sheath in lateroventral view. Scale bars: 0.1 mm (**A–E**); 0.5 mm (**F**).

long; flagellomere II 0.15 [0.12] mm wide, 0.17 [0.15] mm long, as long as individual lengths of remaining flagellomeres (Figs 5C and 7C).

Thorax wide, width across tegulae 1.59 [1.54] mm; pronotum short, with slightly developed anterior notch and prominent hind margin, and with mediolongitudinal furrow dorsally. Mesoscutum with longitudinal sulcus and notauli strongly impressed; mesoscutellum tapering to acute apex; ratio of lengths of prescutum, median longitudinal sulcus between notauli, and mesoscuto-mesoscutellar sulcus and mesoscutellum 2.3/1/5.3 [2.2/1/4.9], notauli close to mesoscutellum. Legs spindly, mesofemur longer than mesotibia. Metafemur length 1.69 [1.43] mm, nearly as long as metatibia (length 1.68 [1.50] mm), thick subapically, narrowed apically. Protibia and metatibia with only one apical spur (Figs 6B, D and 7G), mesotibia with two apical spurs (Figs 6C and 7H); all tarsomeres with stiff apical setae; basitarsi long but

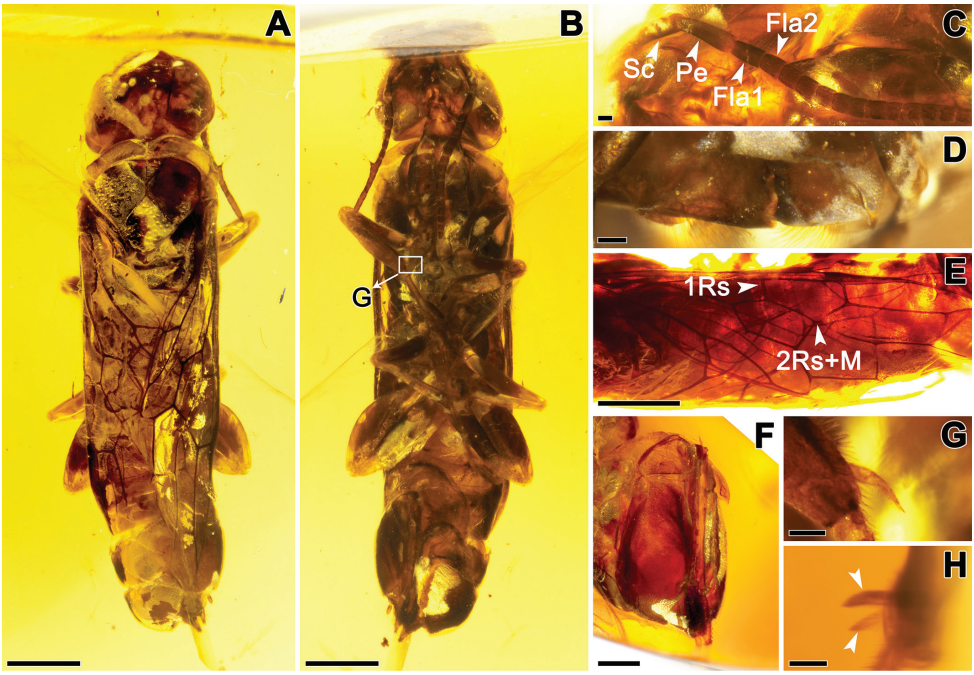

Figure 7. Photographs of *Orthosyntexis thanti* sp. nov., paratype (specimen CNU-HYM-MA2015103) female **A** habitus in dorsal view **B** habitus in ventral view **C** part of antenna **D** mandible in frontal view **E** left forewing **F** ovipositor in lateroventral view **G** protibial spur **H** mesotibial spurs. Scale bars: 1 mm (**A, B**); 0.2 mm (**C**); 0.1 mm (**D–H**). Abbreviations: Fla1 and Fla2, flagellomeres I and II; Pe, pedicel; Sc, scape.

shorter than remaining tarsomeres combined; tarsomere V elongate but shorter than basitarsus; pretarsal claws long, with curved apices and each with a single preapical tooth (Fig. 6E).

Abdomen only slightly narrower than mesothorax. Ovipositor strongly serrate apically, short, not protruding beyond abdominal tip, full length 2.67 [2.51] mm (Figs 6F and 7F).

Forewing with dense microtrichia but no coloration pattern, except for slightly darkened costal area. C and R thick, costal area narrower than C and R widths. Pterostigma completely sclerotized; Sc absent; 1r-rs and 2rs-m absent; 2r-rs issuing from pterostigma at its basal 1/3; 1Rs short and slightly proclival to R, about 0.7× as long as 1M, meeting 1M at right angle (Fig. 7E). 2Rs+M distinct but short, 0.1× as long as 1Rs+M (Fig. 7E). 2r-rs slightly proclival. 2+3M 1.6× [1.2×] as long as 4M. Cell 1mcu pentagonal, about 2.0× [2.1×] as long as wide; cell 2mcu hexagonal, about 1.1× [1.4×] as long as wide. 2Cu 2.1× [1.6×] as long as 1Cu. 1cu-a reclival, nearly 0.8× as long as 1Cu. 1m-cu nearly as long as 3Cu, 3Cu shorter than 4Cu. 2m-cu nearly 0.8× [0.6×] as long as 4M and 1.2× [1.1×] as long as 1m-cu.

Hind wing Sc absent. Cell r closed. 1Rs (about 0.36 [0.32] mm in length) longer than 1M (about 0.26 [0.30] mm in length). 1rs-m (about 0.23 [0.20] mm in length),

with an angle at 2Rs and shorter than 1Rs. 1M straight; m-cu absent; 2M+Cu present (about 0.40 [0.33] mm in length), free abscissa of Cu and cu-a (about 0.40 [0.43] mm in length) developed, 1Cu and cu-a straight.

Phylogenetic analyses

Our morphological phylogenetic analysis, based on 63 morphological characters coded in Winclada (Suppl. materials 2, 3), recovered 18 equally parsimonious topologies (consistency index, 0.40; retention index, 0.56), the strict consensus of which is presented in Figure 8. Anaxyelidae were recovered as monophyletic, supported by seven synapomorphies, e.g.: pedicel length to width ratio ≥ 2 (character 4), 2rs-m of forewing absent (character 28), length ratio of forewing 1Rs to 1M < 1 (character 36), forewing cell 1mcu length to width ratio apparently < 2 (character 42), and 3rs-m of hind wing absent (character 59).

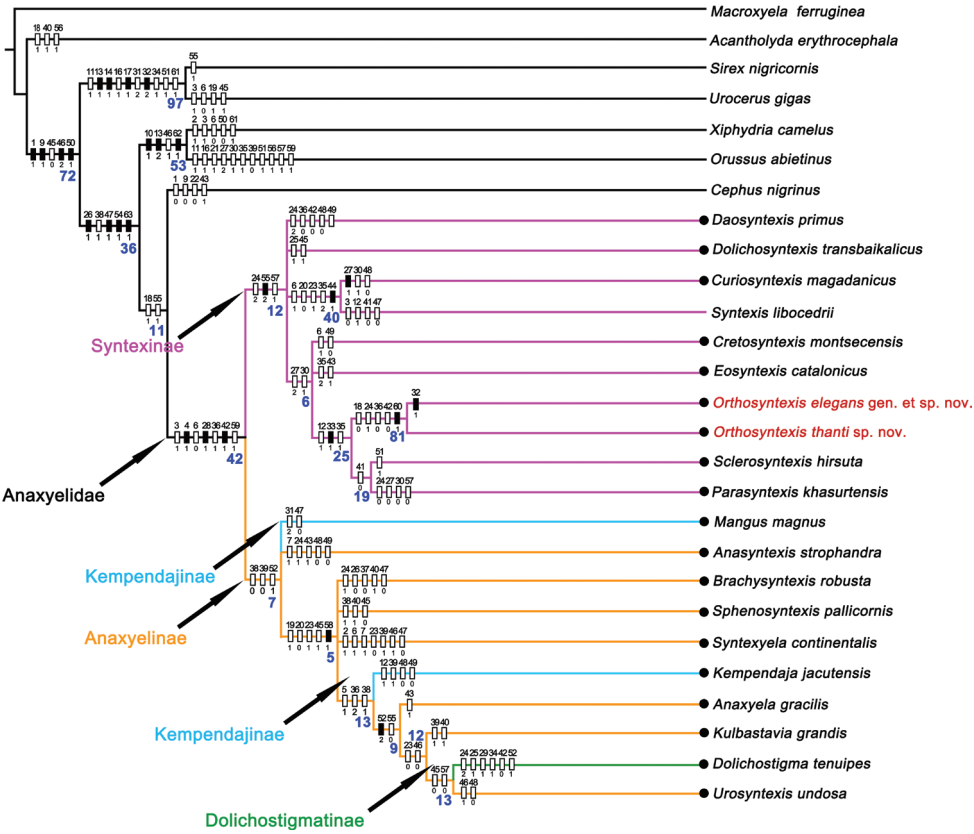

Figure 8. Phylogeny of Anaxyelidae based on 63 morphological characters (Suppl. material 1: File S1 matrix). Strict consensus of 18 trees of length = 195 steps, consistency index = 0.40, and retention index = 0.56. Numbers under branches are bootstrap support values (in blue). Small black bars = unambiguous unique characters; small white bars = homoplasious characters.

The monophyly of *Orthosyntexis* is supported by a unique combination of five homoplasious characters: mesotibia with two apical spurs (character 18), length ratio of the maximum width of pterostigma to 2r-rs nearly = 1 (character 24), length ratio of forewing 1Rs to 1M < 1 (character 36); forewing cell 1mcu length to width ratio ≥ 2 (character 42), and 2M+Cu of hind wing present (character 60). Furthermore, *Orthosyntexis* was recovered as sister to *Sclerosyntexis* + *Parasyntexis* based on: notauli close to mesoscutellum (character 12) and Rs+M bifurcating beyond 1m-cu = 1 (2Rs+M) (character 33).

Regarding the intrafamiliar relationships of Anaxyelidae, two principle branches are supported in the consensus topology (Fig. 8), one equivalent to the subfamily Syntexinae, and the other composed of Dolichostigmatinae, Kempendajinae, and Anaxyelinae, and with the dolichostigmatines and kempendajines rendering anaxyelines paraphyletic. While support values of the two main branches are not great, there are convincing apomorphies supporting these clades. For example, the monophyly of Syntexinae is supported by the ratio of the maximum width of the pterostigma to the length of 2r-rs of forewing nearly = 1 (character 24 length of 2Cu to the length of 1Cu in the hind wing ≥ 5 (character 55), and crossvein m-cu of hind wing absent (character 57). At the same time, the monophyly of Anaxyelinae + Dolichostigmatinae + Kempendajinae is supported by length of 1r-rs to 2Rs of forewing < 1 (character 38), length of Rs+M to 2M of forewing < 1 (character 39), and hind wing crossvein 1rs-m at or quite close to Rs midlength (character 52).

Discussion

The placement of *Orthosyntexis* in Anaxyelidae is well-supported, most notably by the fore- and hind wings each with a single rs-m and the pedicel length to width ratio ≥ 2. Moreover, the genus can be attributed to Syntexinae mainly based on the following combination of characters: forewing with the maximum width of pterostigma not shorter than 2r-rs, 1r-rs absent and hind wing m-cu absent. Given that most of the available fossil anaxyelids are preserved as compressions, often with body structures poorly discernible, there is a natural reliance on wing traits and so most characters currently supporting nodes are derived from the venation. Naturally, as more amber fossils become available, it is hoped that a finer comparison of body structures can be made across living and fossil taxa in the future.

Hitherto, no attempt has been made to explore relationships among anaxyelids in a cladistic framework, likely owing to the fact that there is only one extant species and that many of the known fossils are quite incomplete. Recent phylogenetic treatments of the families of Hymenoptera (e.g., Vilhelmsen 2000, 2001; Sharkey et al. 2012), identified a single putative apomorphy for the family, specifically the longitudinal subdivision of the pronotum, easily observed in our amber fossils. Our analysis recovered a monophyletic Anaxyelidae, even when including the considerable fossil diversity and the lack of critical information from many compression fossils. In addition, our

analysis indicated the pedicel length to width ratio ≥ 2 and the loss of forewing 2rs-m and hind wing 3rs-m to be additional putative apomorphies for the family (Fig. 8).

Zhang and Rasnitsyn (2006) and Kopylov (2019) organized the diversity of Anaxyelidae into four subfamilies. The establishment of Dolichostigmatinae and Kempendajinae was based on four fossil specimens from three species: *Dolichostigma tenuipes* Rasnitsyn 1968, *Kempendaja jacutensis* Rasnitsyn 1968 and *Mangus magnus* Kopylov 2019. The diagnosis of the subfamily Kempendajinae (Rasnitsyn 1980) focused generally on characters of the body and hind wing, which are plesiomorphies; for example, desclerotized pterostigma in the forewing and rs-m located in the distal third of hind wing cell r. Desclerotized pterostigma is also observed in two anaxyelids, *Anaxyela gracilis* Martynov 1925 and *Sphenosyntexis pallicornis* Rasnitsyn 1968. In addition, rs-m in the hind wing is also located in the distal third of cell r in *U. undosa*. Thus, the features used to justify the subfamily Kempendajinae are unreliable and our analysis robustly placed the group within Anaxyelinae. Similarly, the feature used to differentiate Dolichostigmatinae, i.e., large forewing pterostigma also exists in *Dolichosyntexis transbaikalicus* Kopylov 2019. Again, our analysis indicated that the subfamily Dolichostigmatinae is merely a subgroup of Anaxyelinae. Accordingly, we recognize only two monophyletic subfamilies in Anaxyelidae: Syntexinae and Anaxyelinae. Of course, this is only an analysis based on our phylogenetic results, and many fossil specimens provide few useful features due to preservation reasons. Therefore, it is hoped that more fossils of Anaxyelidae will provide more favorable evidence for our analysis in the future.

Recently, the anaxyelid *Sclerosyntexis hirsuta* was described from a single specimen in Kachin amber (Wang et al. 2020). Here, we add two new species, *O. elegans* and *O. thanti*, from the same deposit, based on three specimens. They have thick legs, particularly inflated metatibiae, and a pattern of forewing venation similar to *Sclerosyntexis*, such as 2r-rs joining the pterostigma proximal to pterostigmal midlength, 1r-rs absent, and 2Rs+M present. Furthermore, *Sclerosyntexis* + *Parasyntexis* was recovered as the sister group to *Orthosyntexis* in our phylogenetic estimate for the family.

Although *Orthosyntexis* belongs to the same clade as the modern *Syntexis*, these genera are relatively distantly related within the subfamily, and many features differ significantly between them, e.g., flagellomere I length to width ratio < 3, mesotibia with two apical spurs, 1r-rs absent, 2Rs+M present, hind wing cell r closed, and hind wing 2M+Cu present. However, they do share some similar morphological traits, such as notauli close to the mesoscutellum and 1rs-m at the base of Rs in the hind wing. In addition, the new genus, like extant Anaxyelidae, has the ovipositor apically modified with marginal serrations. Extant Siricoidea use their ovipositor to insert their eggs and spores of a symbiotic fungus into dead or dying trees (Goulet 1993; Grimaldi and Engel 2005). However, there has been no evidence of fungal spores in extinct Anaxyelidae, so a symbiotic relationship between extinct Anaxyelidae and fungi has not been conclusively established, although the distribution of this trait across wood wasps tends to suggest that the extinct diversity had a similar association (e.g., Morgan 1968; Kajimura 2000; Grimaldi and Engel 2005). Nonetheless, conclusive evidence

of a fungal symbiosis in the fossils is lacking and requires further study as more fossil Anaxyelidae are discovered. Indeed, μCT scans of amber-preserved anaxyelids would be critical to look for potential fungal spores carried on adult females or the presence of distinct mycangia. To date, only seven symphytan species have been described in Kachin amber, of which five are syspastoxyelids, one is an anaxyelid, and one is an orussid (Engel et al. 2016; Zhang et al. 2018, 2020; Zheng et al. 2019; Wang et al. 2020, 2021). And eight symphytan specimens have not been described in Kachin amber, of which seven are anaxyelids and one is an orussid (Zhang et al. 2018). Compared with Mesozoic fossil deposits of China and Russia, the number of Symphyta in Kachin amber is quite small. The reason for such a low diversity and abundance may be that the mid-Cretaceous fauna of Kachin amber is characterized by high levels of endemism indicative of an insular biota (Grimaldi et al. 2002; Rasnitsyn and Öhm-Kühnle 2018; Lin et al. 2019; Zhao et al. 2020), as well as its high termophilic (tropical) nature (Grimaldi et al. 2002; Zhang et al. 2018).

Acknowledgements

We are grateful to Hongru Yang, Qiong Wu, Xiangbo Guo, and Yuanyuan Guo (Capital Normal University, Beijing, China) for their helpful advice. We thank the editor Dr. Michael Ohl, and two reviewers, Dr. Lars Vilhelmsen and Dr. Alex Rasnitsyn, as well as an anonymous reviewer for their critical review of the manuscript, which gave considerable insights and improvements. D.R. was supported by grants from the National Natural Science Foundation of China (No. 31730087 and 32020103006). T.P.G. was supported by the National Natural Science Foundation of China (31872277) and the Fok Ying-Tong Education Foundation for Young Teachers in the Higher Education Institutions of China (171016). The authors declare that there are no financial competing interests (political, personal, religious, ideological, academic, intellectual, commercial), nor are there other competing interests in the production of this manuscript.

References

Cruickshank RD, Ko K (2003) Geology of an amber locality in the Hukawng Valley, northern Myanmar. Journal of Asian Earth Sciences 21: 441–455. https://doi.org/10.1016/S1367-9120(02)00044-5

Engel MS, Huang DY, Alqarni AS, Cai CY (2016) An unusual new lineage of sawflies (Hymenoptera) in Upper Cretaceous amber from northern Myanmar. Cretaceous Research 60: 281–286. https://doi.org/10.1016/j.cretres.2015.12.014

Goloboff PA (1997) NoName (NONA), version 2.0. Program and documentation. Tucumán: Fundación Instituto Miguel Lillo.

Goulet H (1993) Superfamilies Cephoidea, Megalodontoidea, Orussoidea, Siricoidea, Tenthredinoidea, and Xyeloidea. In: Goulet H, Huber JT (Eds) Hymenoptera of the World:

An Identification Guide to Families. Research Branch Agriculture Canada Publication, Ottawa, 101–129.

Grimaldi DA, Engel MS (2005) Evolution of the insects. Cambridge University Press, New York.

Grimaldi DA, Engel MS, Nascimbene PC (2002) Fossiliferous Cretaceous amber from Myanmar (Burma): its rediscovery, biotic diversity, and paleontological significance. American Museum Novitates 3361: 1–72. https://doi.org/10.1206/0003-0082(2002)361%3C0001:FCAFMB%3E2.0.CO;2

Heraty J, Ronquist F, Carpenter JM, Hawks D, Schulmeister S, Dowling AP, Murray D, Munro J, Wheeler WC, Schiff N, Sharkey MJ (2011) Evolution of the hymenopteran megaradiation. Molecular Phylogenetics and Evolution 60: 73–88. https://doi.org/10.1016/j.ympev.2011.04.003

Kajimura H (2000) Discovery of mycangia and mucus in adult female xiphydriid woodwasps (Hymenoptera: Xiphydriidae) in Japan. Annals of the Entomological Society of America 93: 312–317. https://doi.org/10.1603/0013-8746(2000)093[0312:DOMAMI]2.0.CO;2

Kopylov DS (2018) Forgotten giants: new Anaxyelidae (Hymenoptera) from the Jurassic of Karatau. Zootaxa 4514: 332–340. https://doi.org/10.11646/zootaxa.4514.3.2

Kopylov DS (2019) New anaxyelids (Hymenoptera: Anaxyelidae) from the Cretaceous of Asia. Zootaxa 4603: 341–353. https://doi.org/10.11646/zootaxa.4603.2.7

Kopylov DS, Rasnitsyn AP, Zhang HC, Zhang Q (2020) Anaxyelidae of Daohugou: oldest occurrences of the relict family in the fossil record. Part1: *Daosyntexis* and *Brachysyntexis*. Alcheringa: An Australasian Journal of Palaeontology 44: 104–114. https://doi.org/10.1080/03115518.2019.1697753

Lin XD, Labandeira CC, Shih CK, Hotton CL, Ren D (2019) Life habits and evolutionary biology of new two-winged long-proboscid scorpionflies from mid-Cretaceous Myanmar amber. Nature Communications 10: e1235. https://doi.org/10.1038/s41467-019-09236-4

Morgan FD (1968) Bionomics of Siricidae. Annual Review of Entomology 13: 239–256. https://doi.org/10.1146/annurev.en.13.010168.001323

Nixon KC (2002) WinClada, version 1.00.08. program and documentation. Cornell University Press, Ithaca.

Ortega-Blanco J, Rasnitsyn AP, Delclòs X (2008) First record of anaxyelid woodwasps (Hymenoptera: Anaxyelidae) in Lower Cretaceous Spanish amber. Zootaxa 1937: 39–50. https://doi.org/10.11646/zootaxa.1937.1.3

Rasnitsyn AP (1968) New Mesozoic sawflies (Hymenoptera, Symphyta). In: Rohdendorf BB, (Ed.) Jurassic Insects of Karatau. Nauka Press, Moscow, 190–236.

Rasnitsyn AP (1969) Origin and evolution of the lower Hymenoptera. Academy of Sciences of the USSR 123: 1–196.

Rasnitsyn AP (1980) Origin and evolution of the Hymenoptera. Academy of Sciences of the USSR 174: 1–192.

Rasnitsyn AP (1988) An outline of evolution of hymenopterous insects (order Vespida). Oriental Insects 22: 115–145. https://doi.org/10.1080/00305316.1988.11835485

Rasnitsyn AP (1990) Hymenoptera. In: Rasnitsyn AP (Ed.) Late Mesozoic insects of Eastern Transbaikalian. Trans. Paleontol. Inst. Acad. Sci. USSR. 239. Nauka Press, Moscow, 1990: 177–205. [in Russian]

Rasnitysyn AP, Jarzembowski EA, Ross AJ (1998) Wasp (Insecta: Vespida = Hymenoptera) from the Purbeck and Wealden (Lower Cretaceous) of southern England and their biostratigraphical and palaeoenvironmental significance. Cretaceous Research 19: 329–391. https://doi.org/10.1006/cres.1997.0114

Rasnitsyn AP, Martínez-Delclòs X (2000) Wasps (Insecta: Vespida = Hymenoptera) from the Early Cretaceous of Spain. Acta Geologica Hispanica 35: 65–95.

Rasnitsyn AP, Öhm-Kühnle C (2018) Three new female *Aptenoperissus* from mid-Cretaceous Burmese amber (Hymenoptera, Stephanoidea, Aptenoperissidae): unexpected diversity of paradoxical wasps suggests insular features of source biome. Cretaceous Research 91: 168–175. https://doi.org/10.1016/j.cretres.2018.06.004

Rohwer SA (1915) A remarkable new genus of Cephidae. Proceedings of the Entomological Society of Washington 17: 114–117.

Ronquist F, Rasnitsyn AP, Roy A, Eriksson K, Lindgren M (1999) Phylogeny of the Hymenoptera: a cladistic reanalysis of Rasnitsyn' s (1988) data. Zoologica Scripta 28: 13–50. https://doi.org/10.1046/j.1463-6409.1999.00023.x

Schulmeister S, Wheeler WC, Carpenter JM (2002) Simultaneous analysis of the basal lineages of Hymenoptera (Insecta) using sensitivity analysis. Cladistics 18: 455–484. https://doi.org/10.1016/S0748-3007(02)00100-7

Sharkey MJ, Carpenter JM, Vilhelmsen L, Heraty JM, Liljeblad J, Dowling PGA, Schulmeister S, Murray D, Deans RA, Ronquist F, Krogmann L, Wheeler CW (2012) Phylogenetic relationships among superfamilies of Hymenoptera. Cladistics 28: 80–112. https://doi.org/10.1111/j.1096-0031.2011.00366.x

Shi GH, Grimaldi DA, Harlow GE, Wang J, Wang J, Yang MC, Lei WY, Li QL, Li XH (2012) Age constraint on Burmese amber based on U–Pb dating of zircons. Cretaceous Research 37: 155–163. https://doi.org/10.1016/j.cretres.2012.03.014

Smith DR (1979) Symphyta. In: Krombein KV, Hurd PJ, Smith DR, Burks BD (Eds) Catalog of Hymenoptera in America North of Mexico. Smithsonian Institution Press, Washington DC, 3–137.

Vilhelmsen L (2000) Cervical and prothoracic skeleto-musculature in the basal Hymenoptera (Insecta): Comparative anatomy and phylogenetic implications. Zoologischer Anzeiger 239: 105–138.

Vilhelmsen L (2001) Phylogeny and classification of the extant basal lineages of the Hymenoptera (Insecta). Zoological Journal of the Linnean Society 131: 393–442. https://doi.org/10.1006/zjls.2000.0255

Vilhelmsen L, Mikó I, Krogmann L (2010) Beyond the wasp-waist: structural diversity and phylogenetic significance of the mesosoma in apocritan wasps (Insecta: Hymenoptera). Zoological Journal of the Linnean Society 159: 22–194. https://doi.org/10.1111/j.1096-3642.2009.00576.x

Wang M, Rasnitsyn AP, Han G, Ren D (2018) A new genus and species of basal horntail (Hymenoptera, Siricidae) from the Lower Cretaceous of China. Cretaceous Research 91: 195–201. https://doi.org/10.1016/j.cretres.2018.06.006

Wang M, Rasnitsyn AP, Li H, Shih CK, Sharkey MJ, Ren D (2016) Phylogenetic analyses elucidate the inter-relationships of Pamphilioidea (Hymenoptera, Symphyta). Cladistics 32: 407–411. https://doi.org/10.1111/cla.12129

Wang YM, Lin XD, Wang M, Shih CK, Ren D, Gao TP (2021) New sawflies from the mid-Cretaceous Myanmar amber (Insecta: Hymenoptera: Syspastoxyelidae). Historical Biology 33: 1212–1221. https://doi.org/10.1080/08912963.2019.1687695

Wang YM, Wang M, Rasnitsyn AP, Shih CK, Ren D, Kopylov DS, Gao TP (2020) A new anaxyelid sawfly (Insecta, Hymenoptera, Siricoidea) in mid-Cretaceous Myanmar amber. Cretaceous Research 109: 104372. https://doi.org/10.1016/j.cretres.2020.104372

Wickman BE (1967) Life history of the incense-cedar wood wasp, *Syntexis libocedrii* (Hymenoptera: Syntexidae). Annals of the Entomological Society of America 60: 1291–1295. https://doi.org/10.1093/aesa/60.6.1291

Zhang HC, Rasnitsyn AP (2006) Two new anaxyelid sawflies (Insecta, Hymenoptera, Siricoidea) from the Yixian Formation of western Liaoning, China. Cretaceous Research 27: 279–284. https://doi.org/10.1016/j.cretres.2005.11.001

Zhang Q, Kopylov DS, Rasnitsyn AP, Zheng Y, Zhang HC (2020) Burmorussidae, a new family of parasitic wasps (Insecta, Hymenoptera) from mid-Cretaceous Burmese amber. Papers in Palaeontology 6: 593–603. https://doi.org/10.1002/spp2.1312

Zhang Q, Rasnitsyn AP, Wang B, Zhang HC (2018) Hymenoptera (wasps, bees and ants) in mid-Cretaceous Burmese amber: a review of the fauna. Proceedings of the Geologists' Association 129: 736–747. https://doi.org/10.1016/j.pgeola.2018.06.004

Zhao ZP, Yin XC, Shih CK, Gao TP, Ren D (2020) Termite colonies from mid-Cretaceous Myanmar demonstrate their early eusocial lifestyle in damp wood. National Science Review 7: 381–390. https://doi.org/10.1093/nsr/nwz141

Zheng Y, Zhang Q, Chen J, Zhang H (2019) A remarkably new basal wasp with uniquely transformed forewing in mid-Cretaceous Burmese amber (Hymenoptera, Syspastoxyelidae). Cretaceous Research 104: 104172. https://doi.org/10.1016/j.cretres.2019.07.002

Supplementary material 1

File S1

Authors: Jia Gao, Michael S. Engel, Chungkun Shih, Dong Ren, Taiping Gao

Data type: Distribution (Word file (.docx))

Explanation note: File S1. List of distribution of living and fossil Anaxyelidae.

Copyright notice: This dataset is made available under the Open Database License (http://opendatacommons.org/licenses/odbl/1.0/). The Open Database License (ODbL) is a license agreement intended to allow users to freely share, modify, and use this Dataset while maintaining this same freedom for others, provided that the original source and author(s) are credited.

Link: https://doi.org/10.3897/jhr.86.73161.suppl1

Supplementary material 2

File S2

Authors: Jia Gao, Michael S. Engel, Chungkun Shih, Dong Ren, Taiping Gao

Data type: Morphological characters (Word file (.docx))

Explanation note: File S2. List of morphological characters and character states for the phylogenetic analyses.

Copyright notice: This dataset is made available under the Open Database License (http://opendatacommons.org/licenses/odbl/1.0/). The Open Database License (ODbL) is a license agreement intended to allow users to freely share, modify, and use this Dataset while maintaining this same freedom for others, provided that the original source and author(s) are credited.

Link: https://doi.org/10.3897/jhr.86.73161.suppl2

Supplementary material 3

File S3

Authors: Jia Gao, Michael S. Engel, Chungkun Shih, Dong Ren, Taiping Gao

Data type: Matrix (Excel file (.xls))

Explanation note: Data matrix of characters used in the phylogenetic analyses.

Copyright notice: This dataset is made available under the Open Database License (http://opendatacommons.org/licenses/odbl/1.0/). The Open Database License (ODbL) is a license agreement intended to allow users to freely share, modify, and use this Dataset while maintaining this same freedom for others, provided that the original source and author(s) are credited.

Link: https://doi.org/10.3897/jhr.86.73161.suppl3

Supplementary material 4

Nex File

Authors: Jia Gao, Michael S. Engel, Chungkun Shih, Dong Ren, Taiping Gao

Data type: Data matrix in nexus file

Explanation note: Data matrix in nexus file of Suppl. material 3: File S3.

Copyright notice: This dataset is made available under the Open Database License (http://opendatacommons.org/licenses/odbl/1.0/). The Open Database License (ODbL) is a license agreement intended to allow users to freely share, modify, and use this Dataset while maintaining this same freedom for others, provided that the original source and author(s) are credited.

Link: https://doi.org/10.3897/jhr.86.73161.suppl4